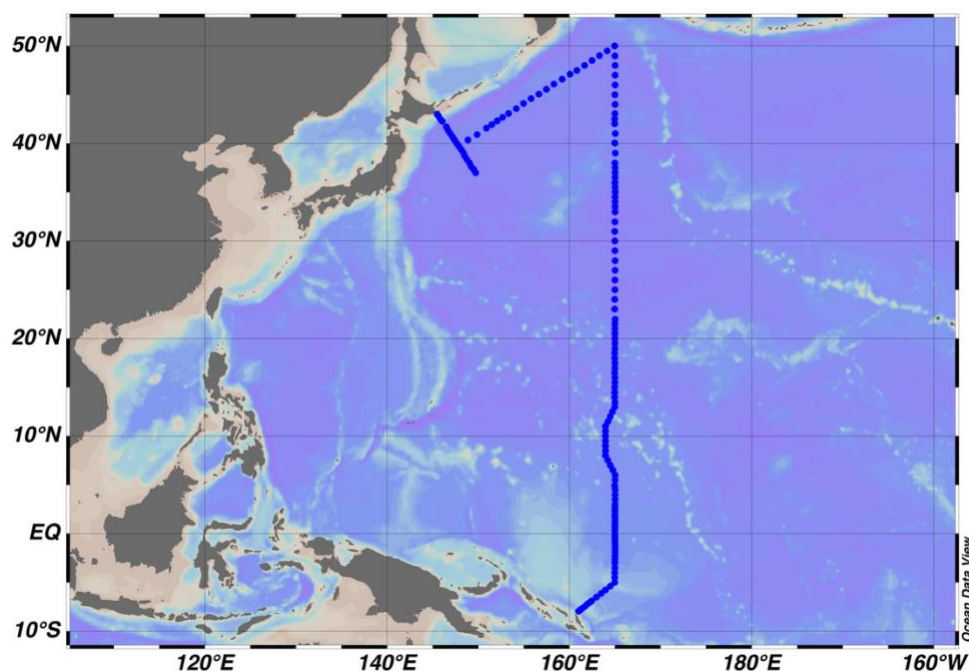


CRUISE REPORT: RF11-06, 07, 08

Created: July 2025



Highlights

Cruise Summary Information

Section Designation	P13
Expedition Designation (ExpoCode)	49UP20110515
Chief Scientist	Toshiya NAKANO (JMA)
Dates	RF11-06: 15 May – 31 May, 2011 RF11-07: 4 June – 27 June, 2011 RF11-08: Leg 1: 5 July – 29 July, 2011 Leg 2: 2 August – 26 August, 2011
Ship	R/V Ryofu Maru
Ports of Call	RF11-06: Tokyo, JP - Tokyo, JP RF11-07: Tokyo, JP - Tokyo, JP RF11-08: Leg 1: Tokyo, JP – Pohnpei, FSM Leg 2: Pohnpei, FSM – Saipan, CNMI
Geographic Boundaries	145° 5"E 50° "N 164° 98"E 7° 97"S
Stations	151
Floats and Drifters Deployed	RF11-06: 3 floats RF11-07: 5 floats RF11-08: 3 floats
Moorings Deployed and Recovered	0

Contact Information:

Toshiya NAKANO

Marine Division

Japan Meteorological Agency (JMA)

Phone: +81-3-3212-8341 Ext. 5163

Email: nakano_t@met.kishou.go.jp

Contents

A. Cruise narrative

C. Hydrographic Measurement Techniques and Calibration

1. CTD/O₂ Measurements

2. Bottle Salinity

3. Bottle Oxygen

4. Nutrients

5. Total Dissolved Inorganic Carbon (DIC) / Total Alkalinity (TA)

6. pH

7. Phytopigment (Chlorophyll-a and phaeopigments)

8. $\delta^{13}\text{C}$ and $\Delta^{14}\text{C}$ of Dissolved Inorganic Carbon

Cruise narrative

1. Highlights

Cruise designation: RF11-06, RF11-07 and RF11-08 (WHP-P13 revisit)

a. EXPOCODE: RF11-06 49UP20110515

RF11-07 49UP20110604

RF11-08 49UP20110705

b. Chief scientist: Toshiya NAKANO (nakano_t@met.kishou.go.jp)

Marine Environment Monitoring and Analysis Center

Marine Division

Global Environment and Marine Department

Japan Meteorological Agency (JMA)

1-3-4, Otemachi, Chiyoda-ku, Tokyo 100-8122, JAPAN

Phone: +81-3-3212-8341 Ext. 5163

FAX: +81-3-3211-6908

c. Ship name: R/V Ryofu Maru

d. Ports of call: RF11-06 Tokyo - Tokyo

RF11-07 Tokyo - Tokyo

RF11-08 Leg1: Tokyo - Pohnpei

Leg 2: Pohnpei - Saipan

e. Cruise dates: RF11-06 15 May 2011 - 31 May 2011

RF11-07 4 June 2011 - 27 June 2011

RF11-08 Leg1: 5 July 2011 - 29 July 2011

Leg2: 2 August 2011 - 26 August 2011

f. Floats and drifters deployed: RF11-06 3 floats

RF11-07 5 floats

RF11-08 3 floats

2. Cruise Summary Information

RF11-06, RF11-07 and RF11-08 cruises were carried out during the period from May 15 to September 5, 2011. The observation line along approximately 165°E meridian was observed by Ocean Research Institute, University of Tokyo, Japan in 1991 and 1993, and by National Oceanographic and Atmospheric Administration, USA in 1992. These cruises were carried out as ‘WHP-P13’, which is a part of WOCE (World Ocean Circulation Experiment) Hydrographic Programme. The stations from Stn.1 (43°N, 145°30'E; RF3984) to Stn.14 (39°40'N, 147°52'E; RF3997) for RF11-06 cruise and from Stn.23 (39°40'N, 147°52'E; RF4007) to Stn.38 (47°N, 160°E) for RF11-07 cruise had been designed as a re-occupation of the WHP-P1 stations observed by Japan Agency for Marine-Earth Science and Technology (JAMSTEC) in 2007.

RF11-06

RF11-06 cruise was carried out during the period from May 15 to May 31, 2011. Before the observation at the first station, all watch standers were drilled in the method of sample drawing and CTD operations near Izu-Oshima (34°40'N, 139°40'E). The cruise started from the coast near Kushiro, Japan, and sailed southeastward. The hydrographic cast of CTDO₂ was started at the first station (Stn.1 (43°N, 145°30'E; RF3984)) on May 17. RF11-06 cruise consisted of 22 stations from Stn.1 to Stn.22 (37°N, 149°50'E; RF4005). Cruise track and station location are shown in Figure 1(a).

Three sub-surface profiling floats (ARVOR: nke Instrumentation, France) were deployed along the cruise track. The information of deployed the floats are listed in Table 1.

RF11-07

RF11-07 cruise was carried out during the period from June 4 to June 27, 2011. Before the observation at the first station, all watch standers were drilled in the method of sample

drawing and CTD operations near Izu-Oshima (34°40'N, 139°40'E). The cruise started from the east of Honshu, Japan, and sailed northeastward along off the Kuril Islands. The hydrographic cast of CTDO₂ was started at the first station (Stn.23 (39°40'N, 147°52'E; RF4007)) on June 6. After observed at Stn.44 (50°N, 165°E; RF4028), she sailed toward south along 165°E meridian. RF11-07 cruise consisted of 33 stations from Stn.23 to Stn.55 (40°N, 165°E; RF4039). Cruise track and station location are shown in Figure 1(b).

Five ARGO floats (PROVOR: nke Instrumentation, France) were deployed at the request of JAMSTEC along the cruise track. The information of deployed floats are listed in Table 1.

RF11-08

RF11-08 cruise was carried out during the period from July 5 to September 5, 2011. In order to ensure a controlled spooling of the armored cable, we rewound the cable at 34°50'N, 142°00'E (about 8000 m depth) before the observation at the first station. The cruise started from 40°N, 165°E, and sailed toward south along approximately 165°E meridian. The hydrographic cast of CTDO₂ was started at the first station (Stn.56 (40°00'N, 165°E; RF4040)) on July 9. Leg 1 consisted of 50 stations from Stn.56 to Stn.105 (9°N, 165°E; RF4089). In order to keep away from the military exercise area, we shifted the nominal longitude of CTDO₂ stations westward between Stn.98 (RF4082) and Stn.111 (RF4095). She called for Pohnpei (Federated States of Micronesia) on July 29, 2011 (Leg 1). She left Pohnpei on August 2, 2011 for Saipan (Commonwealth of the Northern Mariana Islands) and arrived on August 26, 2011 (Leg 2). Leg 2 consisted of 46 stations from Stn.106 (9°N, 164°E; RF4090) to Stn.151 (8°S, 161°E; RF4135). Cruise track and station location are shown in Figure 1(c).

Three ARGO floats (PROVOR: nke Instrumentation, France) were deployed at the request of JAMSTEC along the cruise track. The information of deployed floats are listed in Table 1.

A total of 151 stations (22 for RF11-06, 33 for RF11-07 and 96 for RF11-08) was occupied using a Sea-Bird Electronics (SBE) 36 position carousel equipped with 10-liter Niskin water sample bottles, a CTD system (SBE911plus) equipped with SBE35 deep ocean standards thermometer, JFE Advantech oxygen sensor (RINKO III), Teledyne Benthos altimeter, and Teledyne RD Instruments Lowered Acoustic Doppler Current Profiler (L-ADCP). To examine consistency of data, we carried out the observation twice at 39°40'N, 147°52'E (Stn.14 and Stn.23), 40°N, 165°E (Stn.55 and Stn.56) and 9°N, 165°E (Stn.105 and Stn.106), respectively.

At each station, full-depth CTDO₂ (temperature, conductivity (salinity) and dissolved oxygen) profile and up to 36 water samples were taken and analyzed. Water samples were obtained from 10 dbar to approximately 10 meters above the bottom. In addition, surface water were sampled by stainless steel bucket at each station. Basic sampling layer is designed as so-called staggered mesh as shown in Table 2. We added the sampling layer selected from 25 m/75 m/125 m/350 m/450 m, according as characteristic of ocean structure and water depth. The bottle depth diagram is shown in Figure 2.

Water samples were analyzed for salinity, dissolved oxygen, nutrients, dissolved inorganic carbon (DIC), total alkalinity (TA), pH, CFC-11, -12 and phytopigment (chlorophyll-a and phaeopigments). Samples for ¹⁴C were also collected at the same stations of WHP-P13 in 1992. Underway measurements of partial pressure of carbon dioxide (*p*CO₂), temperature, salinity, chlorophyll-a, subsurface current, bathymetry and meteorological parameters were conducted along the cruise track.

Table 1. Information of deployed floats in RF11-06, RF11-07 and RF11-08.

<i>ARGOS ID</i>	<i>Date and Time of System Reset (UTC)</i>	<i>Date and Time of Deployment (UTC)</i>	<i>Position of deployment</i>	<i>PI</i>	<i>Remark</i>
RF11-06					
064041	May 21, 09:35	May 21, 10:07	39-26.669N, 148-13.147E	JMA	Stn.15 (RF3998)
064213	May 21, 09:31	May 21, 10:08	39-26.613N, 148-13.095E	JMA	Stn.15 (RF3998)
064040	May 22, 00:20	May 22, 01:14	38-43.498N, 148-31.341E	JMA	Stn.17 (RF4000)
RF11-07					
97932	June 4, 16:55	June 4, 17:43	35-10.203N, 141-01.024E	JAMSTEC	
97955	June 5, 04:54	June 5, 06:00	37-08.304N, 144-00.438E	JAMSTEC	
97945	June 17, 21:40	June 17, 22:57	44-00.119N, 165-03.358E	JAMSTEC	Stn.50 (RF4034)
97937	June 19, 01:27	June 19, 02:59	42-02.514N, 164-54.997E	JAMSTEC	Stn.53 (RF4037)
97913	June 21, 21:20	June 21, 22:09	40-07.053N, 165-01.610E	JAMSTEC	Stn.55 (RF4039)
RF11-08					
97951	July 13, 20:20	July 13, 21:31	31-55.845N, 164-59.280E	JAMSTEC	Stn.69 (RF4053)
97939	July 14, 23:12	July 15, 00:27	29-00.311N, 165-00.595E	JAMSTEC	Stn.72 (RF4056)
97943	July 19, 01:05	July 19, 02:10	20-00.022N, 164-58.151E	JAMSTEC	Stn.83 (RF4067)

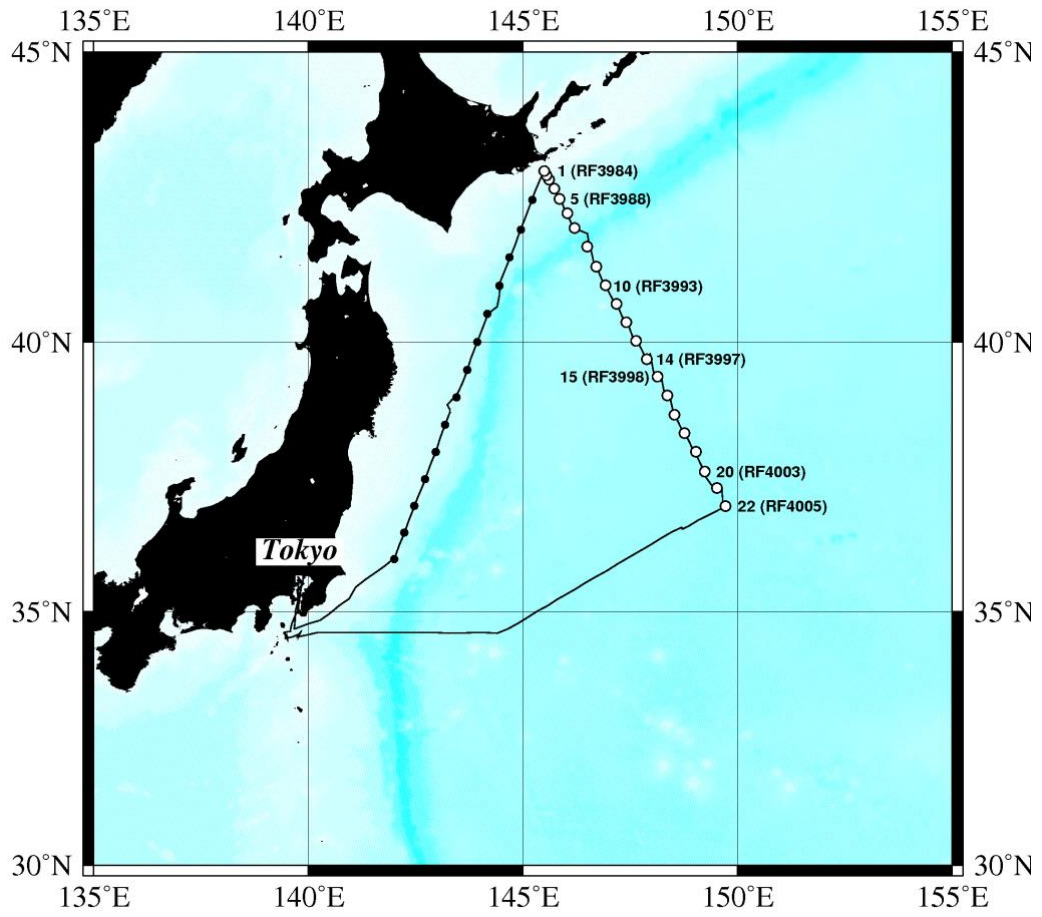


Figure 1(a). Cruise track of RF11-06. Open and closed circles indicate CTD station and X-BT station, respectively.

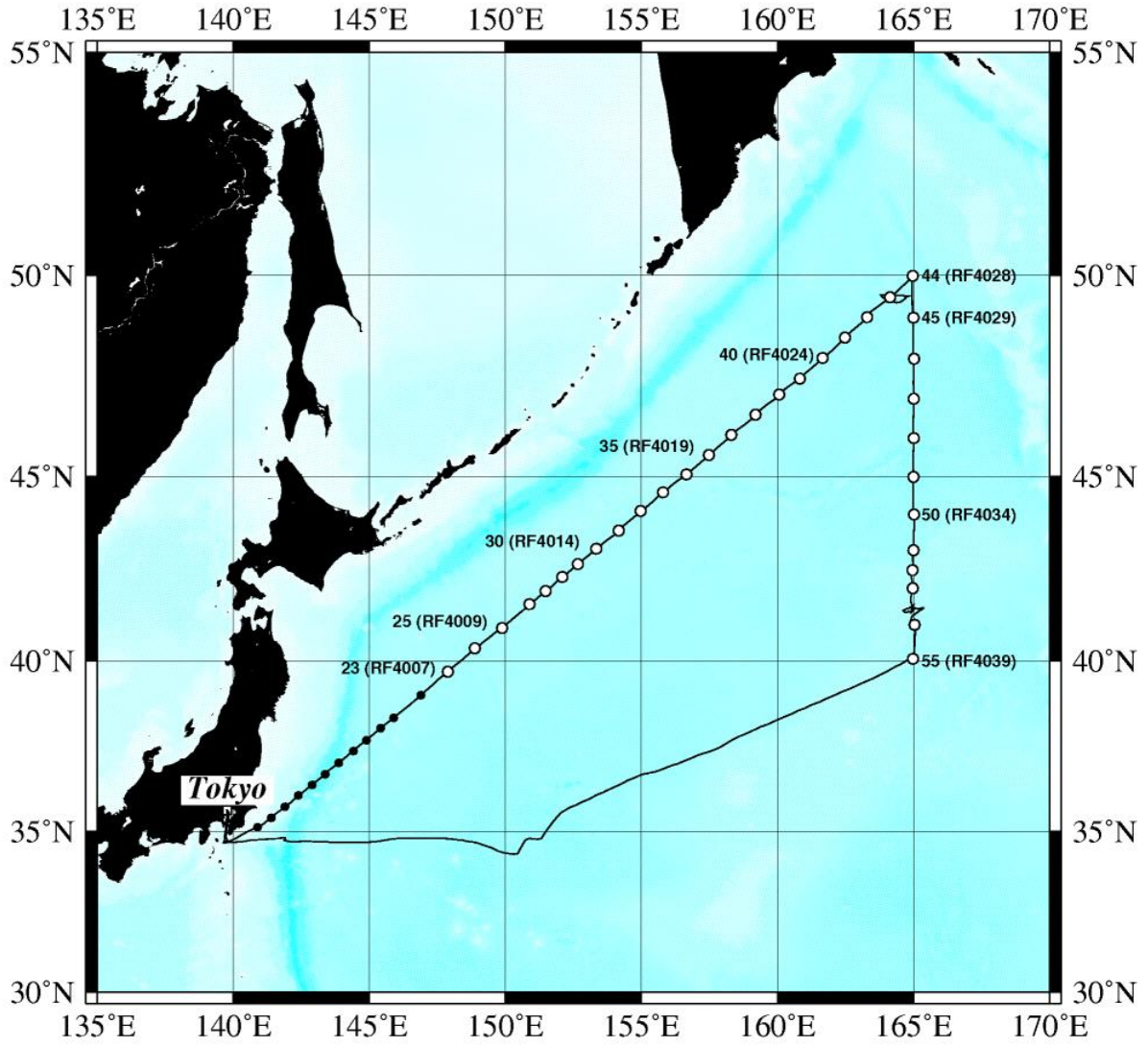


Figure 1(b). Cruise track of RF11-07. Open and closed circles indicate CTD station and X-BT station, respectively.

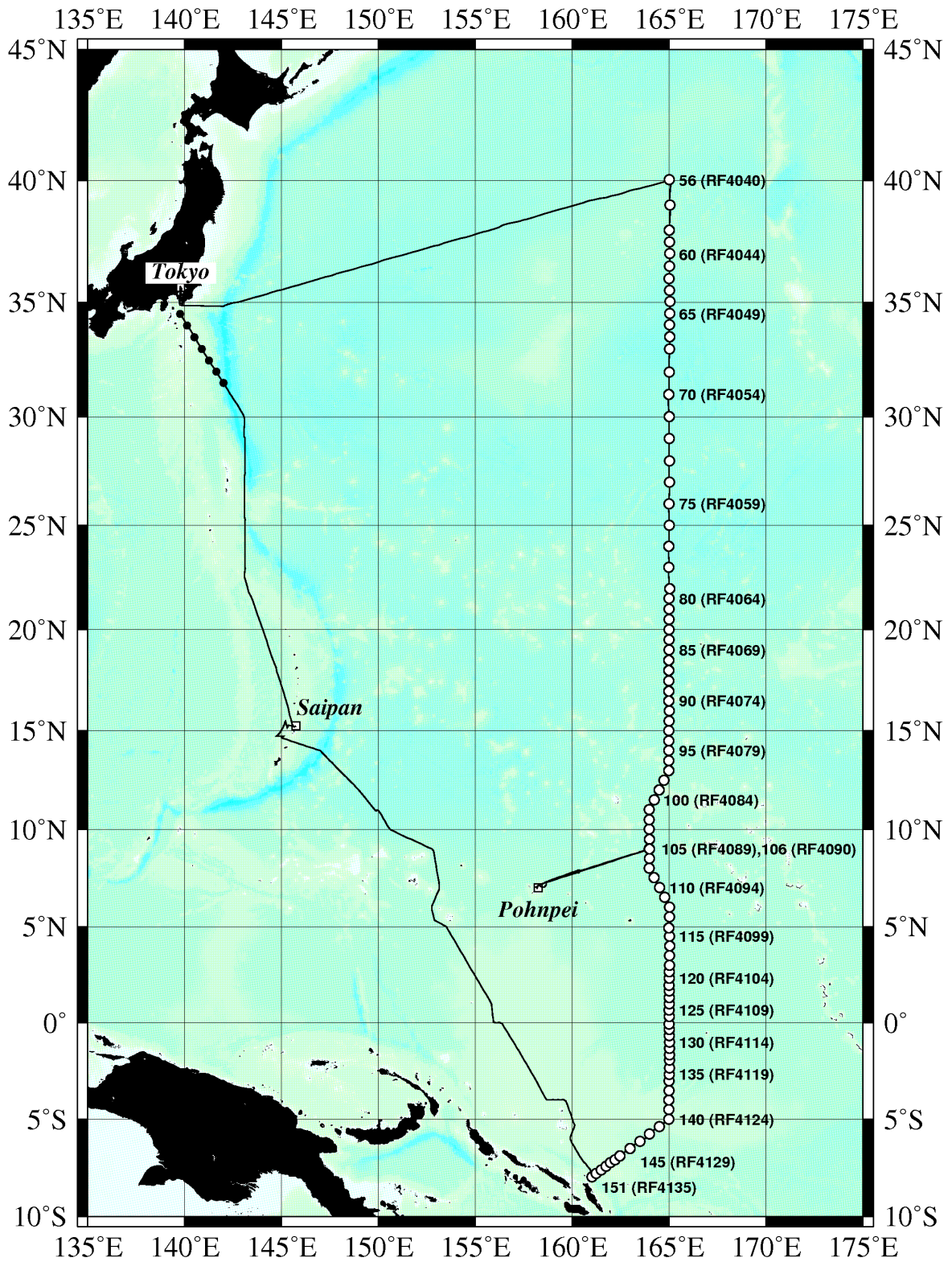


Figure 1(c). Cruise track of RF11-08. Open and closed circles indicate CTD station and X-BT station, respectively.

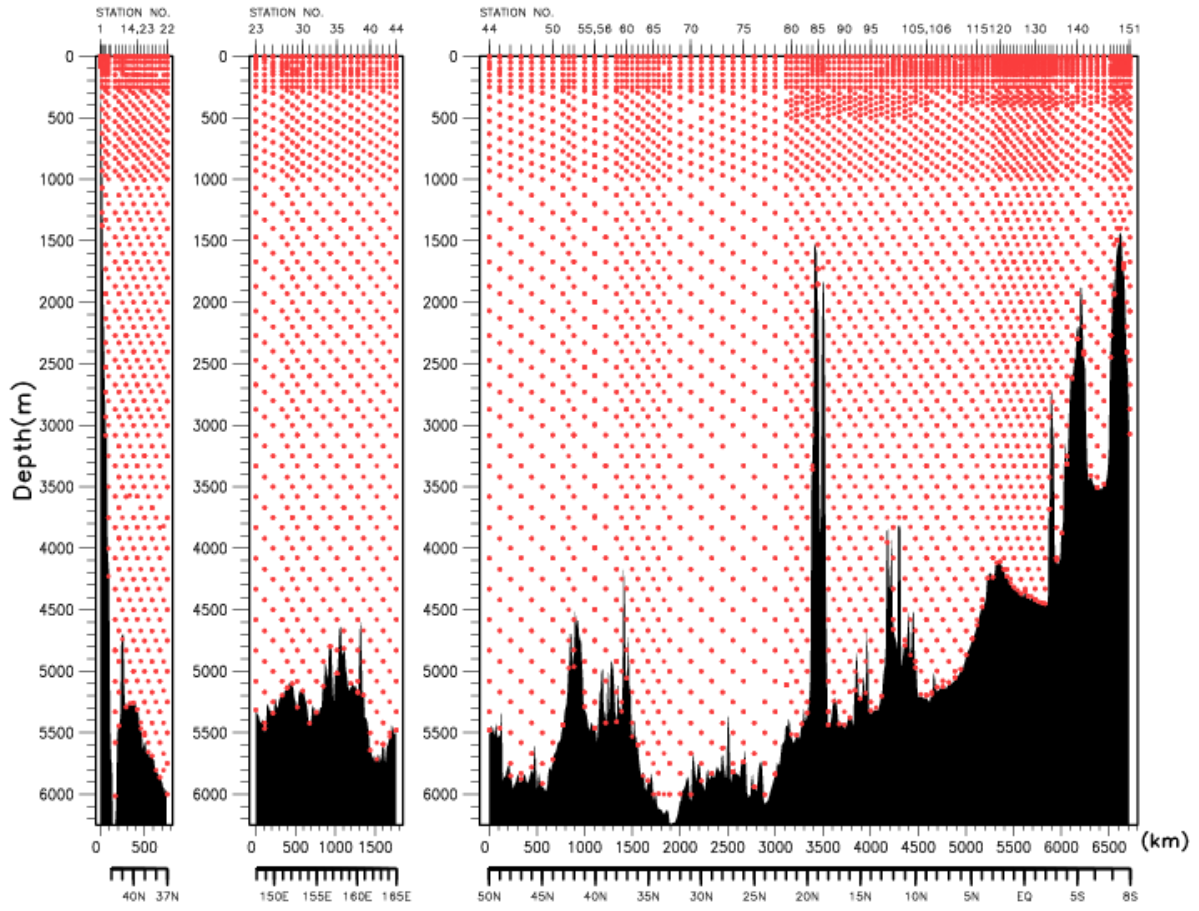


Figure 2. The bottle depth diagram for WHP-P13 revisit.

Table 2. The scheme of sampling layer in meters.

<i>Bottle count</i>	<i>scheme1</i>	<i>scheme2</i>	<i>scheme3</i>
1	10	10	10
2	50	50	50
3	100	100	100
4	150	150	150
5	200	200	200
6	250	250	250
7	300	330	280
8	400	430	370
9	500	530	470
10	600	630	570
11	700	730	670
12	800	830	770
13	900	930	870
14	1000	1070	970
15	1200	1270	1130
16	1400	1470	1330
17	1600	1670	1530
18	1800	1870	1730
19	2000	2070	1930
20	2200	2270	2130
21	2400	2470	2330
22	2600	2670	2530
23	2800	2870	2730
24	3000	3080	2930
25	3250	3330	3170
26	3500	3580	3420
27	3750	3830	3670
28	4000	4080	3920
29	4250	4330	4170
30	4500	4580	4420
31	4750	4830	4670
32	5000	5080	4920
33	5250	5330	5170
34	5500	5580	5420
35	5750	5830	5670
36	Bottom	Bottom	Bottom

Table 3(a). Station data of RF11-06 cruise. The ‘RF’ column indicates the JMA station identification number.

<i>Leg</i>	<i>Station</i>		<i>Position</i>	
	<i>Stn.</i>	<i>RF</i>	<i>Latitude</i>	<i>Longitude</i>
1	1	3984	42-59.53 N	145-29.82 E
1	2	3985	42-55.25 N	145-32.72 E
1	3	3986	42-50.85 N	145-36.45 E
1	4	3987	42-41.38 N	145-43.70 E
1	5	3988	42-30.90 N	145-51.01 E
1	6	3989	42-16.00 N	146-02.06 E
1	7	3990	42-00.75 N	146-12.13 E
1	8	3991	41-41.35 N	146-29.80 E
1	9	3992	41-20.14 N	146-42.38 E
1	10	3993	41-00.56 N	146-55.31 E
1	11	3994	40-40.84 N	147-10.72 E
1	12	3995	40-21.13 N	147-24.26 E
1	13	3996	40-01.21 N	147-37.85 E
1	14	3997	39-41.56 N	147-52.96 E
1	15	3998	39-22.74 N	148-08.12 E
1	16	3999	39-02.30 N	148-21.66 E
1	17	4000	38-41.11 N	148-31.75 E
1	18	4001	38-20.97 N	148-45.65 E
1	19	4002	38-00.47 N	149-01.63 E
1	20	4003	37-38.34 N	149-13.98 E
1	21	4004	37-20.09 N	149-30.97 E
1	22	4005	36-59.71 N	149-43.09 E

Table 3(b). Station data of RF11-07 cruise. The ‘RF’ column indicates the JMA station identification number.

<i>Leg</i>	<i>Station</i>		<i>Position</i>	
	<i>Stn.</i>	<i>RF</i>	<i>Latitude</i>	<i>Longitude</i>
1	23	4007	39-41.20 N	147-53.53 E
1	24	4008	40-21.01 N	148-52.73 E
1	25	4009	40-55.05 N	149-52.79 E
1	26	4010	41-34.59 N	150-53.38 E
1	27	4011	41-56.44 N	151-29.15 E
1	28	4012	42-19.40 N	152-05.32 E
1	29	4013	42-40.36 N	152-39.91 E
1	30	4014	43-05.50 N	153-20.34 E
1	31	4015	43-34.66 N	154-10.27 E
1	32	4016	44-05.77 N	154-58.35 E
1	33	4017	44-35.31 N	155-47.96 E
1	34	4018	45-03.62 N	156-39.25 E
1	35	4019	45-33.64 N	157-28.74 E
1	36	4020	46-04.60 N	158-18.39 E
1	37	4021	46-35.35 N	159-11.81 E
1	38	4022	47-06.13 N	160-03.89 E
1	39	4023	47-29.69 N	160-49.18 E
1	40	4024	48-00.58 N	161-39.39 E
1	41	4025	48-30.44 N	162-28.67 E
1	42	4026	49-00.23 N	163-17.79 E
1	43	4027	49-29.08 N	164-08.39 E
1	44	4028	49-59.80 N	164-58.50 E
1	45	4029	48-59.46 N	164-59.89 E
1	46	4030	47-59.45 N	165-00.88 E
1	47	4031	46-59.64 N	165-00.51 E
1	48	4032	45-59.68 N	165-00.70 E
1	49	4033	44-59.41 N	164-59.94 E
1	50	4034	44-00.16 N	165-01.11 E
1	51	4035	43-02.99 N	164-59.98 E
1	52	4036	42-30.36 N	164-57.80 E
1	53	4037	42-00.81 N	164-58.36 E
1	54	4038	41-00.33 N	165-02.37 E
1	55	4039	40-03.07 N	164-58.78 E

Table 3(c). Station data of RF11-08 cruise. The ‘RF’ column indicates the JMA station identification number.

<i>Leg</i>	<i>Station</i>		<i>Position</i>		<i>Leg</i>	<i>Station</i>		<i>Position</i>	
	<i>Stn.</i>	<i>RF</i>	<i>Latitude</i>	<i>Longitude</i>		<i>Stn.</i>	<i>RF</i>	<i>Latitude</i>	<i>Longitude</i>
1	56	4040	40-02.05 N	165-00.07 E	1	94	4078	14-29.39 N	164-58.65 E
1	57	4041	39-01.05 N	165-02.24 E	1	95	4079	13-59.95 N	164-58.80 E
1	58	4042	37-59.50 N	164-59.77 E	1	96	4080	13-29.27 N	164-58.90 E
1	59	4043	37-30.89 N	165-00.36 E	1	97	4081	12-59.56 N	164-58.25 E
1	60	4044	37-02.44 N	165-01.39 E	1	98	4082	12-29.75 N	164-43.69 E
1	61	4045	36-30.87 N	165-00.85 E	1	99	4083	12-00.16 N	164-28.87 E
1	62	4046	35-59.47 N	164-59.01 E	1	100	4084	11-30.01 N	164-13.86 E
1	63	4047	35-29.65 N	165-00.53 E	1	101	4085	11-00.50 N	163-57.89 E
1	64	4048	35-01.78 N	165-01.87 E	1	102	4086	10-29.30 N	163-58.12 E
1	65	4049	34-30.71 N	165-01.21 E	1	103	4087	10-00.28 N	163-57.98 E
1	66	4050	34-02.22 N	165-01.04 E	1	104	4088	9-29.59 N	163-58.46 E
1	67	4051	33-31.03 N	165-01.22 E	1	105	4089	8-59.64 N	163-58.41 E
1	68	4052	32-59.22 N	165-00.41 E	2	106	4090	9-00.05 N	163-58.09 E
1	69	4053	31-58.31 N	164-59.89 E	2	107	4091	8-30.11 N	163-58.53 E
1	70	4054	30-59.15 N	164-58.88 E	2	108	4092	8-00.44 N	163-58.14 E
1	71	4055	29-59.92 N	165-00.23 E	2	109	4093	7-31.13 N	164-12.97 E
1	72	4056	29-00.40 N	165-00.14 E	2	110	4094	7-00.71 N	164-30.01 E
1	73	4057	27-59.11 N	165-00.46 E	2	111	4095	6-30.55 N	164-45.53 E
1	74	4058	27-00.51 N	165-00.70 E	2	112	4096	6-00.13 N	165-00.52 E
1	75	4059	26-00.21 N	164-59.34 E	2	113	4097	5-30.00 N	165-00.71 E
1	76	4060	24-59.77 N	164-59.76 E	2	114	4098	4-55.06 N	164-58.56 E
1	77	4061	24-00.71 N	164-58.58 E	2	115	4099	4-29.40 N	165-00.59 E
1	78	4062	23-00.62 N	164-58.34 E	2	116	4100	3-59.44 N	165-01.05 E
1	79	4063	21-58.73 N	165-01.24 E	2	117	4101	3-29.25 N	165-00.91 E
1	80	4064	21-30.47 N	164-59.61 E	2	118	4102	2-58.86 N	165-00.94 E
1	81	4065	21-00.01 N	164-59.14 E	2	119	4103	2-38.95 N	165-00.02 E
1	82	4066	20-30.07 N	164-59.47 E	2	120	4104	2-18.95 N	165-00.20 E
1	83	4067	19-59.95 N	164-59.41 E	2	121	4105	1-56.39 N	164-59.37 E
1	84	4068	19-30.34 N	164-59.26 E	2	122	4106	1-39.22 N	165-00.07 E
1	85	4069	19-00.25 N	164-59.28 E	2	123	4107	1-18.47 N	165-00.31 E
1	86	4070	18-30.19 N	164-58.75 E	2	124	4108	0-59.21 N	164-59.87 E
1	87	4071	18-00.01 N	164-58.62 E	2	125	4109	0-39.70 N	164-59.45 E
1	88	4072	17-29.29 N	164-58.90 E	2	126	4110	0-19.93 N	165-00.12 E
1	89	4073	16-58.31 N	164-58.93 E	2	127	4111	0-04.15 S	164-59.61 E
1	90	4074	16-29.43 N	164-58.63 E	2	128	4112	0-20.32 S	164-59.73 E

1	91	4075	15-59.41 N	164-59.70 E	2	129	4113	0-39.82 S	165-00.21 E
1	92	4076	15-28.96 N	164-59.29 E	2	130	4114	1-00.12 S	165-00.90 E
1	93	4077	15-00.00 N	164-58.81 E	2	131	4115	1-19.79 S	165-00.40 E
<i>Leg</i>	<i>Station</i>		<i>Position</i>						
	<i>Stn.</i>	<i>RF</i>	<i>Latitude</i>	<i>Longitude</i>					
2	132	4116	1-40.01 S	165-00.78 E					
2	133	4117	1-56.30 S	165-00.72 E					
2	134	4118	2-20.71 S	165-00.83 E					
2	135	4119	2-40.75 S	165-00.22 E					
2	136	4120	3-00.68 S	164-59.06 E					
2	137	4121	3-30.82 S	164-59.08 E					
2	138	4122	4-00.38 S	164-58.79 E					
2	139	4123	4-30.02 S	164-58.59 E					
2	140	4124	5-00.30 S	164-58.52 E					
2	141	4125	5-23.11 S	164-29.01 E					
2	142	4126	5-45.90 S	163-58.25 E					
2	143	4127	6-08.52 S	163-29.07 E					
2	144	4128	6-30.58 S	162-58.61 E					
2	145	4129	6-54.00 S	162-26.88 E					
2	146	4130	7-05.66 S	162-12.13 E					
2	147	4131	7-14.35 S	161-57.94 E					
2	148	4132	7-25.98 S	161-44.47 E					
2	149	4133	7-36.95 S	161-29.12 E					
2	150	4134	7-47.74 S	161-13.89 E					
2	151	4135	7-58.40 S	161-00.67 E					

3. List of Principal Investigators for all Measurements

The principal investigator (PI) and the person in charge responsible for major parameters measured on the cruise are listed in Table 4.

Table 4(a). List of principal investigator and the person in charge on the ship for RF11-06.

Item	Principal Investigator (PI)	Person in charge on the ship
<u>Hydrography</u>		
CTDO2 / LADCP	Hitomi KAMIYA	Tatsuo NAKAMURA
Salinity	Hitomi KAMIYA	Tatsuo NAKAMURA
Dissolved oxygen	Hitomi KAMIYA	Yusuke TAKATANI
Nutrients	Hitomi KAMIYA	Takahiro KITAGAWA
Phytopigment	Hitomi KAMIYA	Sonoki IWANO
DIC	Hitomi KAMIYA	Shu SAITO
Total Alkalinity	Hitomi KAMIYA	Shu SAITO
pH	Hitomi KAMIYA	Shu SAITO
CFCs	Hitomi KAMIYA	Kazuki ISHIMARU
<u>Underway</u>		
Meteorology	Hitomi KAMIYA	Tatsuo NAKAMURA
Thermo-Salinograph	Hitomi KAMIYA	Shu SAITO
$p\text{CO}_2$	Hitomi KAMIYA	Shu SAITO
Chlorophyll-a	Hitomi KAMIYA	Sonoki IWANO
ADCP	Hitomi KAMIYA	Tatsuo NAKAMURA
Bathymetry	Hitomi KAMIYA	Tatsuo NAKAMURA
<u>Floats</u>		
Sub-surface Profiling float	Hitomi KAMIYA	Toshiya NAKANO

Hitomi KAMIYA (hkamiya@met.kishou.go.jp)

Marine Division, Global Environment and Marine Department, JMA

1-3-4, Otemachi, Chiyoda-ku, Tokyo 100-8122, JAPAN

Phone: +81-3-3212-8341 Ext. 5150 FAX: +81-3-3211-6908

Table 4(b). List of principal investigator and the person in charge on the ship for RF11-07.

Item	Principal Investigator (PI)	Person in charge on the ship
<u>Hydrography</u>		
CTDO2 / LADCP	Hitomi KAMIYA	Tetsuya NAKAMURA
Salinity	Hitomi KAMIYA	Tetsuya NAKAMURA
Dissolved oxygen	Hitomi KAMIYA	Shinichiro UMEDA
Nutrients	Hitomi KAMIYA	Naoki NAGAI
phytopigment	Hitomi KAMIYA	Naoki NAGAI
DIC	Hitomi KAMIYA	Shinji MASUDA
Total Alkalinity	Hitomi KAMIYA	Shinji MASUDA
pH	Hitomi KAMIYA	Shinji MASUDA
CFCs	Hitomi KAMIYA	Takayuki TOKIEDA
¹⁴ C	Yuichiro KUMAMOTO	Shinji MASUDA
<u>Underway</u>		
Meteorology	Hitomi KAMIYA	Tetsuya NAKAMURA
Thermo-Salinograph	Hitomi KAMIYA	Takayuki TOKIEDA
pCO ₂	Hitomi KAMIYA	Takayuki TOKIEDA
Chlorophyll-a	Hitomi KAMIYA	Naoki NAGAI
ADCP	Hitomi KAMIYA	Tetsuya NAKAMURA
Bathymetry	Hitomi KAMIYA	Tetsuya NAKAMURA
<u>Floats</u>		
ARGO float	Toshio SUGA	Toshiya NAKANO

Hitomi KAMIYA (hkamiya@met.kishou.go.jp)

Marine Division, Global Environment and Marine Department, JMA

1-3-4, Otemachi, Chiyoda-ku, Tokyo 100-8122, JAPAN

Phone: +81-3-3212-8341 Ext. 5150 FAX: +81-3-3211-6908

Yuichiro KUMAMOTO (kumamoto@jamstec.go.jp)

Ocean Climate Change Research Program

Research Institute for Global Change (RIGC)

Japan Agency for Marine-Earth Science and Technology (JAMSTEC)

2-15 Natsushima, Yokosuka, Kanagawa, Japan 237-0061

Toshio SUGA (sugat@jamstec.go.jp)

Ocean Climate Change Research Program

Research Institute for Global Change (RIGC)

Japan Agency for Marine-Earth Science and Technology (JAMSTEC)

2-15 Natsushima, Yokosuka, Kanagawa, Japan 237-0061

Table 4(c). List of principal investigator and the person in charge on the ship for RF11-08.

Item	Principal Investigator (PI)	Person in charge on the ship
<u>Hydrography</u>		
CTDO2 / LADCP	Hitomi KAMIYA	Tetsuya NAKAMURA
Salinity	Hitomi KAMIYA	Tetsuya NAKAMURA
Dissolved oxygen	Hitomi KAMIYA	Yusuke TAKATANI
Nutrients	Hitomi KAMIYA	Naoki NAGAI
Phytopigment	Hitomi KAMIYA	Naoki NAGAI
DIC	Hitomi KAMIYA	Shu SAITO
Total Alkalinity	Hitomi KAMIYA	Shu SAITO
pH	Hitomi KAMIYA	Shu SAITO
CFCs	Hitomi KAMIYA	Kazuki ISHIMARU
¹⁴ C	Yuichiro KUMAMOTO	Shu SAITO
<u>Underway</u>		
Meteorology	Hitomi KAMIYA	Tetsuya NAKAMURA

Thermo-Salinograph	Hitomi KAMIYA	Shu SAITO
$p\text{CO}_2$	Hitomi KAMIYA	Shu SAITO
Chlorophyll-a	Hitomi KAMIYA	Naoki NAGAI
ADCP	Hitomi KAMIYA	Tetsuya NAKAMURA
Bathymetry	Hitomi KAMIYA	Tatsuo NAKAMURA
<u>Floats</u>		
ARGO float	Toshio SUGA	Toshiya NAKANO

Hitomi KAMIYA (hkamiya@met.kishou.go.jp)

Marine Division, Global Environment and Marine Department, JMA

1-3-4, Otemachi, Chiyoda-ku, Tokyo 100-8122, JAPAN

Phone: +81-3-3212-8341 Ext. 5150 FAX: +81-3-3211-6908

Yuichiro KUMAMOTO (kumamoto@jamstec.go.jp)

Ocean Climate Change Research Program

Research Institute for Global Change (RIGC)

Japan Agency for Marine-Earth Science and Technology (JAMSTEC)

2-15 Natsushima, Yokosuka, Kanagawa, Japan 237-0061

Toshio SUGA (sugat@jamstec.go.jp)

Ocean Climate Change Research Program

Research Institute for Global Change (RIGC)

Japan Agency for Marine-Earth Science and Technology (JAMSTEC)

2-15 Natsushima, Yokosuka, Kanagawa, Japan 237-0061

4. Scientific Program and Methods

In recent years, the global environmental issues such as global warming and climate change have become one of the major socio-economic concerns, and it has become apparent that the ocean plays a key role in the climate system. For the better understanding and assessment of global environmental conditions, continuous monitoring of climate variables, concentrations of greenhouse gases both in the ocean and in the atmosphere. To meet those requirements, JMA has been conducting operational oceanographic observations by research vessels in the western North Pacific on a seasonal basis. RF11-06, RF11-07 and RF11-08 cruises are one of these activities. The purposes of this cruise are as follows:

- (1) To observe profiles of seawater temperature, salinity, dissolved oxygen, nutrients and carbon parameters, as well as upper ocean current;
- (2) To observe concentrations of greenhouse gases both in the ocean and in the atmosphere;
- (3) To observe bio-geochemical parameters to study carbon cycle in the ocean.

These activities are expected to contribute to international projects related to global environmental issues such as the World Climate Research Programme (WCRP), IOCCP (International Ocean Carbon Coordination Project) and the Global Atmosphere Watch (GAW).

5. Major Problems and Goals not Achieved

RF11-06

Since there was a lot of debris on the sea surface east of Japan after the Tohoku earthquake on March 11, 2011, we stopped to sail and drifted one night at about 38°40'N, 143°18'E on May 16. During the observation at Stn.7(42°N, 146°12'E), the armored cable hitched a radio buoy with fishing net, so we gave up the observation below 2000 m depth and water sampling at the station.

RF11-07

Owing to the troubles in CTD winch and the unfavorable sea state due to the storms, insufficient time was available to complete the section as planned, and station spacing increased to 60 nautical miles between 50°N and 43°N, and between 42°N and 40°N.

RF11-08

Because of the trouble in the previous cruise, RF11-07, the first station of this cruise was changed from 38°N to 40°N, and station spacing increased to 60 nautical miles between 40°N and 38°N, and between 33°N and 22°N.

6. List of Cruise Participants

The cruise participants of the three cruises are listed in Table 5.

Table 5(a). List of cruise participants for RF11-06.

Name	Responsibility	Affiliation
Ayumi HASHIZUME	CTDO / ADCP / LADCP / Salinity	GEMD / JMA
Hiroyuki HATAKEYAMA	Carbon Items/CFCs	GEMD / JMA
Yoshikazu HIGASHI	CTDO / ADCP / LADCP / Salinity	GEMD / JMA
Masaya IKEDA	Dissolved Oxygen	GEMD / JMA
Kazuki ISHIMARU	Carbon Items /CFCs	GEMD / JMA
Sonoki IWANO	Nutrients / Phytopigment	GEMD / JMA
Takahiro KITAGAWA	Nutrients	GEMD / JMA
Kiyoshi MURAKAMI	CTDO / ADCP / LADCP / Salinity	GEMD / JMA
Tatsuo NAKAMURA	Meteorology / Bathymetry	GEMD / JMA
Toshiya NAKANO	Chief Scientist	GEMD / JMA
Hidemi OGAHARA	Dissolved Oxygen	GEMD / JMA
Etsuro ONO	Carbon Items/CFCs	GEMD / JMA
Shu SAITO	Carbon Items/CFCs	GEMD / JMA
Ryosuke SAKAKIBARA	Nutrients	GEMD / JMA
Yusuke TAKATANI	Dissolved Oxygen	GEMD / JMA
Shinichiro UMEDA	Dissolved Oxygen / Phytopigment	GEMD / JMA
Koichi WADA	CTDO / ADCP / LADCP / Salinity	GEMD / JMA

GEMD / JMA: Marine Division, Global Environment and Marine Department, JMA

Table 5(b). List of cruise participants for RF11-07.

Name	Responsibility	Affiliation
Kazutaka ENYO	Carbon Items	GEMD / JMA
Hiroyuki FUJIWARA	Nutrients	GEMD / JMA
Sho HIBINO	Dissolved Oxygen	GEMD / JMA
Nobumi KATO	CTDO / ADCP / LADCP	GEMD / JMA
Tomoyuki KITAMURA	CTDO / ADCP / LADCP	GEMD / JMA
Atsushi KOJIMA	Salinity	GEMD / JMA
Shinji MASUDA	Carbon Items	GEMD / JMA
Kiyoshi MURAKAMI	CTDO / ADCP / LADCP	GEMD / JMA
Tetsuya NAKAMURA	Meteorology / Bathymetry	GEMD / JMA
Naoki NAGAI	Nutrients / Phytopigment	GEMD / JMA
Toshiya NAKANO	Chief Scientist	GEMD / JMA
Ryosuke SAKAKIBARA	Dissolved Oxygen	GEMD / JMA
Naoaki SAKAMOTO	CFCs	GEMD / JMA
Daisuke SASANO	Carbon Items	MRI / JMA
Hiroumi SHIGEOKA	Salinity	GEMD / JMA
Yoshihiro SHINODA	CFCs	GEMD / JMA
Takayuki TOKIEDA	CFCs	GEMD / JMA
Tomohiro UEHARA	Nutrients	GEMD / JMA
Shinichiro UMEDA	Dissolved Oxygen	GEMD / JMA
Koichi WADA	Salinity	GEMD / JMA

GEMD / JMA: Marine Division, Global Environment and Marine Department, JMA

MRI / JMA: Geochemical Research Department, Meteorological Research Institute, JMA

Table 5(c). List of cruise participants for RF11-08.

Name	Responsibility	Affiliation
Hiroyuki FUJIWARA	Nutrients	GEMD / JMA
Sho HIBINO	Dissolved Oxygen	GEMD / JMA
Kazuki ISHIMARU	CFCs	GEMD / JMA
Nobumi KATO	CTDO / ADCP / LADCP	GEMD / JMA
Takahiro KITAGAWA	Nutrients	GEMD / JMA
Tomoyuki KITAMURA	CTDO / ADCP / LADCP	GEMD / JMA
Atsushi KOJIMA	Salinity	GEMD / JMA
Shinya MAEDA	Carbon Items	GEMD / JMA
Shinji MASUDA	Carbon Items	GEMD / JMA
Tetsuya NAKAMURA	Meteorology / Bathymetry	GEMD / JMA
Naoki NAGAI	Nutrients / Phytopigment	GEMD / JMA
Toshiya NAKANO	Chief Scientist	GEMD / JMA
Hiroumi SHIGEOKA	Salinity	GEMD / JMA
Etsuro ONO	CFCs	GEMD / JMA
Hidemi OGAHARA	Dissolved Oxygen	GEMD / JMA
Shu SAITO	Carbon Items	GEMD / JMA
Haruka SUEMATSU	CFCs	GEMD / JMA
Yusuke TAKATANI	Dissolved Oxygen	GEMD / JMA
Masahiro TANIGUCHI	CTDO / ADCP / LADCP	GEMD / JMA
Koichi WADA	Salinity	GEMD / JMA

GEMD / JMA: Marine Division, Global Environment and Marine Department, JMA

C. Hydrographic Measurement Techniques and Calibration

1. CTD/O₂ Measurements

1 November 2019

(1) Personnel

RF 11-06

Kiyoshi MURAKAMI (GEMD/JMA)

Yoshikazu HIGASHI (GEMD/JMA)

Koichi WADA (GEMD/JMA)

Ayumi HASHIZUME (GEMD/JMA)

RF 11-07

Kiyoshi MURAKAMI (GEMD/JMA)

Nobumi KATO (GEMD/JMA)

Tomoyuki KITAMURA (GEMD/JMA)

RF 11-08

Nobumi KATO (GEMD/JMA)

Tomoyuki KITAMURA (GEMD/JMA)

Masahiro TANIGUCHI (GEMD/JMA)

(2) CTD Traction Winch and Motion Compensated Crane Arrangements

The CTD/O₂ system was deployed by using a Traction Winch System with ca. 7000m of 8.03 mm armored cable (Tyco Electronics, USA) and a Motion Compensated Crane (Dynacon, Inc., USA). The system was installed on the *R/V Ryofu Maru* in March, 2010 (Photo C1.1).



Photo C1.1. (Left) The Traction Winch and (right) Motion Compensated Crane.

(3) Overview of the CTD/O₂ system

The CTD/O₂ system, SBE 911plus system (Sea-Bird Electronics, Inc., USA), was used for entire cruise. The system is consisted of a SBE 9plus underwater unit and a SBE 11plus deck unit. The SBE 11plus deck unit is a rack-mountable interface which supplies DC power to under water unit, decodes serial data stream, formats data under microprocessor control, and passes the data to a computer. The real time serial data from the underwater unit is sent to the deck unit. The deck unit decodes the serial data and sends them to a personal computer to display and a storage in a file using SEASAVE data acquisition software (SEASAVE-Win32,

version 7.18).

The SBE 911plus system controls 36-position SBE 32 Carousel Water Sampler (Photo C1.2). The Carousel with a custom frame accepts 10-liter Niskin bottles (General Oceanics, Inc., USA). The SBE 9plus was mounted horizontally in the 36-position carousel frame. Two set of SBE's temperature (SBE 3plus) and conductivity (SBE 4C) sensor modules were used with the SBE 9plus underwater unit. Two modular units of underwater housing pump (SBE 5T) flush water through sensor tubing at a constant rate independent of the CTD's motion (Photo C1.3). Two dissolved oxygen sensors (RINKO III: JFE Advantech Co., Ltd., Japan; http://www.jfe-alec.co.jp/html/english_top.htm) were mounted on CTD housing, by the side of primary T/C sensors (Photo C.1.3). Auxiliary sensors, Deep Ocean Standards Thermometer (SBE 35) and an altimeter (PSA-916D: Teledyne Benthos, Inc., USA) were also used with the SBE 9plus underwater unit. The SBE 35 was mounted at the center of CTD between two pumps and the altimeter was mounted at the same height of pressure sensor of SBE 9plus.



Photo C1.2. (Left)The CTD/O₂ system top view and (right) bottom view.

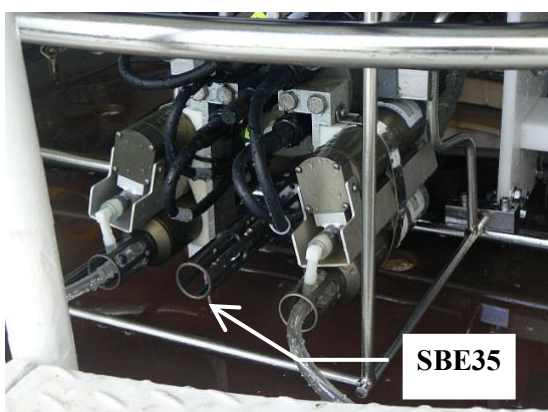


Photo C1.3. (Left) SBE 9plus CTD with SBE35 and (right) RINKO III.

Table C.1.1. Specification and serial number of the CTD/O2 measurements system components.

<i>Deck unit</i>	<i>Serial Number</i>				
SBE 11plus (SBE)	0648				
<i>Under water unit</i>	<i>Serial Number</i>	<i>Range</i>	<i>Accuracy</i>	<i>Stability</i>	<i>Resolution</i>
SBE 9plus (SBE)	31345(RF11-06/RF11-07)	0 to 10000	0.015 %(FS)	0.002%FS/year	0.001 % (FS)
	(Pressure:0722)	psi	1.0 dbar	0.2 dbar/year	0.1 dbar
	35560(RF11-08)	0 to 6800			
	(pressure:0764)	dbar			
<i>Temperature</i>	<i>Serial Number</i>	<i>Range</i>	<i>Accuracy</i>	<i>Stability</i>	<i>Resolution</i>
SBE 3plus (SBE)	5219(RF-11-06,primary)	-5 to 35 °C	0.001 °C	0.0002 °C /month	0.0002 °C
	4815(RF11-06,secondary)				
	5219(RF11-07,primary)				
	4923(RF11-07,secondary)				
	4923(RF11-08,primary)				
	4199(RF11-08,secondary)				
<i>Conductivity</i>	<i>Serial Number</i>	<i>Range</i>	<i>Accuracy</i>	<i>Stability</i>	<i>Resolution</i>
SBE 4C (SBE)	3697(RF11-06,primary)	0 to 7 S/m	0.0003 S/m	0.0003 S/m/month	0.00004 S/m
	2410(RF11-06,secondary)				
	2410(RF11-07,primary)				
	3670(RF11-07,secondary)				
	3670(RF11-08,primary)				
	2842(RF11-08,secondary)				
<i>Pump</i>	<i>Serial Number</i>				
SBE 5T (SBE)	5420(RF11-06,primary)				
	5418(RF11-06,secondary)				
	2778(RF11-07,primary)				
	5501(RF11-07,secondary)				
	5501(RF11-08,primary)				
	3887(RF11-08,secondary)				
<i>Oxygen</i>	<i>Serial Number</i>	<i>Range</i>	<i>Linearity</i>	<i>Response time</i>	<i>Resolution</i>
RINKO III (JFE)	25 (primary,	0 to 200%	±2% (FS)	≤ 1 second	0.01 to 0.04 %
	foil umber:150002A)	(saturation)			
	3 (secondary,				
	foil umner:150001A)				

Table C.1.1. (Continued)

<i>Water sampler</i>	<i>Serial Number</i>		
SBE 32 (SBE)	0734		
<i>Altimeter</i>	<i>Serial Number</i>	<i>Range</i>	<i>Resolution</i>
PSA-916D (TB)	43854	0 to 100 m	1 cm
<i>Water Sampling Bottle</i>			
Niskin Bottle (GO)	•10-Liter	•Bottle O-ring: Viton	
	•No TEFRON coating	•Stainless spring	
SBE: Sea-Bird Electronics Inc., USA		JFE: JFE Advantech Co., Ltd., Japan	
GO: General Oceanics, Inc., USA		TB: Teledyne Benthos, Inc., USA	

(4) Pre-cruise calibration

(4.1) Pressure

Pre-cruise calibration were performed at SBE, Inc., USA. The following coefficients were used in the SEASOFT:

S/N	0722	0764
calibration date	26 Jan 2011	27 Apr 2011
c ₁	−4.802766e+04	−4.318853e+04
c ₂	−2.656902e−01	−4.853949e−01
c ₃	1.418260e−02	1.294200e−02
d ₁	3.830200e−02	3.706500e−02
d ₂	0.000000e+00	0.000000e+00
t ₁	3.012930e+01	3.005385e+01
t ₂	−3.769891e−04	−4.407111e−04
t ₃	4.208190e−06	4.098190e−06
t ₄	1.503050e−09	1.662250e−09
t ₅	0.000000e+00	0.000000e+00

Pressure coefficients are first formulated into

$$c = c_1 + c_2 \times U + c_3 \times U^2$$

$$d = d_1 + d_2 \times U$$

$$t_0 = t_1 + t_2 \times U + t_3 \times U^2 + t_4 \times U^3 + t_5 \times U^4$$

where U is temperature in degrees Celsius. The pressure temperature, U, is determined according to

$$U(\text{degrees Celsius}) = M \times (12 \text{ bit pressure temperature compensation word}) - B$$

The following coefficients were used for in SEASOFT:

$$M = 1.289460e-02 (\text{for } S/N0722), 1.289080e-02 (\text{for } S/N0764)$$

$$B = -8.428240e+00 (\text{for } S/N0722), -8.282450e+00 (\text{for } S/N0764)$$

(in the underwater unit system configuration sheet dated on 26 Jan, 2011 and 27 Apr, 2011).

Finally, pressure is computed as

$$P(psi) = c \times (1 - t_0^2 / t^2) \times \{1 - d \times (1 - t_0^2 / t^2)\}$$

where t is pressure period (μ sec).

Since the pressure sensor measures the absolute value, it inherently includes atmospheric pressure (about 14.7 psi). SEASOFT subtracts 14.7 psi from computed pressure above automatically.

The pressure sensor drift is known to be primarily an offset drift at all pressures rather than a change of span slope. The following coefficients for the sensor drift correction were also used in SEASOFT:

$$\text{Slope} = 1.00001 (\text{for } S/N0722), 0.99993 (\text{for } S/N0764)$$

$$\text{Offset} = -1.5787 (\text{for } S/N0722), -0.6807 (\text{for } S/N0764)$$

The drift-corrected pressure is computed as

$$\text{Drift corrected pressure (dbar)} = \text{slope} \times (\text{computed pressure in dbar}) + \text{offset}$$

(4.2) Temperature (SBE 3plus)

Pre-cruise calibrations were performed at SBE, Inc., USA. The following coefficients were used in SEASOFT:

S/N	5219	4815	4923	4199
calibration date	20 Jan 2011	25 Jan 2011	21 Apr 2011	21 Apr 2011
g	4.35500121e-03	4.34772899e-03	4.35309957e-03	4.39448175e-03
h	6.36469896e-04	6.36030078e-04	6.39308306e-04	6.49614250e-04
i	2.17451382e-05	2.06037339e-05	2.12523653e-05	2.38816372e-05
j	1.94107546e-06	1.71635040e-06	1.79898659e-06	2.22252052e-06
f ₀	1000.000	1000.000	1000.000	1000.000

Temperature (ITS-90) is computed according to

$$\text{Temperature (ITS-90)} = \frac{1}{g + h \times \ln(f_0/f) + i \times \ln^2(f_0/f) + j \times \ln^3(f_0/f)} - 273.15$$

where f is the instrument frequency (Hz).

Time drift of the SBE 3plus temperature sensors based on the laboratory calibrations is shown in Figure C.1.1.

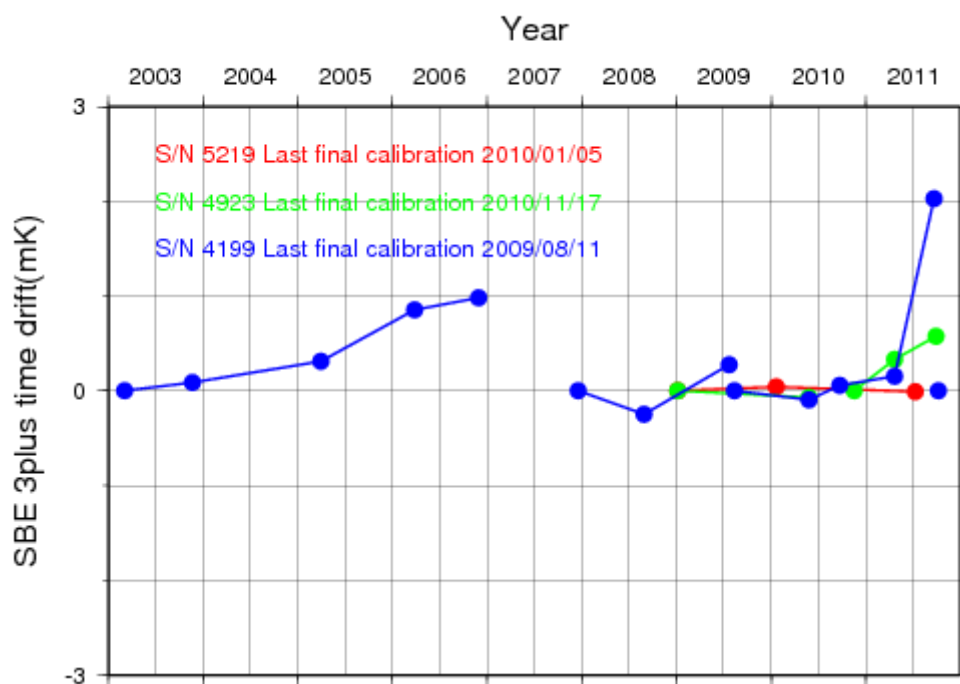


Figure C.1.1. Time drift of the SBE 3plus temperature sensors (S/N 5219, 4923, and 4199) based on laboratory calibrations performed by SBE, Inc. S/N4199 was resecured the temperature probe retaining nut in December 2007, and replaced the main piston O-rings in August 2009, and backfilled with Argon gas October 2011(after the cruise).

(4.3) Conductivity (SBE 4C)

Pre-cruise sensor calibrations were performed at SBE, Inc., USA. The following coefficients were used in SEASOFT:

S/N	3697	2410	3670	2842
calibration date	24 Feb 2011	21 Jan 2011	21 Apr 2011	27 Apr 2011
g	-1.01831055e+0 01	-9.96565291e+0 00	-1.01934873e+0 01	-1.01276306e+0 01
h	1.58514699e+00 0	1.49035343e+00 0	1.57437906e+00 0	1.38837664e+00 0
i	-5.06429589e-0 04	3.06771181e-004	-1.67445862e-0 03	4.89401834e-004
j	1.24905346e-00 4	7.00488899e-00 5	2.35407017e-00 4	3.44921338e-005
CP _{cor}	-9.57e-08	-9.57e-08	-9.57e-08	-9.57e-08
CT _{cor}	3.25e-06	3.25e-06	3.25e-06	3.25e-06

Conductivity of a fluid in the cell is expressed as:

$$C(S/m) = (g + h \times f^2 + i \times f^3 + j \times f^4) / \{10 \times (1 + CT_{cor} \times t + CP_{cor} \times p)\}$$

where f is the instrument frequency (kHz), t is the water temperature (degrees Celsius) and p is the water pressure (dbar).

(4.4) Deep Ocean Standards Thermometer (SBE 35)

In the first place a newly manufactured SBE 35 is first calibrated in a temperature controlled bath against Standard Platinum Resistance Thermometer, and this calibration is referred as the Linearization Calibration. In the next place SBE 35 is calibrated to generate slope and offset coefficients that correct for the time drift from the Linearization Calibration. This calibration is referred Fixed Point Calibrations. Pre-cruise sensor calibrations were performed at SBE, Inc., USA. The following coefficients were stored in EEPROM:

S/N 0069, 23 October, 2006(1st step: Linearization Calibration)

$$\begin{aligned}a_0 &= 4.96812728\text{e-}003 \\a_1 &= -1.39341438\text{e-}003 \\a_2 &= 2.06596098\text{e-}004 \\a_3 &= -1.14827915\text{e-}005 \\a_4 &= 2.44200422\text{e-}007\end{aligned}$$

Linearized temperature (ITS-90) is computed according to

$$\text{Linearized temperature(ITS-90)} = 1/\{a_0 + a_1 \times \ln(n) + a_2 \times \ln^2(n) + a_3 \times \ln^3(n) + a_4 \times \ln^4(n)\} - 273.15$$

where n is the instrument output. Then the SBE 35 is certified by measurements in thermodynamic fixed-point cells of the Triple Point of Water (TPW: 0.0100 degrees Celsius) and Gallium Melt Point (GaMP: 29.7646 degrees Celsius). The slow time drift of the SBE 35 is adjusted by periodic recertification corrections.

S/N 0069, 3 October, 2010 (2nd step: Fixed Point Calibration)

$$\text{Slope} = 1.000009$$

$$\text{Offset} = 0.000313$$

Temperature (ITS-90) is calibrated according to

$$\text{Temperature(ITS-90)} = \text{slope} \times (\text{Linearized temperature}) + \text{offset}$$

The time required per sample = 1.1 * NCYCLES + 2.7 seconds. The 1.1 seconds is total time per an acquisition cycle. NCYCLES is the number of acquisition cycles per sample. The 2.7 seconds is required for converting the measured values to temperature and storing average in EEPROM. In this cruise NCYCLES was set to 2.

(5) Data processing

(5.1) Data Collection

CTD system was powered on at least five minutes in advance of the operation and was powered off after CTD came up from the surface.

The package was lowered into the water from the port side and held about 10 m beneath the surface for about one minute in order to activate the pump. After the pump was activated, the package was lifted to the surface and lowered at a rate of 0.6 m/s approximately to 50m (or more when wave height was high), then the package was stopped to turn on the heave

compensator of the crane. The package was lowered again at a rate of 0.9 m/s to the bottom. For the up cast, the package was lifted at a rate of 0.9 m/s except for bottle firing stops. At each bottle firing stops, the bottle was fired after waiting for about 30 seconds and the package was stayed at least 10 seconds for measurement of the SBE 35 after firing. At 50 m from the surface, the package was stopped to turn off the heave compensator of the crane.

Water samples were collected using a 36-position SBE 32 Carousel Water Sampler with 10-liter Niskin bottles.

The SBE11plus deck unit received the data signal from the CTD. Digitized data were forwarded to a personal computer running the SEASAVE data acquisition software (*SEASAVE-Win32, version 7.18*). Temperature, conductivity, salinity, oxygen and descent/ascent rate profiles were displayed in real-time with the package depth, altimeter reading and sound speed. Differences in temperature, salinity, and oxygen between primary and secondary sensor were also displayed in order to monitor the status of sensors. Note that oxygen data were displayed and monitored in voltage (0–5V).

Altimeter (PSA-916D) was mounted at the same height of pressure sensor of SBE 9plus (Photo C1.4). The altimeter detected the sea floor at 136 of 151 stations, the average distance of beginning detecting the sea floor was 33.4m, and that of final detection of sea floor was 13.8m. The summary of detection of PSA-916D was shown in Figure C.1.2.

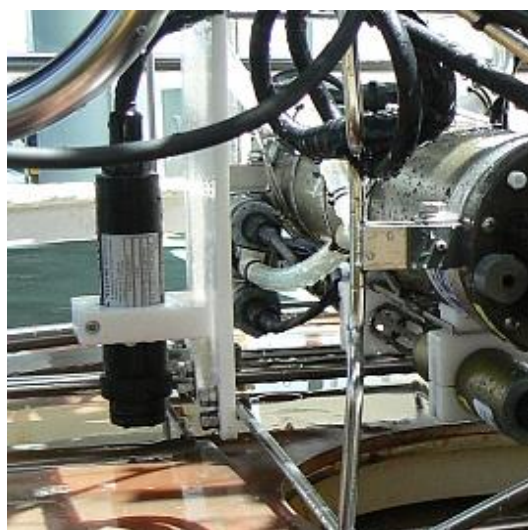


Photo C.1.4. The location of PSA-916D.

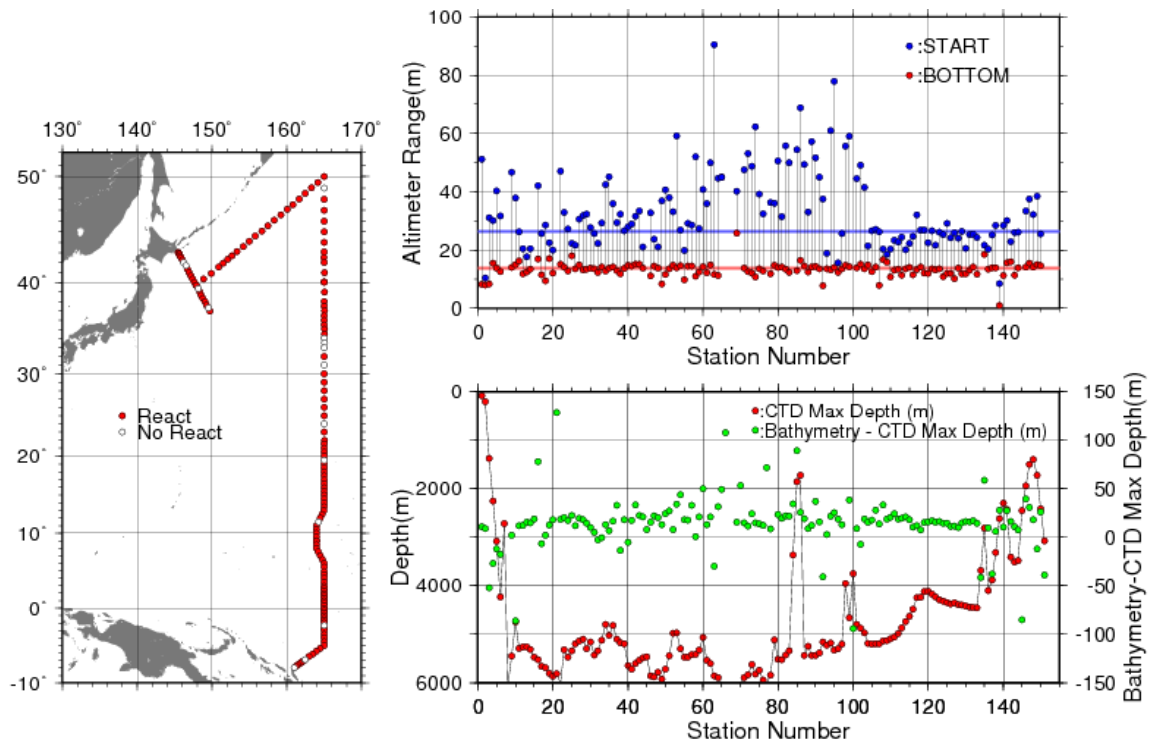


Figure C.1.2. The summary of detection of PSA-916D. The left panel shows the stations of detection, the right panels shows the relationship among PSA-916D, bathymetry and CTD depth.

(5.2) Data Processing

SEASOFT (*SEASOFT-Win32, version 7.18*) consists of modular menu driven routines for acquisition, display, processing, and archiving of oceanographic data acquired with SBE equipment, and is designed to work with a personal computer. Raw data are acquired from instruments and are stored as unmodified data. The conversion module **DATCNV** uses instrument configuration and calibration coefficients to create a converted engineering unit data file that is operated on by all SEASOFT post processing modules.

Each SEASOFT module that modifies the converted data file adds proper information to the header of the converted file permitting tracking of how the various oceanographic parameters were obtained. The converted data is stored in rows and columns of ASCII numbers. The last data column is a flag field used to mark scans as good or bad.

We made the original module for the process of RINKO III and JMA's report. The following are the SEASOFT data processing module and JMA original module sequence and specifications used in the reduction of CTD data in this cruise.

DATCNV converted the raw data to engineering unit data such as scan number, pressure, temperatures, conductivities, RINKO III voltages, time in Julian days, pump status, and flag. **DATCNV** also extracted bottle information where scans were marked with the bottle confirm bit during acquisition. The duration was set to 2.0 seconds, and the offset was set to 0.0

seconds.

DECKP_OFF (original module) cancelled the deck pressure and after this module, spikes in temperature and salinity were eliminated manually.

RINKO_hystoff (original module) cancelled the hysteresis of RINKO III using the method of SBE 43 (Sea-Bird Electronics, 2009) .

SECT_IN (original module) found the first and last scan numbers while pump was activated, and made the surface data while pump was not activated for down cast.

SECTION selected a time span of data based on scan number in order to reduce a file size. The minimum number was set to be the start time when the CTD package was beneath the sea-surface after activation of the pump. The maximum number was set to be the end time when the package came up from the surface.

FILTER performed a low pass filter on pressure with a time constant of 0.15 seconds. In order to produce zero phase lag (no time shift) the filter runs forward first then backwards.

ALIGNCTD converted the time-sequence of RINKO III sensor outputs into the pressure sequence to ensure that all calculations were made using measurements from the same parcel of water. RINKO III sensor output delays 1 second compared to pressure, temperature and conductivity.

ALIGNROS (original module) replace the RINKO III output of the bottle to that of all scan data applied **ALIGNCTD** module.

BOTTOLESUM created a summary of the bottle data. The bottle position, date, time were output as the first two columns. Salinities, pressure, temperatures, conductivities and oxygen voltage were averaged over 2.0 seconds.

CELLTM used a recursive filter to remove conductivity cell thermal mass effects from the measured conductivity. Typical values used were thermal anomaly amplitude $\alpha = 0.03$ and the time constant $1/\beta = 7.0$.

LOOPEDIT marked scans where the CTD was moving less than the minimum velocity of 0.0 m/s (traveling backwards due to ship roll).

BINAVG averaged the data into 1dbar pressure bins. The center value of the first bin was set equal to the bin size. The bin minimum and maximum values are the center value plus and minus half the bin size. Scans with pressures greater than the minimum and less than or equal to the maximum were averaged. Scans were interpolated so that a data record could exist in every dbar.

RSC2ASC (original module) made the data set from 1dbar to the bottom of observation. The RINKO III processes (original module) to make down and up cast data in every dbar were performed after those processes.

(6) Post-cruise calibration

(6.1) Pressure

The CTD pressure sensor offset in the period of this cruise is estimated from the pressure readings on the ship deck. In order to get the calibration data for the pre-cast pressure sensor drift, the CTD deck pressure was averaged over five scan pressure data after the CTD system had been stable on the deck.

Deck pressure was used to cancel the CTD pressure sensor offset in CTD data processing. Time series of the CTD deck pressure is shown in Figure C.1.3. Tendencies of CTD deck pressure and air pressure were almost similar during the cruise.

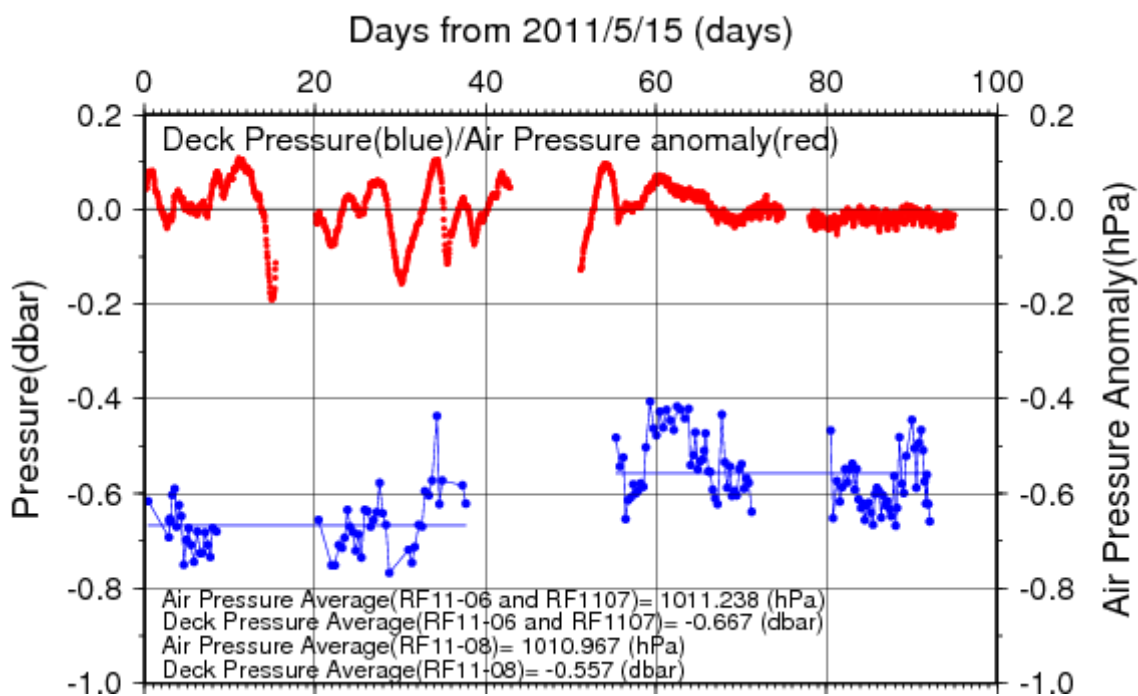


Figure C.1.3. Time series of the CTD deck pressure. Red line indicates atmospheric pressure anomaly. Blue line and dots indicate pre-cast deck pressure and average.

Post-cruise sensor calibrations were performed at SBE, Inc., USA. The pressure sensor drift is known to be primarily an offset drift at all pressures rather than a change of span slope.

S/N 0722, 15 July 2011

Slope = 1.00002(S/N 0722)

Offset = -1.54880(S/N 0722)

S/N 0764, 09 Feb. 2012

$$\text{Slope} = 0.99994(\text{S/N } 0764)$$

$$\text{Offset} = -0.6681(\text{S/N } 0764)$$

The pressure sensor drift was estimated to be 0.09 dbar for S/N 0722 and 0.07 dbar for S/N 0764 at the pressure of 6000 dbar, respectively. The pressure sensor drift was small, so post-cruise calibration is not applied.

(6.2) Temperature

Budeus and Schneider (1998) noted that the CTD temperature sensor (SBE 3plus) showed a pressure sensitivity. The pressure sensitivity for a SBE 3plus sensor is usually less than +2 mK/6000 dbar. It is somewhat difficult to measure this effect in the laboratory and the difficulty is one of the primary reasons to use the SBE 35 at sea for critical work. Also SBE 3plus measurements may be affected by viscous heating (about +0.5 mK) that occurs in a TC duct and does not occur for un-pumped SBE 35 measurements (*Larson and Pederson*, 1996). Furthermore, the SBE 35 calibrations have some uncertainty (about 0.2 mK) and SBE 3plus calibrations have some uncertainty (about 1 mK). So the practical corrections for CTD temperature data can be made by using a SBE 35, correcting the SBE 3plus to agree with the SBE 35 (*Uchida et al.*, 2007).

Post-cruise sensor calibration for the SBE 35 was performed at SBE, Inc., USA.

S/N 0069, 30 September 2011 (2nd step: fixed point calibration)

$$\text{Slope}=1.000003$$

$$\text{Offset}=0.000373$$

The discrepancy between the CTD temperature and the SBE 35 temperature is considered to be a function of pressure and time. But the time drift correction is regarded as 0 due to following reasons; 1) The time drift of the SBE 3plus estimated to be as +0.00007 K/year for S/N 5219, -0.00030 K/year for S/N 4815, -0.00046 K/year for S/N 4923, -0.00430 K/year for S/N 4199 and that of SBE 35 is estimated to be as -0.05 mK during the cruise according to pre-cruise and post-cruise calibrations performed at SBE, 2).

Effect of the viscous heating is assumed to be constant. Since the pressure sensitivity is thought to be constant in time at least during observation period, the CTD temperature is calibrated as

$$\text{Calibrated temperature} = T - (c_0 + c_1 \times P + c_2 \times P^2)$$

where T is the CTD temperature in degrees Celsius, P is pressure in dbar and c_0 , c_1 , c_2 are calibration coefficients.

The calibration is performed for the primary and secondary temperature data. The CTD data created by the software module **BOTTLESUM** are used. (The deviation of CTD temperature from the SBE35 temperature at depth shallower than 1900 dbar is large for determining the coefficients with sufficient accuracy since the vertical temperature gradient is too large in the regions. So the coefficients are determined by least squares method using the data for the depth deeper than 1900 dbar.) The temperature calibration summary is listed in Table C.1.2

at Pressure ≥ 1900 dbar. We adopted secondary conductivity sensor (S/N 2410) RF11-06, so secondary temperature sensor (S/N 4815) is adopted. Except for RF11-06, we adopted primary temperature sensors.

Table C.1.2. Temperature Calibration summary (Pressure ≥ 1900 dbar).

S/N	Num	c_0 (K)	c_1 (K/dbar)	c_2 (K/dbar ²)	Average (K)	STD (K)	Note
5219	769	1.6194e-3	1.7735e-6	-6.4124e-11	0.0000	0.0002	RF11-06 and RF11-07
4815	247	7.8152e-4	3.0001e-7	0.0000	0.0000	0.0002	RF11-06
4923	522	-1.4564e-3	-1.6687e-7	0.0000	-0.0001	0.0001	RF11-07
4923	1239	1.3089e-3	1.3026e-7	0.0000	0.0000	0.0003	RF11-08
4199	1239	-2.0724e-4	1.4673e-7	-6.4823e-11	0.0000	0.0003	RF11-08

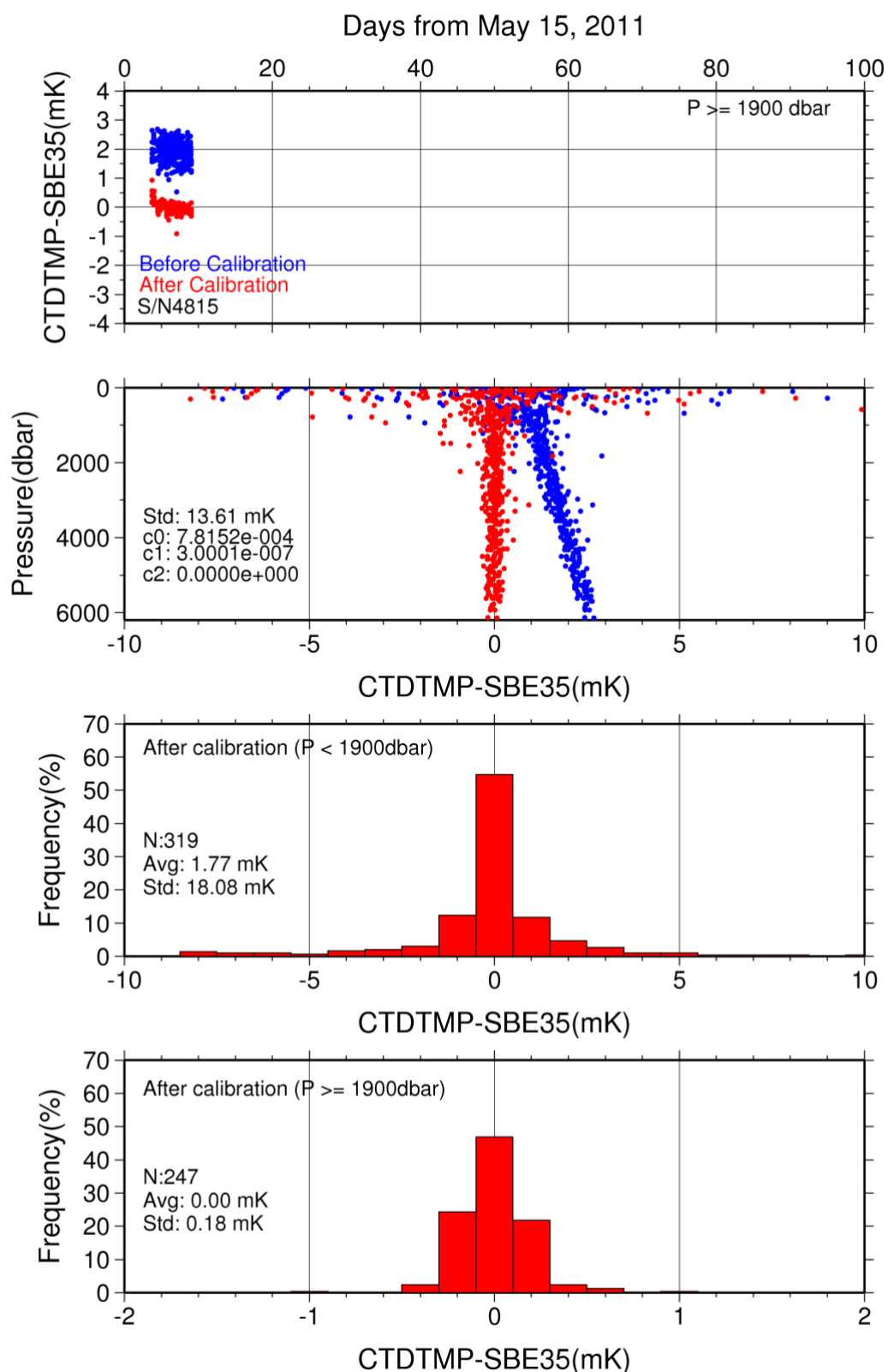


Figure C.1.4. Difference between the CTD temperature (secondary) and the Deep Ocean Standards thermometer (SBE35) at RF11-06. Blue and red dots indicate before and after the calibration using SBE35 data respectively. Lower two panels show histogram of the difference after calibration.

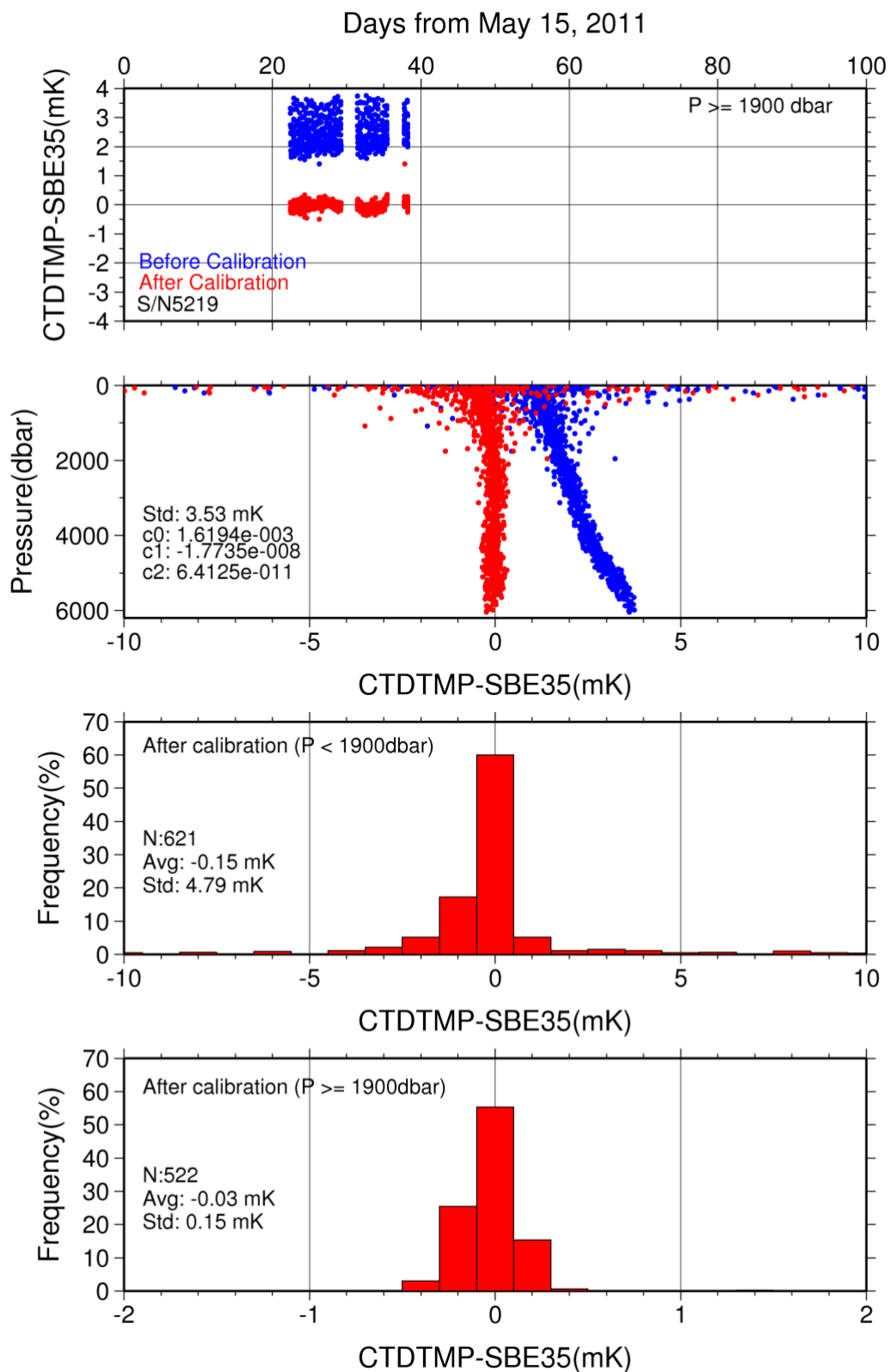


Figure C.1.5. Difference between the CTD temperature (primary) and the Deep Ocean Standards thermometer (SBE35) at RF11-07. Blue and red dots indicate before and after the calibration using SBE35 data respectively. Lower two panels show histogram of the difference after calibration.

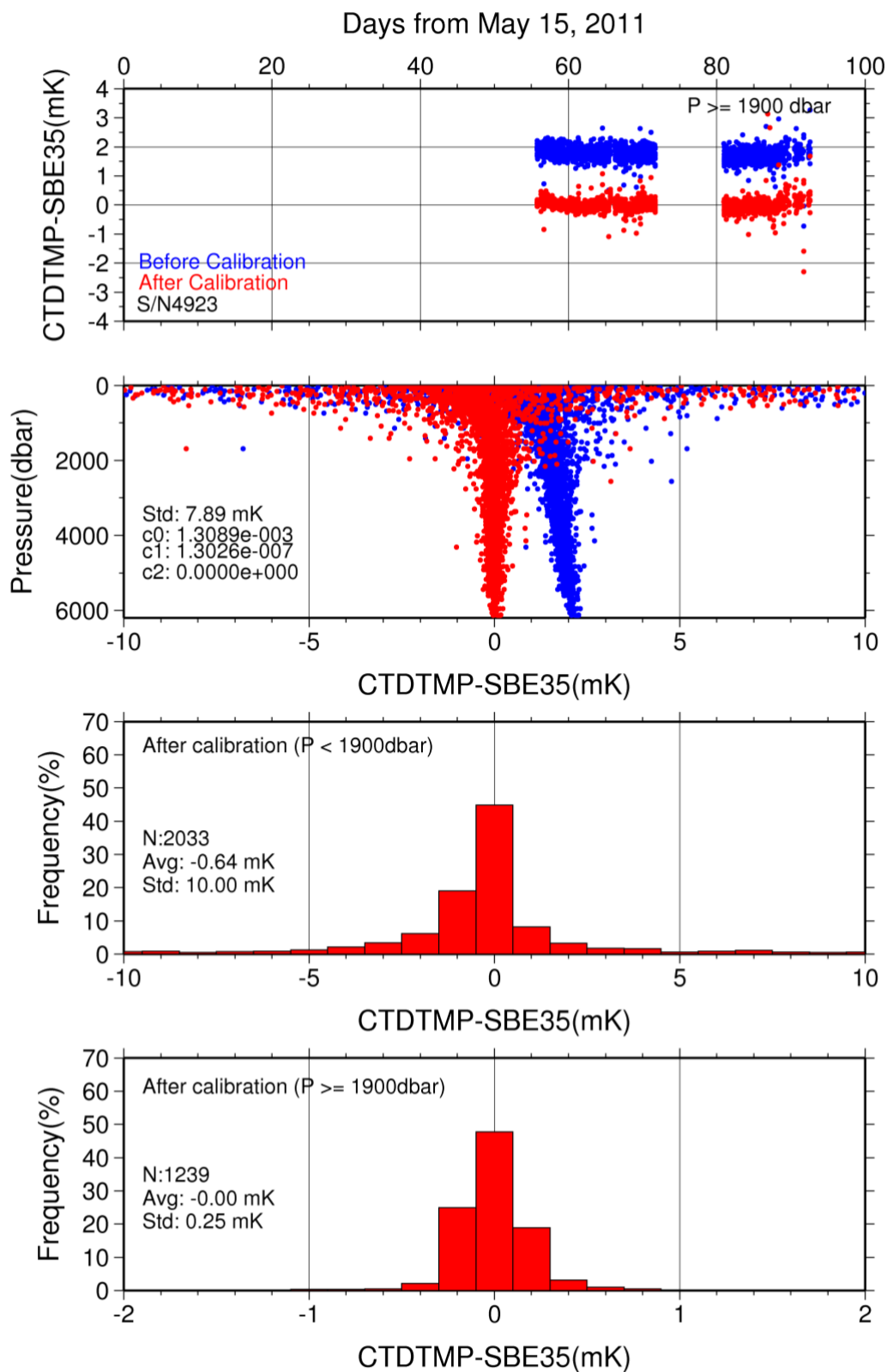


Figure C.1.5. Difference between the CTD temperature (primary) and the Deep Ocean Standards thermometer (SBE35) at RF11-08. Blue and red dots indicate before and after the calibration using SBE35 data respectively. Lower two panels show histogram of the difference after calibration.

(6.3) Salinity

The CTD salinity is computed from pressure, conductivity and temperature according to algorithm of the Practical Salinity Scale of 1978 (PSS78). The discrepancy between the CTD conductivity and the bottle conductivity is considered to be a function of pressure and time according to *McTaggart et al.* (2010).

Post-cruise sensor calibrations were performed in September 2010 at SBE, Inc., USA. According to the conductivity calibration report, the drifts since pre-cruise calibration was -0.00090 /month in PSS78 at 3.0 S/m for primary sensor (S/N3670), so the effect of SBE 4C drift during the cruise was estimated to be less than 0.002 in PSS78. However the time coefficient was set to zero in this cruise because the calibration was performed considering the sudden station-dependent shifts of the CTD conductivity and other calibration coefficients included the effect of slow drift by calibration grouping. So the CTD conductivity is calibrated as below.

$$\text{Calibrated Conductivity} = C - \left(\sum_{i=0}^I c_i \times C^i + \sum_{j=1}^J p_j \times P^j \right)$$

where C is the CTD conductivity and c_i and p_j are calibration coefficients. Coefficient sets of each (I, J) combination was calculated by least square method between CTD conductivity and the bottle conductivity data except for bad bottle data. In calculated coefficient sets, the best (I, J) combination are determined by referring to AIC (*Akaike*, 1974). According to *McTaggart et al.* (2010), maximum of I and J are 2.

The discrepancy between the calibrated CTD conductivity and the bottle conductivity was within 0.0001 S/m for each sensor. The results of post-cruise calibration for the CTD salinity (S/N2410, 3670) are summarized in Figure C.1.6. The calibration coefficients and the data (Num) used for the calibration are listed in Table C.1.3, and the calibration summary are listed in Tables C.1.4 and C.1.5 for S/N 2410 and S/N3670, respectively. We adopted secondary sensor (S/N 2410) RF11-06 because of spike noise in deep layers of primary sensor (S/N 3697). Except for RF11-06, we adopted primary conductivity sensors.

Table C.1.3. Conductivity Calibration Coefficient Summary.

S/N	Num	$c_0(\text{mS/m})$	c_1	$c_2(\text{mS/m})$	$c_3(\text{mS/m})$	Stations
			$p_1(\text{mS/dbar})$	$p_2(\text{mS/m/dbar}^2)$	$p_3(\text{mS/m/dbar}^3)$	
2410	327	$1.8207\text{e-}4$	$9.9995\text{e-}1$	$0.0000\text{e+}0$	$0.0000\text{e+}0$	RF3984
			$-1.6572\text{e-}7$	$1.8620\text{e-}11$	$0.0000\text{e+}0$	-4005
2410	526	$2.5007\text{e-}2$	$9.8494\text{e-}1$	$2.2560\text{e-}3$	$0.0000\text{e+}0$	RF4007
			$-1.2318\text{e-}7$	$1.7698\text{e-}11$	$0.0000\text{e+}0$	-4023
2410	462	$1.1992\text{e-}1$	$8.9902\text{e-}1$	$2.8126\text{e-}2$	$-2.5890\text{e-}3$	RF4024
			$-1.1879\text{e-}7$	$1.3827\text{e-}11$	$0.0000\text{e+}0$	-4039
3670	1109	$5.9325\text{e-}4$	$9.9988\text{e-}1$	$0.0000\text{e+}0$	$0.0000\text{e+}0$	RF4040
			$-7.4659\text{e-}8$	$9.8694\text{e-}12$	$0.0000\text{e+}0$	-4089
3670	1117	$6.7019\text{e-}4$	$9.9984\text{e-}1$	$0.0000\text{e+}0$	$0.0000\text{e+}0$	RF4090
			$-6.0476\text{e-}8$	$6.2312\text{e-}12$	$0.0000\text{e+}0$	-4135

Table C.1.4. Conductivity Calibration Summary for S/N 2410.

Stations	Pressure < 1900dbar			Pressure \geq 1900 dbar		
	Num	Average (mS/cm)	Std (mS/cm)	Num	Average (mS/cm)	Std (mS/cm)
RF3984-4005	156	0.0000	0.0002	171	0.0000	0.0001
RF4007-4023	292	0.0000	0.0002	234	0.0000	0.0000
RF4024-4039	240	0.0000	0.0002	222	0.0000	0.0001

Table C.1.5. Conductivity Calibration Summary for S/N 3670.

Stations	Pressure < 1900dbar			Pressure \geq 1900 dbar		
	Num	Average (mS/cm)	Std (mS/cm)	Num	Average (mS/cm)	Std (mS/cm)
RF4040-4089	592	0.0000	0.0002	517	0.0000	0.0001
RF4090-4135	740	0.0000	0.0002	377	0.0000	0.0001

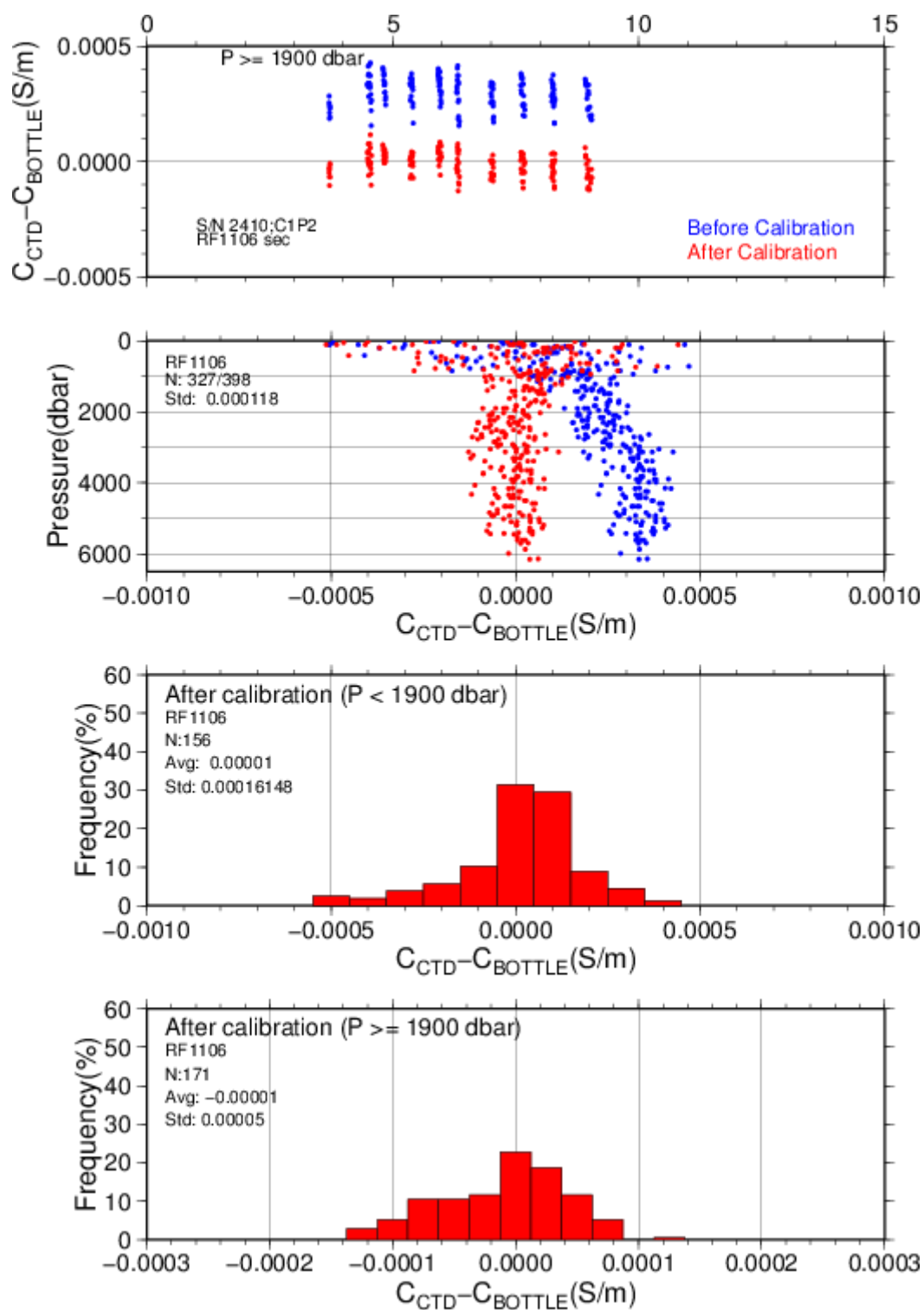


Figure C.1.6-1. Difference between the CTD conductivity and the bottle conductivity at RF11-06. Blue and red dots indicate before and after the calibration using bottle data respectively. Lower two panels show histogram of the difference after calibration.

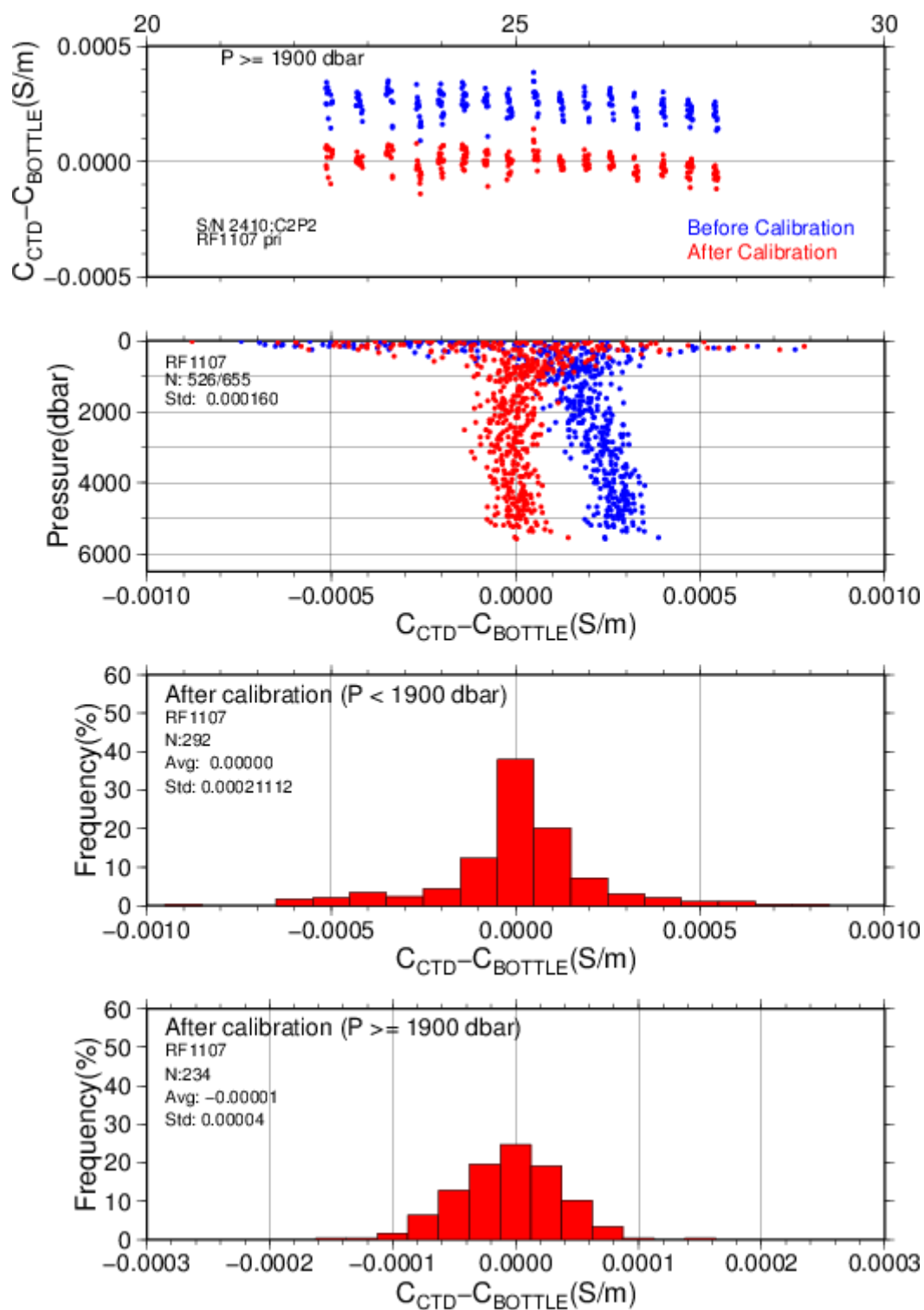


Figure C.1.6-2 Same as Fig. C.1.6-1. But at before half of RF11-07 (using Autosal salinometer S/N 69677).

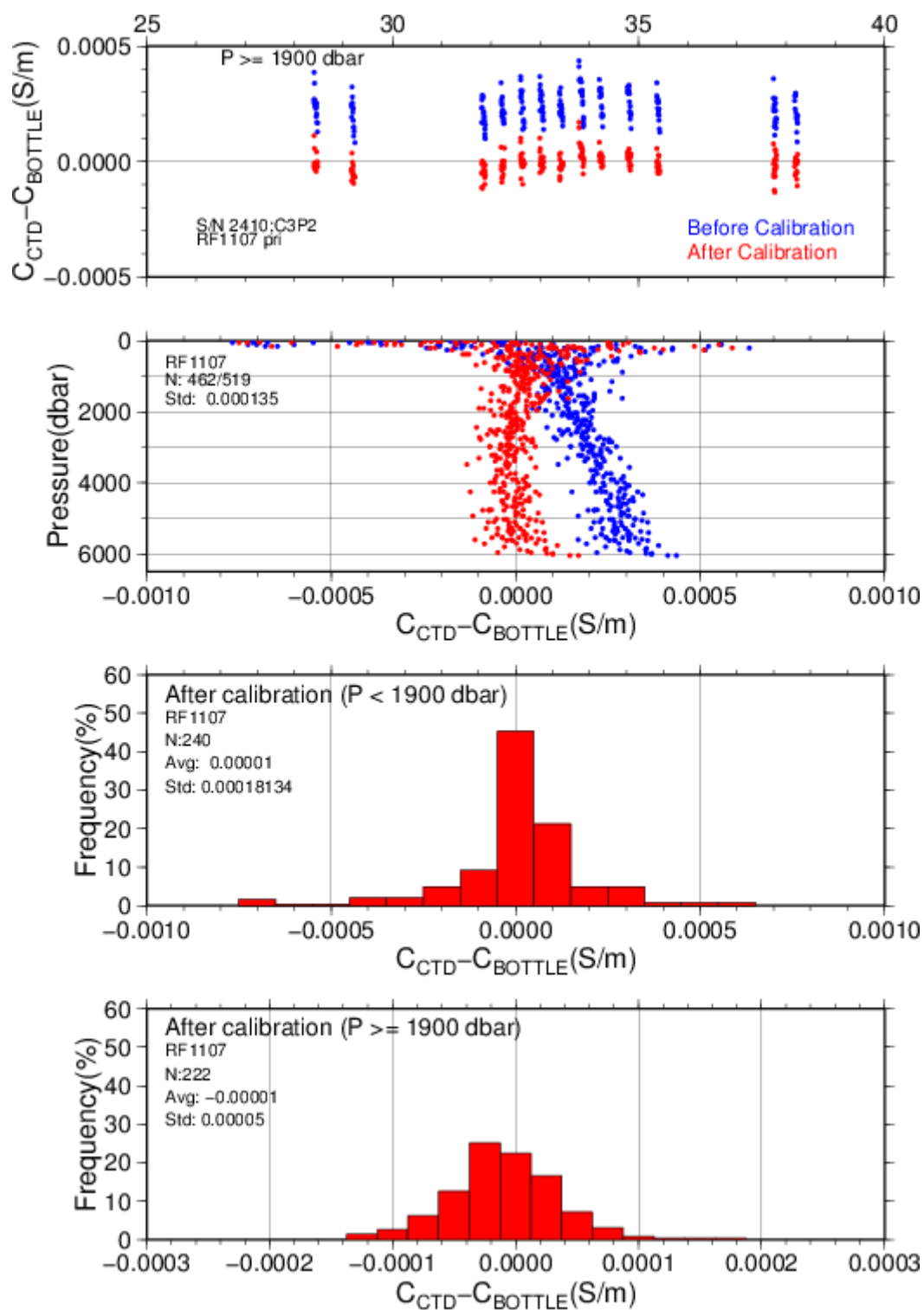


Figure C.1.6-3 Same as Fig. C.1.6-1. But at after half of RF11-07 (using Autosal salinometer S/N 66286).

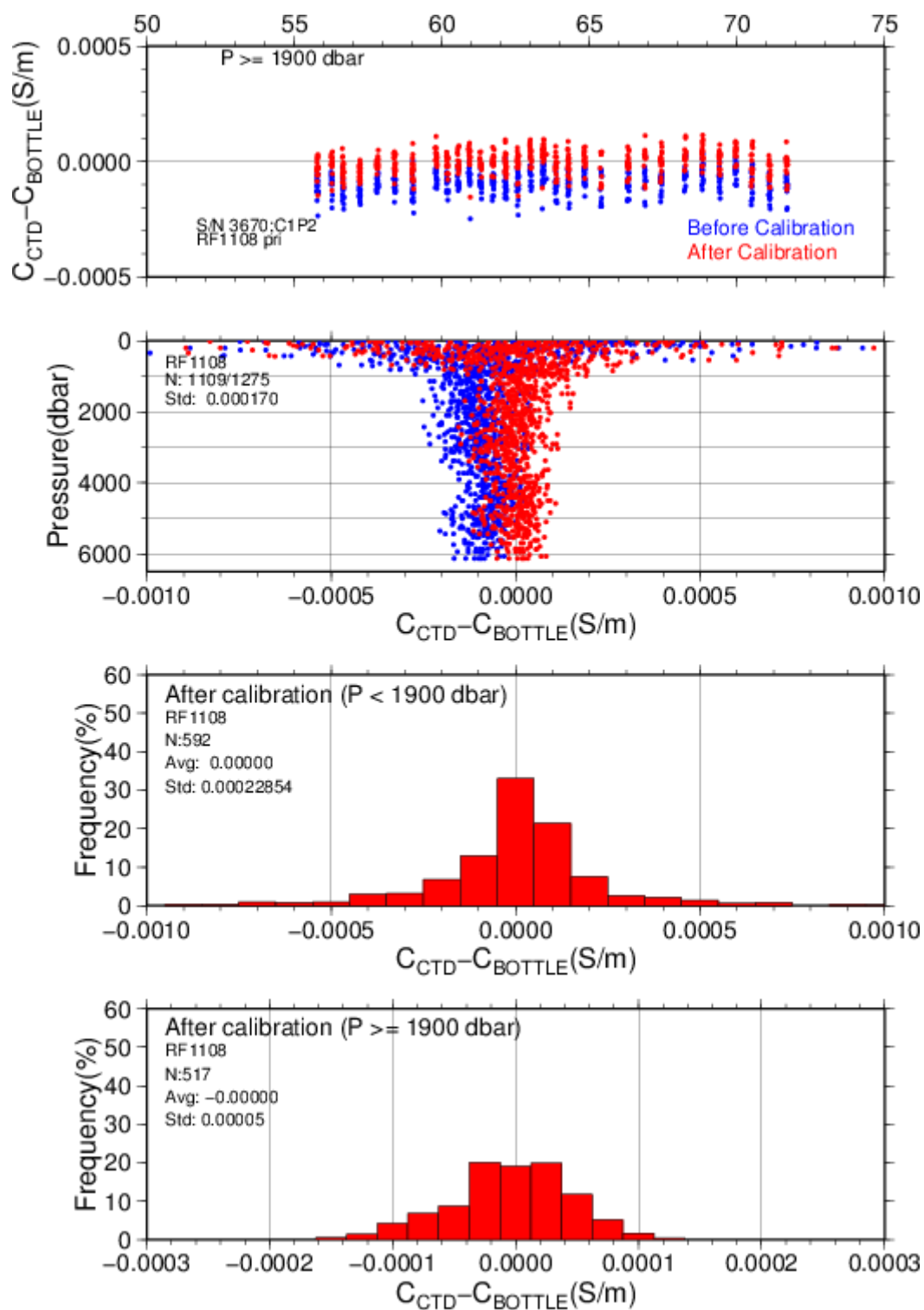


Figure C.1.6-4 Same as Fig. C.1.6-1. But at RF11-08 1Leg.

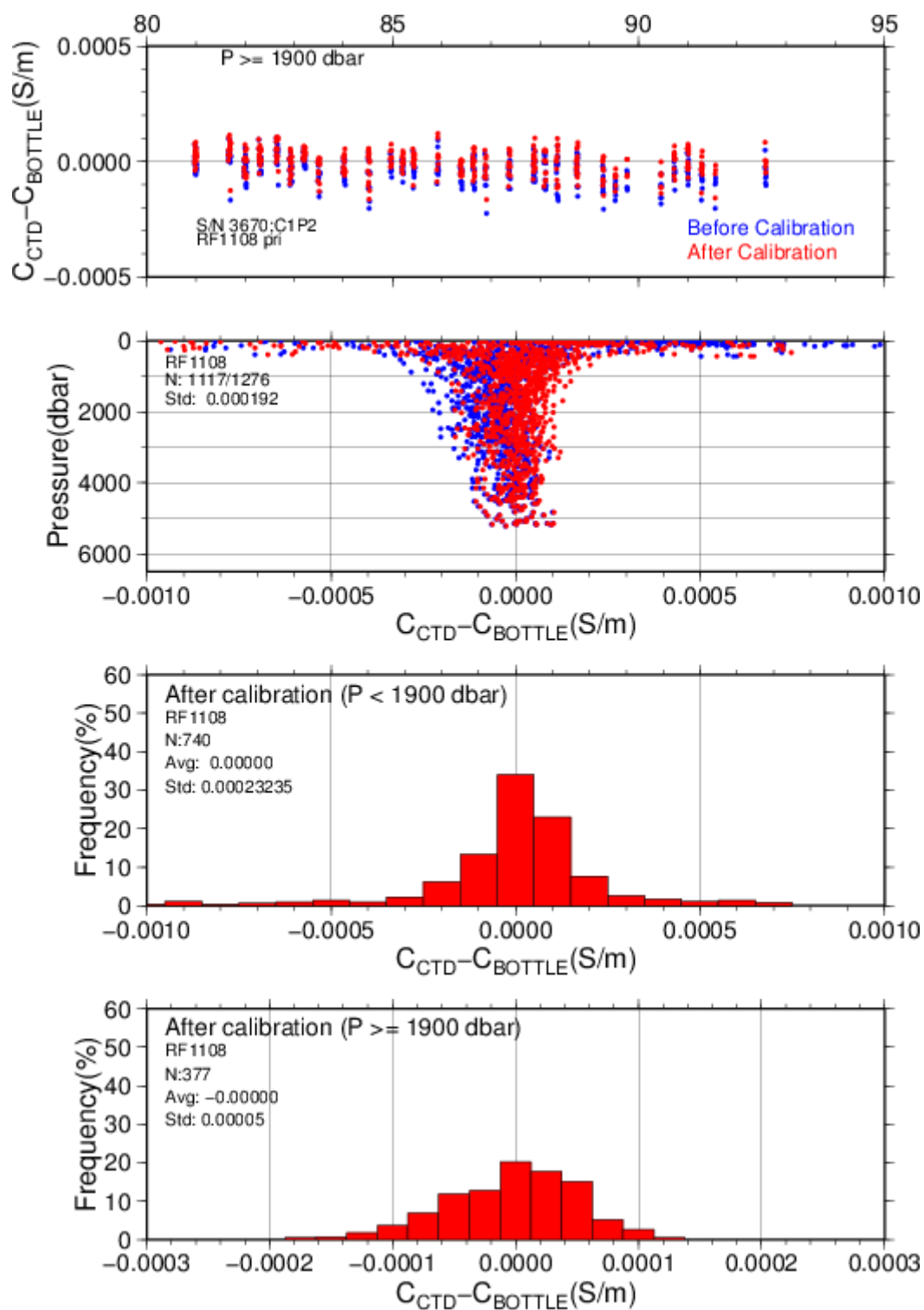


Figure C.1.6-5 Same as Fig. C.1.6-1. But at RF11-08 2Leg.

(6.4) Oxygen

RINKO III (JFE Advantech Co., Ltd., Japan) is based on the ability of selected substance to act as dynamic fluorescence quenchers. RINKO III model is designed to use with a CTD system which accept an auxiliary analog sensor, and is designed to operate down to 7000 m. The CTD oxygen is calculated using RINKO III output (voltage) by the Stern-Volmer equation, according to a method by *Uchida et al.* (2008). The formulas are as follows:

$$P_0 = 1.0 + c_4 \times t$$

$$P_c = c_5 + c_6 \times v + c_7 \times T + c_8 \times T \times v$$

$$K_{sv} = c_1 + c_2 \times t + c_3 \times t^2$$

$$coef = (1.0 + c_9 \times P/1000)^{1/3}$$

$$[O_2] = \{(P_0 / P_c - 1.0) / K_{sv} \times coef\}$$

Where ***P*** is the pressure in dbar, ***t*** is the potential temperature, ***v*** is RINKO output voltage in volt, ***T*** is elapsed time of the sensor from the beginning of first station in calculation group in day and ***[O₂]*** is the dissolved oxygen saturation, dissolved oxygen is calculated from ***[O₂]***, ***potential temperature*** and ***salinity*** by *Garcia and Gordon* (1992) in μmol/kg. Calibration coefficients (***c₁–c₉***) are determined by minimizing the sum of absolute deviation with weight between CTD oxygen and bottle dissolved oxygen by quasi-newton method (*Shanno*, 1970). The weight was given as a function of pressure as :

$$\text{Weight} = \min[10, \exp\{\log(10) \times P/PR\}]$$

Where PR is threshold of the pressure (950dbar). This function is similar to *Uchida et al.* (2009) .In general, the calibration was performed for each Leg. Calibration coefficients are listed in Table C.1.6. The data summary is listed in Tables C.1.7 and C.1.8. We adopted primary sensor (S/N 025).

Table C.1.6. Dissolved Oxygen Calibration Coefficients Summary.

S/N	Stations	c ₁	c ₂	c ₃	c ₄	c ₅
		c ₆	c ₇	c ₈	c ₉	
025	RF3984–4005	1.68490	1.89371e–2	3.53537e–4	–1.52601e–3	–7.44388e–2
		2.99657e–1	–1.19918e–5	1.58654e–3	7.84063e–2	
025	RF4007–4039	1.69390	1.57929e–2	4.68976e–4	–2.49529e–3	–7.74877e–2
		3.06369e–1	–3.47191e–4	1.27465e–3	7.74917e–2	
025	RF4040–4089	1.69392	2.73785e–2	1.56298e–4	6.33790e–6	–7.68831e–2
		3.14086e–1	3.16921e–4	8.01871e–4	8.14669e–2	
025	RF4090–4135	1.64771	2.21551e–2	4.10892e–5	–1.00585e–3	–5.12331e–2

		$3.13087\text{e-}1$	-8.48546e- 5	$7.32350\text{e-}4$	$8.76030\text{e-}2$	
--	--	---------------------	--------------------------	---------------------	---------------------	--

Table C.1.6. (Continued)

S/N	Stations	c ₁	c ₂	c ₃	c ₄	c ₅
		c ₆	c ₇	c ₈	c ₉	
003	RF3984–4005	1.69730	2.24366e–2	3.51487e–4	–7.05213e–4	–8.45472e–2
		3.13506e–1	6.39698e–5	1.36512e–3	7.56368e–2	
003	RF4007–4039	1.70196	1.76936e–2	4.88653e–4	–1.87179e–3	–8.55821e–2
		3.18589e–1	–3.48760e–4	1.10083e–3	7.61634e–2	
003	RF4040–4089	1.69444	2.85727e–2	1.77568e–4	2.81331e–4	–8.64729e–2
		3.24891e–1	1.81317e–4	6.51621e–4	7.93843e–2	
003	RF4090–4135	1.63809	2.39508e–2	3.97281e–5	–6.77574e–4	–6.06154e–2
		3.22285e–1	–1.59634e–4	5.99810e–4	8.44855e–2	

Table C.1.7. Dissolved Oxygen Calibration Summary for primary sensor.

Stations	Pressure < 950dbar			Pressure ≥ 950dbar		
	Num	Average of deviation (μmol/kg)	STD of deviation (μmol/kg)	Num	Average of deviation (μmol/kg)	STD of deviation (μmol/kg)
RF3984 – 4005	158	0.06	1.38	216	0.00	0.31
RF4007 – 4039	404	0.06	1.31	603	–0.01	0.43
RF4040 – 4089	448	–0.01	1.01	661	0.00	0.30
RF4090 – 4135	584	0.03	0.94	534	–0.01	0.30

Table C.1.8. Dissolved Oxygen Calibration Summary for secondary sensor.

Stations	Num	Average of deviation (μmol/kg)	STD of deviation (μmol/kg)	Num	Average of deviation (μmol/kg)	STD of deviation (μmol/kg)
RF3984 – 4005	158	0.05	1.35	216	0.00	0.33
RF4007 – 4039	404	0.06	1.29	603	–0.01	0.42
RF4040 – 4089	448	–0.01	1.02	661	–0.00	0.31
RF4090 – 4135	584	0.04	0.91	534	0.01	0.30

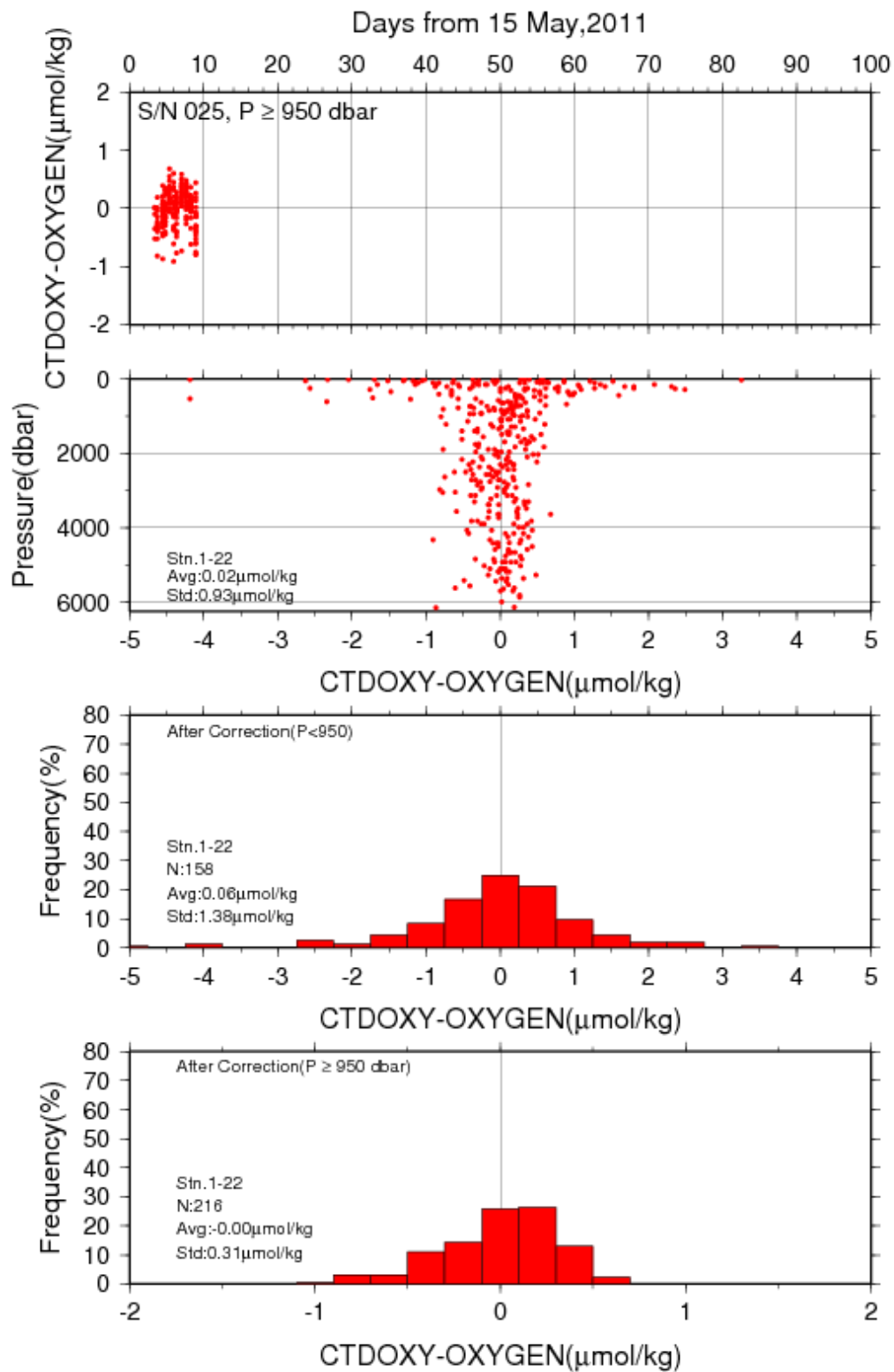


Figure C.1.7. Difference between the CTD oxygen and bottle dissolved oxygen in RF11-06. Red dots in upper two panels indicate the result of calibration. Lower two panels show histogram of the difference between calibrated oxygen and bottle oxygen.

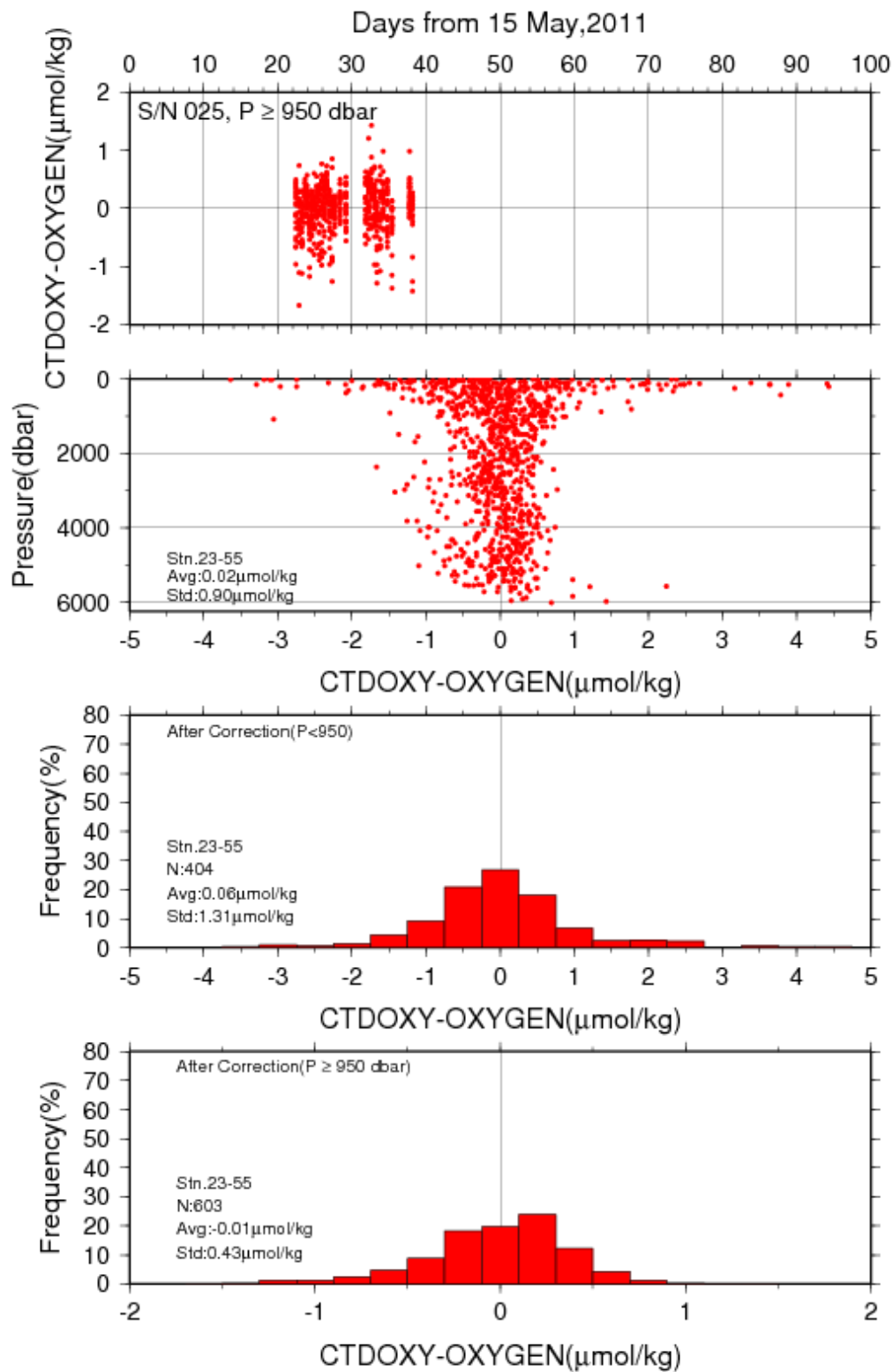


Figure C.1.8. Difference between the CTD oxygen and bottle dissolved oxygen in RF11-07. Red dots in upper two panels indicate the result of calibration. Lower two panels show histogram of the difference between calibrated oxygen and bottle oxygen.

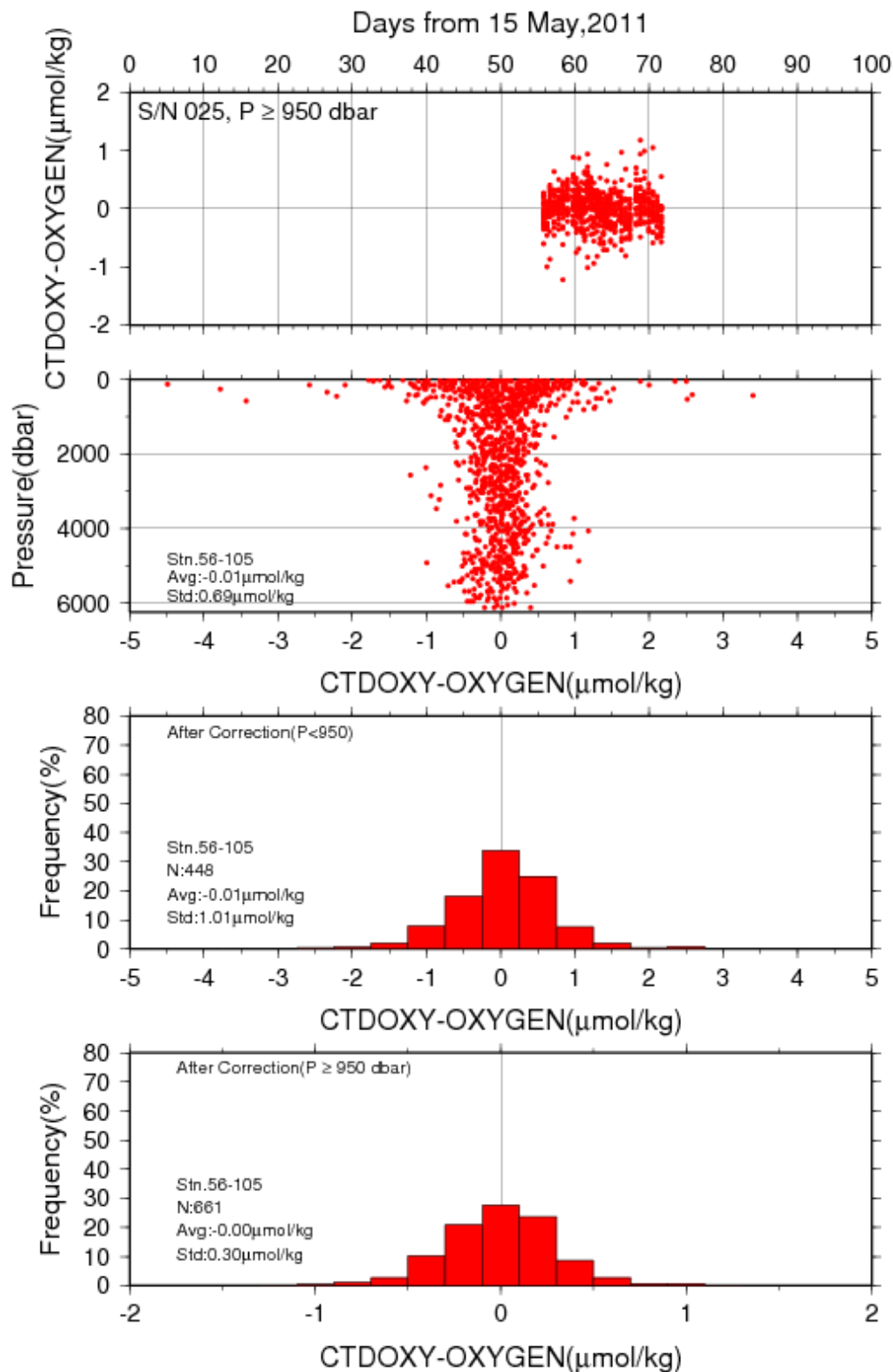


Figure C.1.9. Difference between the CTD oxygen and bottle dissolved oxygen in RF11-08 Leg 1. Red dots in upper two panels indicate the result of calibration. Lower two panels show histogram of the difference between calibrated oxygen and bottle oxygen.

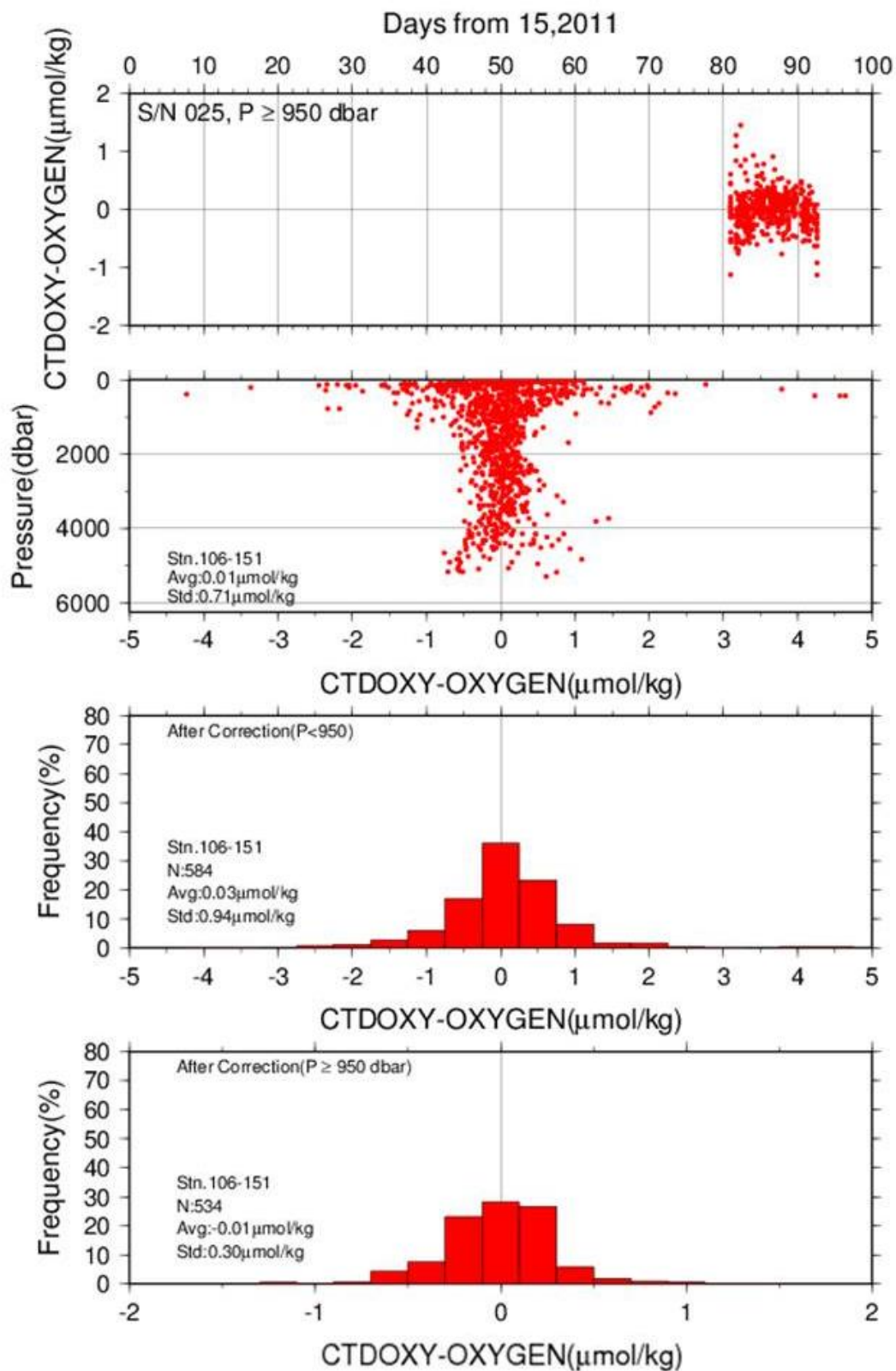


Figure C.1.9. Difference between the CTD oxygen and bottle dissolved oxygen in RF11-08 Leg 2. Red dots in upper two panels indicate the result of calibration. Lower two panels show histogram of the difference between calibrated oxygen and bottle oxygen.

References

- McTaggart, K. E., G. C. Johnson, M.C.Johnson, F.M.Delahoyde, and J.H.Swift (2010): The GO-SHIP Repeat Hydrography Manual: A Collection of Expert Reports and guidelines. IOCCP Report No **14**, ICPO Publication Series No. 134, version 1, 2010
- Budeus. G., and W. Schneider (1998): In-situ temperature calibration: A remark on instruments and methods. *International WOCE Newsletter*, No.**30**, WOCE International Project Office, Southampton, United Kingdom, 16-18.
- Larson, N., and A.M. Pedersen (1996): Temperature measurements in flowing water: Viscous heating of sensor tips. *Proc. of the First IGHEM Meeting, Montreal, QC, Canada, International Group for Hydraulic Efficiency Measurement*. [Available online at http://www.seabird.com/technical_references/viscous.htm]
- Uchida, H., K. Ohyama, S. Ozawa, and M. Fukasawa (2007): In-situ calibration of the Sea-Bird 9plus CTD thermometer. *J. Atmos. Oceanic Technol.***24**, 1961-1967.
- Akaike, H. (1974): A new look at the statistical model identification. *IEEE Transactions on Automatic Control*, **19**:716 – 722.
- Uchida, H., T. Kawano, I. Kaneko, and M. Fukasawa (2008): In-situ calibration of optode-based oxygen sensors. *J. Atmos. Oceanic Technol.*, **25**, 2271-2281.
- Garcia, H. E., and L. I. Gordon (1992): Oxygen solubility in seawater: Better fitting equations. *Limnol. Oceanogr.*, **37**, 1307-1312.
- Shanno, David F. (1970): Conditioning of quasi-Newton methods for function minimization. *Math. Comput.* **24**, 647-656. MR 42 #8905
- Sea-Bird Electronics (2009): SBE 43 dissolved oxygen (DO) sensor – hysteresis corrections, *Application note no. 64-3*, 7 pp.
- Kawano, T., H. Uchida and T. Doi (2009): WHP P01, P14 REVISIT DATA BOOK, JAMSTEC, Yokosuka, Japan.

2. Bottle Salinity

1 November 2019

(1) Personnel

RF 11-06

Kiyoshi MURAKAMI (GEMD/JMA)

Yoshikazu HIGASHI (GEMD/JMA)

Koichi WADA (GEMD/JMA)

Ayumi HASHIZUME (GEMD/JMA)

RF 11-07

Koichi WADA (GEMD/JMA)

Hiroumi SHIGEOKA (GEMD/JMA)

Atsushi KOJIMA (GEMD/JMA)

RF 11-08

Koichi WADA (GEMD/JMA)

Hiroumi SHIGEOKA (GEMD/JMA)

Atsushi KOJIMA (GEMD/JMA)

(2) Station occupied

A total of 106 stations (RF1106: 12, RF1107: 29, RF1108: 65) were occupied for bottle salinity. Station location and sampling layers of bottle salinity are shown in Figure C.2.1.

Figure C.2.1 Station location (left panel) and sampling layers of bottle salinity (right panel).

(3) Instruments and method

(3.1) Salinity sample collection

The bottles in which the salinity samples are collected and stored are 250 ml colorless transparent glass bottles with screw caps. Each bottle was rinsed three times with sample water and was filled to the shoulder of the bottle. The screw caps were also thoroughly rinsed. Salinity samples were wiped with dry clothes and stored for more than 24 hours in the same laboratory as the salinity measurement was made.

(3.2) Instruments and methods

The salinity analysis was carried out on AUTOSAL Laboratory Salinometer model 8400B (Guildline Instruments Ltd., Canada), which was modified by addition of an Ocean Science International peristaltic-type sample intake pump and two Guildline platinum thermometers model 9450. One thermometer monitored an ambient temperature and the other monitored a bath temperature. The resolution of the thermometers was 1 mK. The measurement system was almost same as *Aoyama et al (2003)*. Ambient temperature in laboratory was monitored by one thermometer. The salinometer was operated in a ship's laboratory air-conditioned at a bath temperature of 24 °C. Ambient temperature varied from approximately 21.0 to 23.5 °C, while bath temperature is very stable and varied within ± 0.001 °C on rare occasion. A measure of a double conductivity ratio of a sample is taken as a median of thirty-one readings. Data collection was started after 10 seconds and it took about 10 seconds to collect 31 readings by a personal computer. Data were sampled for the fourth and the fifth filling of the cell. In case the difference in the double conductivity ratio between this two fillings was smaller than 0.00003, the average value of the two double conductivity ratios was used to calculate the bottle salinity with the algorithm for practical salinity scale, 1978 (*UNESCO, 1981*). If the difference was greater than or equal to 0.00003, we measured the sixth filling of the cell. In case the double conductivity ratio of the sixth filling did not satisfy the criteria above, we measured the next filling of the cell and chose proper two fillings which satisfied the criteria. We continued these process at most ninth fillings.

(4) Result

Sample was measured by three AUTOSAL salinometers (RF1106: S/N67642, the first of RF1107: S/N69677, the second half of RF1107 and RF1108: S/N66286).

Standardization control was set to 4.06, 5.72, 4.79 in each salinometeres (S/N67642, S/N69677, S/N66286) and all the sample measurements were done by this setting. During the whole measurement, STANDBY and ZERO were stable (STANDBY: 5436 ± 0003 , 6011 ± 0001 , 5239 ± 0001 , ZERO: 0.00000, 0.00002, 0.00002, in each salinometeres). We used IAPSO Standard Seawater batch P153 whose conductivity ratio was 0.99979 (double conductivity ratio is 1.99958) as the standard for salinity. We measured 2 or 3 ampoules of

P153 for each station, total amount was 365. There were 6 bottles whose conductivities are extremely high or low.

Figure C.2.2 shows the history of ambient temperature, bath temperature, raw and corrected double conductivity ratio of standard sea water (P153) and time drift of P153 but for bad ampoules. The average of corrected double conductivity ratio was 1.999580 and the standard deviation was 0.00001, which was equivalent to 0.0002 in salinity. The correction of AUTOSAL drift for salinity measurements was from 0 to 10 digits.

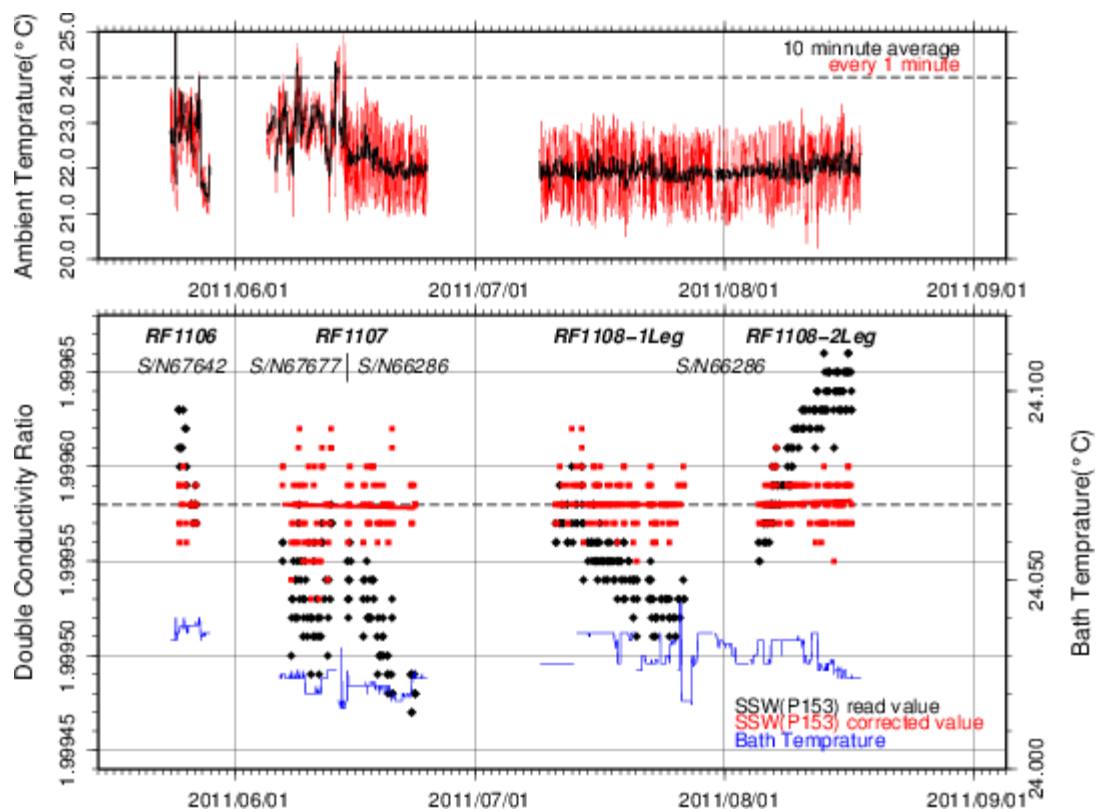


Figure C.2.2 The upper panel shows time-series of ambient temperature during cruise. The lower panel, black dots and red dots indicate raw and corrected time-series of the double conductivity ratio of the standard sea water (P153), red line indicates corrected standard sea water for each period, gray line indicates the label value double conductivity ratio of P153 and blue line indicates time-series of bath temperature during cruise.

(5) Sub-Standard Water

We also used sub-standard seawater which was filtered by pore size of 10 micrometer and stored in a 20 liter cubitainer made of polyethylene and stirred for at least 24 hours before measuring. It was measured every about five samples in order to check possible sudden drift of the salinometer. During the whole measurements, there was no detectable sudden drift of the salinometer.

(6) Replicate and Duplicate Samples

We took 451 pairs of replicate samples and 229 pairs of duplicate samples during the cruise. Figure C.2.3 and Figure C.2.4 show the absolute difference among replicate and duplicate samples in salinity, respectively. There were 59 bad measurements in replicate pairs and 36 bad measurements of sampling in duplicate pairs. Excluding those bad and questionable measurements, the mean absolute difference and standard deviation 392 pairs of replicate samples was 0.0004 ± 0.0004 in salinity and that of 193 pairs of duplicate samples was 0.0006 ± 0.0006 in salinity. Note that standard deviation was calculated by a procedure (SOP23) in *DOE (1994)*.

Table C.2.1 Summary of assigned quality control flags

Flag	Definition	Salinity
2	Good	2969
4	Bad (Faulty)	288
6	Replicate measurements	392
Total number of samples		3649

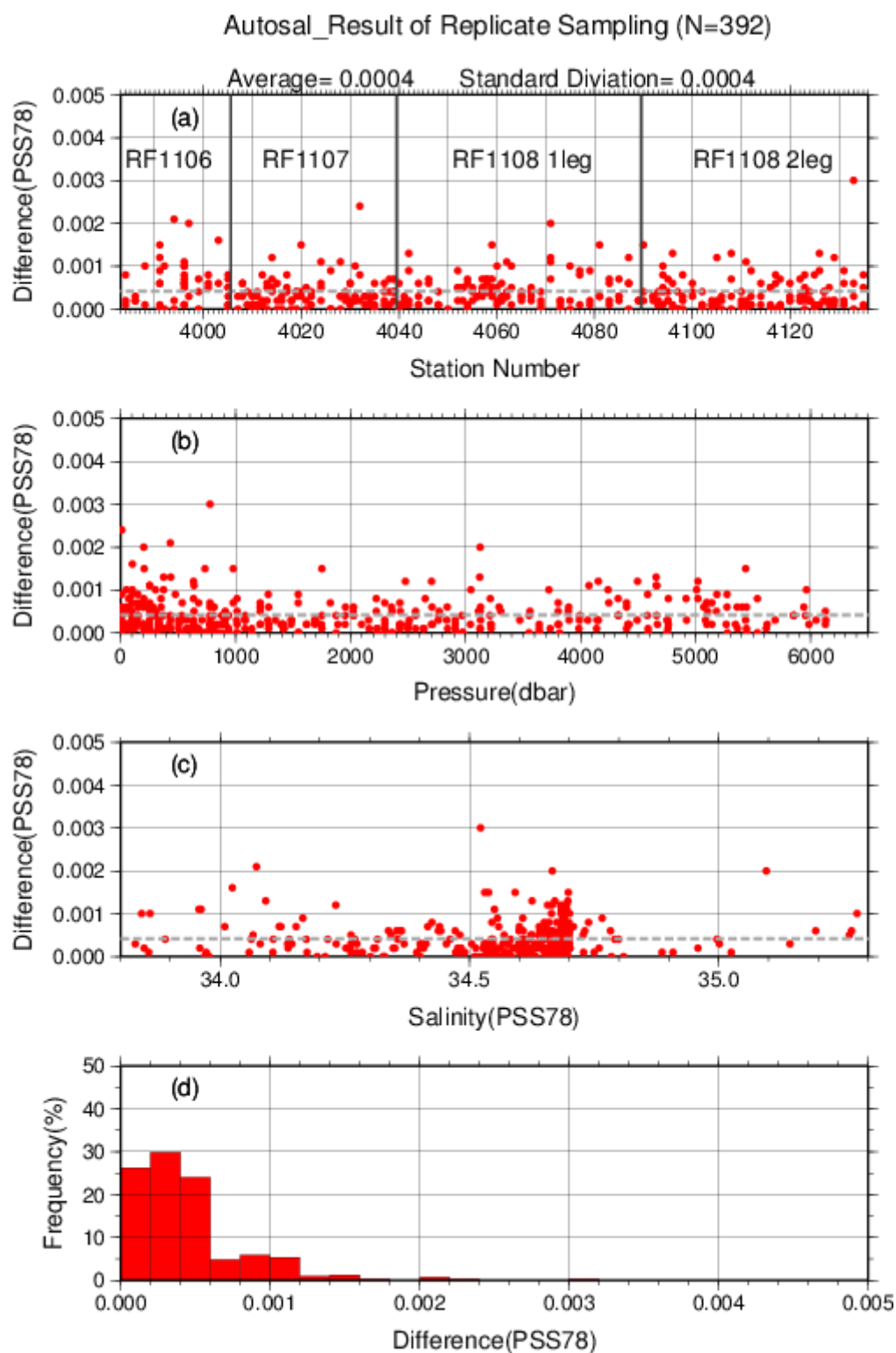


Figure C.2.3 Result of replicate samplings during this cruise against (a) station number, (b) sampling pressure and (c) salinity. Dotted line denotes the average of replicate samplings. Bottom panel (d) shows histogram of the result of replicate samplings.

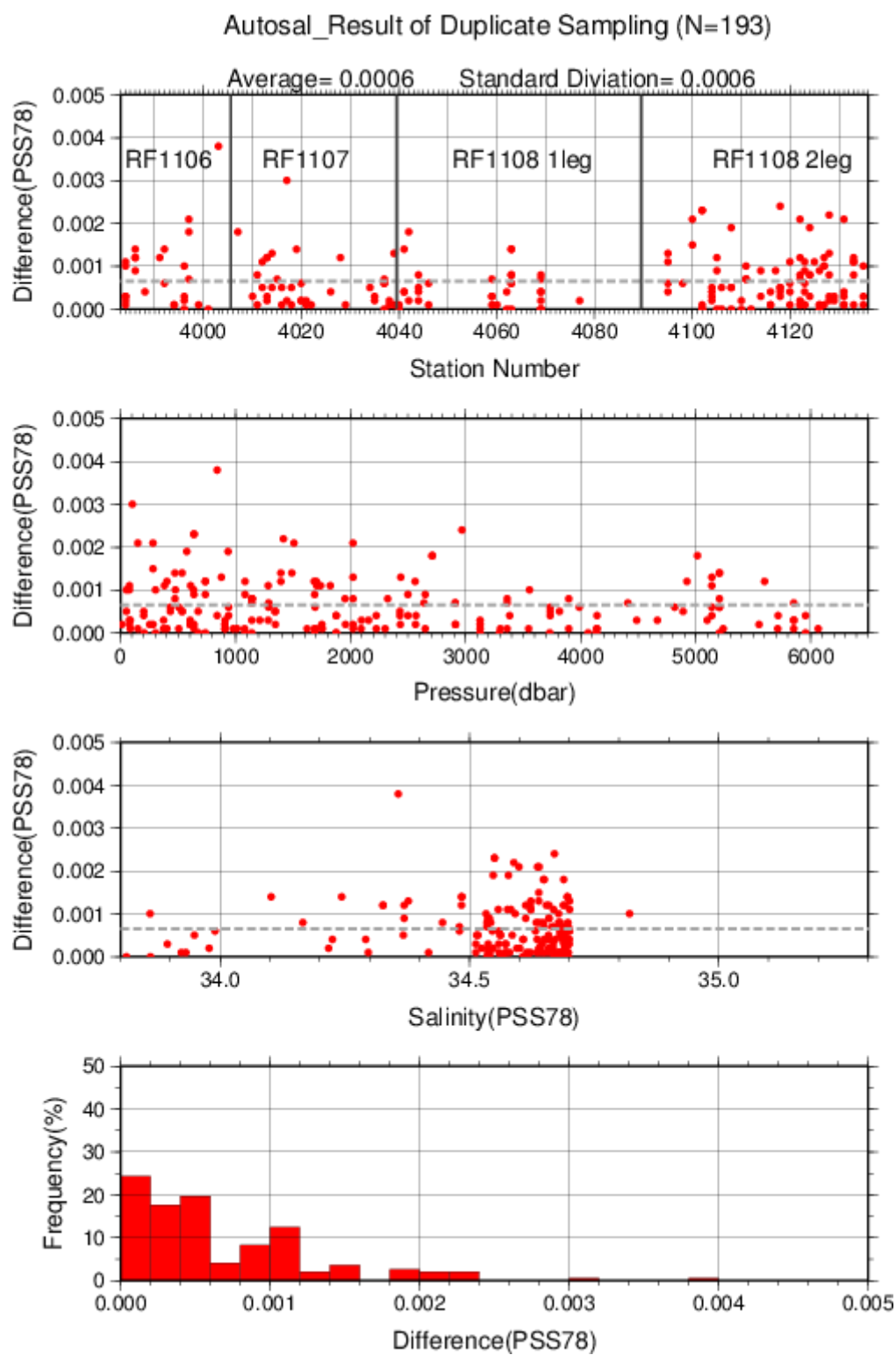


Figure C.2.4 Same as Fig.C.2.3 but for duplicate samplings.

References

- Aoyama, M., T. Joyce, T. Kawano and Y. Takatsuki (2003): Standards seawater comparison up to P129. *Deep-sea Research, 1, Vol. 49, 1103-1114.*
- UNESCO (1981): Tenth report of the Joint Panel on Oceanographic Tables and Standards. *UNESCO Tech. Papers in Mar. Sci., 36, 25 pp.*
- DOE (1994): Handbook of methods for the analysis of the various parameters of the carbon dioxide system in sea water; version 2. *A.G. Dickson and C. Goyet (eds), ORNL/CDIAC-74.*

3. Bottle Oxygen

1 November 2019

(1) Personnel

RF11-06

Hidemi OGAHARA (GEMD/JMA)

Masaya IKEDA (GEMD/JMA)

Yusuke TAKATANI (GEMD/JMA)

Ryosuke SAKAKIBARA (GEMD/JMA)

RF11-07

Shinichiro UMEDA (GEMD/JMA)

Sho HIBINO (GEMD/JMA)

Ryosuke SAKAKIBARA (GEMD/JMA)

RF11-08

Hidemi OGAHARA (GEMD/JMA)

Yusuke TAKATANI (GEMD/JMA)

Sho HIBINO (GEMD/JMA)

(2) Station occupied

A total of 106 stations (RF11-06: 12, RF11-07: 29, RF11-08 Leg 1: 32, RF11-08 Leg 2: 33) were occupied for bottle oxygen. Station location and sampling layers of bottle oxygen are shown in Figure C.3.1.

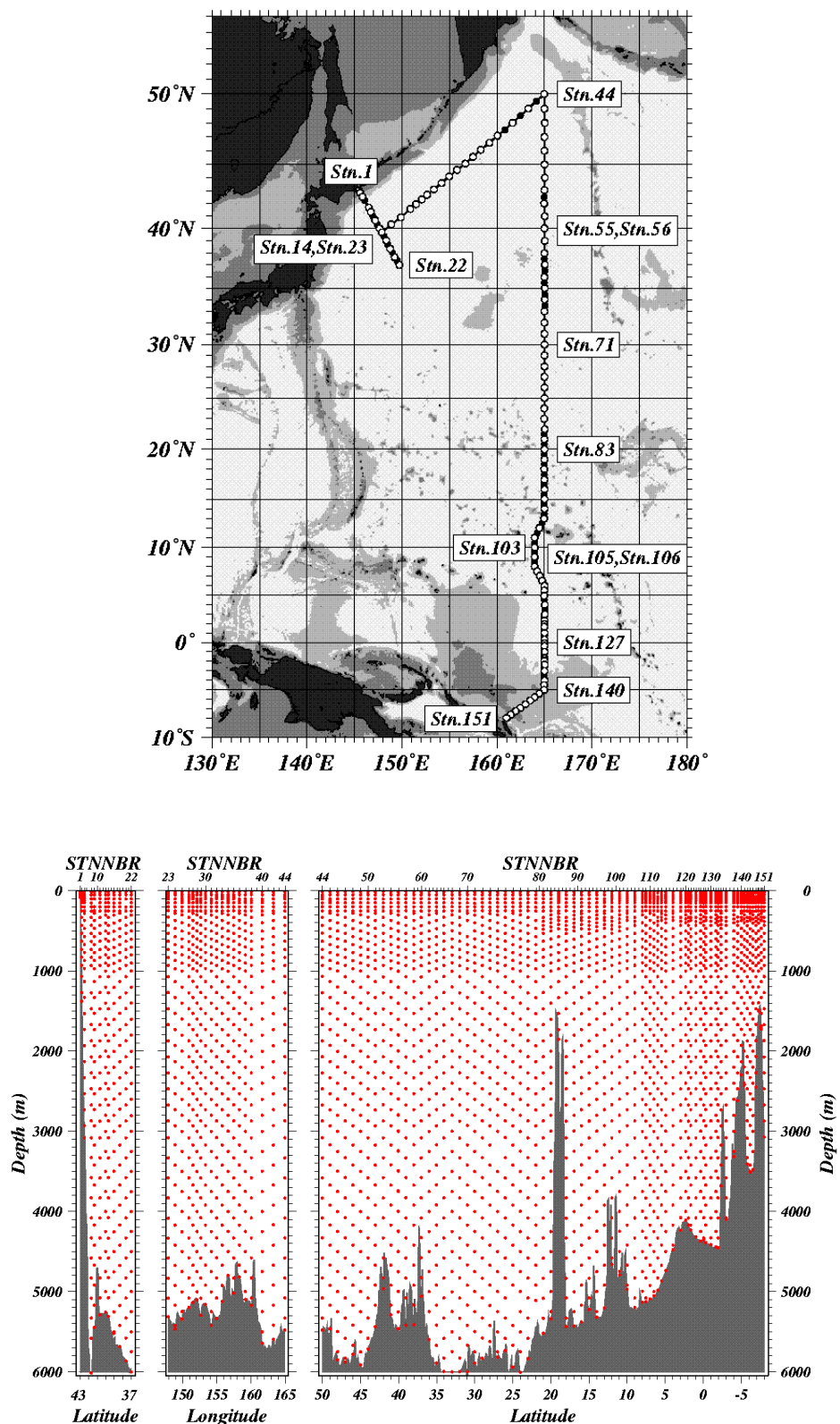


Figure C.3.1 (Upper panel) CTD station location. Open circles denote DO sampling stations and closed circles denote no DO sampling stations. (Bottom panels) Sampling layers of bottle oxygen.

(3) Reagents

·Manganous chloride solution (3 M)(Pickling Reagent-I)

Dissolved 600 g of $\text{MnCl}_2 \cdot 4\text{H}_2\text{O}$ in deionized water, then dilute the solution with deionized water to a final volume of 1 L. $\text{MnCl}_2 \cdot 4\text{H}_2\text{O}$ (Lot. STJ5288) used to make pickling reagent-I was guaranteed reagent manufactured by Wako Pure Chemical industries, Ltd.

·Sodium hydroxide (8 M) / sodium iodide solution (4 M) (Pickling Reagent-II)

Dissolved 320 g of NaOH in about 500 ml of deionized water, allow to cool, then add 600 g NaI and dilute with deionized water to a final volume of 1 L. NaOH (Lot. STN1103 and STN2682) and NaI (Lot. STF2442) used to make pickling reagent-II were guaranteed reagent manufactured by Wako Pure Chemical industries, Ltd.

·Sulfuric acid solution (5 M)

Slowly add 280 ml concentrated H_2SO_4 to roughly 500 ml of deionized water. After cooling the final volume should be 1 L. H_2SO_4 (Lot. EPL2000) used to make sulfuric acid solution was guaranteed reagent manufactured by Wako Pure Chemical industries, Ltd.

·Sodium thiosulfate (0.04 M)

Dissolved 50 g of $\text{Na}_2\text{S}_2\text{O}_3 \cdot 5\text{H}_2\text{O}$ and 0.4 g of Na_2CO_3 in deionized water, then dilute the solution with deionized water to a final volume of 5 L. $\text{Na}_2\text{S}_2\text{O}_3 \cdot 5\text{H}_2\text{O}$ (Lot. SDF1608) and Na_2CO_3 (Lot. WKF1312) used to make sodium thiosulfate were guaranteed reagent manufactured by Wako Pure Chemical industries, Ltd.

·Potassium iodate (0.001667 M)

Dry high purity KIO_3 for two hours in an oven at 130°C . After weight out accurately KIO_3 , dissolve it in deionized water in a 5 L flask. Concentration of potassium iodate is determined by a gravimetric method. KIO_3 (Lot. 62404E) used to make potassium iodate was manufactured by MERCK & CO., Inc., and a purity of KIO_3 that is traceable to NIST (National Institute of Standards and Technology) standard reference material is $99.75 \pm 0.05 \%$. The normality of the standard potassium iodate solution made by Merck reagent was corrected by the factor as 1.0026 from the result of the inter-laboratory comparison with the standard potassium iodate solution made by National Metrology Institute of Japan reagent (JMA, 2013).

(4) Instruments

Detector; DOT-01X automatic photometric titrator manufactured by Kimoto Electronic Co. Ltd.

Burette for sodium thiosulfate;

APB-510 manufactured by Kyoto Electronic Co. Ltd. / 10 ml of titration vessel

Burette for potassium iodate;

Multipette stream 4986 and Combitip plus manufactured by eppendorf / 10 ml of tip vessel

Bottle top dispenser for pickling reagent-I and II;

CalibrexTM 520 manufactured by SOCOREX ISBA S.A.

(5) Seawater sampling

Following procedure is based on a determination method in IOCCP Report No.14 (Langdon, 2010). Seawater samples were collected from 10 liter Niskin sample bottles attached the CTD-system and a stainless steel bucket for the surface. Seawater for bottle oxygen measurement was transferred from the Niskin sample bottle and a stainless steel bucket to a volumetrically calibrated dry glass bottles (ca. 120 ml, standard deviation of calibration = 0.009 ml). At least three times volume of the glass of sample water was overflowed. Two reagent solutions (Reagent-I and II) of 1 ml (standard deviation of calibration = 0.003 ml) each were added immediately, sample temperature was then measured by a thermometer. After the stopper was inserted carefully into the glass, the sample glass was shaken vigorously to mix the content and to disperse the precipitate finely. The precipitate has settled at least halfway down the glass, the glass was then shaken again vigorously to disperse the precipitate. The sample glasses containing pickled samples were stored in a laboratory until they were titrated. To prevent air from entering the flask, deionized water was added to the neck of the flask after sampling.

(6) Sample measurement

At least 30 minutes after the re-shaking, the pickled samples were measured on board. 1 ml sulfuric acid solution and a magnetic stirrer bar were added into the sample glass and stirring began. Samples were titrated by sodium thiosulfate solution whose molarity was determined by potassium iodate solution. Temperature of sodium thiosulfate during titration was recorded by a thermometer. The titrations were carried out using the titration apparatus, named DOT-01X. Dissolved oxygen concentration ($\mu\text{mol/kg}$) was calculated by the sample temperature at the fixation, CTD salinity, glass volume, and titrated volume of the sodium thiosulfate solution.

(7) Standardization

Concentration of sodium thiosulfate titrant (ca. 0.04 M) was determined by potassium iodate solution. Table C.3.1 shows a list of potassium iodate solution used in this cruise. Using a calibrated volumetric dispenser, 10 ml (standard deviation of calibration = 0.0009 ml) of the standard potassium iodate solution was added to a glass with 100 ml of deionized water. Then, 1 ml of sulfuric acid solution, and 1 ml of pickling reagent solution-II and I were added into the glass in order. Amount of titrated volume of sodium thiosulfate (usually 5 times measurements average) gave the molarity of the sodium thiosulfate titrant. Figure C.3.2 and Table C.3.2 show the results of the standardization during this cruise. The sodium thiosulfate titrant of each batch was a mean of titrated volume of sodium thiosulfate on each day and a standard deviation of a concentration at 20 °C of sodium thiosulfate on each day was an uncertainty caused by the standardization. A sodium thiosulfate of one batch was assumed to be one sodium thiosulfate titrant. The uncertainty of dissolved oxygen that caused by the standardization was estimated 0.04-0.11 %.

Table C.3.1 List of the standard potassium iodate solution in this cruise.

KIO ₃ batch	Conc. at 20°C (N)
KIO ₃ _20110119_2	0.010027±0.000003
KIO ₃ _20110412_2	0.010574±0.000003

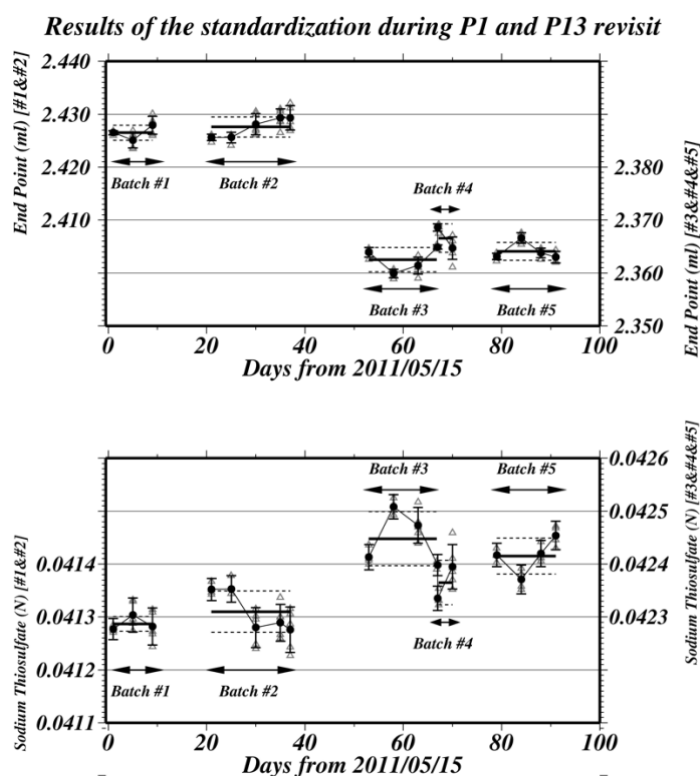


Figure C.3.2 Results of the standardization. Upper panel shows results of end point, bottom panel shows results of calculated concentration at 20°C of sodium thiosulfate. Crosses show each value for each standardization samples, and closed circles show the mean at each standardizations. Thick lines and dotted lines denote the means and 1 σ error for each batch of sodium thiosulfate, respectively.

Table C.3.2 Results of the standardization.

Cruise	Date (UTC)	KIO ₃		Na ₂ S ₂ O ₃ (ml)		Stations
		Batch	Bottle	Batch	End Point	
RF11-06	2011/5/16	20110119_2	4	#1	2.4265	RF3984
	2011/5/20	20110119_2	5	#1	2.4261	
	2011/5/24	20110119_2	6	#1	2.4279	RF4005
Na ₂ S ₂ O ₃ _#1					2.4268±0.0010	
RF11-07	2011/6/5	20110119_2	7	#2	2.4256	
	2011/6/10	20110119_2	8	#2	2.4256	RF4007
	2011/6/14	20110119_2	9	#2	2.4282	
	2011/6/19	20110119_2	10	#2	2.4293	RF4039
	2011/6/22	20110119_2	11	#2	2.4293	
Na ₂ S ₂ O ₃ _#2					2.4276±0.0019	
RF11-08	2011/7/8	20110119_2	12	#3	2.3639	RF4040
	2011/7/13	20110119_2	13	#3	2.3599	
	2011/7/18	20110119_2	14	#3	2.3614	RF4076
	2011/7/21	20110119_2	15	#3	2.3649	
	Na ₂ S ₂ O ₃ _#3					2.3625±0.0023
Leg 1	2011/7/21	20110119_2	15	#4	2.3686	RF4077–
	2011/7/25	20110119_2	16	#4	2.3647	RF4089
Na ₂ S ₂ O ₃ _#4					2.3666±0.0027	
RF11-08	2011/8/2	20110119_2	17	#5	2.3631	
	2011/8/8	20110119_2	18	#5	2.3666	RF4090
Leg 2	2011/8/11	20110119_2	19	#5	2.3638	
	2011/8/15	20110119_2	20	#5	2.3630	RF4135
Na ₂ S ₂ O ₃ _#5					2.3641±0.0017	

(8) Determination of the blank

The oxygen in the pickling reagents-I (1 ml) and II (1 ml) was assumed to be 7.6×10^{-8} mol (Murray *et al.*, 1968). The blank from the presence of redox species apart from oxygen in the reagents (the pickling reagents-I, II, and the sulfuric acid solution) was determined as follows. Using a calibrated volumetric dispenser, 1 ml of the standard potassium iodate solution was added to a glass with 100 ml of deionized water. Then, 1 ml of sulfuric acid solution, and 1 ml of pickling reagent solution-II and I were added into the glass in order. First, the sample was titrated to the end-point by sodium thiosulfate solution. Then, the sample was titrated again to the end-point after added a further 1 ml of the standard potassium iodate solution. The blank was determined by difference between the first (1 ml of KIO₃) titrated volume of the sodium thiosulfate and the second (2 ml of KIO₃) one. Because reagents set were prepared two sets

(set A and B), the blank in each sets were determined. Usually, the results of 5 times blank determinations were averaged (Table C.3.3). The standard deviation of the blank determination during this cruise was 0.0006-0.0011 ml (set A) and 0.0004–0.0015 ml (set B), c.a. 0.02–0.07 %.

Table C.3.3 Result of the blank determinations.

Cruise	Date (UTC)	Na ₂ S ₂ O ₃ Batch	Blank (ml)		Stations
			Set A	Set B	
RF11-06	2011/5/16	#1	0.0011	0.0024	Stn.1
	2011/5/20	#1	0.0016	0.0015	
	2011/5/24	#1	0.0032	0.0021	Stn.22
			Set A	0.0020±0.0011	
			Set B	0.0020±0.0004	
RF11-07	2011/6/5	#2	0.0022	0.0033	
	2011/6/10	#2	0.0028	0.0000	Stn.23
	2011/6/12	#2	0.0021	0.0008	
	2011/6/14	#2	0.0013	0.0034	Stn.55
	2011/6/19	#2	0.0033	0.0017	
	2011/6/22	#2	0.0020	0.0004	
			Set A	0.0023±0.0007	
RF11-08 Leg 1			Set B	0.0016±0.0015	
	2011/7/8	#3	0.0024	0.0017	
	2011/7/13	#3	0.0011	0.0035	Stn.56
	2011/7/18	#3	0.0027	0.0034	
	2011/7/21	#3	0.0020	0.0022	Stn.105
	2011/7/25	#4	0.0021	0.0021	
			Set A	0.0020±0.0006	
RF11-08 Leg 2			Set B	0.0026±0.0008	
	2011/8/3	#5	0.0016	0.0017	
	2011/8/8	#5	0.0022	0.0010	Stn.106
	2011/8/12	#5	0.0023	0.0018	
	2011/8/15	#5	0.0031	0.0016	Stn.155
			Set A	0.0023±0.0006	
			Set B	0.0015±0.0004	

(9) Reagent blank

The blank determined in section (8), pure water blank ($V_{\text{blk, dw}}$) can be represented by equation (i),

$$V_{\text{blk, dw}} = V_{\text{blk, ep}} + V_{\text{blk, reg}} \quad (\text{i})$$

where

$V_{\text{blk, ep}}$ = blank due to differences between the measured end-point and the equivalence point;

$V_{\text{blk, reg}}$ = blank due to oxidants or reductants in the reagent.

Here, the reagent blank ($V_{\text{blk, reg}}$) was determined by following procedure. 1 ml of the standard potassium iodate solution and 100 ml of deionized water were added to two glasses each. 1 ml of sulfuric acid solution, pickling reagent solution-II and I each were added into the first glass in order. Then, two times volume of the reagents (2 ml of sulfuric acid solution, pickling reagent solution-II and I each) was added to the second glass. The reagent blank was determined by difference between the first (3 ml of the total reagent volume added) titrated volume of the sodium thiosulfate and the second (6 ml of the total reagent volume added) one. We also carried out experiments for three and four times volume of the reagents. The results are shown in Figure C.3.3.

The relation between difference of the titrant ($\text{Na}_2\text{S}_2\text{O}_3$) volume and the volume of the reagents added (V_{reagent}) is expressed by equation (ii),

$$\text{Difference of the titrant volume} = -0.0013V_{\text{reagent}} \quad (\text{ii})$$

$V_{\text{blk, reg}}$ was estimated to be about -0.004 ml, suggesting that about $0.02 \mu\text{mol}$ of reductants was contained in every 3 ml of the reagents added.

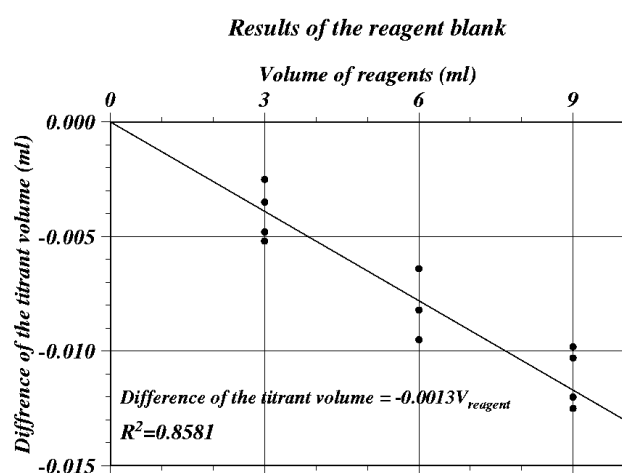


Figure C.3.3 Blank (ml) due to redox species apart from oxygen in the reagents.

(10) Sample blank

Blank due to redox species other than oxygen in the sample ($V_{\text{blk, spl}}$) can be a potential source of measurement error. The total blank during the seawater measurement, the seawater blank ($V_{\text{blk, sw}}$) can be represented by equation (iii).

$$V_{\text{blk, sw}} = V_{\text{blk, spl}} + V_{\text{blk, dw}} \quad (\text{iii})$$

If the pure water blank ($V_{\text{blk, dw}}$) that is determined in section (9) is identical both in pure water and in seawater, the difference between the seawater blank and the pure water one gives the sample blank ($V_{\text{blk, spl}}$).

Here, $V_{\text{blk, spl}}$ was determined by following procedure. Seawater sample was collected in the calibrated volumetric glass (c.a. 120 ml) without the pickling. Then 1 ml of the standard potassium iodate solution, sulfuric acid solution, and pickling reagent solution-II and I each were added into the glass in order. Additionally, a glass contained 100 ml of deionized water and 1 ml of the standard potassium iodate solution, sulfuric acid solution, pickling reagent solution-II and I was prepared. The difference of the titrant volumes of the seawater glass and the deionized water one gave the sample blank ($V_{\text{blk, spl}}$).

We measured vertical profiles of the sample blank at 4 stations (Table C.3.4). The sample blank ranged from 0.55 to 2.48 $\mu\text{mol/kg}$ and its vertical and horizontal variations are large. This result does not agree to reported values ranged from 0.4 to 0.8 $\mu\text{mol/kg}$ (Culberson et al., 1991). It does not have been known about the magnitude and variability of the seawater blank, so this result should be discussed carefully. Ignorant of the sample blank will cause systematic errors in the oxygen calculations, but these errors are expected to be the same to all investigators and not to affect the comparison of results from different investigators (Culberson, 1994).

Table C.3.4 Results of the sample blank determinations during this cruise.

Station: Stn.6 42.27°N/146.03°E		Station: Stn.19 38.01°N/149.03°E		Station: Stn.39 47.49°N/160.82°E		Station: Stn.52 42.51°N/164.96°E	
Pres. (dbar)	Blank ($\mu\text{mol/kg}$)	Pres. (dbar)	Blank ($\mu\text{mol/kg}$)	Pres. (dbar)	Blank ($\mu\text{mol/kg}$)	Pres. (dbar)	Blank ($\mu\text{mol/kg}$)
11.1	2.02	51.6	1.74	51.3	0.90	202.5	0.74
76.7	2.01	104.2	2.48	151.3	0.73	304.9	0.61
253.6	1.68	255.3	2.10	282.4	0.82	304.9	0.63
253.6	1.51	405.7	1.26	282.4	0.81	708.3	0.55
607.9	0.77	1214.8	1.99	473.8	0.78	1215.2	0.67
809.1	1.01	2433.8	0.97	879.4	0.81	1620.1	0.57
1011.8	0.81	3046.0	1.22	1547.8	1.01	1620.1	0.69
2028.1	1.19	3301.8	1.22	2364.6	0.99	2230.1	0.66
3046.7	1.49	3557.2	1.47	2364.6	0.91	2841.4	0.66
3046.7	1.42	4326.3	1.08	3989.9	0.99	3559.7	0.73
3558.8	1.67	5098.9	1.06	3989.9	0.87	4585.8	0.62
4072.1	2.07	5098.9	1.98	5302.1	0.90	4585.8	0.75

		5929.6	1.48				
--	--	--------	------	--	--	--	--

(11) Replicate sample measurement

Replicate samples were carried out at every bottle oxygen observation stations. Total amount of the replicate sample pairs in good measurement (flag=6) was 406, and total amount of the removed pair (flag=3 or 4) was 22. The average and the standard deviation of the replicate measurement during this cruise were 0.19 ± 0.17 $\mu\text{mol/kg}$. The standard deviation was calculated by a procedure (SOP23) in DOE (1994). The difference between the replicate sample pairs did not depended on sampling pressure, measurement date and concentration of sample (Figure C.3.4). The averages and the standard deviations during RF11-06, RF11-07, RF11-08 Leg1 and Leg 2 were 0.20 ± 0.17 (n=42), 0.19 ± 0.18 (n=104), 0.19 ± 0.17 (n=129) and 0.17 ± 0.16 (n=131) $\mu\text{mol/kg}$, respectively.

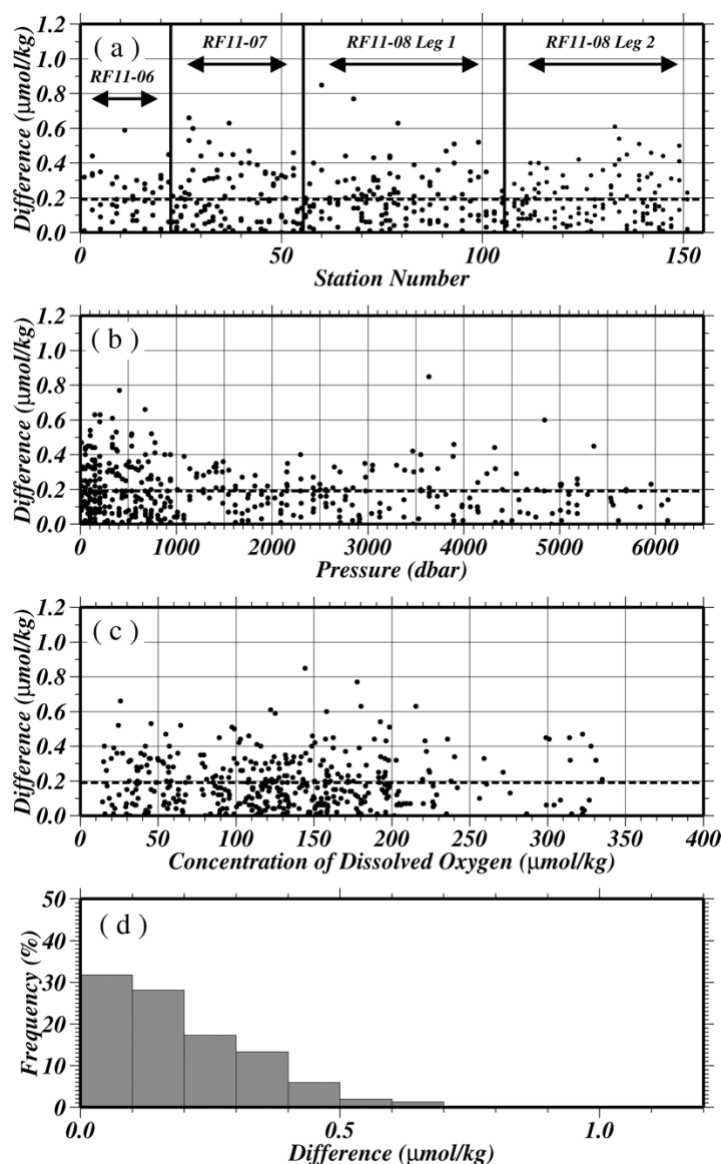


Figure C.3.4 Result of replicate samplings during this cruise against (a) station number, (b) sampling pressure and (c) concentration of dissolved oxygen. Dotted line denotes the

average of replicate samplings. Bottom panel (d) shows histogram of the result of replicate samplings.

(12) Duplicate sample measurement

Duplicate samples that were seawater samples from two Niskin sample bottles that were collected at same depth were carried out at some bottle oxygen observation stations also. Total amount of the duplicate sample pairs in good measurement (flag=2) was 152, and total amount of the removed pair (flag=3 or 4) was 22. The average and the standard deviation of the duplicate measurement during this cruise were 0.24 ± 0.21 $\mu\text{mol/kg}$. The difference between the duplicate sample pairs did not depended on sampling pressure, measurement date and concentration of sample (Figure C.3.5). The averages and the standard deviations during RF11-06, RF11-07, RF11-08 Leg1 and Leg 2 were 0.27 ± 0.26 (n=21), 0.20 ± 0.19 (n=35), 0.26 ± 0.22 (n=21) and 0.24 ± 0.21 (n=75) $\mu\text{mol/kg}$, respectively.

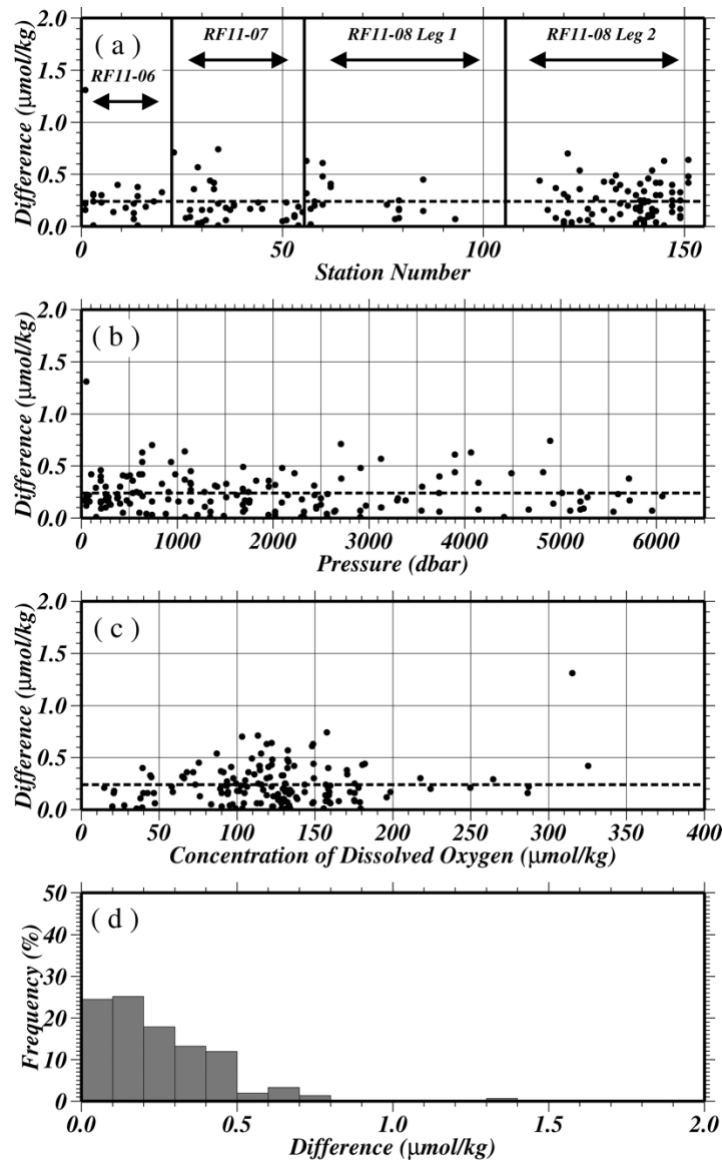


Figure C.3.5 Result of duplicate samplings during this cruise against (a) station number, (b) sampling pressure and (c) concentration of dissolved oxygen. Dotted line denotes the average of duplicate samplings. Bottom panel (d) shows histogram of the result of duplicate

samplings.

(13) Mutual comparison between each standard potassium iodate

During the cruise, we performed the mutual comparison between two standard potassium iodate of difference Lot. in order to confirm the accuracy of our oxygen measurement and the bias of a standard potassium iodate. We measured concentration of a KIO₃ (KIO₃_20110412_2) against another KIO₃ (KIO₃_20110119_2), and checked the difference between measurement value and theoretical one (Table C.3.5, Figure C.3.6). Error weighted means of measurement results of KIO₃_20110412_2 were 0.010579±0.000011 N. The averaged value of the KIO₃_20110412_2 was so close to the theoretical value (0.010574±0.000003 N) that was prepared in laboratory. A good agreement among two standard potassium iodate confirmed that there was no systematic shift in our oxygen measurements during this cruise.

Table C.3.5 Results of mutual comparison of KIO₃_20110412_2 against KIO₃_20110119_2

Date (UTC)	KIO ₃ Batch	Measurement Value (N)
2011/5/16	20110412_2_4	0.010580±0.000007
2011/5/20	20110412_2_5	0.010564±0.000012
2011/5/24	20110412_2_6	0.010570±0.000013
2011/6/5	20110412_2_7	0.010593±0.000008
2011/6/10	20110412_2_8	0.010580±0.000008
2011/6/14	20110412_2_9	0.010581±0.000013
2011/6/19	20110412_2_10	0.010567±0.000013
2011/6/22	20110412_2_11	0.010568±0.000013
2011/7/8	20110412_2_12	0.010579±0.000008
2011/7/13	20110412_2_13	0.010583±0.000012
2011/7/18	20110412_2_14	0.010592±0.000011
2011/7/21	20110412_2_15	0.010581±0.000008
2011/7/21	20110412_2_15	0.010583±0.000007
2011/7/25	20110412_2_16	0.010580±0.000013
2011/8/2	20110412_2_17	0.010580±0.000007
2011/8/8	20110412_2_18	0.010561±0.000008
2011/8/11	20110412_2_19	0.010577±0.000008
2011/8/15	20110412_2_20	0.010601±0.000009
Weighted Mean		0.010579±0.000011

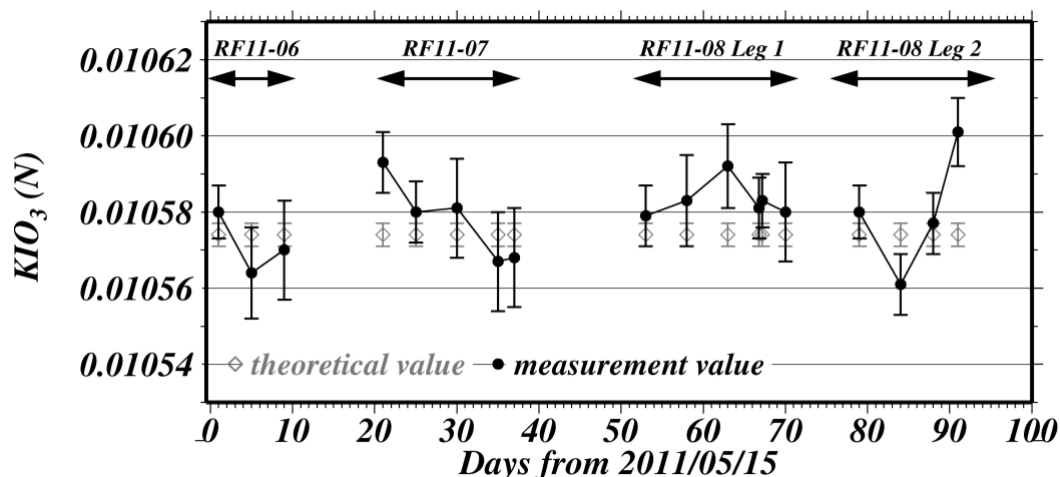


Figure C.3.6 Results of mutual comparison of KIO₃_20110412_2 against KIO₃_20110119_2. Closed circles show mean of measurement value with 1 σ error at each mutual comparison, and gray opened diamonds and error bar show the theoretical value and the uncertainty of the standard potassium iodate.

(14) CSK standard measurements

The CSK standard solution is commercial potassium iodate solution (0.0100 N) for analysis of oxygen in seawater. During the cruise, we measured concentration of the CSK standard solution (Lot EPJ3885) against our KIO₃ standard (Batch 20110119_2) in order to confirm the accuracy of our oxygen measurement (Table C.3.5, Figure C.3.6). Error weighted means of measurement results of CSK standard solution were 0.010006 ± 0.000012 N. The averaged value of the CSK standard solution was so close to the certified value (0.0100 N). A good agreement among two standard potassium iodate confirmed that there was no systematic shift in our oxygen measurements during this cruise.

Table C.3.5 Results of CSK standard measurements against KIO₃_20110119_2..

Date (UTC)	Measurement Value (N)
2011/5/16	0.010003±0.000008
2011/5/20	0.010014±0.000013
2011/5/24	0.010001±0.000015
2011/6/5	0.010018±0.000009
2011/6/10	0.010013±0.000011
2011/6/14	0.010005±0.000015
2011/6/19	0.010000±0.000014
2011/6/22	0.010006±0.000014
2011/7/8	0.010000±0.000009
2011/7/13	0.010018±0.000014
2011/7/18	0.010012±0.000013
2011/7/21	0.010010±0.000009
2011/7/21	0.010001±0.000007
2011/7/25	0.009998±0.000013
2011/8/2	0.010010±0.000009
2011/8/8	0.009991±0.000009
2011/8/11	0.010007±0.000009
2011/8/15	0.010006±0.000009
Weighted Mean	0.010006±0.000012

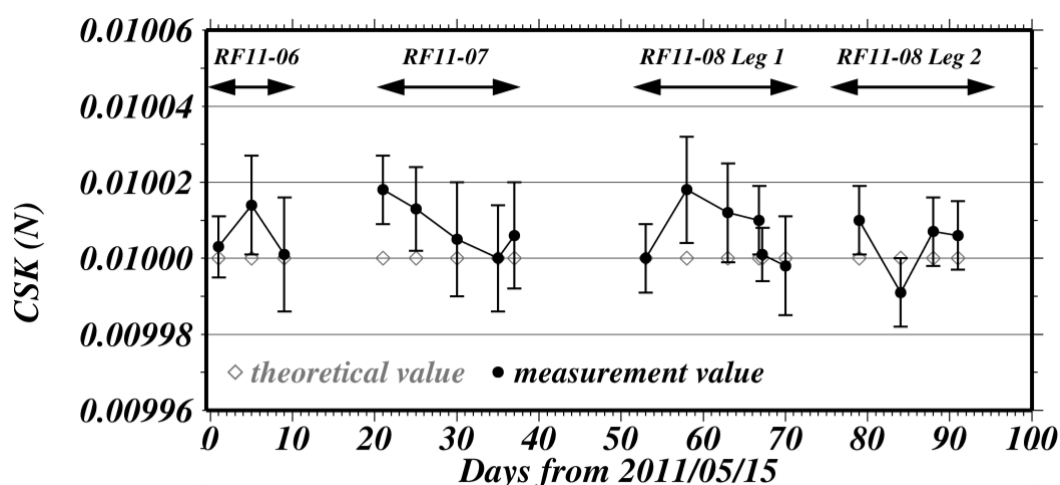


Figure C.3.6 Results of CSK standard measurements against KIO₃_20110119_2.. Closed circles show mean of measurement value with 1 σ error at each mutual comparison, and gray opened diamonds and error bar show the theoretical value and the uncertainty of the standard potassium iodate.

(15) Quality control flag assignment

Quality flag values were assigned to oxygen measurements using the code defined in IOCCP Report No.14 (Swift, 2010). Measurement flags of 2 (good), 3 (questionable), 4 (bad), 5 (not repeated), and 6 (replicate measurement) have been assigned (Table C.3.6). The replicate data were averaged and flagged 6 if both of them were flagged 2. If either of them was flagged 3 or 4, a datum with “younger” flag was selected. For the choice between 2, 3, or 4, we basically followed a flagging procedure as listed below:

- a. Vertical sections against pressure and potential density were drawn. Any points not lying on a generally smooth curve were noted.
- b. Dissolved oxygen was then plotted against potential temperature, salinity and nutrients. If a datum deviated from a group of plots, it was flagged 3.
- c. If a datum was deviated from the mean $\pm 3\sigma$ on the section, datum flag was degraded from 2 to 3, or from 3 to 4.
- d. We Compared bottle oxygen with CTD oxygen at the sampling depth. If a datum deviated from CTD oxygen, datum flag was degraded from 2 to 3, or from 3 to 4.
- e. If the bottle flag was 4 (did not trip correctly), a datum was flagged 4 (bad). If the bottle flag was 3 (leaking) or 5 (unknown problem), a datum was flagged based on steps a, b, c, and d.

Table C.3.6 Summary of assigned quality control flags.

Flag	Definition	
2	Good	4118
3	Questionable	44
4	Bad (Faulty)	72
5	Not reported	1
6	Replicate Measurements	406*
Total number of samples		4235*

*Samples of flag 6 are counted as flag 2

(16) Uncertainty in Oxygen data of this cruise

The reproducibility in this cruise determined by replicate samples and duplicate samples in section (11) and (12) was 0.19 ± 0.17 $\mu\text{mol/kg}$ and 0.24 ± 0.21 $\mu\text{mol/kg}$. Bottle oxygen data in this cruise were calculated based on IOCCP Report No.14 (Langdon, 2010). In these results, various uncertainty were included (ex. standardization, calibration of glass bottles, precision of burette etc.). The standard uncertainty of bottle oxygen data in this cruise by considering above uncertainty that can be estimated theoretically is shown in Table C.3.7. For example, when it assumes that seawater temperature is 20 degrees and salinity is 34.5, the standard uncertainty of 4ml/l (174.39 $\mu\text{mol/kg}$) DO concentration sample in RF11-06 is about 0.42

μmol/kg. However, it is impossible to estimate an accurate uncertainty because there is no reference material.

Table C.3.7 The standard uncertainty of bottle oxygen in this cruise

DO (ml/l)	RF11-06 (ml/l)	RF11-07 (ml/l)	RF11-08 Leg 1 (ml/l)	RF11-08 Leg 2 (ml/l)
0.3	0.0081	0.0100	0.0083	0.0089
0.5	0.0081	0.0101	0.0084	0.0089
1.0	0.0080	0.0101	0.0083	0.0089
1.5	0.0080	0.0102	0.0084	0.0089
2.0	0.0081	0.0105	0.0085	0.0089
3.0	0.0086	0.0113	0.0092	0.0094
4.0	0.0095	0.0125	0.0104	0.0103
5.0	0.0107	0.0141	0.0119	0.0115
6.0	0.0122	0.0159	0.0136	0.0130
7.0	0.0138	0.0179	0.0155	0.0146
8.0	0.0155	0.0200	0.0175	0.0163

(coverage factor; k=1)

(17) Results

(17.1) Comparison at cross-point during this cruise

Cross-points during this cruise were three points. The first cross-point of Stn.14 (RF3997) and Stn.23 (RF4007) was located at 39°40'N/147°50'E, the second cross-point of Stn.55 (RF4039) and Stn.56 (RF4040) was located at 40°N/165°E, the third cross-point of Stn.105 (RF4089) and Stn.106 (RF4090) was located at 9°N/164°E. Each cross-point was conducted two times at interval of about two weeks, about twenty days, about a week, respectively.

Dissolved oxygen profiles of the two hydrocasts at each cross-point agreed well (Figure C.3.7). In the layers deeper than 4,000 dbar, the difference between the two hydrocasts at each cross-point was calculated to be 0.48 ± 0.29 μmol/kg, -0.05 ± 0.70 μmol/kg, -0.11 ± 0.61 μmol/kg, respectively.

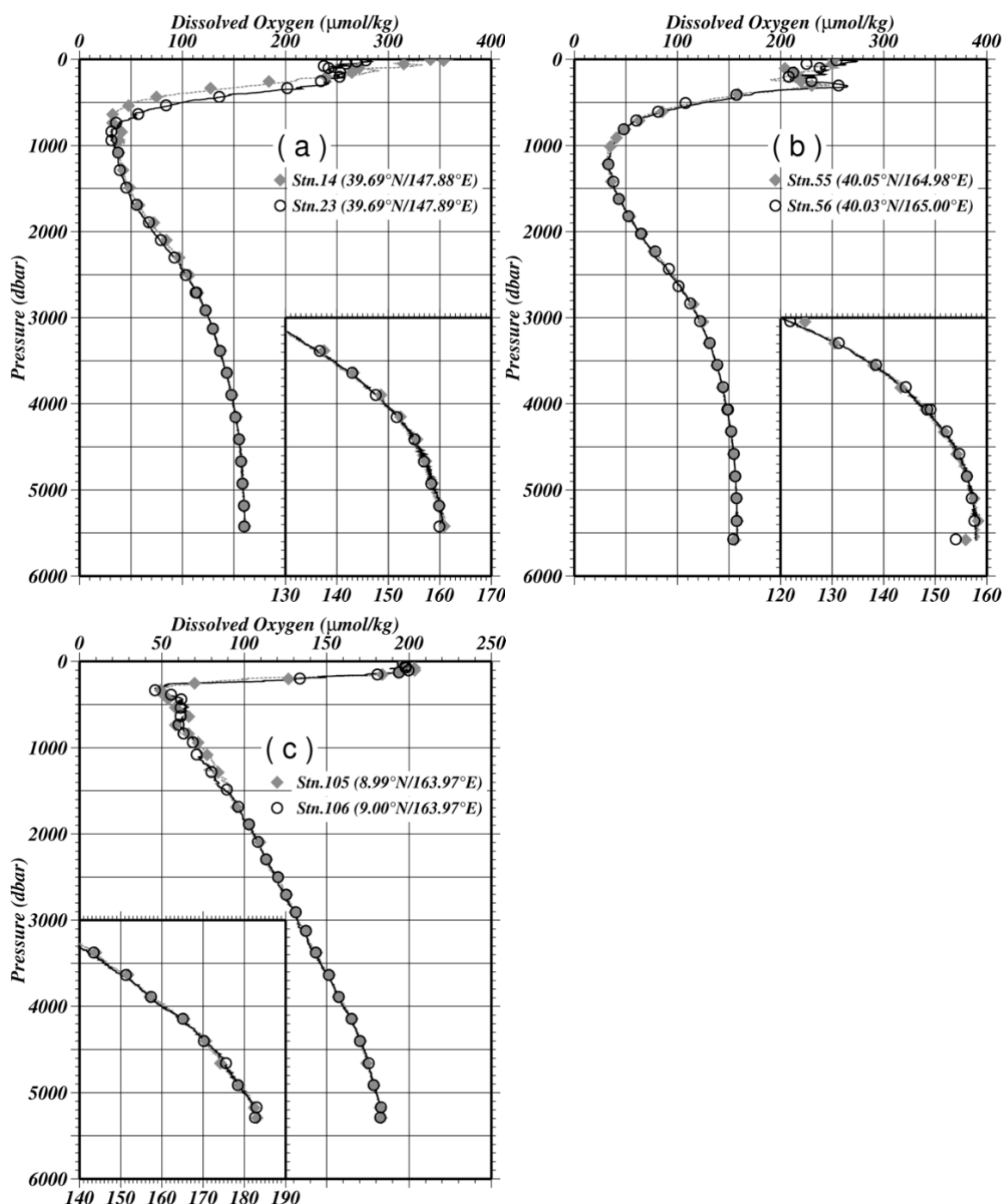


Figure C.3.7 Comparison of dissolved oxygen profiles between the first hydrocast (gray diamonds) and the second one (open circles) at the cross-point of (a) 39°40'N/147°52'E, (b) 40°N/165°E and (c) 9°N/164°E. Lines denote the profiles of the oxygen sensor.

(17.2) Comparison at cross-point of WHP sections

WHP-P13 has some cross-points among other WHP lines. Around 47°N/165°E, WHP-P13 line intersects WHP-P1 line. WHP-P1 was observed three times in 1985, 1999 and 2007. Around 30°N/165°E, 24°N/165°E and 9°N/164°E, WHP-P13 line intersects WHP-P2 line, WHP-P3 line and WHP-P4 line, respectively. WHP-P2 was observed two times in 1994 and 2004, WHP-P3 was observed two times in 1985 and 2005/06, WHP-P4 was observed one

time in 1989. Dissolved oxygen profiles between one in this cruise and in 2000s at each cross points agreed well (Figure C.3.8). But it was found that oxygen data in this cruise were significantly lower than those in 1980s and 1990s in deep layers. This difference should be discussed carefully. The difference between this cruise and other cruise below 4,000 dbar are shown in Table C.3.8.

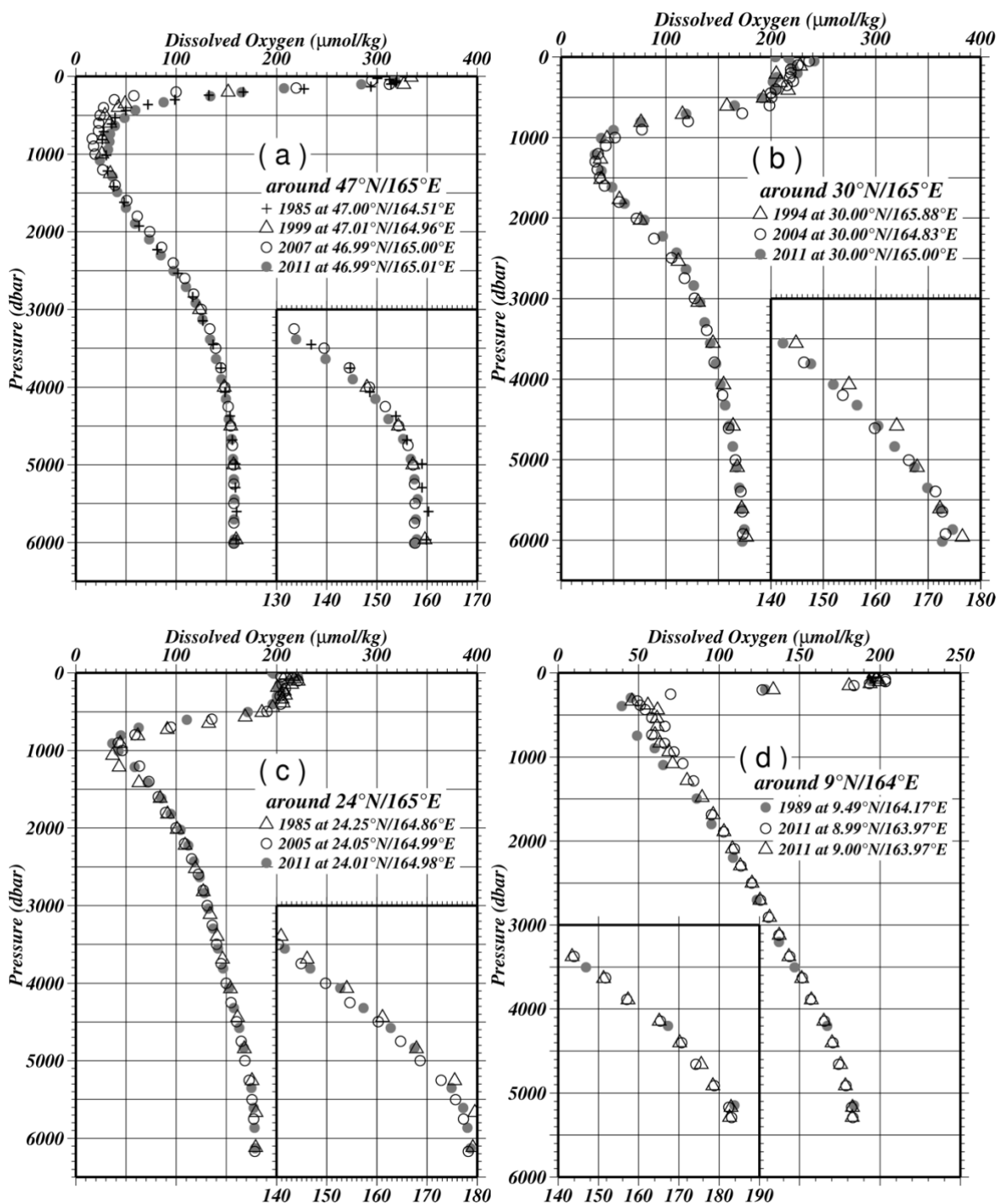


Figure C.3.8 Comparison of dissolved oxygen profiles at the cross-point of (a) WHP-P1, (b) WHP-P2, (c) WHP-P3 and (d) WHP-P4.

Table C.3.8 Difference between oxygen data in this cruise and in WHP cruise below 4,000 dbar.

Cruise	Year	Difference ($\mu\text{mol/kg}$)
P1	1985	-1.51 ± 0.68
	1999	-0.72 ± 0.56
	2007	-0.26 ± 0.59
P2	1994	-1.73 ± 1.51
	2004	0.23 ± 0.76
P3	1985	-1.28 ± 0.62
	2005/06	0.99 ± 0.45
P4	1989	(Stn.105) -1.68 ± 0.85
		(Stn.106) -1.60 ± 0.58

(17.3) Comparison with WHP-P13 oxygen data in 1990s

WHP-P13 was observed three times, the first and third in 1991 and 1993 by University of Tokyo, the second in 1992 by National Oceanographic and Atmospheric Administration (NOAA). We compared oxygen data in this cruise and ones in each cruises (Figure C.3.9). In deep layers, dissolved oxygen has been decreased from 1991 or 1993. On the other hand, in the comparison with data in 1992, change in each region is not constant. Especially, dissolved oxygen in the subtropical zone from 10°N to 20°N has been increased greatly. Below 4,000 dbar, the difference in average is shown in Figure C.3.10 and Table C.3.9. Because it is necessary to consider offset value in each cruise, these differences should be discussed carefully.

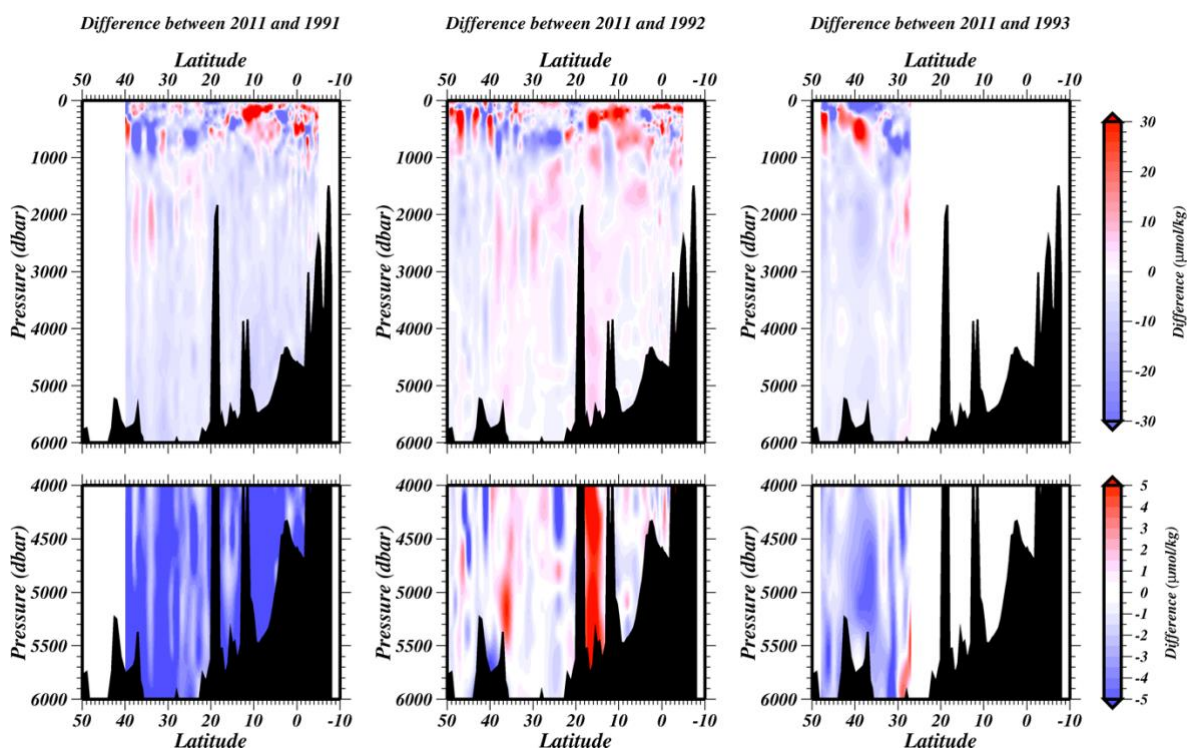


Figure C.3.9 Difference of dissolved oxygen between (left) 2011 and 1991 (2011 data minus 1991 data), (center) 2011 and 1992 (2011 data minus 1992 data), (right) 2011 and 1993 (2011 data minus 1993 data) against pressure.

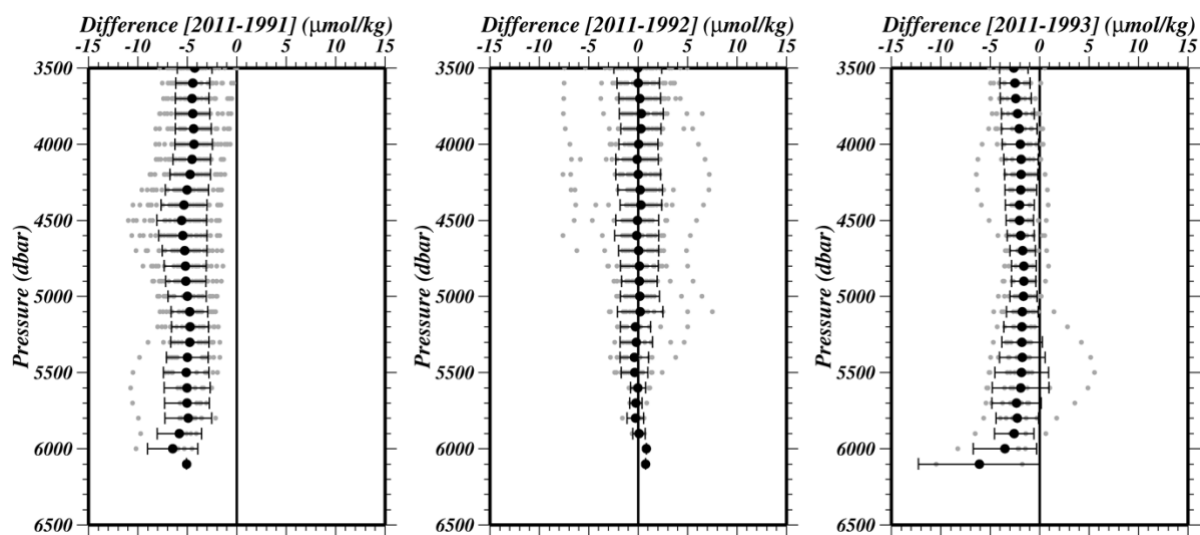


Figure C.3.10 Difference of dissolved oxygen on each 100 dbar. Black closed circles denote the mean of differences with 1σ error.

Table C.3.9 Difference in average below 4,000 dbar.

	Difference in average
1991	-5.01±2.13
1992	0.00±1.96
1993	-1.93±1.87

Reference

- Cullberson, A.H. (1994), Dissolved oxygen, in *WHPO Pub. 91-1 Rev. 1*, November 1994, Woods Hole, Mass., USA.
- Cullberson, A.H., G. Knapp, M.C. Stalcup, R.T. Williams, and F. Zemlyak (1991), A comparison of methods for the determination of dissolved oxygen in seawater, *WHPO Pub. 91-2*, August 1991, Woods Hole, Mass., USA.
- DOE (1994), Handbook of methods for the analysis of the various parameters of the carbon dioxide system in sea water; version 2. A.G. Dickson and C. Goyet (eds), ORNL/CDIAC-74.
- Gouretski, V.V. and K. Jancke (2001), Systematic errors as the causes for an apparent deep water property variability: global analysis of the WOCE and historical hydrographic data, *Prog. Oceanogr.*, 48, 337-402.
- JAMSTEC, WHP P03 REVISIT DATA BOOK (2001), edited by T. Kawano and H. Uchida, JAMSTEC.
- JMA, WHP P09 REVISIT CRUISE REPORT (2013)
- Johson, G.C., P.E. Robbins, and G.E. Hufford (2001), Systematic adjustments of hydrographic sections for internal consistency, *J. Atmos. Oceanic Technol.*, 18, 1234-1244.
- Langdon, C. (2010), Determination of dissolved oxygen in seawater by Winkler titration using the amperometric technique, *IOCCP Report No.14, ICPO Pub. 134, 2010 ver.1*
- Murray, C.N., J.P. Riley and T.R.S. Wilson (1968), The solubility of oxygen in Winkler reagents used for the determination of dissolved oxygen, *Deep-Sea Res.*, **15**, 237-238
- Swift, J. H. (2010): Reference-quality water sample data: Notes on acquisition, record keeping, and evaluation. *IOCCP Report No.14, ICPO Pub. 134, 2010 ver.1*

4. *Nutrients*

Updated 8 July 2020

(1) Personnel

RF 11-06

Sonoki IWANO (GEMD/JMA)

Takahiro KITAGAWA (GEMD/JMA)

Shinichiro UMEDA (GEMD/JMA)

RF 11-07

Naoki NAGAI (GEMD/JMA)

Hiroyuki FUJIWARA (GEMD/JMA)

Tomohiro UEHARA (GEMD/JMA)

RF 11-08

Naoki NAGAI (GEMD/JMA)

Takahiro KITAGAWA (GEMD/JMA)

Hiroyuki FUJIWARA (GEMD/JMA)

(2) Station occupied

A total of 148 stations (RF 11-06: 19, RF 11-07: 33, RF 11-08 leg1: 50, leg2: 46) were occupied for nutrients. Station location and sampling layers of nutrients are shown in Figure C.4.1.

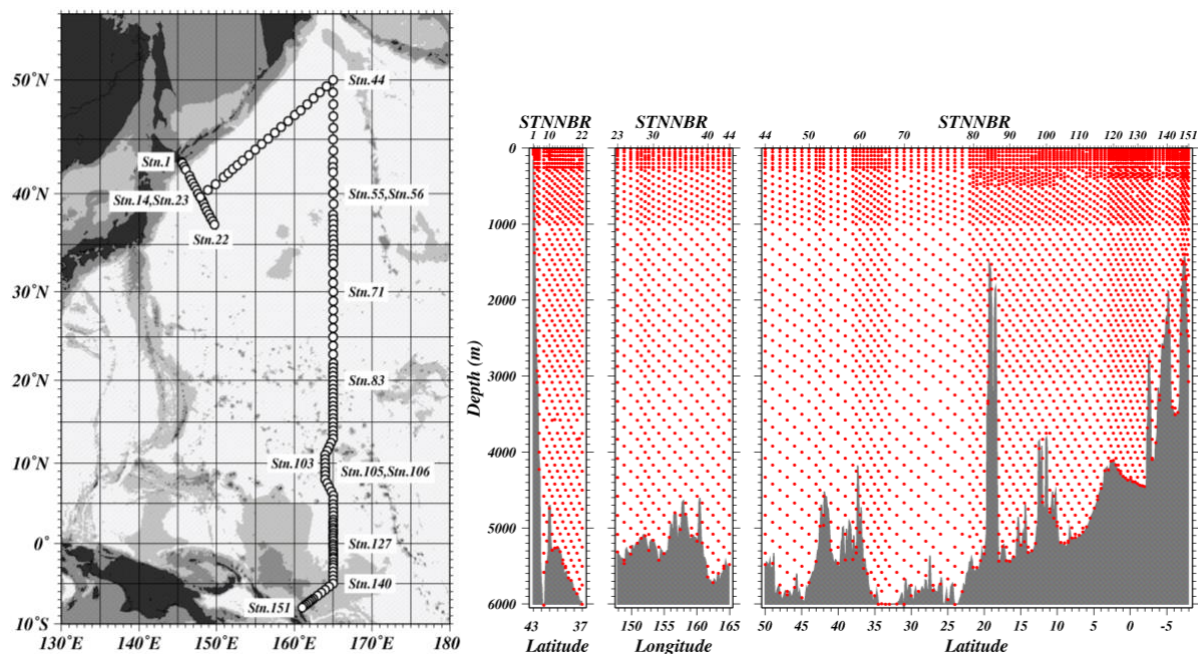


Figure C.4.1 Station location (left) and sampling layers (right) of nutrients.

(3) Instrument and Method

(3.1) Analytical detail using Auto Analyzer III systems (BLTEC)

The nutrients analyses were carried out on 4-channel Auto Analyzer III (BLTEC). Measured Parameters are nitrate + nitrite, nitrite, phosphate and silicate.

Nitrate + nitrite and nitrite are analyzed according to the modification method of *Armstrong* (1967). The sample nitrate is reduced to nitrite in a cadmium tube inside of which is coated with metallic copper. The sample stream with its equivalent nitrite is treated with an acidic, sulfanilamide reagent and the nitrite forms nitrous acid which reacts with the sulfanilamide to produce a diazonium ion. N-1-Naphthylethylene-diamine added to the sample stream then couples with the diazonium ion to produce a red, azo dye. With reduction of the nitrate to nitrite, both nitrate and nitrite react and are measured; without reduction, only nitrite reacts. Thus, for the nitrite analysis, no reduction is performed and the alkaline buffer is not necessary.

The phosphate analysis is a modification of the procedure of *Murphy and Riley* (1962). Molybdic acid is added to the seawater sample to form phosphomolybdic acid which is in turn reduced to phosphomolybdous acid using L-ascorbic acid as the reductant.

The silicate method is analogous to that described for phosphate. The method used is essentially that of *Grasshoff et al.* (1983), wherein silicomolybdic acid is first formed from the silicate in the sample and added molybdic acid, then the silicomolybdic acid is reduced to silicomolybdous acid, or "molybdenum blue," using L-ascorbic acid as the reductant.

The flow diagrams and reagents for each parameter are shown in Figures C.4.2-C.4.5.

(3.2) Nitrate Reagents

Ammonium chloride (buffer), 0.7 M (0.04 % w/v);

Dissolve 190 g Ammonium chloride, NH_4Cl , in ca. 5000 ml of milli-Q water, add about 5 ml Ammonia(aq.), adjust pH 8.2-8.5.

Sulfanilamide, 0.06 M (1 % w/v);

Dissolve 5 g Sulfanilamide, $4\text{-NH}_2\text{C}_6\text{H}_4\text{SO}_3\text{H}$, in 430 ml milli-Q water, add 70 ml concentrated HCl. After mixing, 1 ml Brij-35 (22 % w/w) is added.

N-1-Naphthylethylene-diamine dihydrochloride (NEDA), 0.004 M (0.1 % w/v);

Dissolve 0.5 g NEDA, $\text{C}_{10}\text{H}_7\text{NH}_2\text{CH}_2\text{CH}_2\text{NH}_2 \cdot 2\text{HCl}$, in 500 ml milli-Q water.

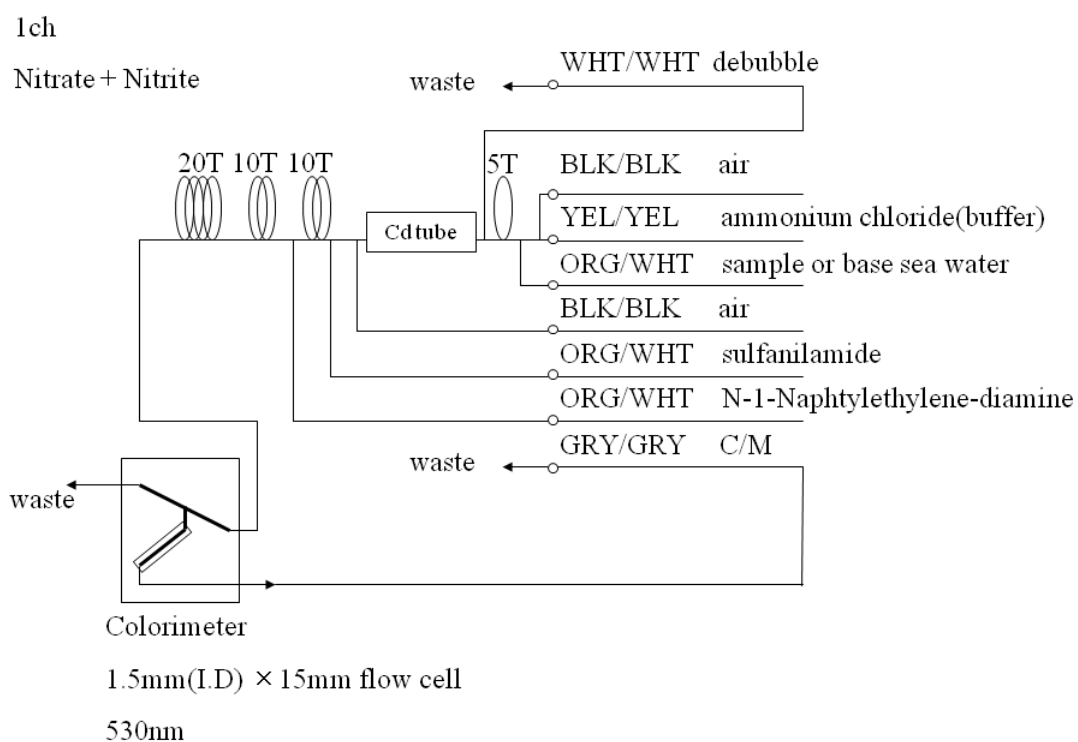


Figure C.4.2 1ch. (Nitrate + nitrite) Flow diagram.

(3.3) Nitrite Reagents

Sulfanilamide, 0.06 M (1 % w/v);

Dissolve 5 g Sulfanilamide, 4-NH₂C₆H₄SO₃H, in 430 ml milli-Q water, add 70 ml concentrated HCl. After mixing, 1 ml Brij-35 (22 % w/w) is added.

N-1-Naphtylethylene-diamine dihydrochloride (NEDA), 0.004 M (0.1 % w/v);

Dissolve 0.5 g NEDA, C₁₀H₇NH₂CH₂CH₂NH₂·2HCl, in 500 ml milli-Q water.

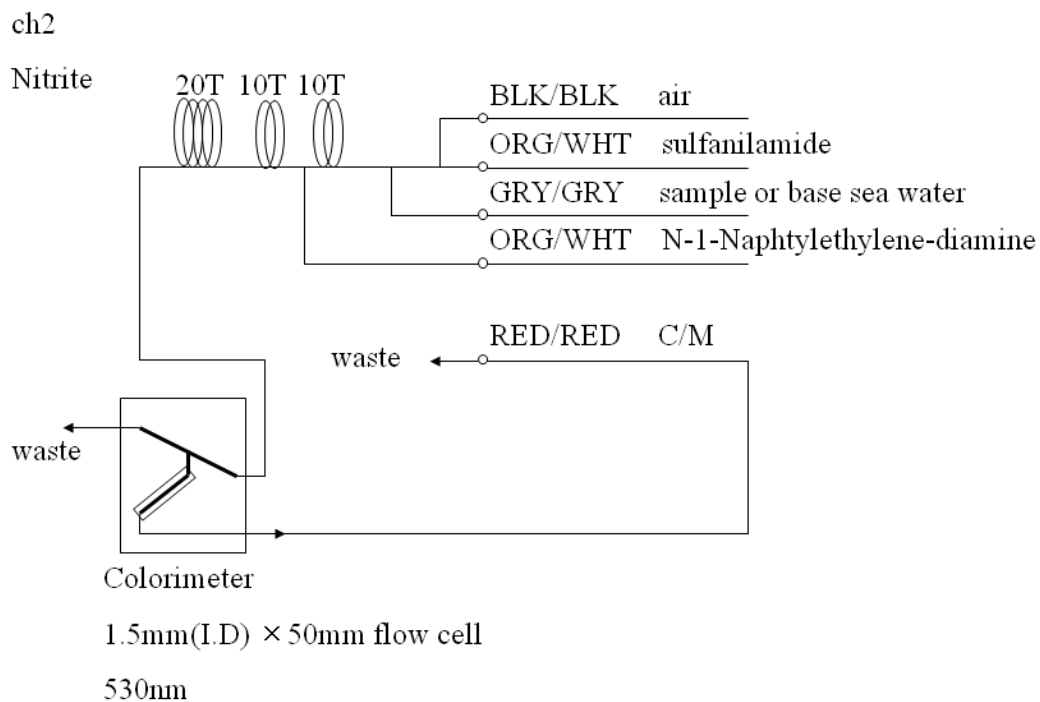


Figure C.4.3 2ch. Nitrite Flow diagram.

(3.4) Phosphate Reagents

Ammonium molybdate, 0.005 M (0.6 % w/v);

Dissolve 3 g Ammonium molybdate(VI) tetrahydrate, $(\text{NH}_4)_6\text{Mo}_7\text{O}_{24}\cdot 4\text{H}_2\text{O}$, and 0.05 g Potassium antimonyl tartrate, $\text{C}_8\text{H}_4\text{K}_2\text{O}_{12}\text{Sb}_2\cdot 3\text{H}_2\text{O}$, in 400 ml milli-Q water and add 100 ml H_2SO_4 (12.6N). After mixing, 2 ml Sodium dodecyl sulfate (15 % solution in water) is added.

L(+)-Ascorbic acid, 0.08 M (1.5 % w/v);

Dissolve 4.5 g L(+)-Ascorbic acid, $\text{C}_6\text{H}_8\text{O}_6$, in 300 ml milli-Q water. After mixing, 5 ml Acetone is added. Freshly prepared before every measurement.

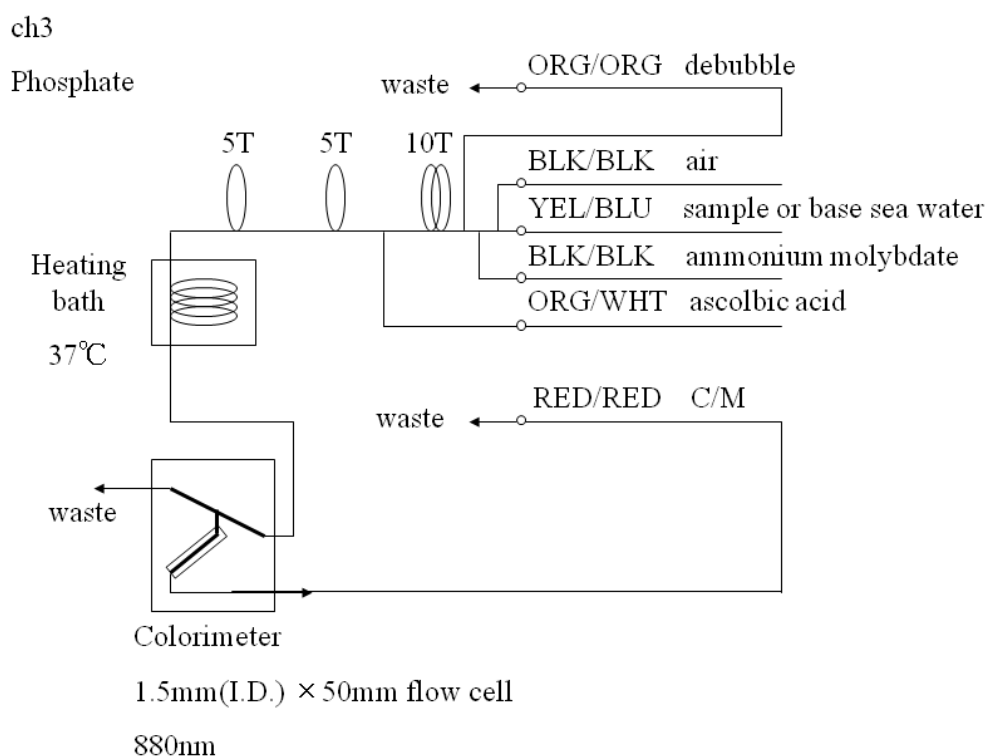


Figure C.4.4 3ch. Phosphate Flow diagram.

(3.5) Silicate Reagents

Ammonium molybdate, 0.005 M (0.6 % w/v);

Dissolve 3 g Ammonium molybdate(VI) tetrahydrate, $(\text{NH}_4)_6\text{Mo}_7\text{O}_{24}\cdot 4\text{H}_2\text{O}$, in 500 ml milli-Q water and added 5 ml H_2SO_4 (12.6N). After mixing, 2 ml Sodium dodecyl sulfate (15 % solution in water) is added.

Oxalic acid, 0.4 M (5 % w/v);

Dissolve 25 g Oxalic acid dihydrate, $(\text{COOH})_2\cdot 2\text{H}_2\text{O}$, in 500 ml milli-Q water.

L(+)-Ascorbic acid, 0.08 M (1.5 % w/v);

Dissolve 4.5 g L(+)-Ascorbic acid, $\text{C}_6\text{H}_8\text{O}_6$, in 300 ml milli-Q water. After mixing, 5 ml Acetone is added. Freshly prepared before every measurement.

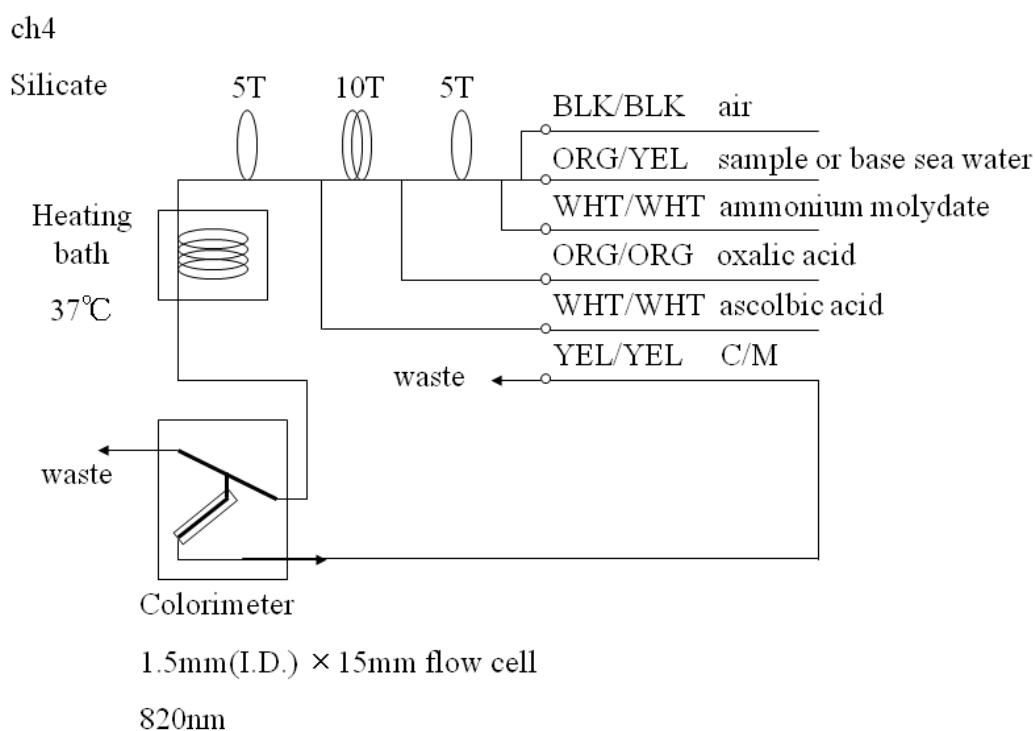


Figure C.4.5 4ch. Silicate Flow diagram.

(3.6) Sampling procedures

Seawater samples were collected from 10 liter Niskin sample bottles attached CTD-system and a stainless steel bucket for the surface. Sampling of nutrients followed that oxygen and trace gases. Samples were drawn into 10 ml polymethylpenten vials with sample drawing tubes. These were rinsed three times before filling and vials were capped immediately after the drawing.

No transfer was made and the vials were set an auto sampler tray directly. Samples were analyzed immediately after collection.

(3.7) Data processing

Raw data from Auto Analyzer III were treated as follows;

- Check the shape of each peak and position of peak values taken, and then change the positions of peak values taken if necessary.
- Baseline correction was done basically using liner regression.
- Reagent blank correction was done basically using liner regression.
- Carry-over correction was applied to peak heights of each sample.
- Sensitivity correction was applied to peak heights of each sample.
- Refraction error correction was applied to peak heights of each seawater sample.
- Calibration curve to get nutrients concentration were assumed quadratic expression.
- Load pressure and salinity from CTD data to calculate density of seawater.
- Convert data from $\mu\text{mol/l}$ to $\mu\text{mol/kg}$.

(4) Nutrients standards

(4.1) Volumetric Laboratory Ware of in-house standards

All volumetric ware used were gravimetrically calibrated. Polymethylpenten volumetric flasks were gravimetrically calibrated at the temperature of use within 3-6 K.

Volumetric flasks

The weights obtained in the calibration weightings were corrected for the density of water and air buoyancy.

Pipettes and pipettors

All pipettes have nominal calibration tolerances of 0.1 % or better. These were gravimetrically calibrated in order to verify and improve upon this nominal tolerance.

(4.2) Reagents, general considerations

Specifications

For nitrate standard, “potassium nitrate 99.995 suprapur” provided by Merck, CAS No. : 7757-79-1, was used.

For phosphate standard, “potassium dihydrogen phosphate anhydrous 99.995 suprapur” provided by Merck, CAS No. : 7778-77-0, was used.

For nitrite standard, “sodium nitrite GR for analysis ACS, Reag. Ph Eur” provided by Merck, CAS No. : 7632-00-0, was used.

For the silicate standard, we use “Silicon standard solution traceable to SRM from NIST SiO_2 in NaOH 0.5 mol/l 1000 mg/l Si CertiPUR” provided by Merck, which lot number is HC074650 is used. The silicate concentration is certified by NIST-SRM3150 with the uncertainty of 0.5 %. Factor of HC074650 was signed 1.000, however we reassigned the factor as 0.975 from the result of comparison with HC814662.

Ultra pure water

Ultra pure water (Milli-Q water) freshly drawn was used for preparation of reagents, higher concentration standards and for measurement of reagent and system blanks.

Low Nutrient Seawater (LNSW)

Surface water having low nutrient concentration was taken and filtered using 10 µm pore size membrane filter. This water is stored in 20 liter flexible container with paper box.

(4.3) Concentrations of nutrients for A, B and C standards

Concentrations of nutrients for A, B and C standards are set as shown in Table C.4.1.1-C.4.1.2. RF11-06 and RF11-07 cruises used standard concentration were table C.4.1.1 and RF11-08 cruise used standard concentration was table C.4.1.2. The C standard is prepared according recipes as shown in Table C.4.2. All volumetric laboratory tools were calibrated prior the cruise as stated in chapter (4.1). Then the actual concentration of nutrients in each fresh standard was calculated based on the ambient, solution temperature and determined factors of volumetric lab. wares. The calibration curves for each run were obtained using 5 levels, C-1, C-2, C-3, C-4 and C-5.

Table C.4.1.1 Nominal concentrations of nutrients for A, B and C standards at RF11-06 and RF11-07.

Unit: µmol/l

	A	B	C-1	C-2	C-3	C-4	C-5 (Full scale)
NO ₃	28700	570	LNSW*	1/4 Full scale	2/4 Full scale	3/4 Full scale	47.5
NO ₂	12500	250	LNSW*	1/4 Full scale	2/4 Full scale	3/4 Full scale	1.98
PO ₄	2180	43.5	LNSW*	1/4 Full scale	2/4 Full scale	3/4 Full scale	3.46
Si	35600	2250	LNSW*	1/4 Full scale	2/4 Full scale	3/4 Full scale	178

Table C.4.1.2 Nominal concentrations of nutrients for A, B and C standards at RF11-08.

Unit: µmol/l

	A	B	C-1	C-2	C-3	C-4	C-5 (Full scale)
NO ₃	27400	546	LNSW*	1/4 Full scale	2/4 Full scale	3/4 Full scale	45.5
NO ₂	12500	250	LNSW*	1/4 Full scale	2/4 Full scale	3/4 Full scale	1.98
PO ₄	2120	42.3	LNSW*	1/4 Full scale	2/4 Full scale	3/4 Full scale	3.36
Si	35600	2070	LNSW*	1/4 Full scale	2/4 Full scale	3/4 Full scale	165

Table C.4.2 Working calibration standard recipes.

C Std.	B-1 Std.	B-2 Std.
C-5 (Full scale)	20 ml	2 ml
	LNSW*	C-5 (Full scale)
C-1	40 ml	0 ml
C-2	30 ml	10 ml
C-3	20 ml	20 ml
C-4	10 ml	30 ml
C-5	0 ml	40 ml

B-1 Std.: Mixture of nitrate, phosphate and silicate.

B-2 Std.: Nitrite.

LNSW*: 22 ml milli-Q water in 250 ml volumetric flask, and LNSW add to marked line.

(4.4) Renewal of in-house standard solutions

In-house standard solutions as stated in (4.3) were renewed as shown in Table C.4.3.

Table C.4.3 Timing of renewal of in-house standards.

NO ₃ ,NO ₂ ,PO ₄ ,Si	Renewal
A-1 Std.(NO ₃)	no renewal
A-2 Std.(NO ₂)	no renewal
A-3 Std.(PO ₄)	no renewal
A-4 Std.(Si)	commercial prepared solution
B Std.	
B-1 Std.	maximum 10 days
B-2 Std.	maximum 18 days
C Std.	Renewal
mixture of B-1 and B-2 Std.	Every measurement

B-1 Std.: Mixture of nitrate, phosphate and silicate.

B-2 Std.: nitrite.

(5) Use of RMNS

The reference material of nutrients in seawater (hereafter RMNS), which was prepared by the General Environmental Technos Co. Ltd. (Kanso Technos), was used every analysis at each hydrographic station. According to *Aoyama et al.* (2010), the RMNS homogeneity is 0.1 % - 0.2 % in high concentration range, and stability is 48 – 71 months. By the use of RMNSs for

the analysis of seawater, it is expected to secure stable comparability and uncertainty of data. If RMNS will be certified in the future, the traceability of our analysis value will be secured. Aoyama et al. (2010) assigned nutrients concentrations for RMNS lot BE and BF and the measured concentrations by Kanso Technos for lot BS and BT as shown in Table C.4.4.

Table C.4.4 INSS assigned concentration of RMNSs. Unit: $\mu\text{mol/kg}$

	Nitrate	Phosphate	Silicate
RMNS-BS*	$0.058^{**}\pm 0.012$	0.054 ± 0.004	2.411 ± 0.0674
RMNS-BT*	18.15 ± 0.056	1.296 ± 0.0065	42.02 ± 0.21
RMNS-BE	36.70 ± 0.04	2.662 ± 0.005	99.20 ± 0.08
RMNS-BF	41.39 ± 0.05	2.809 ± 0.006	150.61 ± 0.14

* RMNS-BS,BT data at KANSO Technos.

** The value are below quantifiable detection limit (QDL), use these value as a guide.

(5.1) RMNSs for this cruise

RMNS lots BS, BT, BE and BF were prepared to use every analysis at every hydrographic station. All RMNS lots were renewed every run on the same day. The RMNS bottles were stored at a room in the ship.

It is noted that nutrient data in our report are calibrated not on RMNS but on in-house standard solutions. Therefore, to calculate data based on RMNS, it is necessary that values of nutrient concentration in our report are correlated with RMNS values measured in the same analysis run. The result of RMNS measurements is attached as 49UP20110515_P13_nut_RM_measurement.csv.

(5.2) Assigned concentration of RMNSs

We assigned nutrients concentrations for RMNS lots BS, BT, BE and BF shown in Table C.4.5 based on the analysis during the cruise. The measured concentration of RMNS lot BE during the cruise are shown in Figure C.4.6–C.4.8 as quality control charts. The concentration variations in these figures represent largely differences of the in-house standard. The concentrations of RMNSs were in close agreement with expected values within the range of uncertainty.

Table C.4.5 Assigned concentration of RMNSs. Unit: $\mu\text{mol/kg}$

	Nitrate + nitrite	Phosphate	Silicate
RMNS-BS	0.05 ± 0.04	0.04 ± 0.01	1.76 ± 0.12
RMNS-BT	18.68 ± 0.06	1.28 ± 0.01	42.24 ± 0.17
RMNS-BE	36.89 ± 0.08	2.65 ± 0.01	102.08 ± 0.30
RMNS-BF	41.53 ± 0.08	2.79 ± 0.01	154.41 ± 0.41

Note: N (BS,BE)=145 (Silicate=143), N(BT,BF)=124 (Silicate=122) at data flag 2.

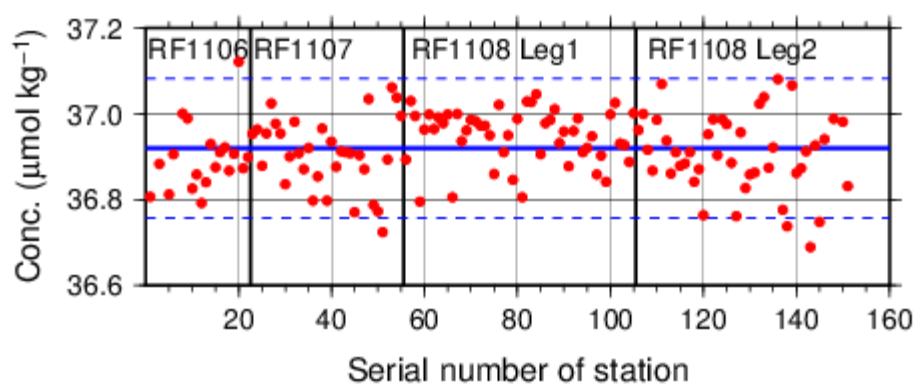


Figure C.4.6. Result of RMNS lot BE concentrations of nitrate + nitrite during the cruise.

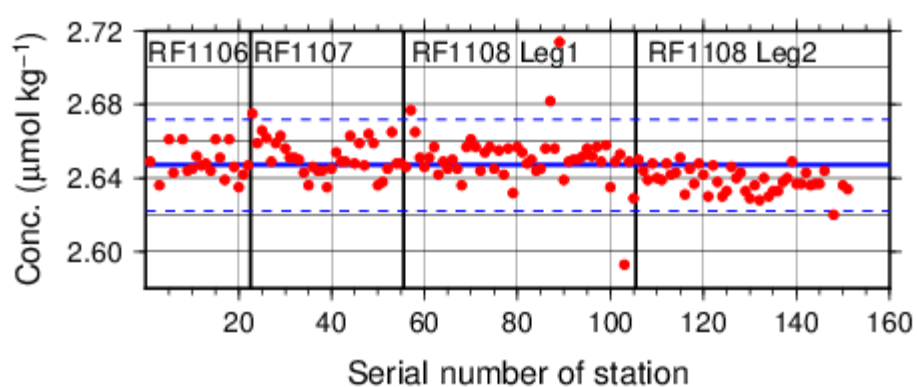


Figure C.4.7. Result of RMNS lot BE concentrations of phosphate during the cruise.

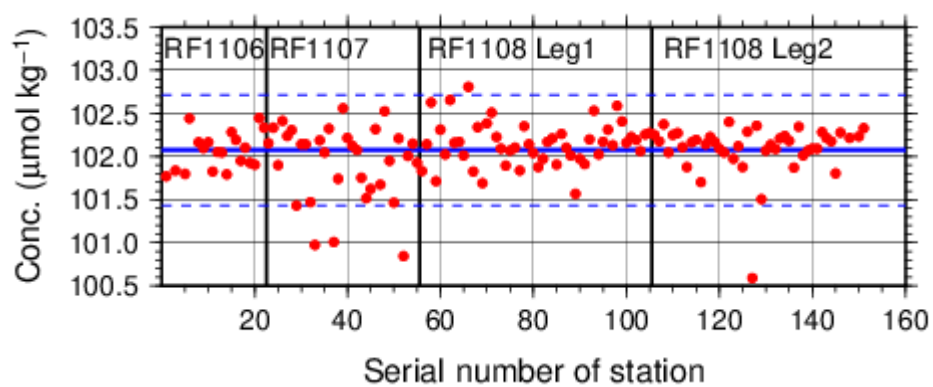


Figure C.4.8. Result of RMNS lot BE concentrations of silicate during the cruise.

(5.3) Relative standard deviation of RMNSs measurement

The relative standard deviation of lot BS, BT, BE and BF throughout the cruise are shown in Table C.4.6.

Table C.4.6 Relative standard deviation of RMNSs lot BS, BT, BE and BF measurements in each run throughout cruise.

	Nitrate + nitrite CV %	Phosphate CV %	Silicate CV %
RMNS-BS	87.18	32.45	6.83
RMNS-BT	0.34	0.99	0.38
RMNS-BE	0.22	0.49	0.30
RMNS-BF	0.19	0.44	0.24

Note: N=123, N(Silicate)=121.

(6) Quality control

(6.1) Precision of nutrients analyses during the cruise

Precision of nutrients analyses during the cruise was evaluated based on 7 measurements of the C-5 (full scale) standard in each run. Summary of precisions are shown in Table C.4.7.

During this cruise, analytical precisions were 0.15 % for nitrate, 0.15 % for phosphate and 0.13 % for silicate in terms of mean of precision, respectively. The time series of precision are shown in Figures C.4.9–C.4.11.

Table C.4.7 Summary of precision during the cruise.

	Nitrate + nitrite CV %	Phosphate CV %	Silicate CV %
Median	0.14	0.13	0.12
Mean	0.15	0.15	0.13
Maximum	0.38	0.36	0.33
Minimum	0.04	0.06	0.03
Number	146	146	144

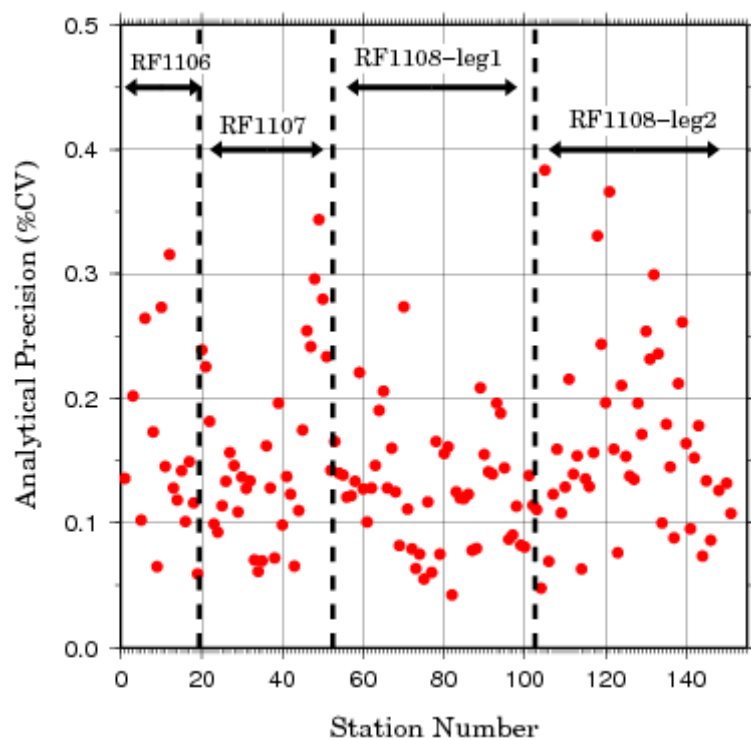


Figure C.4.9 Time series of precision of nitrate + nitrite for RF1106-08.

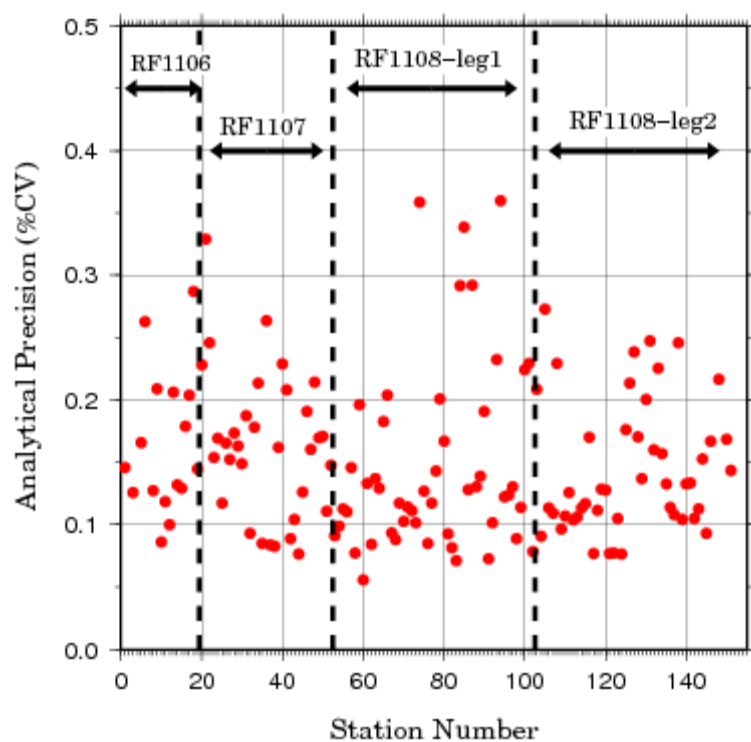


Figure C.4.10 Time series of precision of phosphate for RF1106-08.

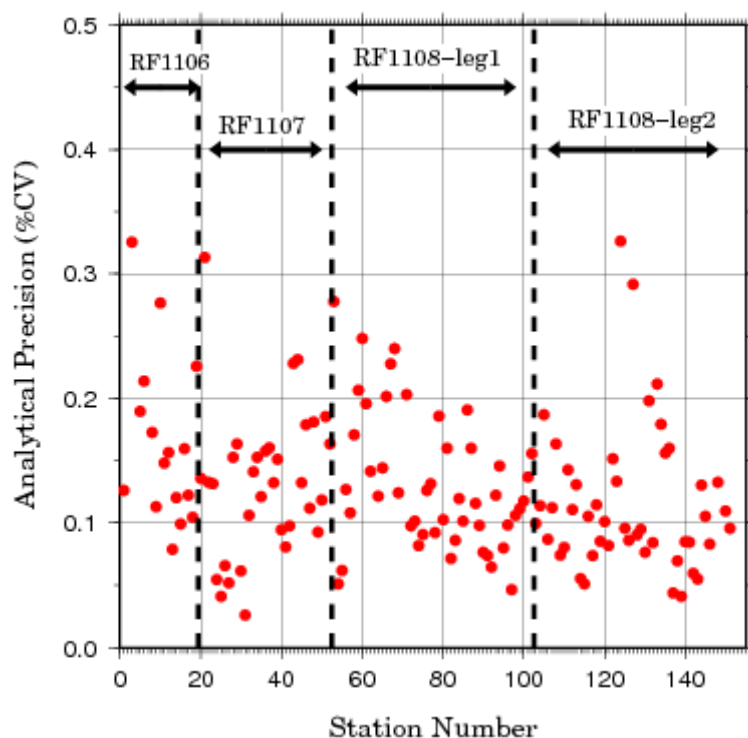


Figure C.4.11 Time series of precision of silicate for RF1106-08.

(6.2) Replicate sample measurement

Replicate sample were analyzed at every hydrographic station. Total amount of the replicate sample pairs was 589. Summary of replicate sample measurements are shown in Table C.4.8, and Figure C.4.12 - C.4.14. During this cruise, the average difference and standard deviation of replicate measurement were 0.046 ± 0.046 ($\mu\text{mol/kg}$) for nitrate+nitrite, 0.004 ± 0.004 ($\mu\text{mol/kg}$) for phosphate and 0.116 ± 0.114 ($\mu\text{mol/kg}$) for silicate, respectively.

Table C.4.8 Average difference of replicate samples in each run throughout cruise.

Unit: $\mu\text{mol/kg}$		
Nitrate + nitrite	Phosphate	Silicate
0.046 ± 0.046	0.004 ± 0.004	0.116 ± 0.114

Note: N=587(nitrate + nitrite), N=572(phosphate), N=563(silicate) at flag 2.

RF1106-08_NO₃ Result of Replicate Sampling (N=587)

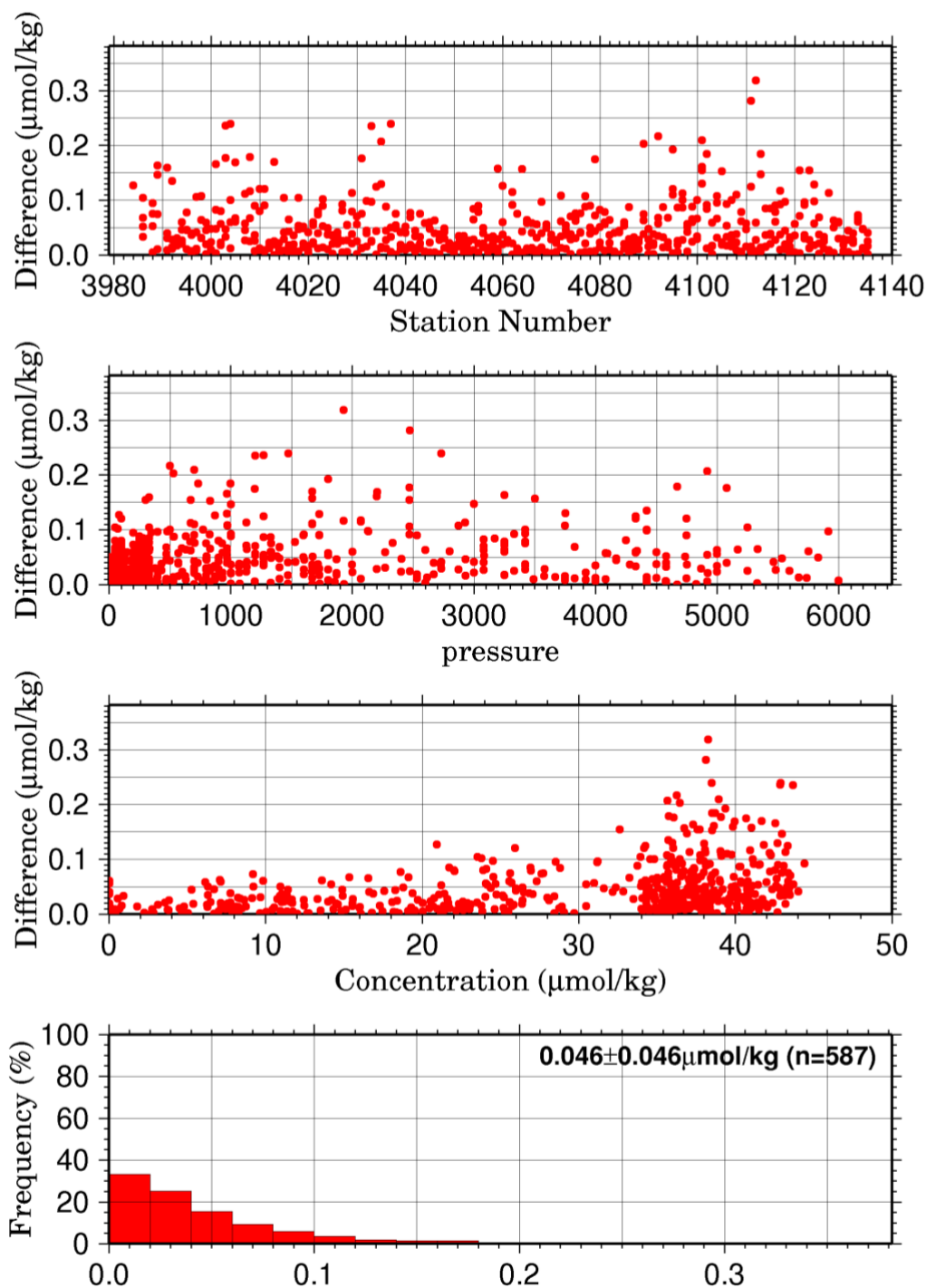


Figure C.4.12 Result of nitrate + nitrite replicate samplings (N=587) during RF1106-08 against (a) station number, (b) sampling pressure, (c) concentration and (d) histogram of the result of replicate samplings.

RF1106-08_PO₄ Result of Replicate Sampling (N=572)

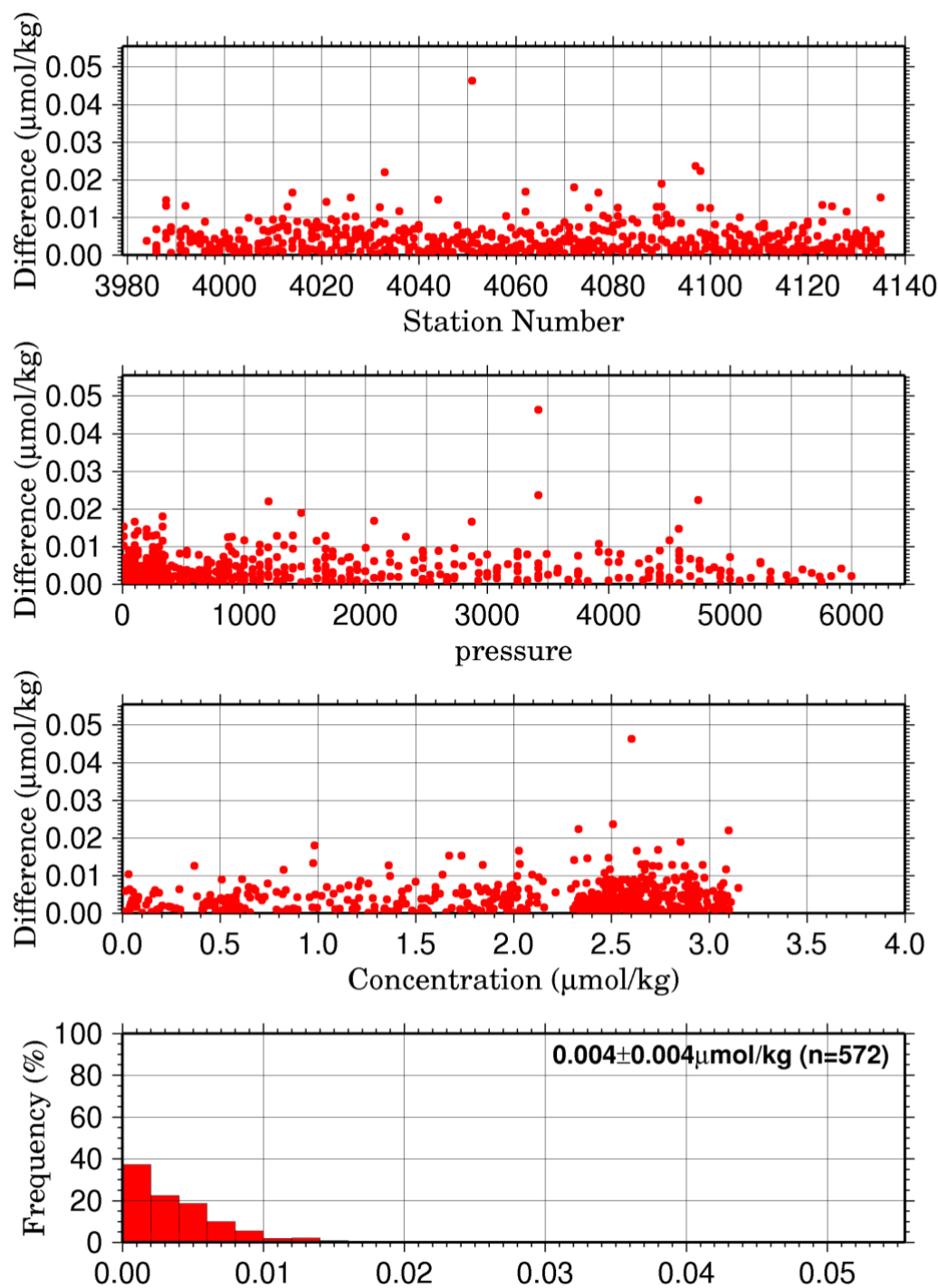


Figure C.4.13 Result of phosphate replicate samplings (N=572) during RF1106-08 against (a) station number, (b) sampling pressure, (c) concentration and (d) histogram of the result of replicate samplings.

RF1106-08_SiO₂ Result of Replicate Sampling (N=563)

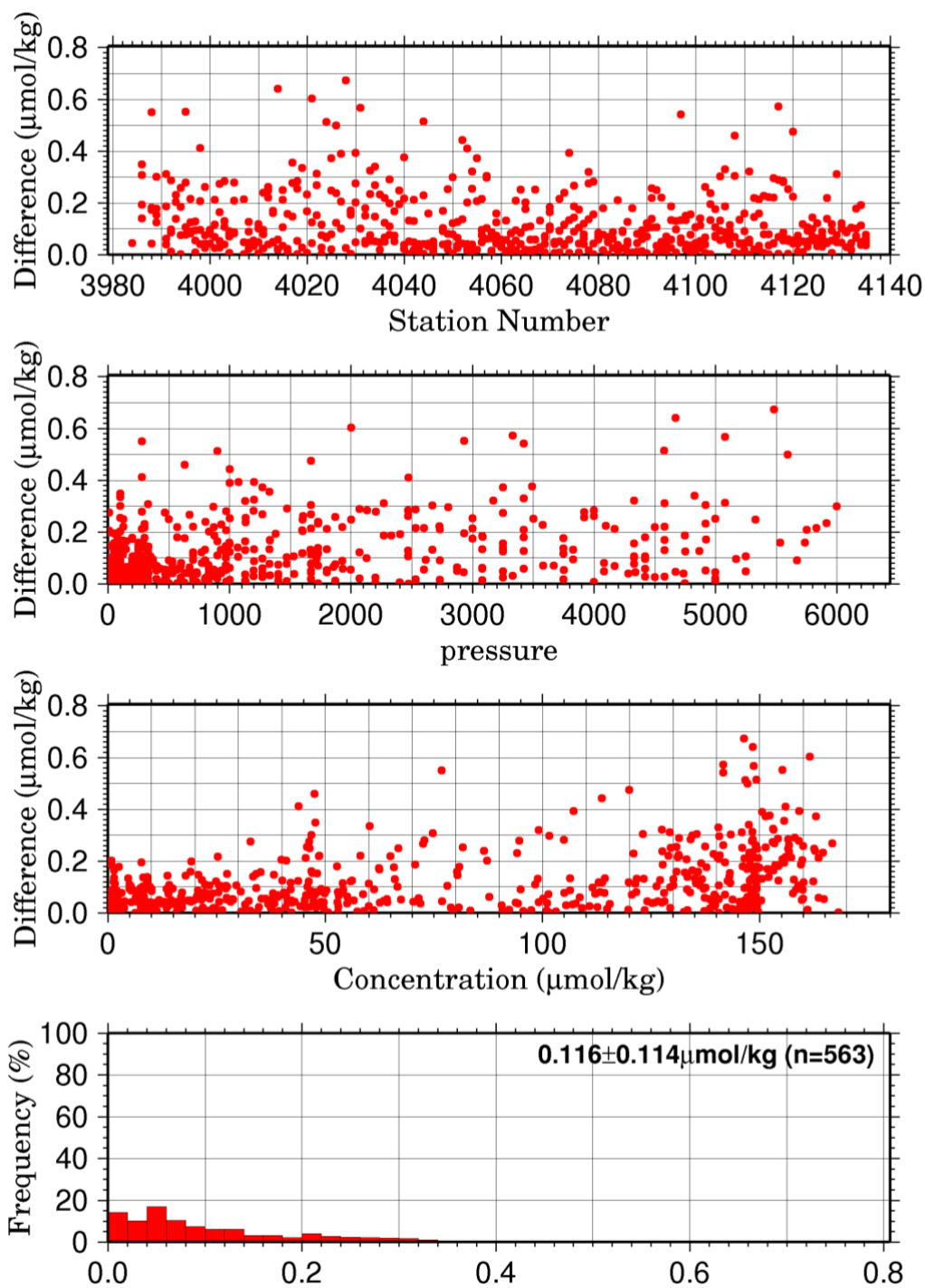


Figure C.4.14 Result of silicate replicate samplings (N=563) during RF1106-08 against (a) station number, (b) sampling pressure, (c) concentration and (d) histogram of the result of replicate samplings.

(6.3) Duplicate sample measurement

Duplicate samples were analyzed at every hydrographic station. Total amount of the duplicate sample pairs was 254. Summary of duplicate sample measurements are shown in Table C.4.9, and Figure C.4.15 – C.4.17. During this cruise, the average difference and standard deviation of replicate measurement were 0.069 ± 0.061 ($\mu\text{mol/kg}$) for nitrate+nitrite, 0.005 ± 0.005 ($\mu\text{mol/kg}$) for phosphate and 0.170 ± 0.156 ($\mu\text{mol/kg}$) for silicate, respectively.

Table C.4.9 Average difference of duplicate samples in each run throughout cruise.

Unit: $\mu\text{mol/kg}$		
Nitrate + nitrite	Phosphate	Silicate
0.069 ± 0.061	0.005 ± 0.005	0.170 ± 0.156

Note: N=253(nitrate + nitrite), N=246(phosphate), N=238(silicate) at flag 2.

RF1106-08_NO₃ Result of Duplicate Sampling (N=253)

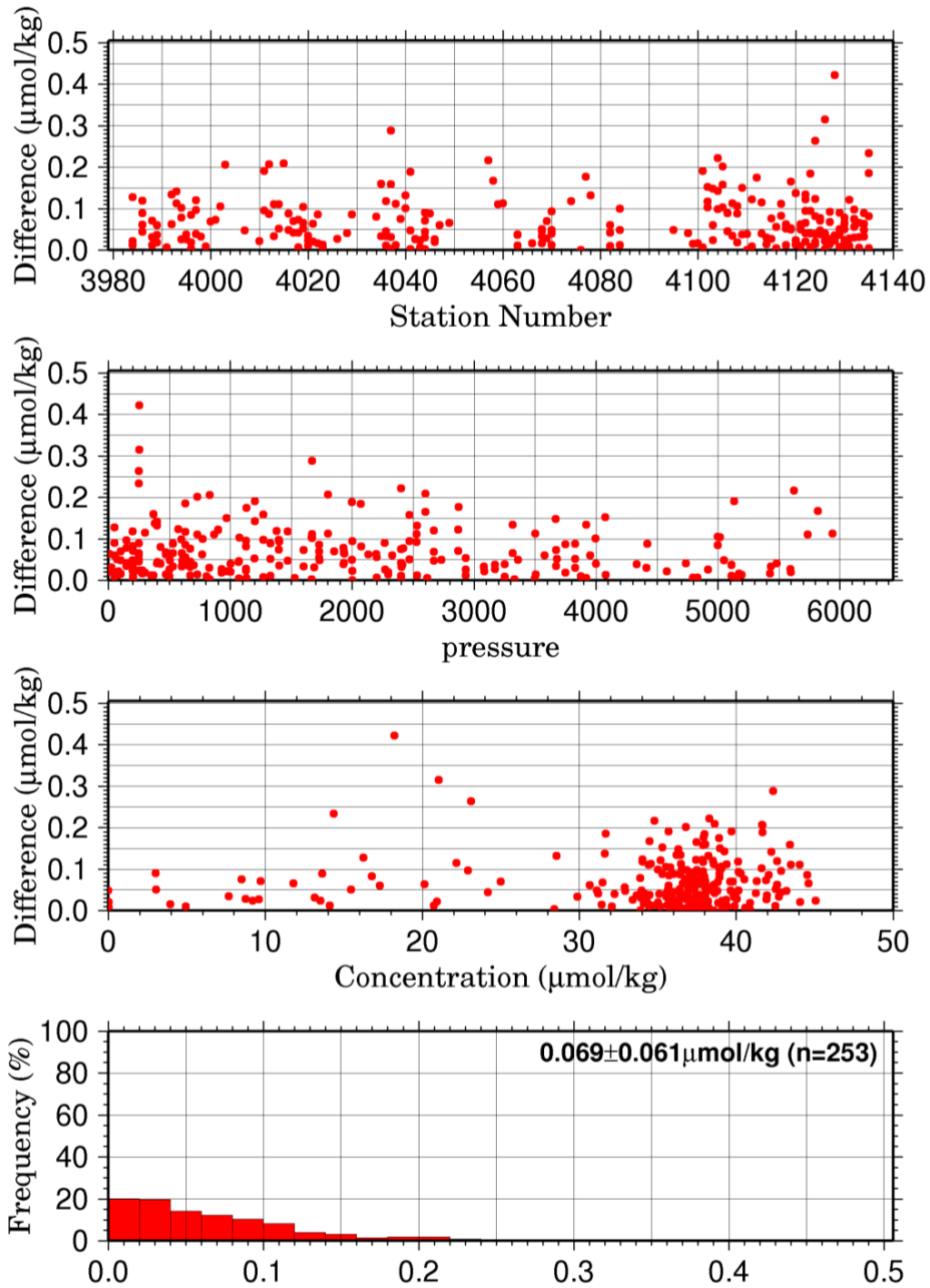


Figure C.4.15 Result of nitrate + nitrite duplicate samplings (N=253) during RF1106-08 against (a) station number, (b) sampling pressure, (c) concentration and (d) histogram of the result of duplicate samplings.

RF1106-08_PO₄ Result of Duplicate Sampling (N=246)

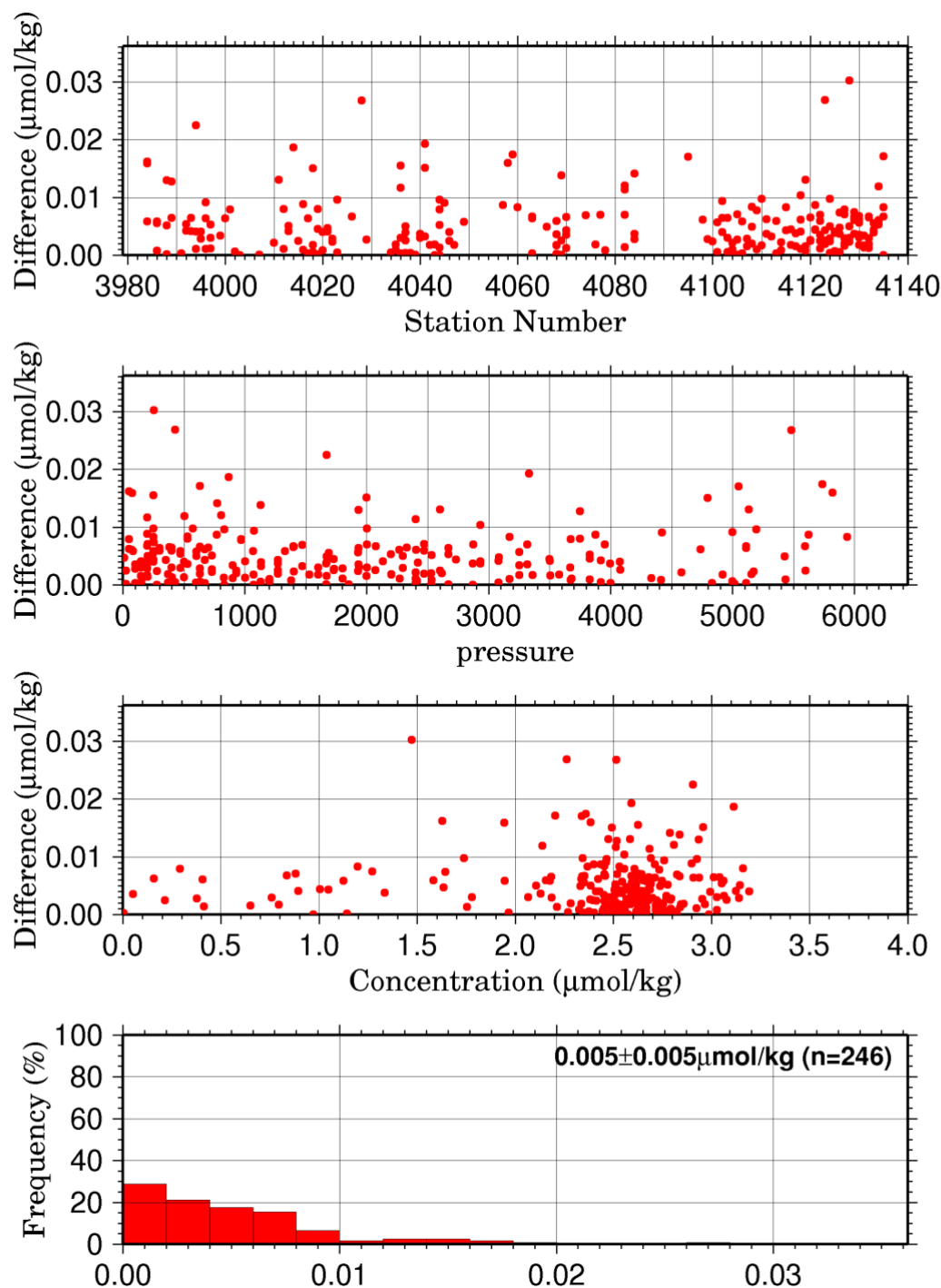


Figure C.4.16 Result of phosphate duplicate samplings (N=246) during RF1106-08 against (a) station number, (b) sampling pressure, (c) concentration and (d) histogram of the result of duplicate samplings.

RF1106-08_SiO₂ Result of Duplicate Sampling (N=238)

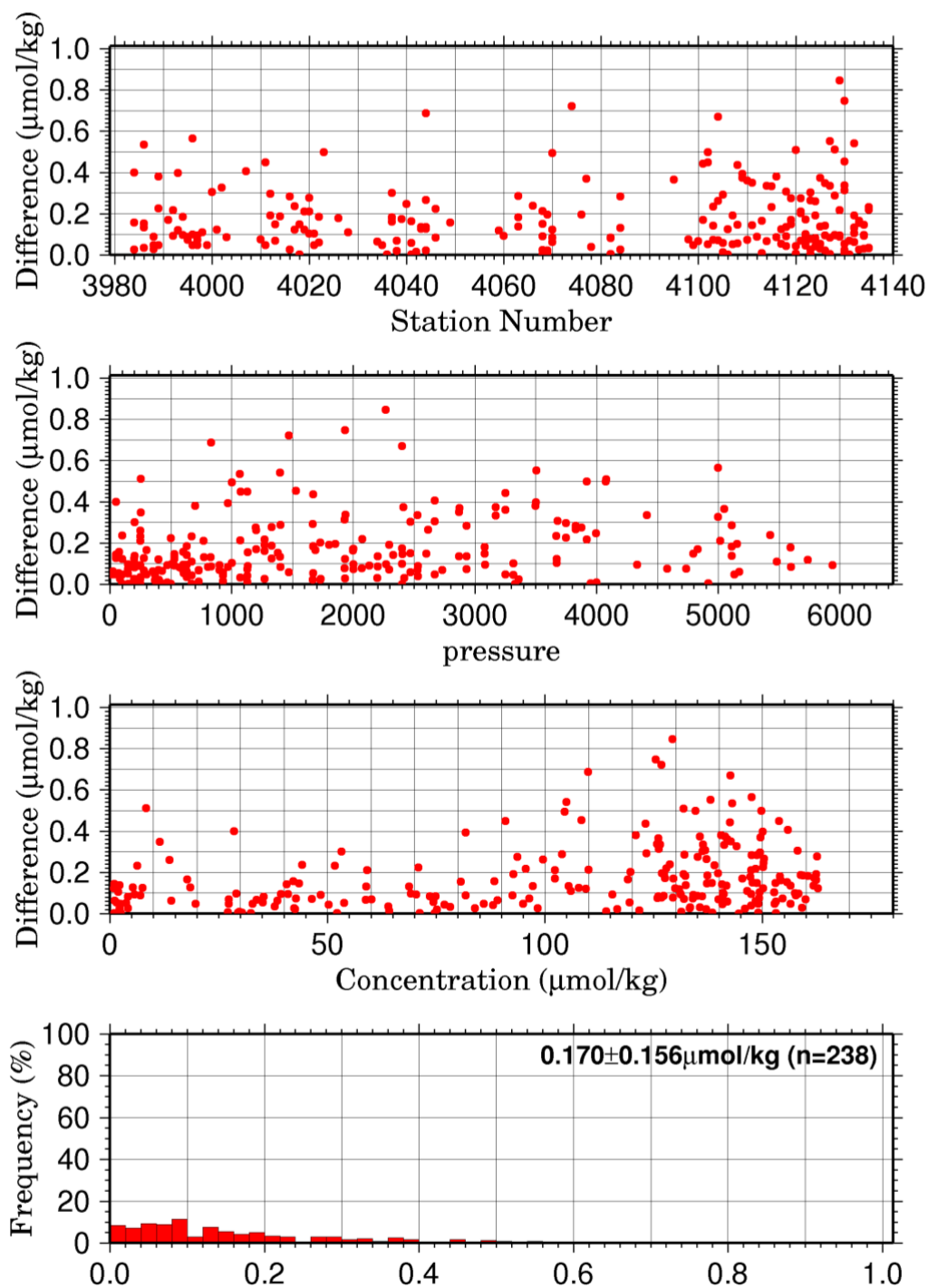


Figure C.4.17 Result of silicate duplicate samplings (N=238) during RF1106-08 against (a) station number, (b) sampling pressure, (c) concentration and (d) histogram of the result of duplicate samplings.

(7) Uncertainty

(7.1) Uncertainty associated with concentration level: U_c

The 124 sets of RMNS will be analyzed during the cruise to make empirical equations to estimate uncertainty of concentrations of seawater samples throughout cruise. The average value and CV for each RMNS level will be calculated, graphed, and a curve fit determined. The empirical equation (7.1) is an example of the curve fit between nutrients concentration C_x and the uncertainty at each concentration level.

$$\text{Uncertainty for parameter } \overline{X(\%)} = a + b(1/C_x) + c(1/C_x)^2 \quad (7.1)$$

Where C_x is concentration of sample for parameter X.

Empirical equations eqs. (7.2), (7.3) and (7.4) were used to estimate uncertainty of measurement of nitrate, phosphate and silicate during this cruise. The equations are based on analysis of 44 sets of RMNS lots BS, BT, BE and BF. Figure C.4.18 – C.4.20 show graphic presentations of eq.(7.2)–(7.4).

Nitrate + nitrite Concentration C_n in $\mu\text{mol/kg}$:

Uncertainty of measurement of nitrate (%) =

$$\sqrt{0.1049 + 3.7977 \times (1/C_n) - 0.0048 \times (1/C_n)^2} \quad (7.2)$$

Where C_n is nitrate concentration of sample.

Phosphate Concentration C_p in $\mu\text{mol/kg}$:

Uncertainty of measurement of phosphate (%) =

$$\sqrt{0.0634 + 1.0565 \times (1/C_p) - 0.0014 \times (1/C_p)^2} \quad (7.3)$$

Where C_p is phosphate concentration of sample.

Silicate Concentration C_s in $\mu\text{mol/kg}$:

Uncertainty of measurement of silicate (%) =

$$\sqrt{0.203 + 6.431 \times (1/C_s) + 8.367 \times (1/C_s)^2} \quad (7.4)$$

Where C_s is silicate concentration of sample.

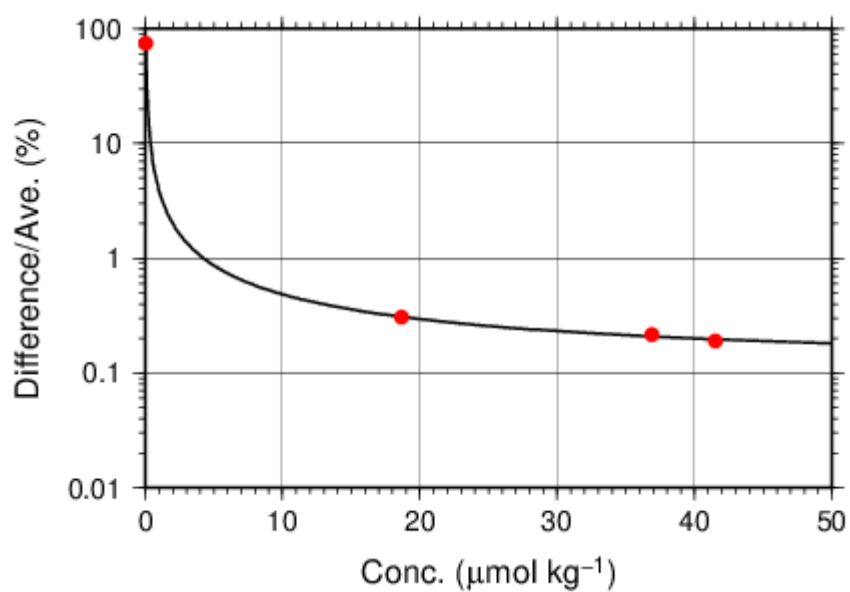


Figure C.4.18 Uncertainty of nitrate + nitrite concentration level.

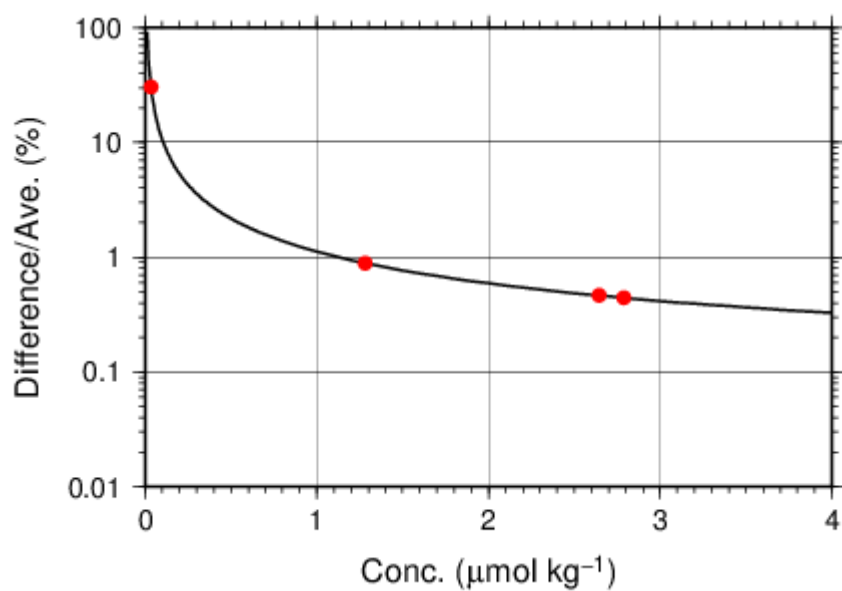


Figure C.4.19 Uncertainty of phosphate concentration level.

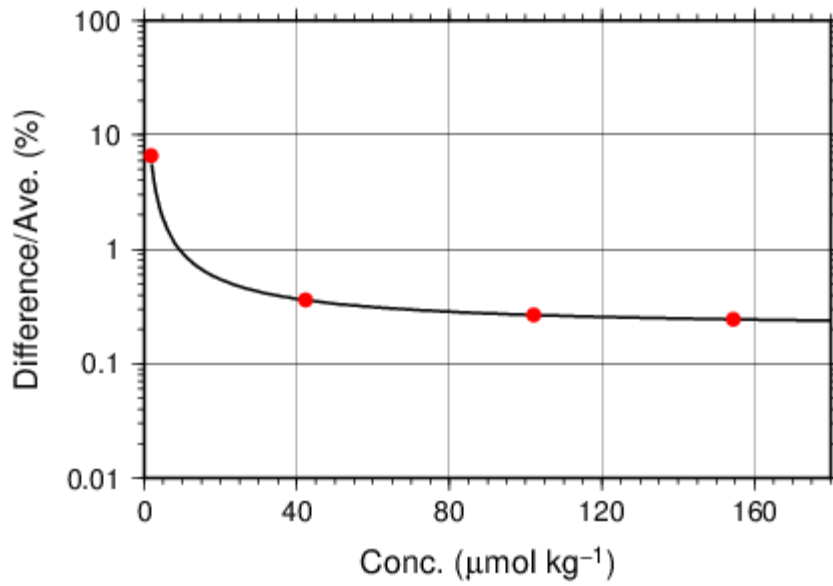


Figure C.4.20 Uncertainty of silicate concentration level.

(7.2) Uncertainty of analysis between runs: U_s

Uncertainty of analysis between runs (U_s) was estimated from relative standard deviation of RMNS throughout cruise as shown in subsection (5.3).

(7.3) Uncertainty of analysis in a run: U_a

Uncertainty of analysis (U_a) was estimated from relative standard deviation of precision throughout cruise as shown in subsection (6.1).

(7.4) Conclusive uncertainty of nutrient measurements of samples: U

To determine the conclusive uncertainty of nutrient measurements of samples, we use two functions depending on U_a value acquired at each run as follows:

When U_a was small and measurement was well-controlled condition, the conclusive uncertainty of nutrient measurements of samples, U , might be as below:

$$|U = U_c. \quad (7.5)$$

When U_a was relative large and the measurement might have some problems, the conclusive uncertainty of nutrient measurements of samples, U , can be expanded as below:

$$|U = \sqrt{U_c^2 + U_a^2}. \quad (7.6)$$

(8) Problems/improvements occurred and solutions

At Stn.63 (Lat. 35-30.20°N / Long. 164-59.74°E, RF4047) and Stn.70 (Lat. 30-59.91°N / Long. 164-59.82°E, RF4054), we got a problem on silicate measurements. They were judged that they were not possible to analyze because sample peaks were wavy. Pump tubes were replaced after the analysis.

Stn.67 (Lat. 33-29.39°N / Long. 165-00.33°E, RF4051), silicate concentration calculated it by having carried out the moving average of the raw data for 11 seconds.

(9) Results

(9.1) Comparison at cross-stations during this cruise

Cross-stations during this cruise were three stations. The first was located at 39-40°N/147.52°E, second was located at 40°N/165°E, last was located at 9°N/164°E. At stations of Stn.14 (RF3997) and Stn.23 (RF4007), hydrocast sampling for nutrients (nitrate, nitrite, phosphate, silicate) were conducted two times at interval of about 16 days. At stations of Stn.55 (RF4039) and Stn.56 (RF4040), hydrocast sampling for nutrients were conducted two times at interval of about 17 days. At stations of Stn.105 (RF4089) and Stn.106 (RF4090), hydrocast sampling for nutrients were conducted two times at interval of about 9 days. Each nutrients parameter profiles of the three hydrocasts agreed well within the range of uncertainty.

These profiles are shown in Figures C.4.21 – C.4.29.

Comparison of Nitrate+Nitrite at cross-stations(39°40'N,147°50'E) during p01-p13 revisit

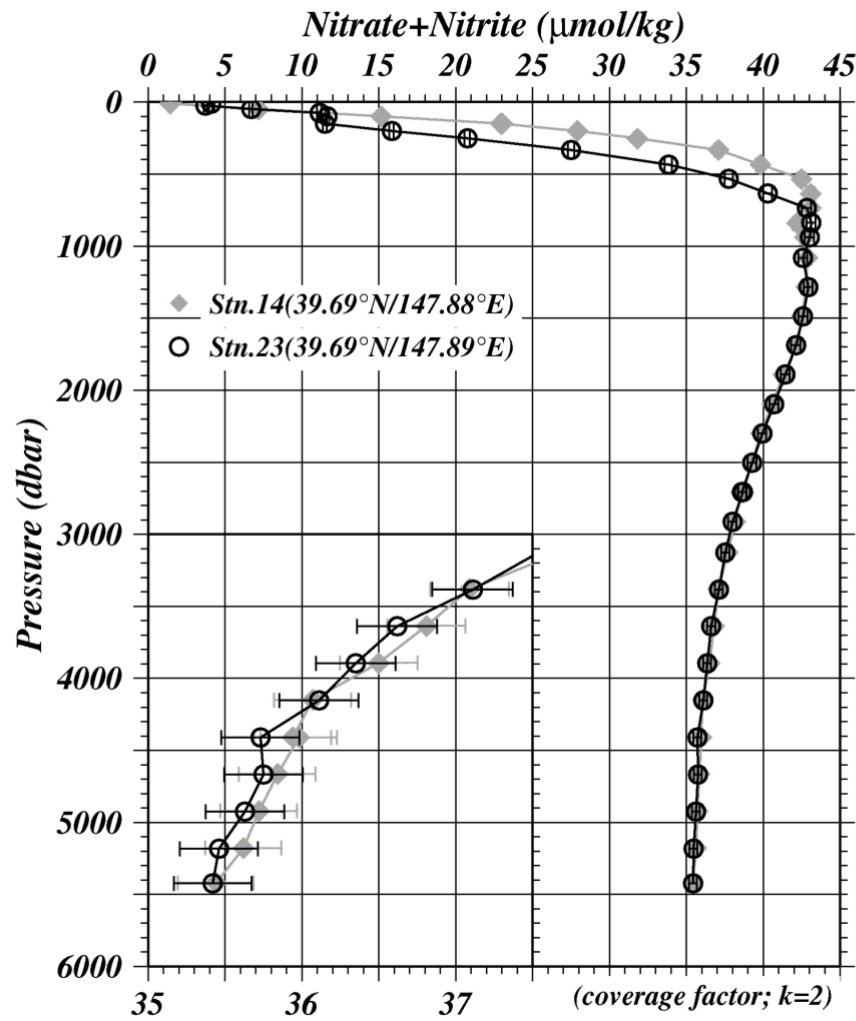


Figure C.4.21 Comparison of nitrate + nitrite profiles between the first hydrocast (painting diamonds) and the second one (circle) at the cross-stations of 39°40'N/147°50'E.

Comparison of Phosphate at cross-stations(39°40'N,147°50'E) during p01-p13 revisit

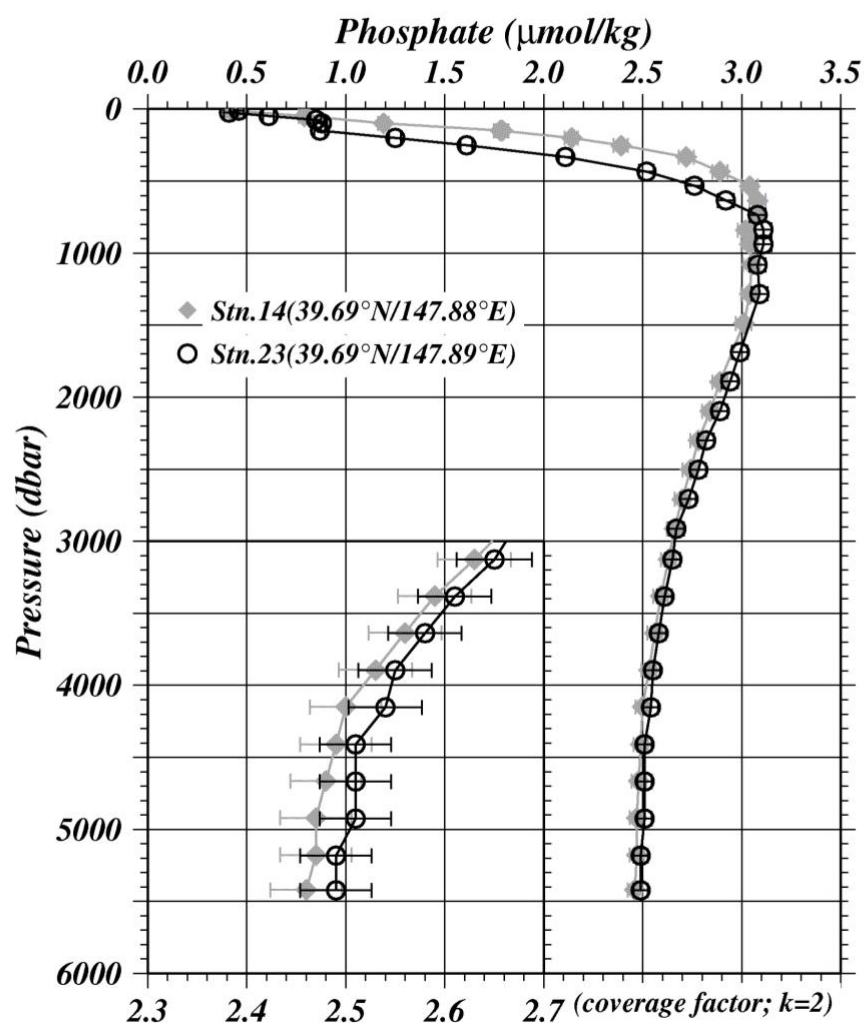


Figure C.4.22 Comparison of phosphate profiles between the first hydrocast (painting diamonds) and the second one (circle) at the cross-stations of 39°40'N/147°50'E.

Comparison of Silicate at cross-stations(39°40'N,147°50'E) during p01-p13 revisit

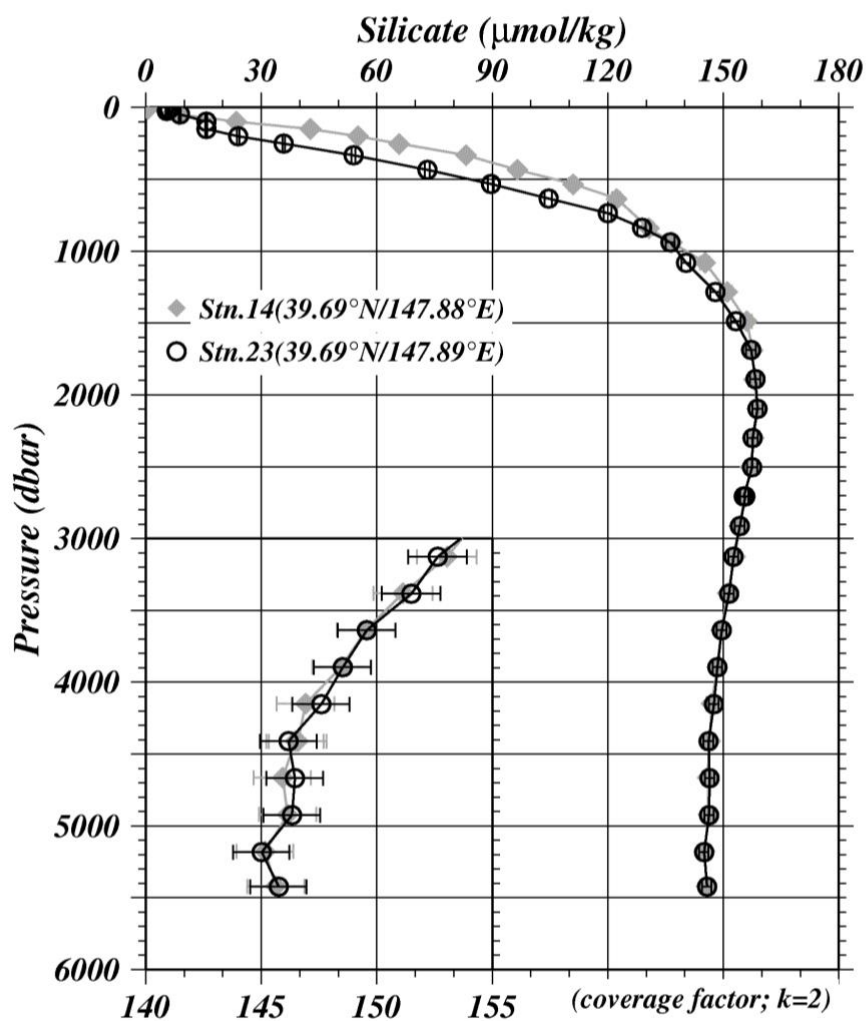


Figure C.4.23 Comparison of silicate profiles between the first hydrocast (painting diamonds) and the second one (circle) at the cross-stations of 39°40'N/147°50'E.

Comparison of Nitrate+Nitrite at cross-stations(40°N,165°E) during p01-p13 revisit

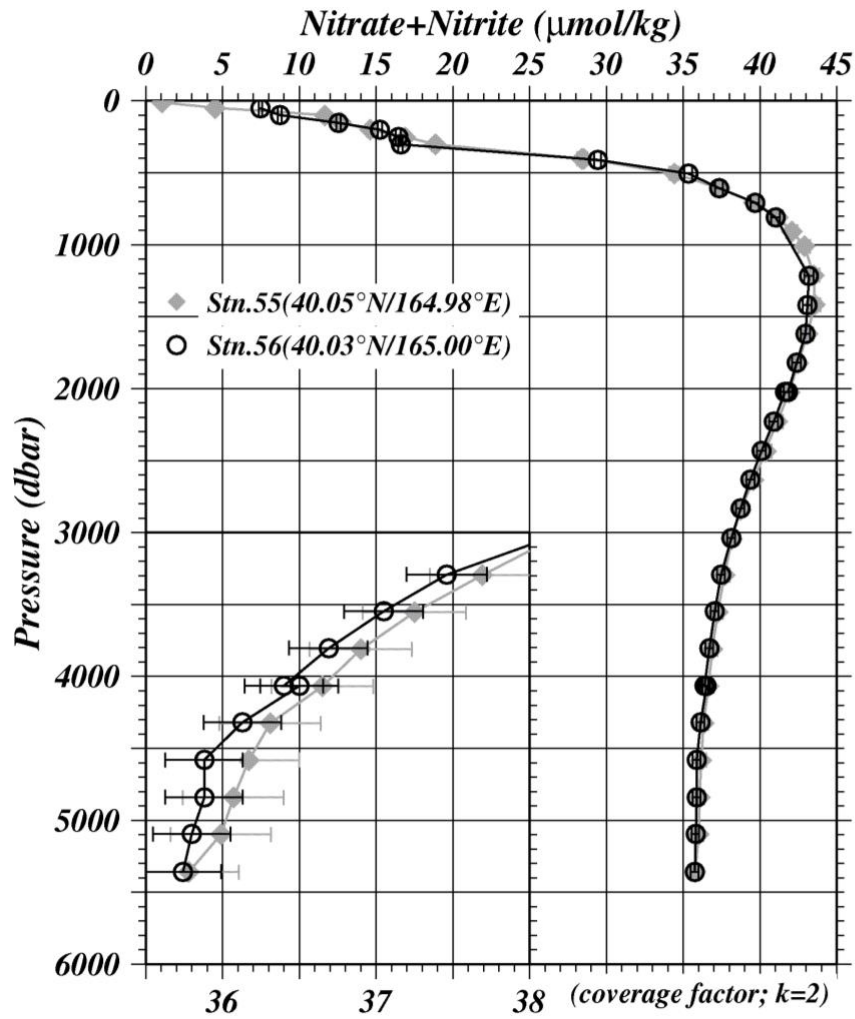


Figure C.4.24 Comparison of nitrate + nitrite profiles between the first hydrocast (painting diamonds) and the second one (circle) at the cross-stations of 40°N/165°E.

Comparison of Phosphate at cross-stations(40°N,165°E) during p01-p13 revisit

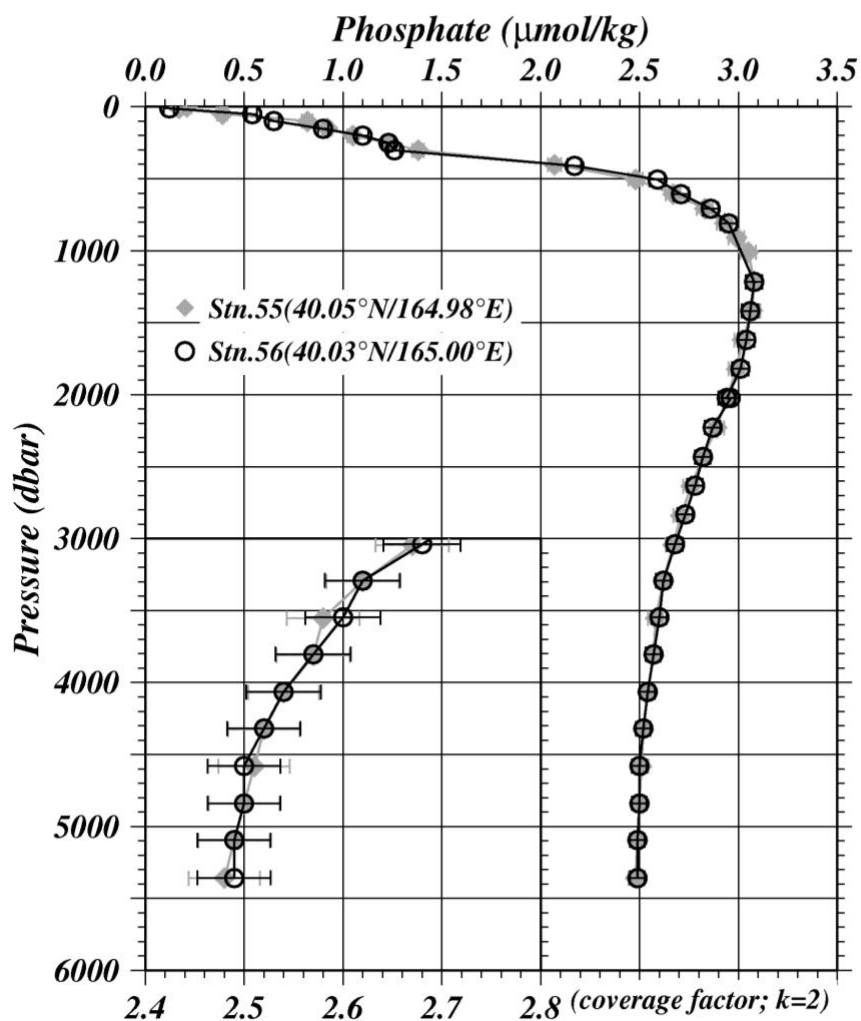


Figure C.4.25 Comparison of phosphate profiles between the first hydrocast (painting diamonds) and the second one (circle) at the cross-stations of 40°N/165°E.

Comparison of Silicate at cross-stations(40°N,165°E) during p01-p13 revisit

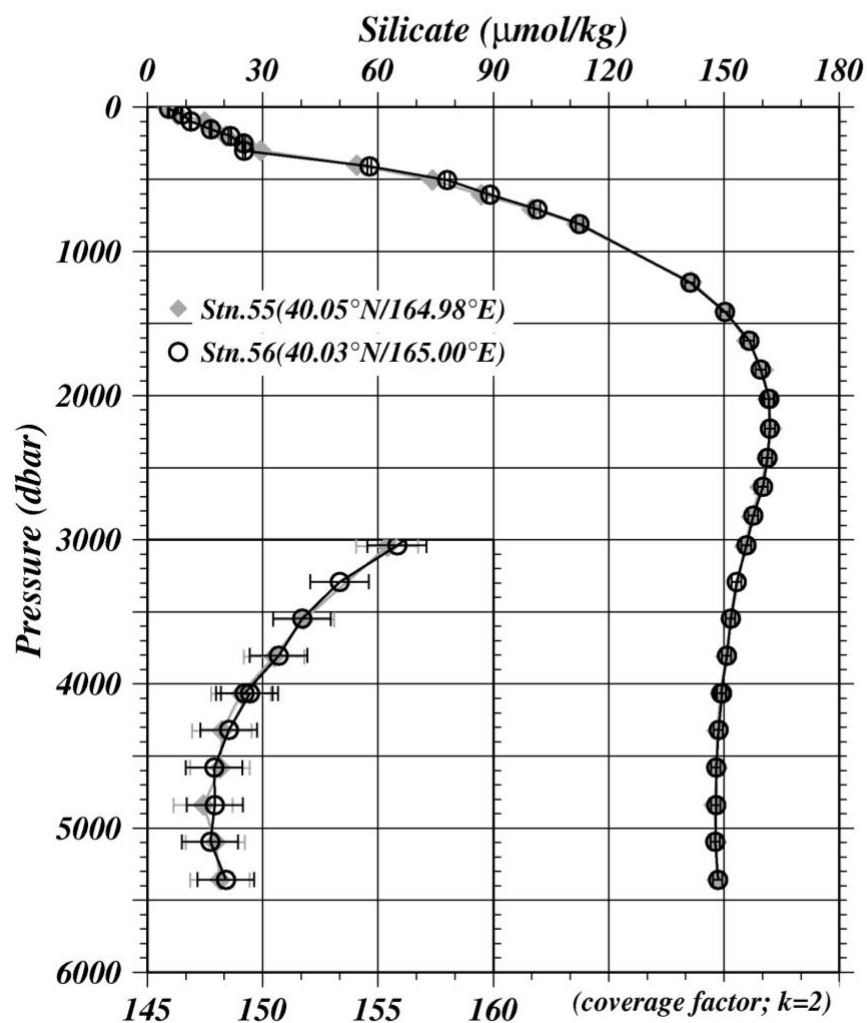


Figure C.4.26 Comparison of silicate profiles between the first hydrocast (painting diamonds) and the second one (circle) at the cross-stations of 40°N/165°E.

Comparison of Nitrate+Nitrite at cross-stations(9°N,164°E) during p01-p13 revisit

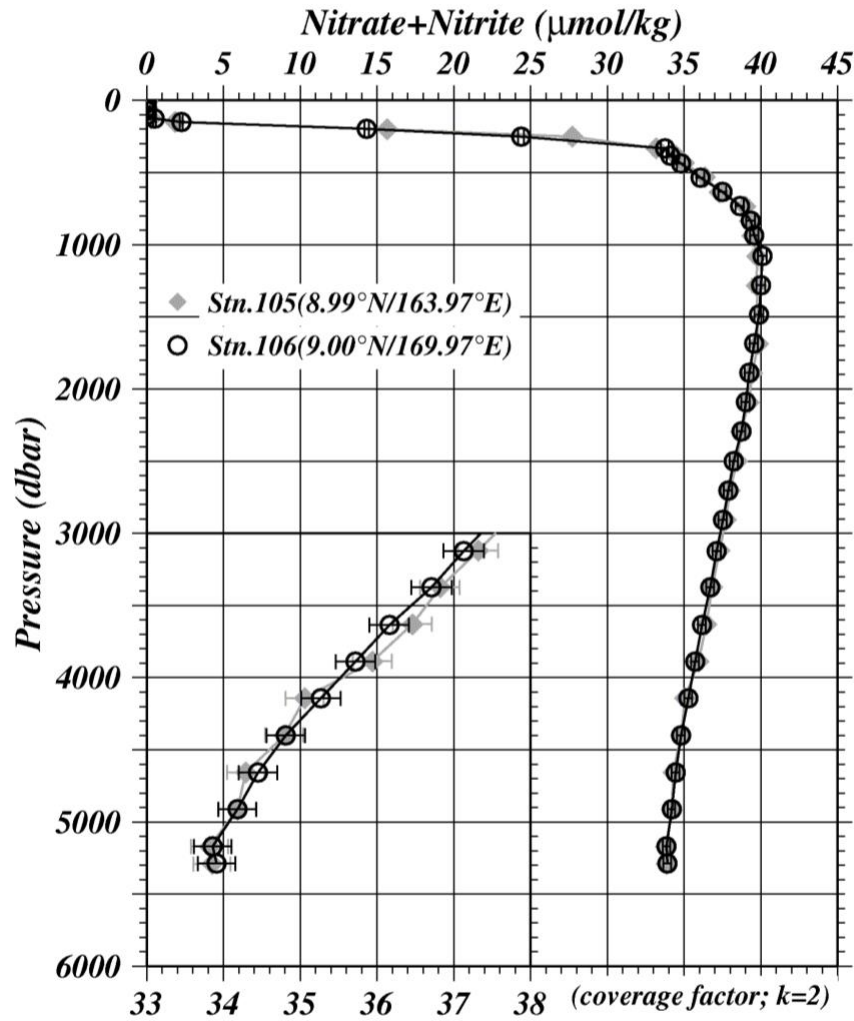


Figure C.4.27 Comparison of nitrate + nitrite profiles between the first hydrocast (painting diamonds) and the second one (circle) at the cross-stations of 9°N/164°E.

Comparison of Phosphate at cross-stations(9°N,164°E) during p01-p13 revisit

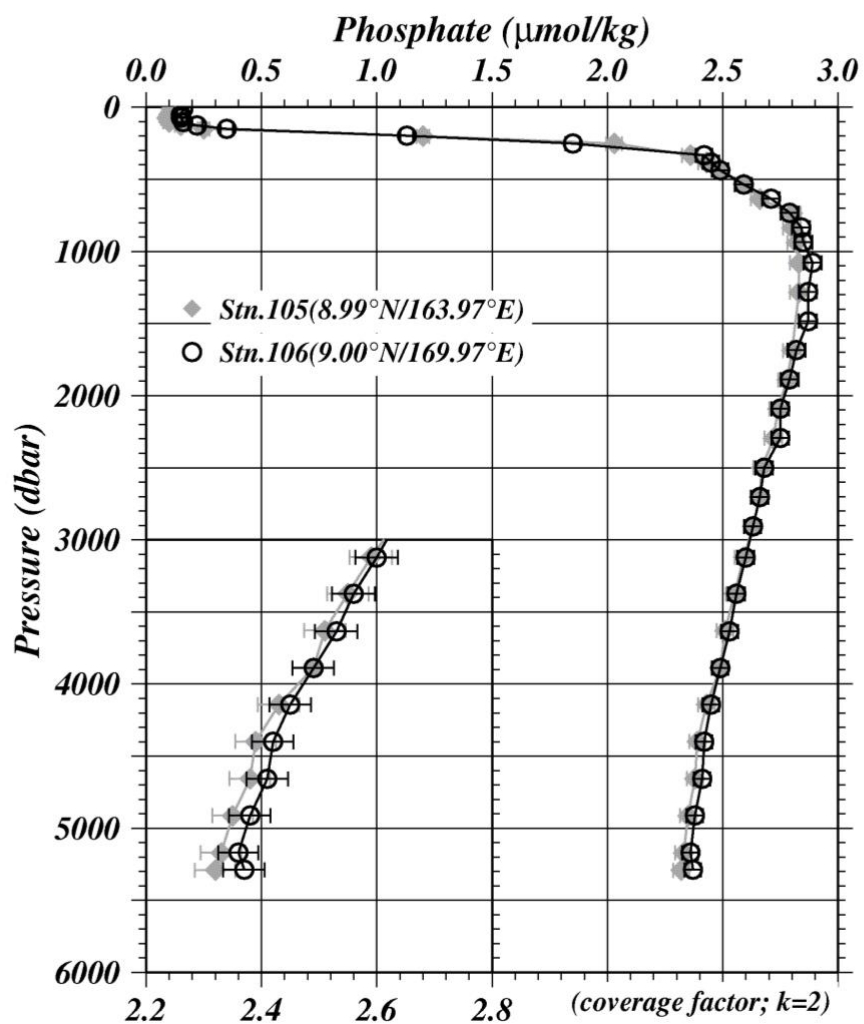


Figure C.4.28 Comparison of phosphate profiles between the first hydrocast (painting diamonds) and the second one (circle) at the cross-stations of 9°N/164°E.

Comparison of Silicate at cross-stations(9°N,164°E) during p01-p13 revisit

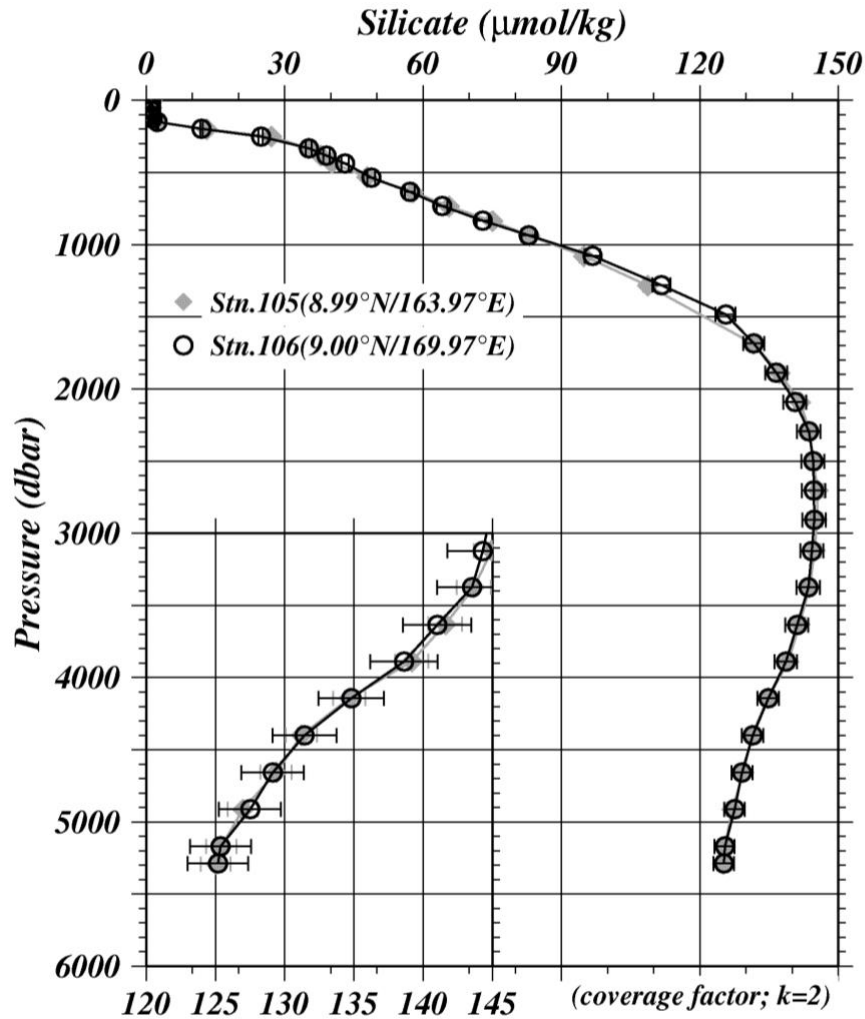


Figure C.4.29 Comparison of silicate profiles between the first hydrocast (painting diamonds) and the second one (circle) at the cross-stations of 9°N/164°E.

(9.2) Comparison at cross-stations of WHP-P1 section in 1985, 1999 and 2007.

We compared our nutrients data with gridded data of WHP-P1 at a cross point, around 47°N/165°E. WHP-P1 line was observed three times, the first cruise was observed in 1985 by R/V Thomas G. Thompson belonged to Scripps Institution of Oceanography (SIO), the second was observed in 1999 by R/V KAIYO-MARU belong to Japan Agency for Marine-Earth Science and Technology (JAMSTEC) and the third was observed in 2007 by R/V MIRAI belong to JAMSTEC. Our nutrients data at P13 revisit and JAMSTEC data in 2007 are comparable directly through the RMNS. However, SIO data in 1985 and JAMSTEC data in 1999 may have inter-cruise differences because they did not measure the RMNS in their cruise. Summary of compared these data profiles shown in Figure C.4.30 – C.4.32.

Comparison of Nitrate at cross-stations of WHP-P01 in 1985, 1999 and 2007

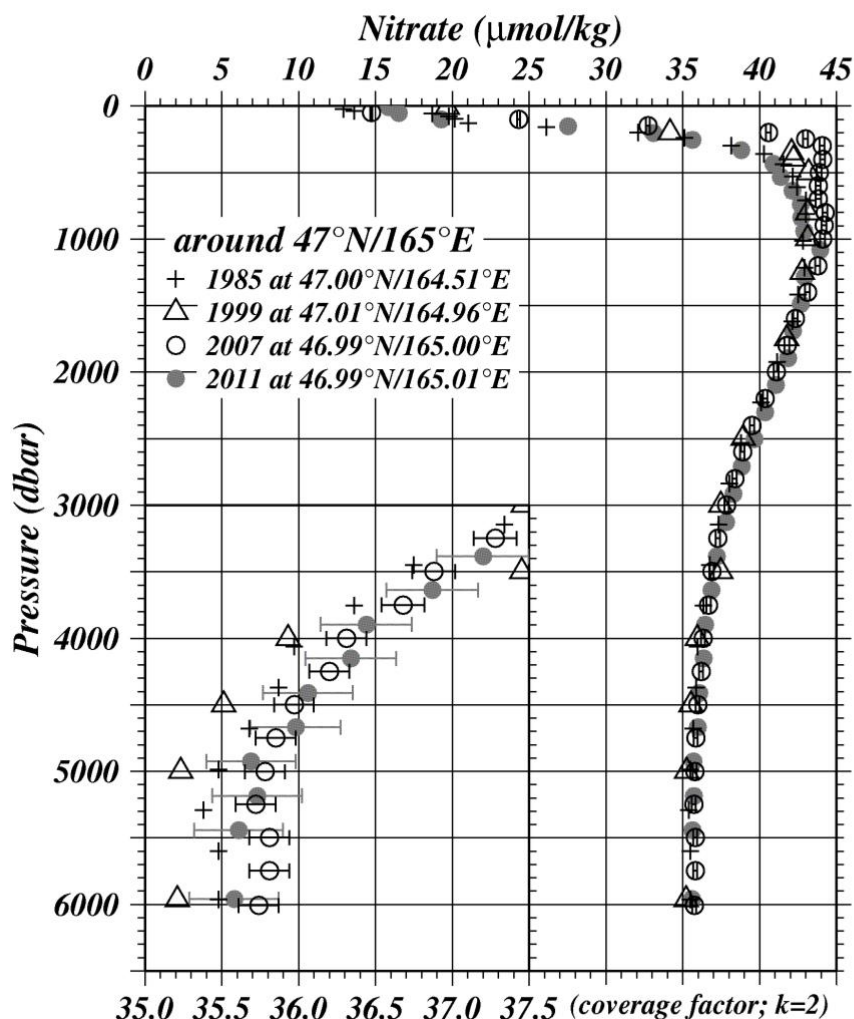


Figure C.4.30 Comparison of nitrate + nitrite profiles at cross-station of WHP-P1. Cross, triangle, circle, painting circle show the WHP-P1 in 1985 by SIO, WHP-P1 in 1999 by JAMSTEC, WHP-P1 in 2007 by JAMSTEC and WHP-P13 revisit in 2011 by JMA, respectively.

Comparison of Phosphate at cross-stations of WHP-P01 in 1985, 1999 and 2007

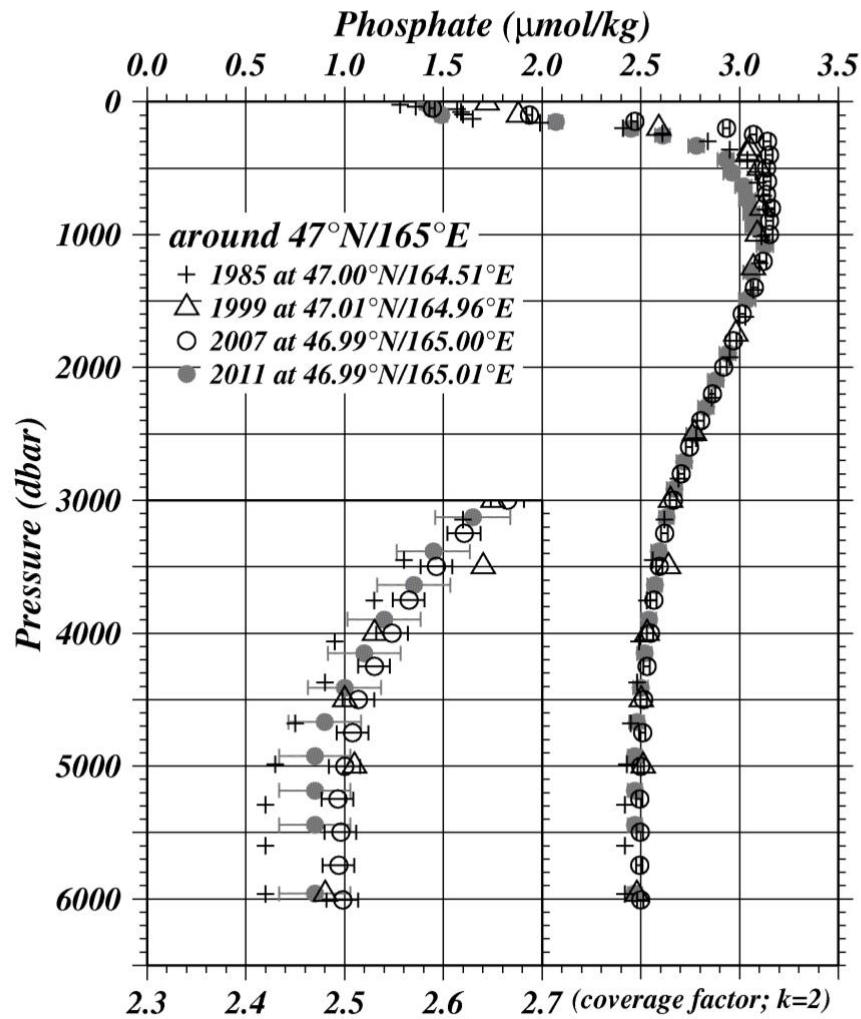


Figure C.4.31 Comparison of phosphate profiles at cross-station of WHP-P1. Cross, triangle, circle, painting circle show the WHP-P1 in 1985 by SIO, WHP-P1 in 1999 by JAMSTEC, WHP-P1 in 2007 by JAMSTEC and WHP-P13 revisit in 2011 by JMA, respectively.

Comparison of Silicate at cross-stations of WHP-P01 in 1985, 1999 and 2007

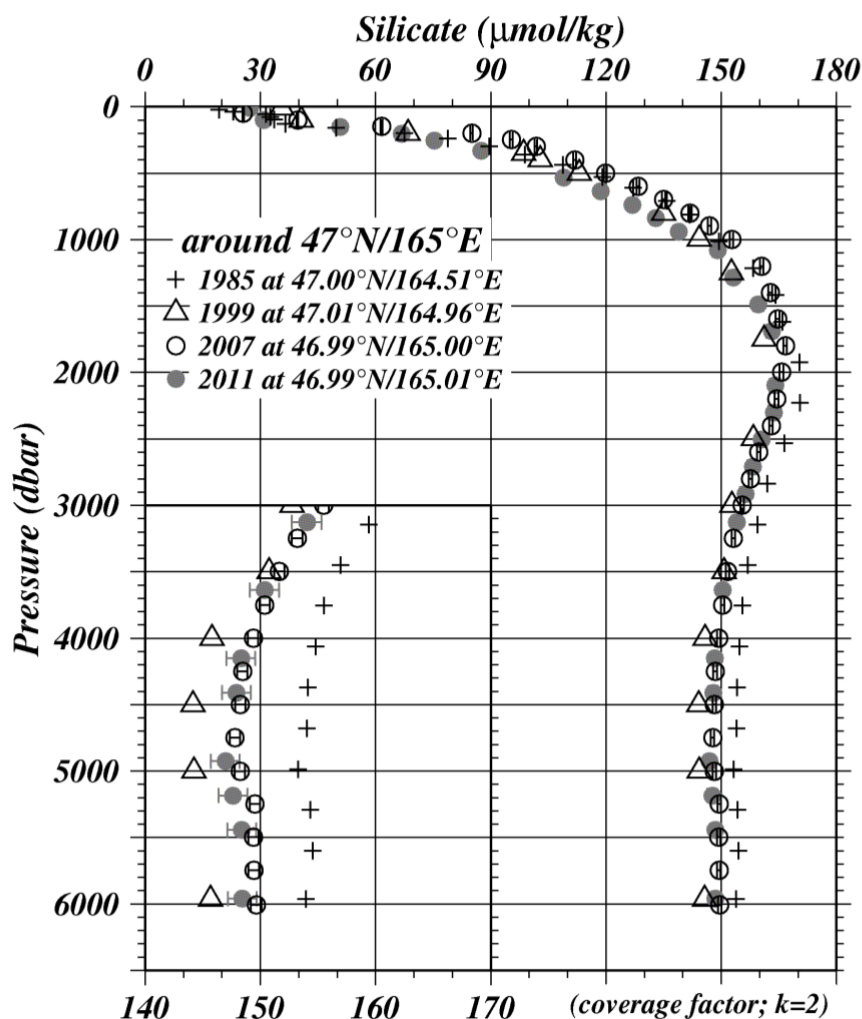


Figure C.4.32 Comparison of silicate profiles at cross-station of WHP-P1. Cross, triangle, circle, painting circle show the WHP-P1 in 1985 by SIO, WHP-P1 in 1999 by JAMSTEC, WHP-P1 in 2007 by JAMSTEC and WHP-P13 revisit in 2011 by JMA, respectively.

(9.3) Comparison at cross-stations of WHP-P2 section in 1994 and 2004.

We compared our nutrients data with gridded data of WHP-P2 at a cross point around 30°N/165°E. WHP-P2 line was observed two times, the first cruise was observed in 1994 by R/V KAIYO-MARU belong to Tohoku National Fisheries Research Institute (NRIFS), the second was observed in 2004 by R/V Melville belonged to Scripps Institution of Oceanography (SIO). These data may have inter-cruise differences because they did not measure the RMNS in their cruise. Summary of compared these data profiles shown in Figure C.4.33 – C.4.35.

Comparison of Nitrate+Nitrite at cross-stations of WHP-P02 in 1994 and 2004

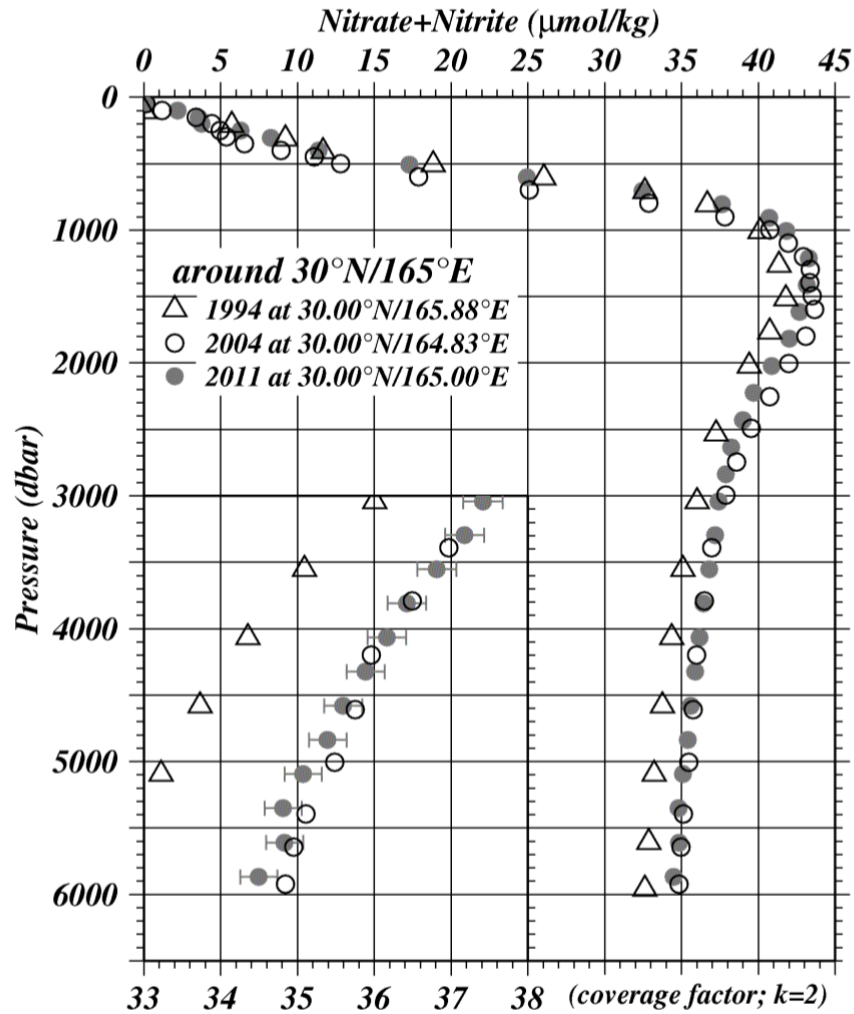


Figure C.4.33 Comparison of nitrate + nitrite profiles at cross-station of WHP-P2. Triangle, circle, painting circle show the WHP-P2 in 1994 by NRIFS, WHP-P2 in 2004 by SIO and WHP-P13 revisit in 2011 by JMA, respectively.

Comparison of Phosphate at cross-stations of WHP-P02 in 1994 and 2004

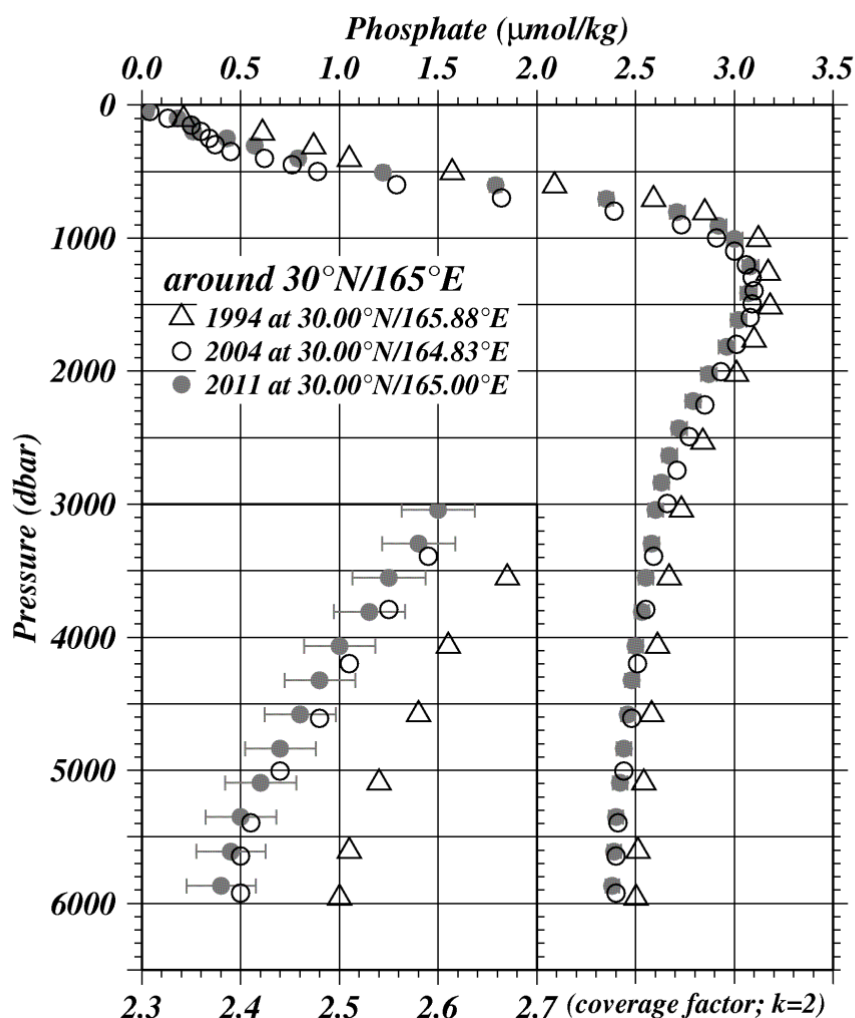


Figure C.4.34 Comparison of phosphate profiles at cross-station of WHP-P2. Triangle, circle, painting circle show the WHP-P2 in 1994 by NRIFS, WHP-P2 in 2004 by SIO and WHP-P13 revisit in 2011 by JMA, respectively.

Comparison of Silicate at cross-stations of WHP-P02 in 1994 and 2004

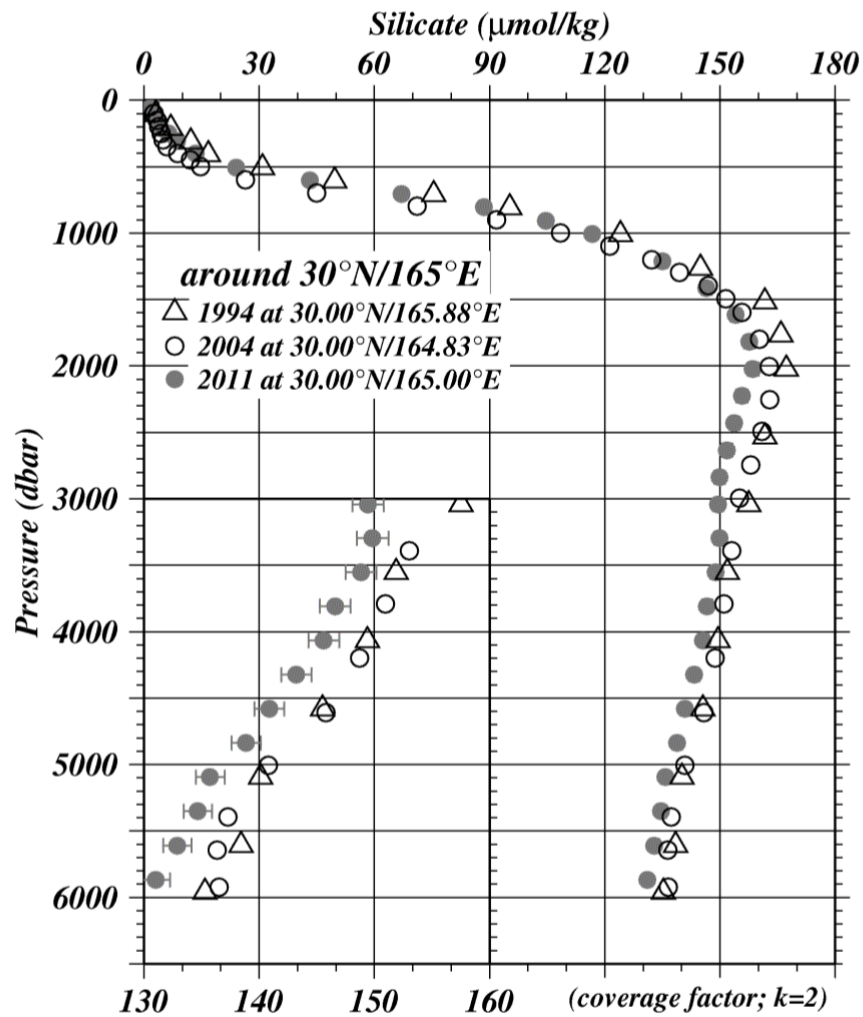


Figure C.4.35 Comparison of silicate profiles at cross-station of WHP-P2. Triangle, circle, painting circle show the WHP-P2 in 1994 by NRIFS, WHP-P2 in 2004 by SIO and WHP-P13 revisit in 2011 by JMA, respectively.

(9.4) Comparison at cross-stations of WHP-P3 section in 1985 and 2005/06.

We compared our nutrients data with gridded data of WHP-P3 at a cross point around 24°N/165°E. WHP-P3 line was observed two times, the first cruise was observed in 1985 by R/V Thomas G. Thompson belonged to SIO and the second was observed in 2005/06 by R/V Mirai belong to Japan Agency for Marine-Earth Science and Technology (JAMSTEC). Our nutrients data at P13 revisit and JAMSTEC data in 2005/06 are comparable directly through the RMNS. However, SIO data in 1985 may have inter-cruise differences because they did not measure the RMNS in their cruise. Summary of compared these data profiles shown in Figure C. 4.36– C.4.38.

Note: Silicate data of WHP-P3 revisit (JAMSTEC, 2007) is corrected by a scale factor provided by M. Aoyama, PI of nutrients of the cruise (personal communication).

Comparison of Nitrate at cross-stations of WHP-P03 in 1985 and 2005

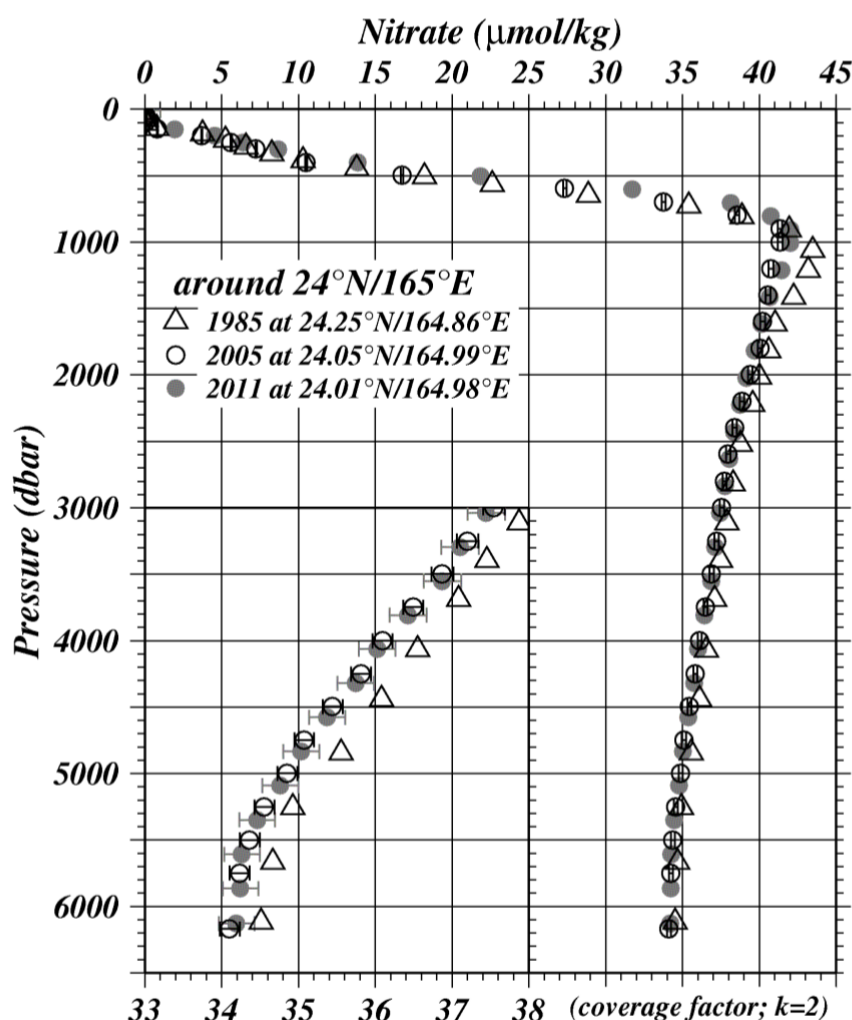


Figure C.4.36 Comparison of nitrate + nitrite profiles at cross-station of WHP-P3. Triangle, circle, painting circle show the WHP-P3 in 1985 by SIO, WHP-P3 in 2005/06 by JAMSTEC and WHP-P13 revisit in 2011 by JMA, respectively.

Comparison of Phosphate at cross-stations of WHP-P03 in 1985 and 2005

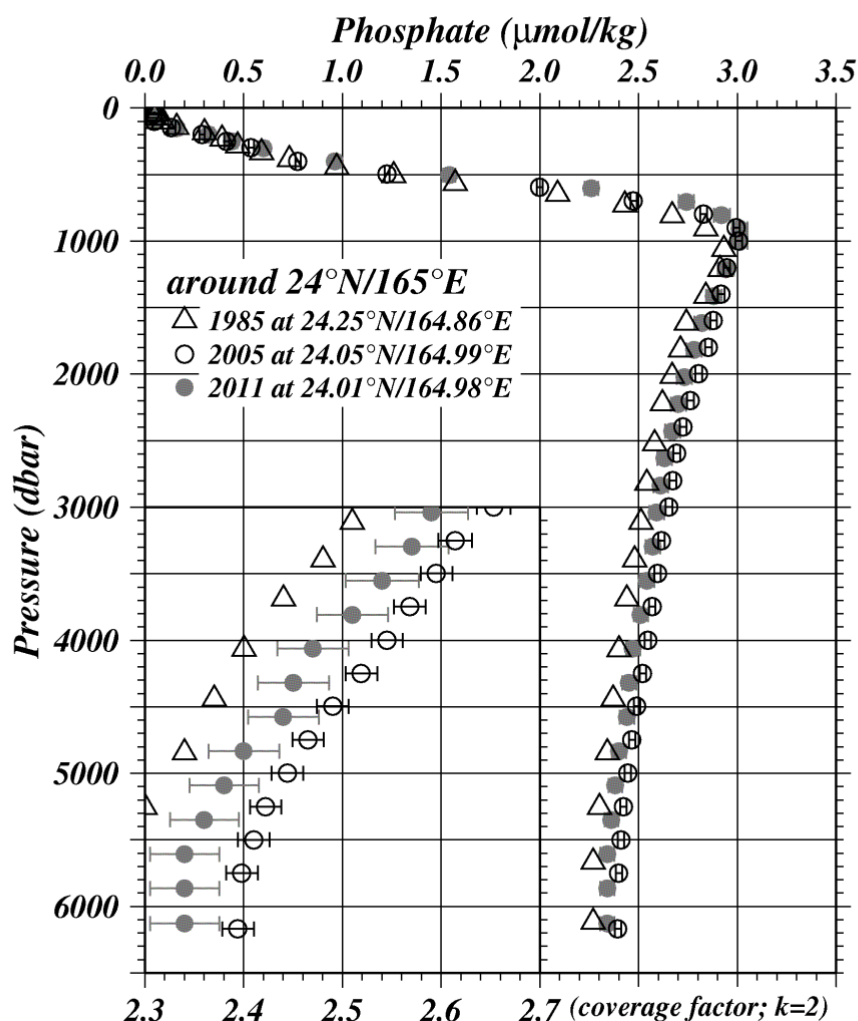


Figure C.4.37 Comparison of phosphate profiles at cross-station of WHP-P3. Triangle, circle, painting circle show the WHP-P3 in 1985 by SIO, WHP-P3 in 2005/06 by JAMSTEC and WHP-P13 revisit in 2011 by JMA, respectively.

Comparison of Silicate at cross-stations of WHP-P03 in 1985 and 2005

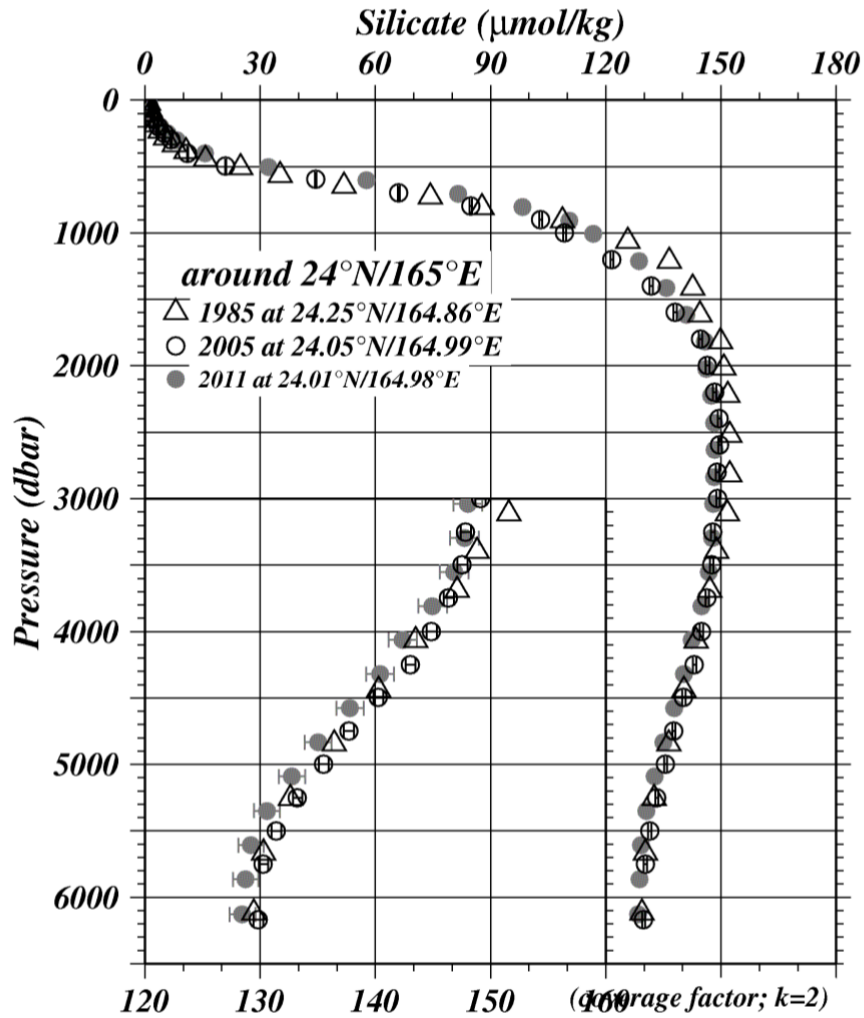


Figure C.4.38 Comparison of silicate profiles at cross-station of WHP-P3. Triangle, circle, painting circle show the WHP-P3 in 1985 by SIO, WHP-P3 in 2005/06 by JAMSTEC and WHP-P13 revisit in 2011 by JMA, respectively. Observed in 2005/06 JAMSEC data is corrected by standard factor, it depends on Aoyama M, this cruise PI.

(9.5) Comparison at cross-stations of WHP-P4 section in 1989

We compared our nutrients data with gridded data of WHP-P4 at cross point around 9°N/164°E. WHP-P4 line was observed in 1989 by R/V Moan Wave belonged to University of Hawaii (UH). Their data may has inter-cruise differences because They did not measure the RMNS in their cruise. Summary of compared these data profiles shown in Figure C.4.39 – C.4.41.

Comparison of Nitrate at cross-stations of WHP-P04 in 1989

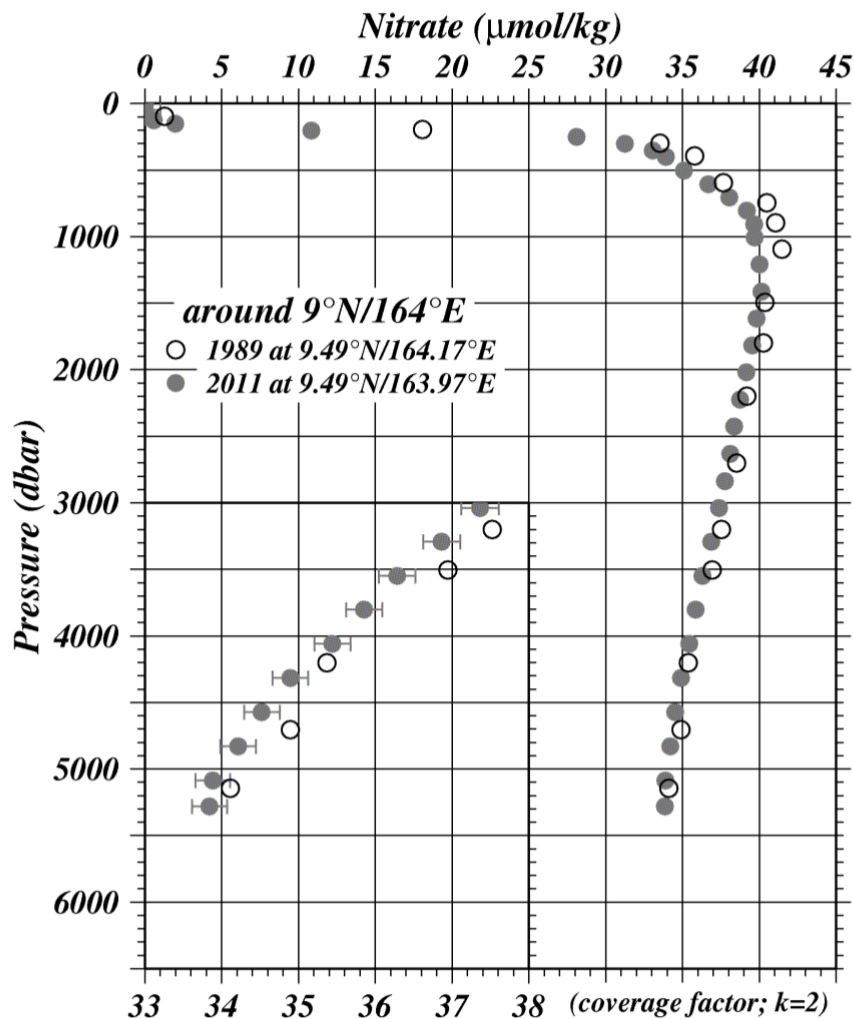


Figure C.4.39 Comparison of nitrate + nitrite profiles at cross-station of WHP-P4. Circle, painting circle show the WHP-P4 in 1989 by UH and WHP-P13 revisit in 2011 by JMA, respectively.

Comparison of Phosphate at cross-stations of WHP-P04 in 1989

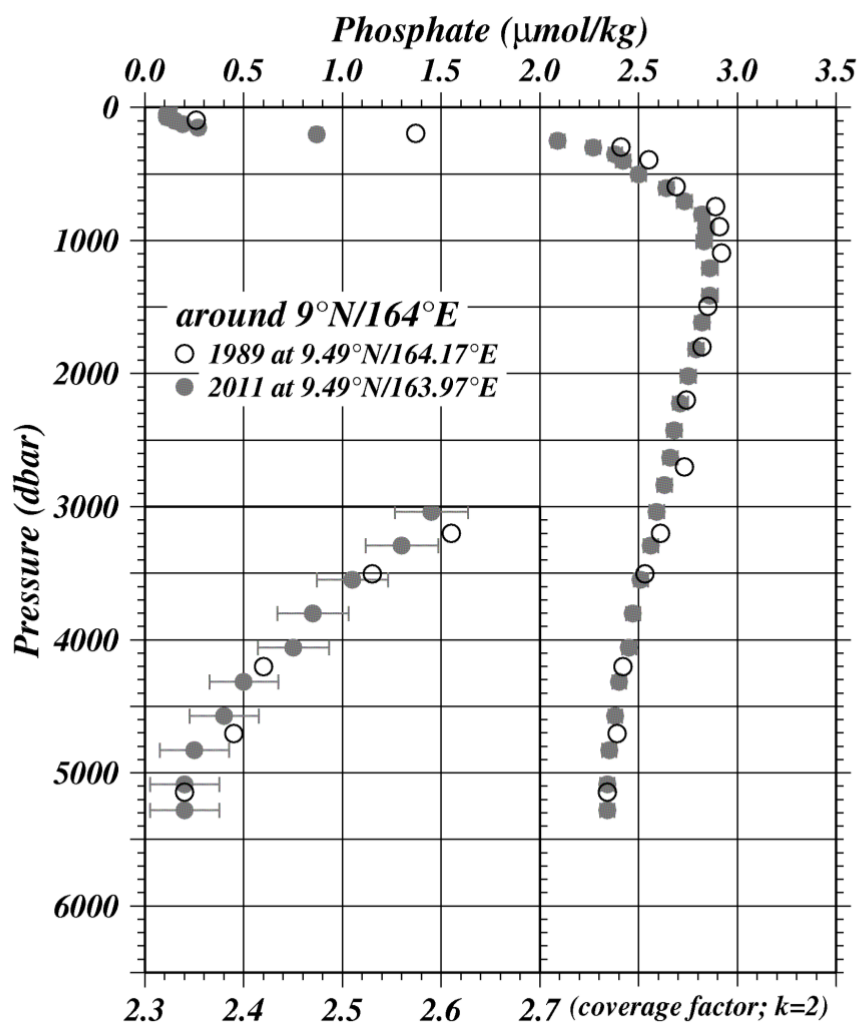


Figure C.4.40 Comparison of phosphate profiles at cross-station of WHP-P4. Circle, painting circle show the WHP-P4 in 1989 by UH and WHP-P13 revisit in 2011 by JMA, respectively.

Comparison of Silicate at cross-stations of WHP-P04 in 1989

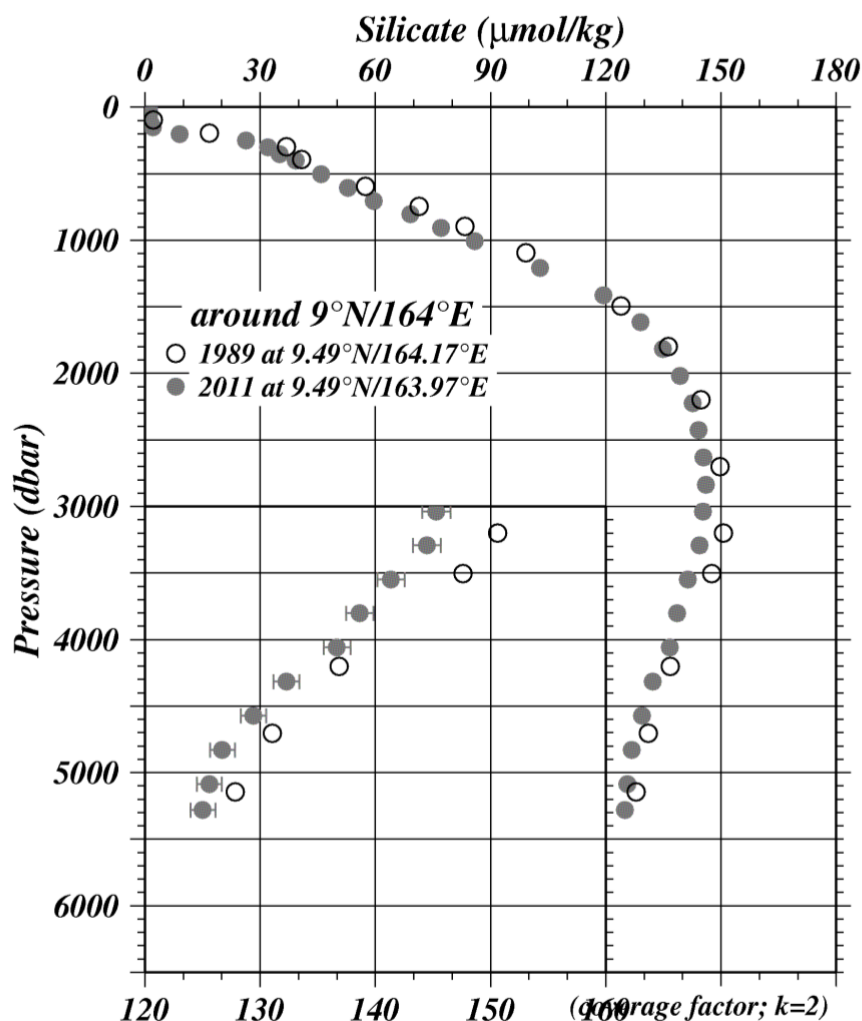


Figure C.4.41 Comparison of silicate profiles at cross-station of WHP-P4. Circle, painting circle show the WHP-P4 in 1989 by UH and WHP-P13 revisit in 2011 by JMA, respectively.

References

- Grasshoff, K., Ehrhardt, M., Kremling K. et al. (1983), *Methods of seawater analysis*. 2nd rev, Weinheim: Verlag Chemie, Germany, West.
- Murphy, J., and Riley, J.P. (1962), *Analytica chimica Acta* **27**, 31-36.
- Armstrong, F. A. J., C. R. Stearns and J. D. H. Strickland (1967), The measurement of upwelling and subsequent biological processes by means of the Technicon TM Autoanalyzer TM and associated equipment, *Deep-Sea Res.*, **14**(3), 381–389.
- JAMSTEC (2007), WHP P3 REVISIT DATA BOOK, WHP P03 REVISIT in 2005.
- Aoyama, M., A. G. Dickson, D. J. Hydes, A. Murata, J. R. Oh, P. Roose and E. Malcom. S. Woodward (2010), Comparability of nutrients in the world's ocean, *INSS international workshop 10-12 Feb. 2009, Paris*

Aoyama, M., S. Becker, K. Sato and D. Schuller (2009), Plan of use of RMNS during the CLIVAR P6 revisited cruise by R/V Melville. (unpublished manuscript).

5. Total Dissolved Inorganic Carbon (DIC) and Total Alkalinity (TA)

1 November 2019

(1) Personnel

Shu SAITO (GEMD/JMA, RF11-06 and RF11-08)
Kazutaka ENYO (GEMD/JMA, RF11-07)
Hiroyuki HATAKEYAMA (GEMD/JMA, RF11-06)
Kazuki ISHIMARU (GEMD / JMA, RF11-06)
Nobuya MAEDA (GEMD/JMA, RF11-08)
Shinji MASUDA (GEMD/JMA, RF11-07 and RF11-08)
Etsuro ONO (GEMD / JMA, RF11-06)
Daisuke SASANO (MRI/JMA, RF11-07)
Naohiro KOSUGI (MRI/JMA, analyses at laboratory on land)

(2) Overview

The concentration of total dissolved inorganic carbon (DIC) and total alkalinity (TA) were determined simultaneously from a single bottle of seawater sample by using two sets of custom-made DIC/TA analyzer manufactured by Nippon ANS Co. Ltd. (apparatus-A and apparatus-B). DIC was determined by coulometric analysis (*Johnson et al.*, 1985, 1987) using an automated CO₂ extraction unit and a coulometer (2009 model, Nippon ANS Co. Ltd.). TA was determined by one-step volumetric addition of hydrochloric acid (HCl) followed by the spectrophotometric analysis of pH with the sulfonephthalein indicator dye bromocresol green (*Breland and Byrne*, 1993) using an automated titration system equipped with CCD image sensor spectrophotometers (Hamamatsu, TA-CCD-A).

At each station, the precision of analysis was monitored using the Certified Reference Material (CRM) for DIC and TA (batches 103, 107 and 110) supplied by Dr. Andrew G. Dickson in Scripps Institution of Oceanography and a non-certified working reference material prepared at our laboratory from surface seawater taken in the western North Pacific. A reference gas of 1.5% CO₂ in air (Japan Fine Products) was also routinely measured to monitor the performance of the coulometric cell assembly. We standardized the DIC measurements with the analytical results of CRMs and their certified DIC concentrations. Concentration of hydrochloric acid (HCl) in the titrant for TA analysis was also monitored by the analytical result of CRMs and their certified TA values. The overall precisions of measurements as estimated from the replicate measurements of CRMs during the course of cruise were 1.7 $\mu\text{mol kg}^{-1}$ for DIC and 0.9 $\mu\text{mol kg}^{-1}$ for TA.

(3) Samplings

Measurements of DIC and TA in the full water column were made at a total of 88 stations (cruise RF11-06: 8, cruise RF11-07: 23, and cruise RF11-08: 57) (Figure C.5.1). Intervals of

sampling stations were 1° in latitude in open ocean zone and from 34 nautical miles to 75 nautical miles in offshore regions near Japan and near Papua New Guinea. In addition to full water column observations, DIC and TA of each layer from the marine surface to depth 800m were analyzed at 6 stations from 2°20'N to 2°20'S. Consequently, the station intervals were from 20' to 40' near equator.

Samples obtained at 5 stations in cruise RF11-06 were preserved by injecting HgCl₂ solution and were analysed at Meteorological Research Institute (MRI/JMA). All other samples were analysed on board.

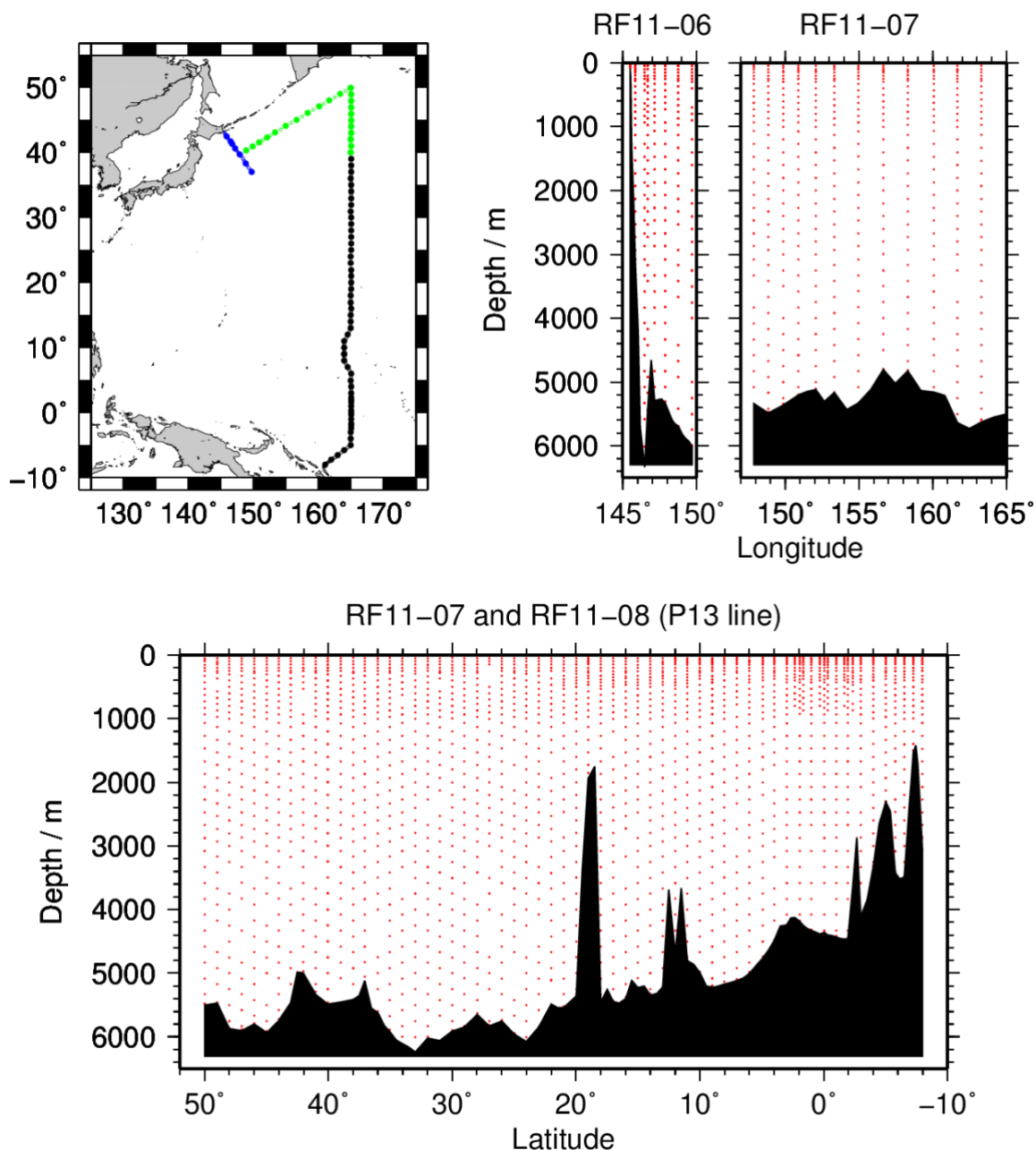


Figure C.5.1. Station locations (top left panel) and sampling layers of DIC and TA (top right and bottom panels). The colour of plots in top left panel indicates the cruise; blue: RF11-06, green: RF11-07 and black: RF11-08, respectively.

Samples for the measurements of DIC and TA were drawn according to the procedures outlined by *Dickson et al.* (2007) from 10-litters Niskin bottles into clean 300 cm³ Schott Duran[®] borosilicate glass bottles using silicone tubing. To minimize CO₂ exchange with the ambient air, samples for DIC/TA were drawn next to those for CFCs and dissolved oxygen. Samples of near-surface seawater were collected from the underway seawater supply from the sea-chest (approx. 5 m).

Total of 241 pairs of replicate samples from the same Niskin bottle and total of 124 pairs of duplicate samples from different Niskin bottles tripped at the same depth were drawn for quality assurance of measurements.

Schott Duran[®] glass bottles were filled smoothly from the bottom after overflowing double a volume while taking care of not entraining any bubbles.

After creating 2 cm³ of headspace by removing sample to allow thermal expansion, the sample bottles were sealed with ground glass stoppers lubricated with Apiezon[®] grease (L). At stations RF-3984, 3988, 3991, 4056, 4060, 4104, 4110, 4112, 4116, 4118, at which more than 80 samples (corresponding to two stations) were waiting for analyses, 0.2 cm³ of saturated mercury (II) chloride solution was added to the samples as a preservative. At other stations, no mercury (II) chloride was added and measurements of DIC and TA were started immediately and ended within 30 hours after samplings. Multiplying 1.00067 (= 300.2 / 300.0), changes in DIC and TA induced by the addition of HgCl₂ solution were corrected for the dilution effect. Samples were immersed in a thermostated water bath (25.0 °C) for approx. 1 hour prior to analysis.

(4) Dissolved Inorganic Carbon (DIC)

(4-1) Instrumentation and procedures

The unit for DIC measurement in the coupled DIC/TA analyzer consists of a coulometer with a quartz coulometric titration cell (8 cm outer diameter), a CO₂ extraction unit and a reference gas injection unit. The CO₂ extraction unit, which is connected to a bottle of 20% v/v phosphoric acid and a carrier N₂ gas supply, includes a sample pipette (approx. 12 cm³) and a CO₂ extraction chamber, two thermoelectric cooling units and switching valves. The coulometric titration cell and the sample pipette are water-jacketed and are connected to a thermostated (25 °C) water bath. The automated procedures of DIC analysis in seawater were as follows (Ishii et al, 1998):

(a) Approximately 2 cm³ of 20% v/v phosphoric acid was injected to an “extraction chamber”, *i.e.*, a glass tube (approx. 20 mm outer diameter and 20 cm in length) with a coarse glass frit placed near the bottom. Purified N₂ (Japan Fine Products, G1 grade >99.99995%) was then allowed to flow through the extraction chamber for 2 minutes to purge CO₂ and other volatile acids dissolved in the phosphoric acid.

- (b) A portion of sample seawater was delivered from the sample bottle into the sample pipette of CO₂ extraction unit by pressurizing the headspace in the sample bottle. After temperature of the pipette was recorded, the sample seawater was transferred into the extraction chamber and mixed with phosphoric acid to convert all carbonate species to CO₂ (aq).
- (c) The acidified sample seawater was then stripped of CO₂ with a stream of purified N₂ (130 cm³ min⁻¹) for 10 minutes. After being dehumidified in a series of two thermoelectric cooling units (2 °C), the evolved CO₂ in the N₂ stream was introduced into the carbon cathode solution (UIC Inc.) in the coulometric titration cell and then CO₂ was electrically titrated. The detail mechanism of titration is described in the document at web site; <http://www.uicinc.com/SystemSheets/Principles%20of%20Operation%20CO2.pdf>.

The entire sequence takes about 13 minutes for a sample. Once every 5 samples, additional 5 minutes are allowed for titration to evaluate the “background count level” of the coulometer.

Cathode and anode solutions of the coulometer were renewed at the beginning of DIC measurements at each station. After conditioning of the solutions, the amount of CO₂ in 1.5% CO₂ in air taken in an electro polished stainless-steel flask (approx. 60 cm³) was measured in order to monitor the performance of the coulometer. A bottle of Certified Reference Material (CRM, batches 103, 107 and 110) prepared by Dr. A.G. Dickson at Scripps Institution of Oceanography was measured at each run of solutions. A working reference material (SSW-M and SSW-N) prepared from western North Pacific surface water was also measured at the beginning, in the middle, and at the end of measurements at a station.

(4-2) Calculation of DIC

Concentration of DIC (C_T) in moles per kilogram of seawater (mol kg⁻¹) was calculated from equation (1):

$$C_T = N_S / (c \cdot V_S \cdot \rho_S), \quad (1)$$

where N_S is the net counts of coulometer, c is the coulometer calibration factor, *i.e.*, the counts of coulometer per mole of carbon, V_S is the sample volume (volume of pipette), and ρ_S is the density of seawater that is calculated from the salinity of sample and its temperature in the pipette.

Net counts of coulometer, N_S , is the counts for sample at 10 minutes after starting CO₂ extraction/titration (N_{10}) subtracted by background count level N_B per 10 minute, *i.e.*,

$$N_S = N_{10} - N_B. \quad (2)$$

Background count levels were measured once every five sample measurements. We evaluated this using equation (3) from the increase of coulometer count from 10 minutes (N_{10}) to 15 minutes (N_{15}) after starting CO₂ extraction/titration when CO₂ in sample seawater is expected to have been completely evolved.

$$N_B = (N_{15} - N_{10}) \cdot 10 / (15 - 10) \quad (3)$$

In this cruise, N_B values were quite large and varied from 0.28 to 1.60. Therefore, we evaluated N_B values more frequently (five times in some runs of measurements). At the same time, we recorded the coulometer count at 10 minute after starting extraction of volatile acids from phosphoric acid (N_{PB}) and used it as the alternative of N_B . N_B or N_{PB} values for each run of five samples measurements were used to calculate N_S .

(4-3) Results of DIC measurements of CRMs and working reference materials

The value of $c \cdot V_S$ was determined for each DIC measurement of CRM (Batch 103, 107 and 110) from equation (4):

$$c \cdot V_S = N_S / (C_{T, CRM} \cdot \rho_{25}), \quad (4)$$

where $C_{T, CRM}$ denotes the certified DIC concentration of CRM. The results are shown in Figure C.5.2a. Values of $c \cdot V_S$ were averaged over the same leg for each apparatus, and were used for the calculations of DIC in sample seawaters (Table C.5.1). The relative standard deviations of $c \cdot V_S$ values were 0.09 % at a whole.

Standard deviation of the differences in DIC concentration of CRM between analysed values and certified values was $\pm 3.0 \mu\text{mol kg}^{-1}$ ($n = 182$) for apparatus A and $\pm 2.5 \mu\text{mol kg}^{-1}$ ($n = 136$) for apparatus B (Figure C.5.2b). The repeatability as estimated from the difference in the replicate analyses from a bottle of CRM (equation 5) was $\pm 1.7 \mu\text{mol kg}^{-1}$ (Figure C.5.2c).

$$\sigma_{\text{repli}} = \sqrt{\sum_{i=1}^n d_i^2 / 2n} \quad (5)$$

Standard deviation of the difference in DIC of working reference materials between analysed values and mean values were $\pm 2.7 \mu\text{mol kg}^{-1}$ ($n = 153$) for apparatus A and $\pm 2.8 \mu\text{mol kg}^{-1}$ ($n = 109$) for apparatus B (Figure C.5.3).

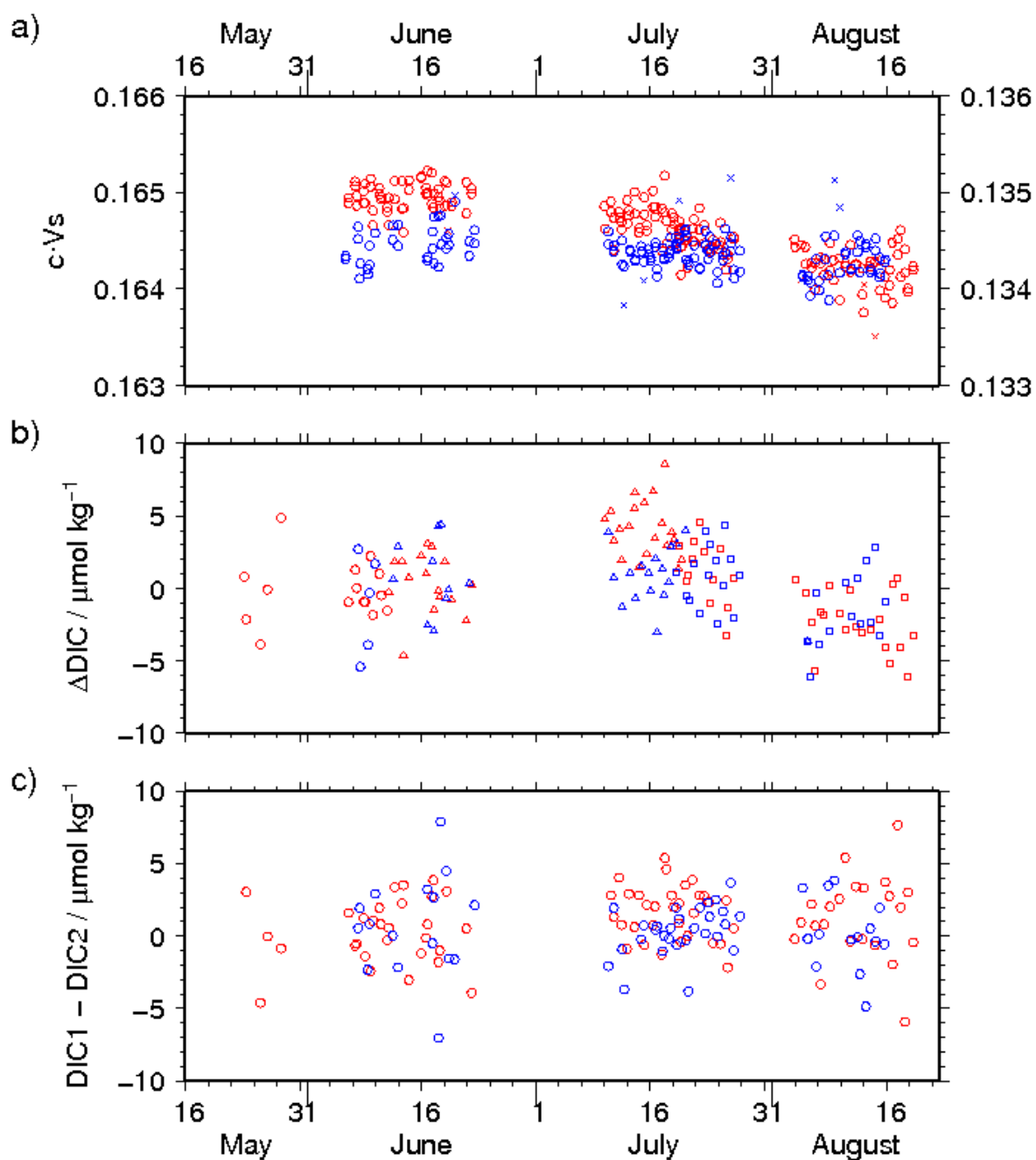


Figure C.5.2. The result of measurements of DIC in CRM. a) Calibration factor $c \cdot V_s$. Circle and cross denote good and bad measurements, respectively. Colour denotes the apparatus used (as well as the following); red: apparatus A, blue: apparatus B. Left vertical axis is for red plots and right vertical axis is for blue plots. b) Difference in DIC between measured and certified values. The shape of plots denotes the batch used; circle: 103, triangle: 107 and square: 110. c) Difference in DIC between two measurements from a bottle.

Table C.5.1. Summary of calibration factor, $c \cdot V_s$.

Mean \pm standard deviation of accepted $c \cdot V_s$ / gC kg mol⁻¹ values. The number of bottles analyzed is in parenthesis. Standard deviation estimated from replicate analyses from a bottle (equation 5) is shown in lower line.

Cruise	Apparatus	
	A	B
RF11-06	0.199684 \pm 0.000297 (10)	----
RF11-07	0.164964 \pm 0.000110 (27) 0.000118	0.134482 \pm 0.000174 (18) 0.000153
RF11-08 leg 1	0.164738 \pm 0.000124 (20) ^{*1} 0.000142 0.164482 \pm 0.000126 (15) ^{*2} 0.000123	0.134377 \pm 0.000121 (32) 0.000083
RF11-08 leg 2	0.164243 \pm 0.000141 (24) 0.000180	0.134242 \pm 0.000169 (15) 0.000082

^{*1} For measurements before 19 July, 2011. ^{*2} For measurements after 20 July, 2011.

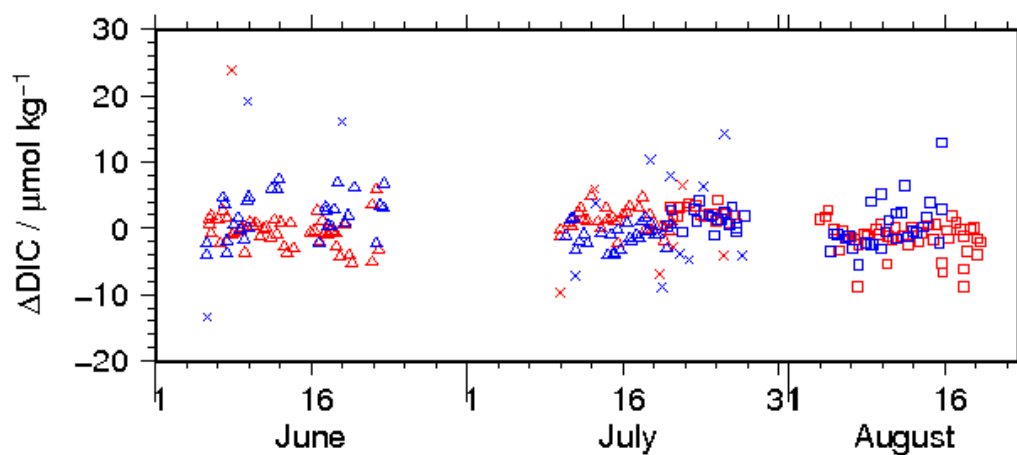


Figure C.5.3 Differences in the measured DIC of working reference materials from mean values of each batch. The shape of plots denotes the batch; triangle: batch M, square: batch N and cross: bad measurements. The color of plots denotes the apparatus; red: apparatus A, blue: apparatus-B.

(5) Total Alkalinity

(5-1) Instrumentation and procedures

TA is measured by one-step volumetric addition of hydrochloric acid (HCl) to a known amount of sample seawater with prompt spectrophotometric measurement of excess acid using the sulfonephthalein indicator bromocresol green (BCG) (*Breland and Byrne, 1993*). The unit for TA measurements in the coupled DIC/TA analyzer consists of sample treatment unit (Nippon ANS) with a calibrated sample pipette and an open titration cell that are water-jacketed and connected to a thermo stated (25 °C) water bath, an auto syringe (PSD/8, Hamilton) connected to a bottle (Schott Duran®, 1 dm³) of titrant stored at 25 °C, and a double-beam spectrophotometric system with two CCD image sensor spectrometers (C10083CAH, Hamamatsu Photonics) combined with a high power Xenon lamp (HPX-2000, Ocean Optics). The mixture of 0.05N HCl and 40 μmol dm⁻³ BCG in 0.65M NaCl solution was used as titrant to automatically titrate the sample as follows:

- (a) A portion of sample seawater was delivered into the sample pipette (approx. 42 cm³) after the other portion is delivered into the DIC unit for a DIC measurement. After the temperature of pipette was recorded, the sample was transferred into a cylindrical quartz cell (4 cm outer diameter).
- (b) An absorption spectrum of sample seawater in the visible light domain was then measured, and the absorbances at wavelengths of 444 nm, 509 nm, 616 nm and 730 nm as well as the temperature in the cell were recorded.
- (c) The titrant that includes 0.05N HCl was added to the sample seawater by using the auto syringe so that pH of sample seawater becomes in the range between 3.85 and 4.05 after the next step (d).
- (d) While the acidified sample was being stirred, the evolved CO₂ was purged with the stream of purified N₂ bubbled into the sample at approx. 200 cm³ min⁻¹ for 5 minutes.
- (e) After leaving the bubbled acidified sample still for 1 minute, the absorbance of bromocresol green in the sample was measured in the same way as described in (b), and pH (in total hydrogen ion scale, pH_T) of the acidified seawater was precisely determined spectrophotometrically.

A typical titration including rinse, fill and discharge takes about 13 minutes.

The data of absorbance (*A*) and temperature (*T*) were processed to calculate the concentration of excess acid (*Breland and Byrne, 1993*):

$$\begin{aligned} \text{pH}_T &= -\log_{10}([\text{H}^+]_T/\text{mol kg-seawater}^{-1}) \\ &= 4.2699 + 0.02578 \cdot (35 - S) + \log\{(R_{25} - 0.00131)/(2.3148 - 0.1299 \cdot R_{25})\} \\ &\quad - \log(1 - 0.001005 \cdot S) \end{aligned} \quad (6)$$

$$R_{25} = R_T \cdot \{1 + 0.00907 \cdot (25 - (T/^\circ\text{C}))\} \quad (7)$$

$$R_T = (A_{616}^{SA} - A_{616}^S - A_{730}^{SA} + A_{730}^S) / (A_{444}^{SA} - A_{444}^S - A_{730}^{SA} + A_{730}^S) \quad (8)$$

S is salinity of sample in PSS-78 that was measured separately. \overline{A}_λ^S and $\overline{A}_\lambda^{SA}$ denotes absorbance of seawater and acidified seawater, respectively, at wavelength λ nm.

The concentration of excess acid $[H^+]_T$ determined is then combined with the volume of sample seawater (V_S / dm³), the volume of titrant (V_A / dm³) added to the sample, and molarity of hydrochloric acid (M_A / mol dm⁻³) in the titrant to calculate total alkalinity (A_T) in the unit of moles per kg of sea water (mol kg⁻¹):

$$A_T = (-[H^+]_T \cdot (V_S + V_A) \cdot \rho_{SA} + M_A \cdot V_A) / (V_S \cdot \rho_S) \quad (9)$$

ρ_S and ρ_{SA} denotes the density of seawater sample before and after the addition of titrant, respectively. Here we assumed that ρ_{SA} is equal to ρ_S , since the density of titrant has been adjusted to that of seawater by adding sodium chloride and the volume of titrant (approx. 2.5 cm³) is no more than approx. 6% of seawater sample.

(5-2) Volume of sample seawater, V_S

The volumes of sample seawater, V_S , *i.e.*, the volume of pipette in the TA measurement unit of DIC/TA analyzer, was calibrated gravimetrically and summarized in Table C.5.2.

Table C.5.2 Summary of sample volumes of seawater V_S for TA measurements.

Apparatus	Volume / ml
A	42.0375
B	42.1978

(5-3) Preparation of titrant (0.05N HCl)

76 g of sodium chloride (NaCl) (Wako Pure Chemical Industries, Ltd.) and 0.12 g of bromocresol green (BCG) (Acros Organics) were dissolved in 200 cm³ of 0.5 mol dm⁻³ HCl solution (Wako Pure Chemical Industries, Ltd.). The solution was diluted with deionised water to a final volume of 2 dm³ at 25 °C. The concentration of HCl, NaCl and BCG was 0.05 mol dm⁻³, 0.65 mol dm⁻³ and 40 µmol dm⁻³, respectively. Sodium chloride was added to make the density and the ionic strength of the solution close to those of seawater.

(5-4) Results of TA measurements of CRMs and working reference materials

Measurements of TA for CRMs (batch 103, 107 and 110) were made and the apparent molarity of hydrochloric acid (M_A / mol dm⁻³) in the titrant was determined from equation (10):

$$M_A = (A_{T, CRM} \cdot V_S \cdot \rho_S + [H^+]_T \cdot V_S \cdot \rho_{SA}) / V_A. \quad (10)$$

The analytical results of M_A was averaged for each bottle of titrant unless the drift of molarity was clearly seen (Figure C.5.4a), and was used to calculate the TA in sample seawaters (Table C.5.3).

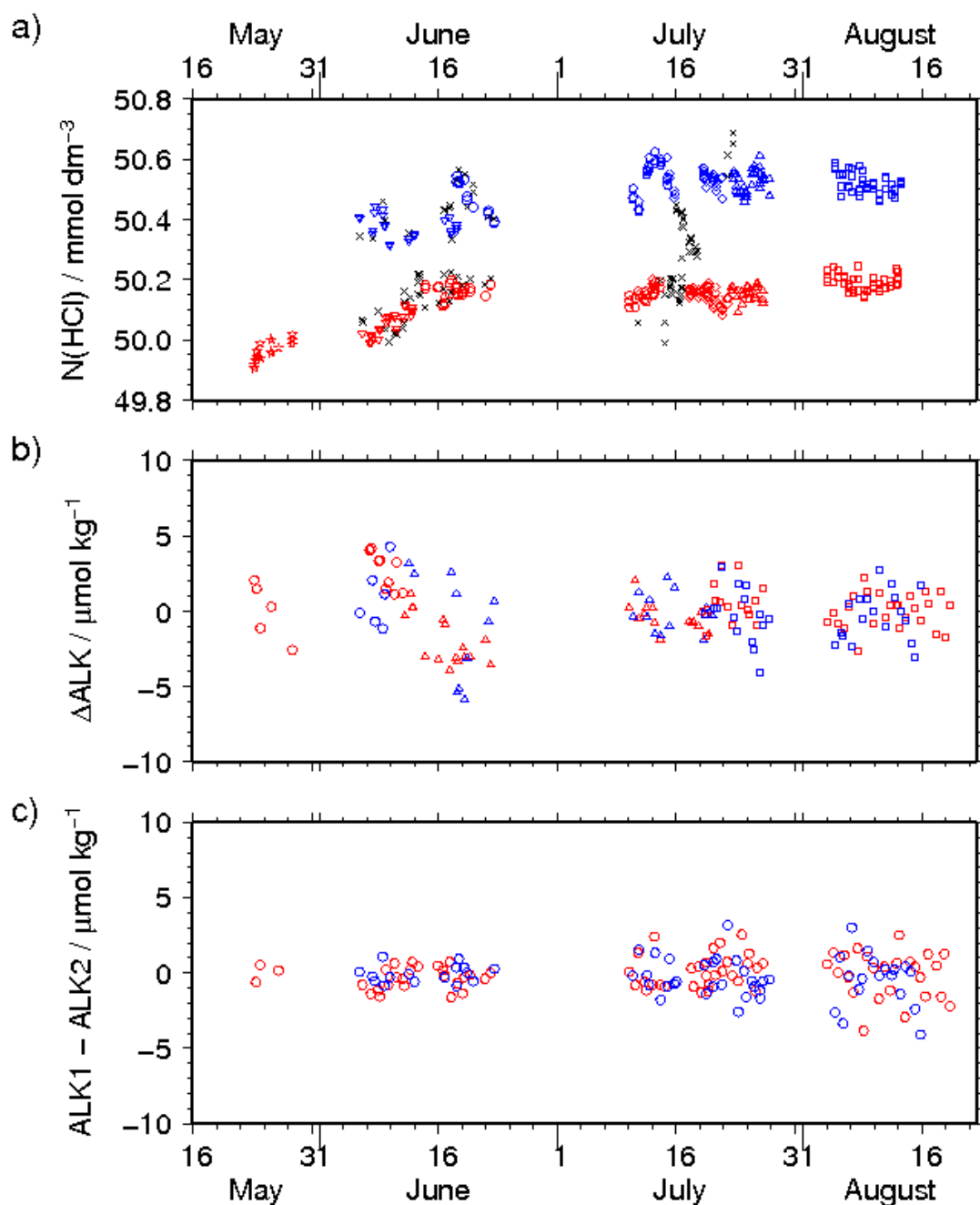


Figure C.5.4. The result of measurements of TA in CRM. a) Apparent concentration of acid in HCl titrant solution. The shape of the plots denotes the bottle of titrant (7 bottles were used for each apparatus). Cross indicates bad measurements. The colour of plots denotes the apparatus; red: apparatus A and blue: apparatus B. b) Difference in TA between measured and certified values. The shape of plots denotes the batch used; circle: 103, triangle: 107 and

square: 110. c) Difference in TA between two measurements from a bottle.

Table C.5.3 Summary of acid titrant concentration for TA analyses

Mean \pm standard deviation of accepted molarity of HCl in titrants. The number of analyses is in parenthesis.

Cruise	Apparatus_Batch	Date	Concentration / mmol dm ⁻³
RF11-06	A_1	23 May – 28 May	49.964 \pm 0.032 (14)
RF11-07	A_2	6 Jun. – 11 Jun.	50.037 \pm 0.030 (22)
	A_3	11 Jun. – 13 Jun.	50.101 \pm 0.012 (7)
	A_4	13 Jun. – 22 Jun.	50.162 \pm 0.021 (26)
RF11-08	A_5	10 Jul. – 22 Jul.	50.149 \pm 0.025 (63) ^{*1}
	A_6	23 Jul. – 26 Jul.	50.156 \pm 0.025 (24) ^{*1}
	A_7	4 Aug. – 12 Aug.	50 190 \pm 0.026 (44)
	A_8	13 Aug. – 26 Aug.	50.173 \pm 0.024 (36)
RF11-07	B_1	6 Jun. – 9 Jun.	50.380 \pm 0.046 (13)
	B_2	12 Jun. – 18 Jun.	50.362 \pm 0.024 (12)
	B_3	18 Jun. – 23 Jun.	50.476 \pm 0.057 (13)
RF11-08	B_4	10 Jul. – 14 Jul.	50.541 \pm 0.060 (20) ^{*2}
	B_5	14 Jul. – 21 Jul.	50.531 \pm 0.030 (30) ^{*2}
	B_6	23 Jul. – 13 Aug.	50.521 \pm 0.035 (79) ^{*2}
	B_7	13 Aug. – 15 Aug.	50.558 \pm 0.031 (14)

*1 Fluctuation of apparent concentration was large due to the bubbles in a titrant syringe.

*2 Apparent concentration varied large by unidentified reason.

Apparent concentrations of HCl varied large in cruise RF11-08. One reason for this was bubbles in titrant syringe of apparatus A. When bubbles exist in the syringe, actually injected volume of titrant decreases. This causes higher pH_T in acidified seawater resulting apparently lower HCl concentration in titrant. In this case, the concentration of HCl in titrant was not corrected but the actual volumes of titrant injected were corrected. On the other hand, the reason for the fluctuation of apparent HCl concentration in titrant of apparatus B was sometimes not identified. In this case, the HCl molarity was not included for average calculation and the TA was calculated using apparent HCl molarity at the station. These corrected data were flagged 3 (questionable. See section (6)).

When the bubbles in titrant syringe were injected, actual volumes of titrant were estimated for each sample using following procedure.

a) Actual volume of titrant injected to sample was estimated so that the measured CRM value was identical to the certified value. Then, the ratio (C) of actual volume to nominal volume was calculated.

b) Apparent absorbance at 509 nm that was equivalent to the nominal volume 2.00 cm³ was calculated. This absorbance value was denoted hereafter as “A₅₀₉₍₂₎”. Then, the ratio

C was expressed as a linear function of A_{509} (2).

c) The volume ratio C for each sample was estimated from the equation obtained at b). Then, actual volume was estimated from C multiplied nominal volume of titrant.

Standard deviation of the differences in TA of CRM between analysed values and certified values was $\pm 2.3 \mu\text{mol kg}^{-1}$ ($n = 236$) for apparatus A and $\pm 1.9 \mu\text{mol kg}^{-1}$ ($n = 179$) for apparatus B (Figure C.5.4b). The repeatability as estimated from the absolute difference in the replicate analyses of CRMs was $\pm 0.9 \mu\text{mol kg}^{-1}$ (Figure C.5.4c).

Standard deviation of the difference in TA of working reference materials between analysed values and mean values were $\pm 2.2 \mu\text{mol kg}^{-1}$ ($n = 166$) for apparatus A and $\pm 1.7 \mu\text{mol kg}^{-1}$ ($n = 92$) for apparatus B (Figure C.5.5).

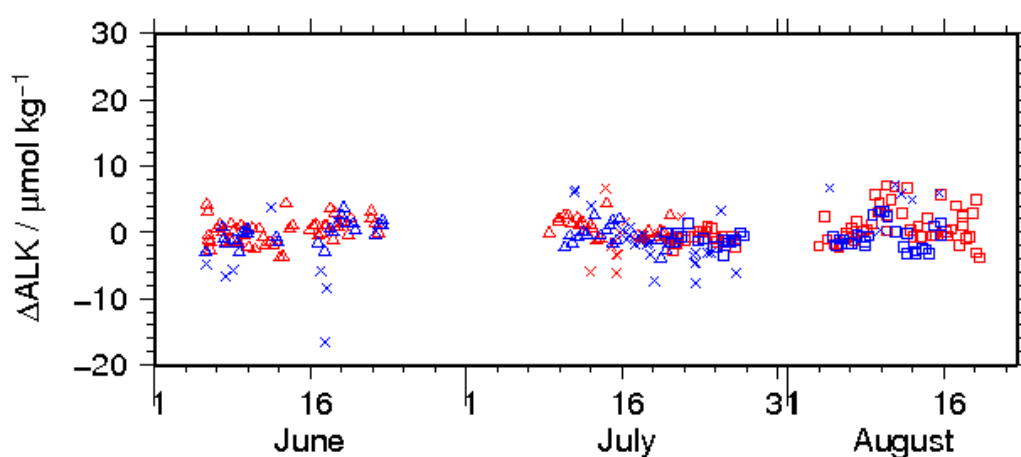


Figure C.5.5. Differences in TA of working reference materials between measured value and mean for each batch. The shape of plots denotes the batch; triangle: batch M, square: batch N and cross: bad measurements. The colour of plots denotes the apparatus; red: apparatus A, blue: apparatus-B.

(6) Assignment of quality flag

Quality code was assigned for each of DIC and TA measurements according to the WHP quality code definitions for water sample measurements (*Swift and Diggs, 2008, Swift, 2010*). Summary of assigned quality flags is shown in Table C.5.4. Data from replicate samples were averaged and flagged 6 if both flags have been assigned 2. If either of flags has been assigned 3 or 4, younger flag was selected.

Table C.5.4. Summary of assigned quality flags.

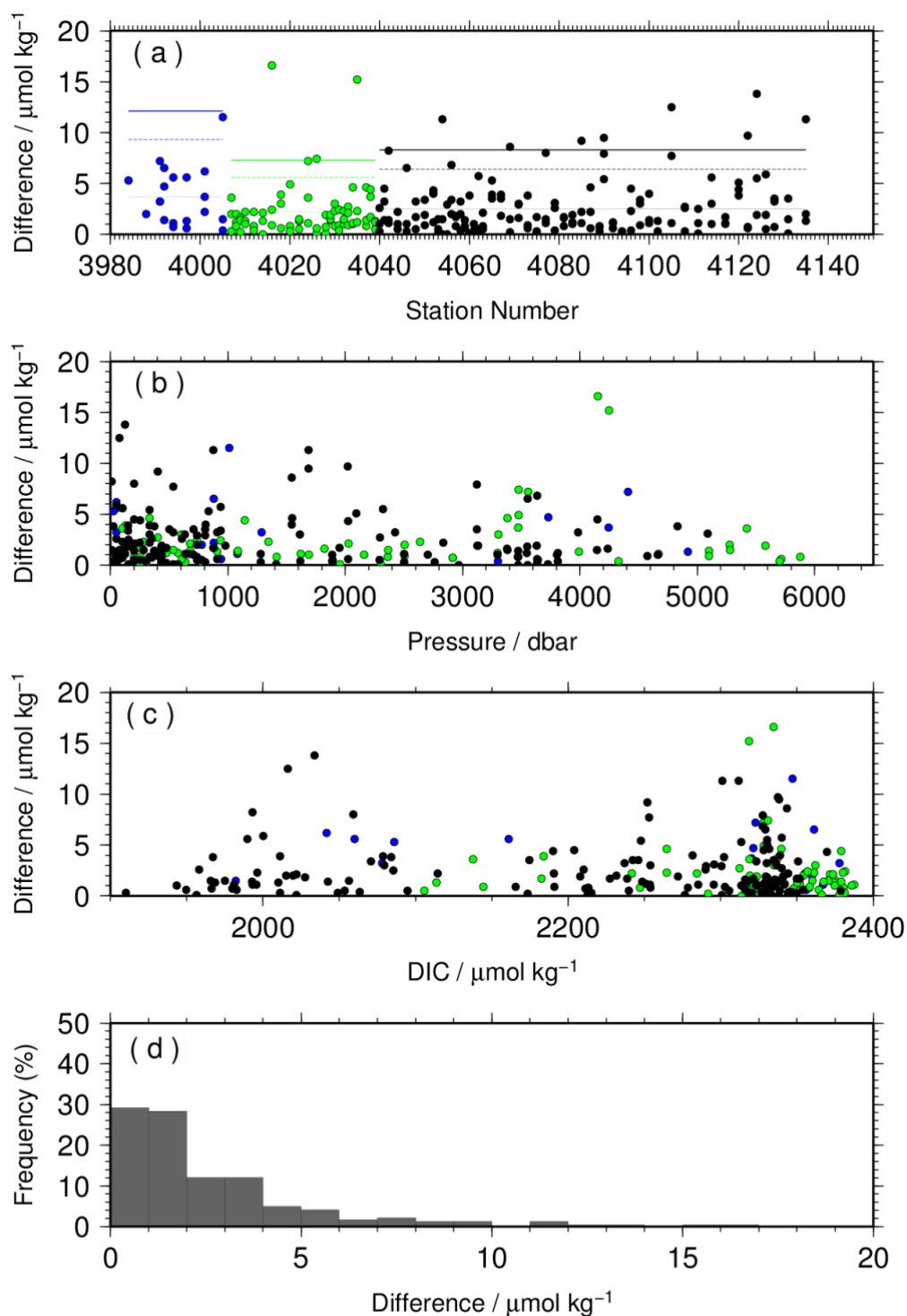
Flag	Definition	DIC	TA
2	Good	2967	2866
3	Questionable	154	260
4	Bad (Faulty)	11	6
5	Not reported	0	0
6	Replicate measurements	192	197
Total number of samples		3132	3132

*Samples of flag 6 are counted as flag 2.

(7) Results of replicate and duplicate sample measurements

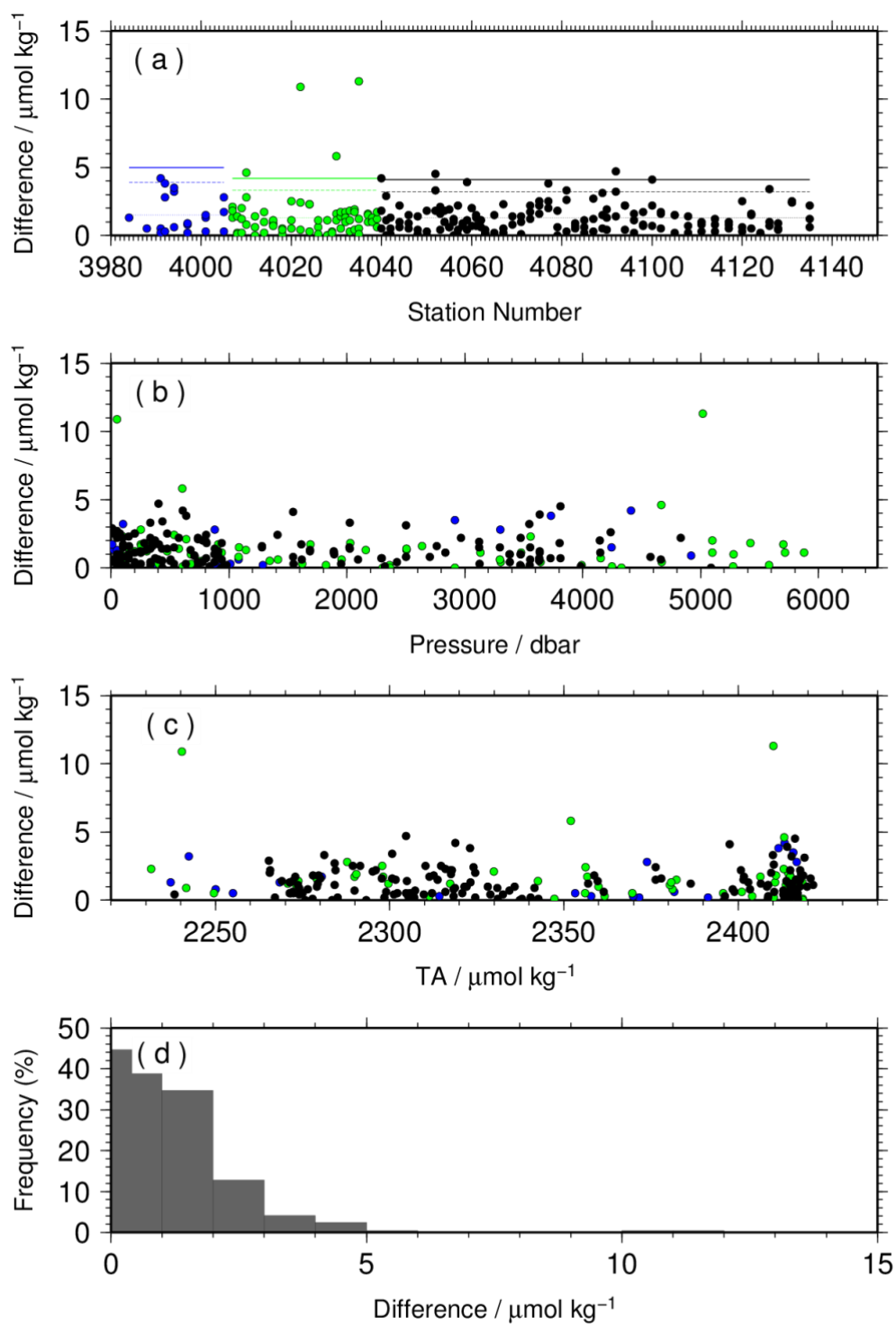
Total of 241 pairs of replicate samples, drawn from a same Niskin bottle, were collected at every stations for DIC and TA measurements. The average of difference in the pairs of measurements (including QF=2 and 3) was $2.5 \mu\text{mol kg}^{-1}$ for DIC ($n = 239$) and $1.3 \mu\text{mol kg}^{-1}$ for TA ($n = 241$). Total of 124 pairs of duplicate samples, drawn from a different Niskin bottle tripped at the same depth, were also collected at every station for DIC and TA measurements. The average of difference in the pairs of measurements (including QF 2 and 3) was $2.7 \mu\text{mol kg}^{-1}$ for DIC ($n = 124$) and $1.1 \mu\text{mol kg}^{-1}$ for TA ($n = 123$).

Summary of replicates are shown in Figures C.5.6 and C.5.7 and in Table C.5.5. Summary of duplicates are shown in Table C.5.6. The average and standard deviation were calculated using a procedure described in SOP23 in *Dickson et al.* (2007).



GM 2014 Feb 13 08:12:45

Figure C.5.6. Absolute differences in DIC between measurements of replicate samples (n = 239) during the cruises RF11-06 (blue), RF11-07 (green) and RF11-08 (black) versus (a) station number, (b) sampling depth, and (c) concentration of DIC. The histogram of absolute difference is shown in (d).



GM 2014 Feb 13 08:07:40

Figure C.5.7. Same as Figure C.5.6 but for TA ($n = 241$).

Table C.5.5 Summary for the measurements of replicate samples.

	DIC / $\mu\text{mol kg}^{-1}$		TA / $\mu\text{mol kg}^{-1}$	
Number of measurement pairs (Accepted / Sampled)	RF11-06:	20 / 20	RF11-06:	20 / 20
	RF11-07:	69 / 69	RF11-07:	69 / 69
	RF11-08:	150 / 152	RF11-08:	152 / 152
	Total:	239 / 241	Total:	241 / 241
Average of absolute difference	RF11-06:	3.7	RF11-06:	1.5
	RF11-07:	2.2	RF11-07:	1.3
	RF11-08:	2.5	RF11-08:	1.3
	Total:	2.5	Total:	1.3
Standard deviation of measurements	RF11-06:	3.3	RF11-06:	1.4
	RF11-07:	2.5	RF11-07:	1.4
	RF11-08:	2.6	RF11-08:	1.1
	Total:	2.6	Total:	1.2

Table C.5.6. Summary for the measurements of duplicate samples.

	DIC / $\mu\text{mol kg}^{-1}$		TA / $\mu\text{mol kg}^{-1}$	
Number of measurement pairs (Accepted / Sampled)	RF11-06:	15 / 15	RF11-06:	15 / 15
	RF11-07:	31 / 31	RF11-07:	31 / 31
	RF11-08:	78 / 78	RF11-08:	77 / 77
	Total:	124 / 124	Total:	123 / 123
Average of absolute difference	RF11-06:	2.9	RF11-06:	0.8
	RF11-07:	1.9	RF11-07:	1.1
	RF11-08:	3.0	RF11-08:	1.3
	Total:	2.7	Total:	1.2
Standard deviation of measurements	RF11-06:	2.5	RF11-06:	0.7
	RF11-07:	1.8	RF11-07:	1.0
	RF11-08:	3.0	RF11-08:	1.2
	Total:	2.7	Total:	1.1

(8) Comparisons at cross-over stations within this cruise

There were two cross-over stations that were occupied multiple times within this cruise. The one was located at 40°N, 165°E. This station was occupied twice; station 55 (RF4039) on 21 June and station 56 (RF4040) on 9 July. The other was located at 9°N, 165°E. This station was occupied twice; station 105 (RF4089) on 25 July and station 106 (RF4090) on 3 August. Vertical profiles of DIC and TA at these stations are shown in Figures C.5.8 and C.5.9.

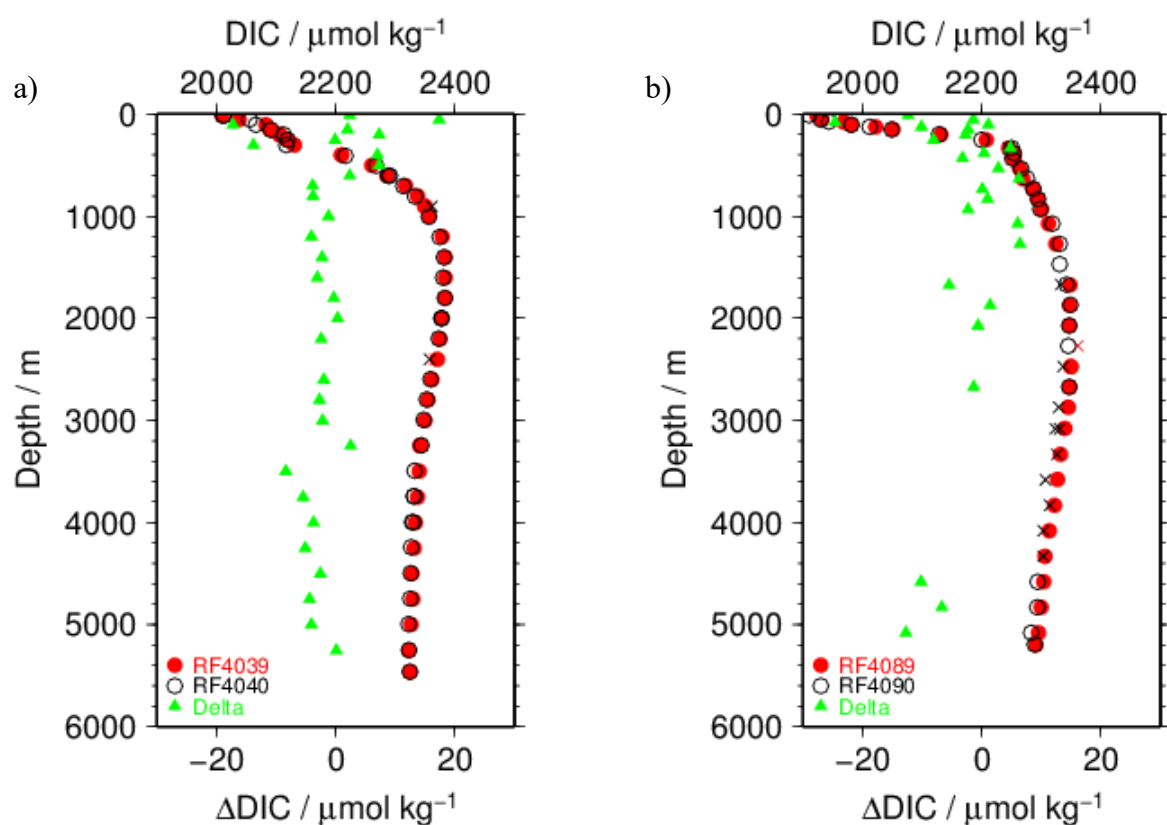


Figure C.5.8 Comparison of DIC observed in this study at same location in different legs of this cruise. a) 40N, 165E in cruise RF11-07 (station RF4039) and in cruise RF11-08 (station RF4040); b) 9N, 165E in leg1 (station RF4089) and leg2 (station RF4090) of cruise RF11-08. Circle and cross plots are acceptable and questionable values, respectively. The colour denotes the station shown in the legend. Triangle plot is the difference in DIC analysed at same location in different legs.

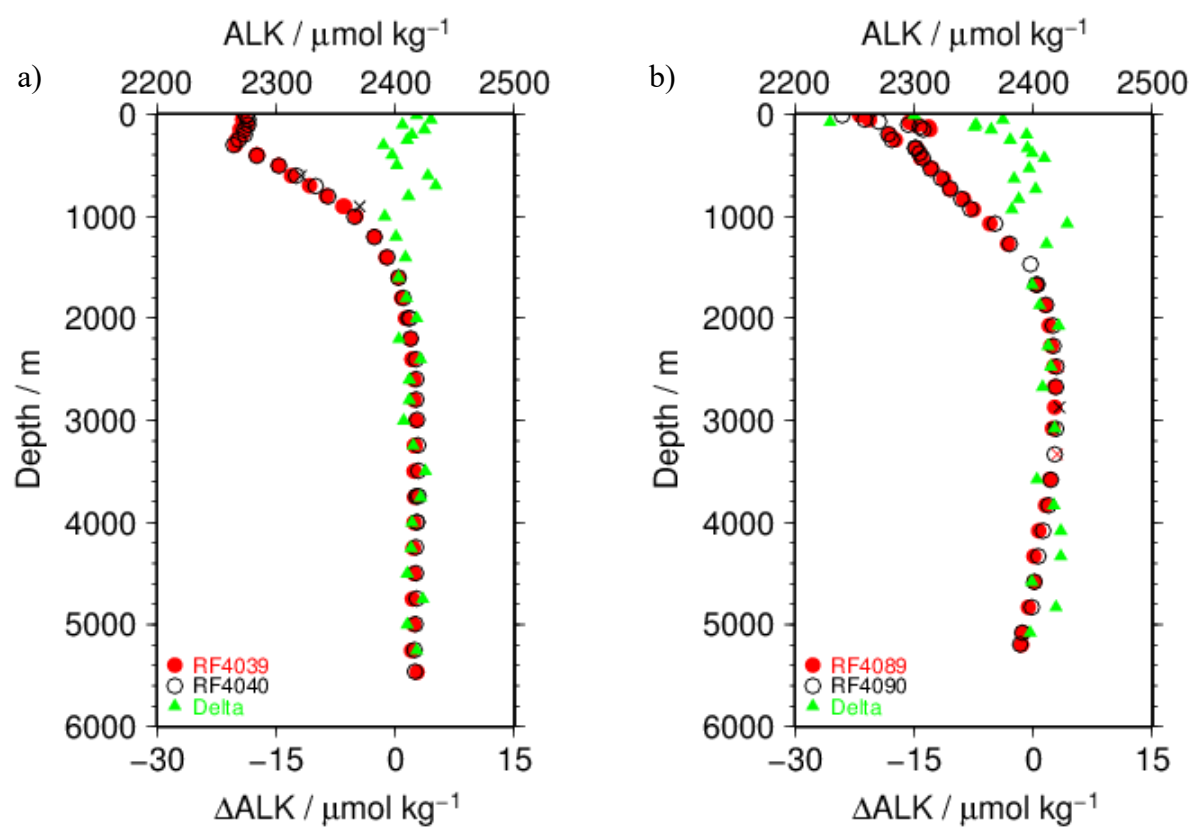


Figure C.5.9. Same as Figure C.5.8 but for TA.

(9) Comparisons at cross-over stations with other WHP and its revisit cruises

The WHP section P13 intersects section P1 at 47°N, 165°E, section P2 at 30°N, 165°E and section P3 at 24°N, 165°E. DIC and TA in section P2 have been observed twice in the past; first in the cruise 49K6KY9401_1 of *R/V Kaiyo-Maru* in 1994 and second in the cruise 318M200406 of *R/V Melville* in 2004, and those in section P3 has been observed in the cruise 49NZ20051127 of *R/V Mirai* in 2005/2006. Summary of the comparisons of vertical profiles at cross-over stations are shown in Figure C.5.10 and C.5.11.

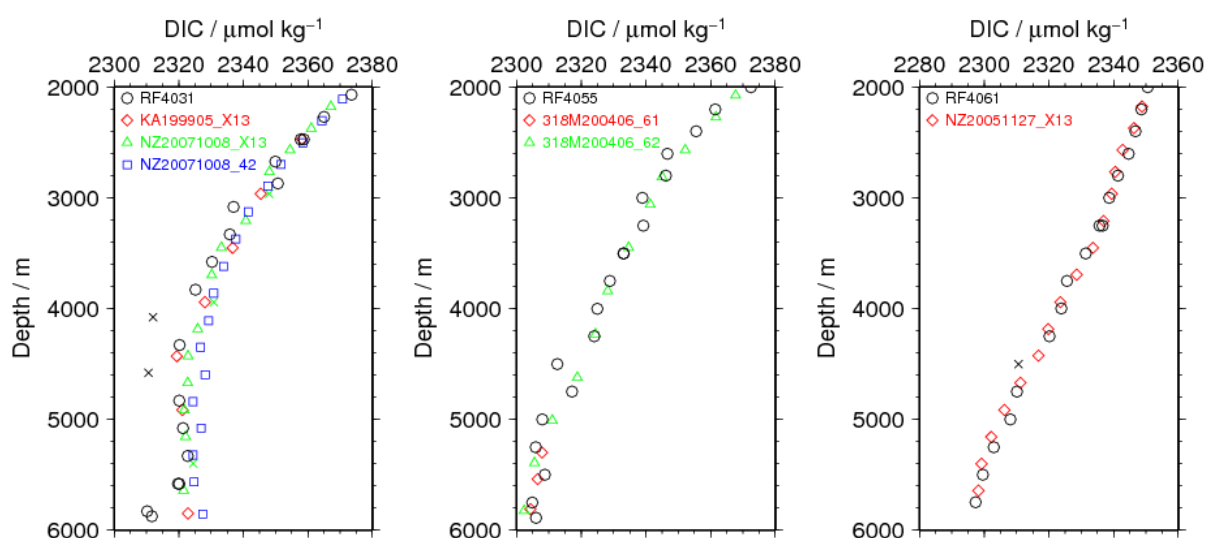


Figure C.5.10. Vertical profiles of DIC with WHP P1e (left panel: P1 in 1999 (diamond), P1 in 2007 (triangle and square) and P13 in 2011 (circle)), with P2 (middle panel: P2 in 2004 (diamond and triangle) and P13 in 2011 (circle)) and with WHP P3 (right panel: P3 in 2005/06 (diamond) and P13 in 2011 (circle)) at cross-over stations.

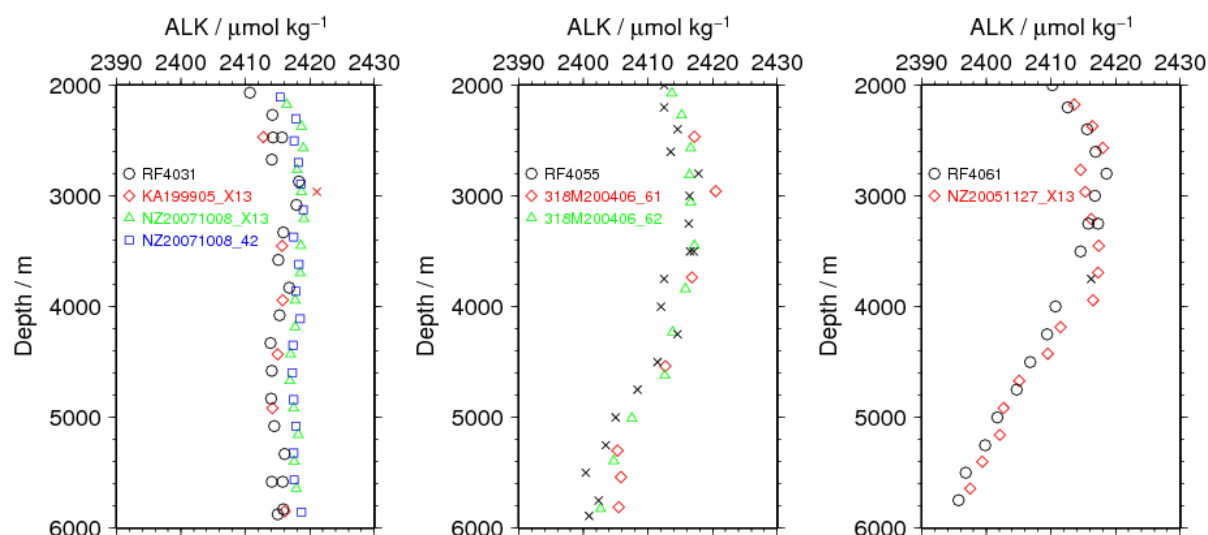


Figure C.5.11. Same as Figure C.5.10 but for TA.

References

- Breland II, J. A. and R. H. Byrne (1993), Spectrophotometric procedures for determination of sea water alkalinity using bromocresol green, *Deep-Sea Res. I*, 470, 629-641.
- Dickson, A. G., Sabine, C. L. and Christian, J. R. (Eds.) (2007), Guide to best practices for ocean CO₂ measurements. PICES Special Publication 3, 191 pp.
- Ishii, M., H. Y. Inoue, H. Matsueda, and E. Tanoue (1998), Close coupling between seasonal biological production and dynamics of dissolved inorganic carbon in the Indian Ocean sector and the western Pacific Ocean sector of the Antarctic Ocean, *Deep Sea Res. Part I*, 45, 1187–1209, doi:10.1016/S0967-0637(98)00010-7.
- Johnson, K. M., A. E. King and J. McN. Sieburth (1985), Coulometric TCO₂ analyses for marine studies; an introduction. *Marine Chemistry*, **16**, 61-82.
- Johnson, K. M., J. McN. Sieburth, P. J. IeB Williams and L Brändström (1987), Coulometric total carbon dioxide analyses for marine studies: Automation and calibration. *Marine Chemistry*, **21**, 117-133.
- Kaneko, I., Y. Takatsuki, H. Kamiya and S. Kawae (1998), Water property and current distributions along the WHP-P9 section (137°-142°E) in the western North Pacific. *J. Geophys. Res.*, **103**, 12959-12984.
- Swift, J. H. and S. C. Diggs (2008), A Guide to Submitting CTD/Hydrographic/Tracer Data and Associated Documentation to the CLIVAR and Carbon Hydrographic Data Office (Appendix C: Description of WHP-Exchange Format for CTD/Hydrographic Data)., <http://cchdo.ucsd.edu/policies.html>.
- Swift, J. H. (2010): Reference-quality water sample data, Notes on acquisition, record keeping, and evaluation. *IOCCP Report No.14, ICPO Pub. 134, 2010 ver.1*

6. Hydrogen ion index (pH)

1 November 2019

(1) Personnel

Shu SAITO (GEMD/JMA, RF11-06 and RF11-08)

Kazutaka ENYO (GEMD/JMA, RF11-07)

Hiroyuki HATAKEYAMA (GEMD/JMA, RF11-06)

Kazuki ISHIMARU (GEMD / JMA, RF11-06)

Nobuya MAEDA (GEMD/JMA, RF11-08)

Shinji MASUDA (GEMD/JMA, RF11-07 and RF11-08)

Etsuro ONO (GEMD / JMA, RF11-06)

Daisuke SASANO (MRI/JMA, RF11-07)

(2) Station occupied

A total of 82 stations (RF11-06: 8, RF11-07: 23, RF11-08: 51) were occupied for hydrogen ion index (pH). Station location and sampling layers of pH are shown in Figure C.6.1.

(3) Method

(3.1) Principle

The pH analysis was made using spectrometry of indicator dye *m*-cresol purple (*Saito et al.*, 2008; *Clayton and Byrne*, 1993). The pH was reported as the value at temperature of 25°C in “total hydrogen ion scale”. In order to state clearly the scale of pH, we mention hereafter as “pH_T” that is defined by equation (1),

$$\text{pH}_T = -\log_{10}([\text{H}^+]_T/C^0) \quad (1)$$

where, $[\text{H}^+]_T$ denotes the concentration of hydrogen ion expressed in the total hydrogen ion scale: $[\text{H}^+]_T = [\text{H}^+]_F(1 + [\text{SO}_4]_T/K_{\text{HSO}_4^-})$, where, $[\text{H}^+]_F$ is the concentration of free hydrogen ion, $[\text{SO}_4]_T$ is the total concentration of sulphate ion and $K_{\text{HSO}_4^-}$ is acid dissociation constant of hydrogen sulphate ion (*Dickson*, 1990). C^0 in equation (1) is the standard value of concentration (1 mole per kilogram of seawater, mol kg⁻¹).

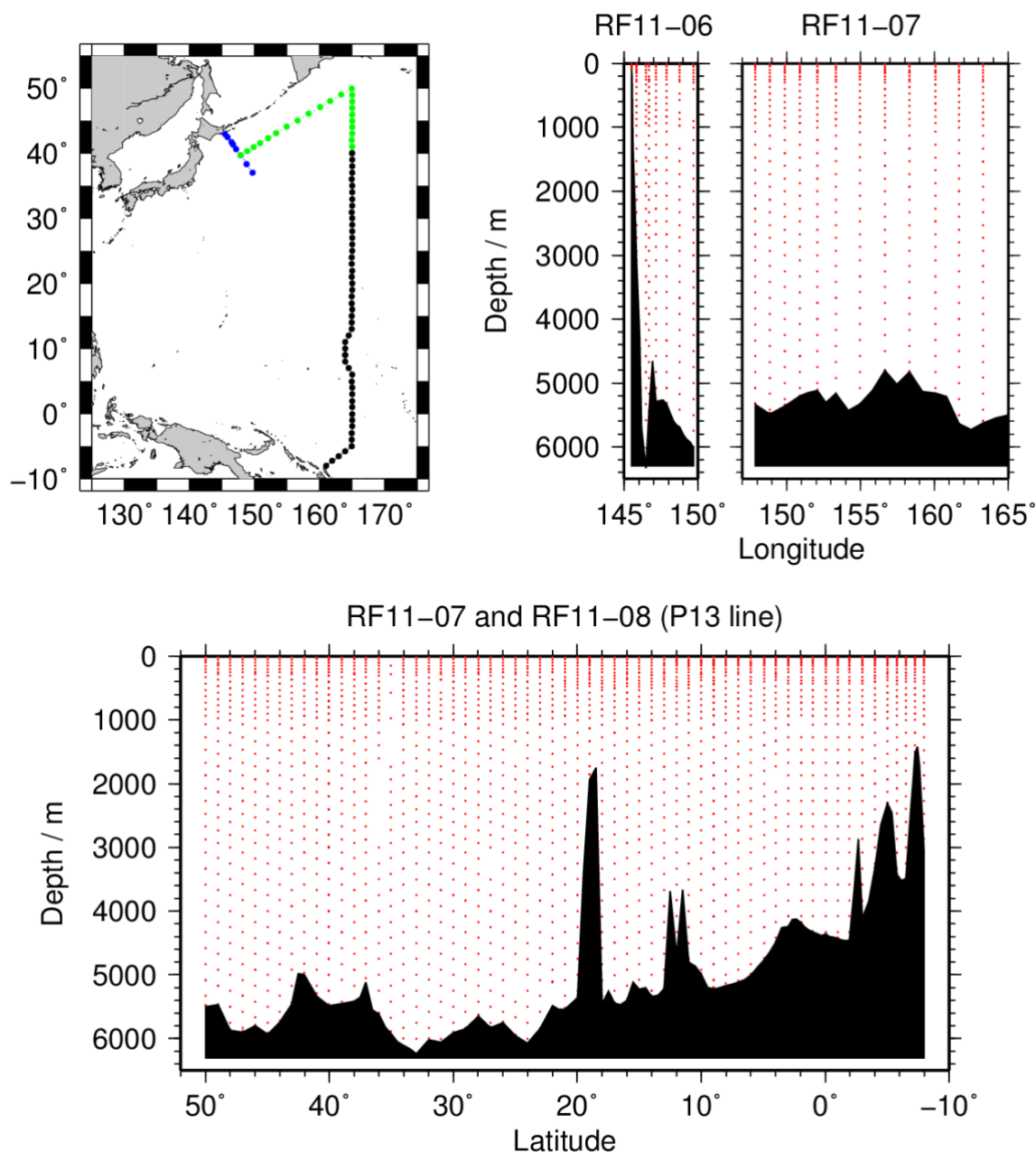


Figure C.6.1. Station location (left panel) and sampling layers of pH (right panels)

(3.2) pHr Reagents

- *m*-Cresol purple solution

The air in a borosilicate glass flask (2 dm³) was replaced by pure nitrogen. 0.67 g of *m*-cresol purple sodium salt (pure water soluble, 199250050, ACROS) was dissolved in 1 kg of deionised water prepared with water purifier “Autopure WR700” (Yamato Scientific Co. Ltd.). Small amount of diluted NaOH solution (approx. 0.25 mol dm⁻³) was added to regulate the pH (free hydrogen ion scale) of indicator solution to 7.9 ± 0.1 . The pH of indicator solution was monitored using glass electrode pH meter.

Custom-made pH_T analysers (2009 model; Japan ANS Co., Ltd, Tokyo, Japan) was prepared and operated in the cruise. The analyser comprised of a sample dispensing unit (box **1** in Figure C.6.2), a pre-treatment unit combined with an automated syringe (PSD/8, HAMILTON; box **2** in Figure C.6.2), and two (sample and reference) spectrophotometers (C10083CAH, Hamamatsu Photonics) combined with a high power xenon light source (HPX-2000, Ocean Optics) (box **3** in Figure C.6.2). Whole analyser system was controlled by a personal computer (EX/522PDET3, TOSHIBA) using a custom-made software (Japan ANS Co., Ltd) that runs on an operating system Windows XPTM.

[illegible]

C6-3

The analysis procedure was as follows:

- a) Seawater was ejected from a sample loop (thick line in Figure C.6.2)
- b) A portion of sample (approx. 30 cm³) was introduced into a sample loop including spectrophotometric cell. The spectrophotometric cell was flushed two times with sample in order to remove air bubbles.
- c) An absorption spectrum of seawater in the visible light range was measured. Absorbance at wavelengths of 434 nm, 488 nm, 578 nm and 730 nm as well as cell temperature were recorded. To eject air bubbles from the cell, the sample was moved four times (approx. 30 cm each in loop tube whose inner diameter was 1/16 inch) and the absorbance was recorded at each stop.
- d) 10 µl of indicator *m*-cresol purple solution was injected to the loop.
- e) Circulating 2 minutes 40 seconds through the loop tube, seawater sample and indicator dye was mixed together. The final *m*-cresol purple concentration in the sample was approx. 0.55 µmol dm⁻³.
- f) Absorbance of *m*-cresol purple plus seawater was measured in the same way described above (c).

(4) Seawater Sampling

Samples for pH_T analysis were drawn with the similar way of dissolved inorganic carbon (see chapter C05) from 10-liter Niskin bottles into clean 300 cm³ borosilicate bottles (Shibata) using silicone rubber tubing on the petcock. To avoid contamination from the air, samples for pH_T were drawn next to the sampling of dissolved inorganic carbon (DIC) and total alkalinity (TA). Surface sample was collected from continuous flow line pumped from sea-chest. In order to avoid CO₂ exchange with the air, the end of tubing was inserted to the bottom of the bottle, and then the sample was dispensed smoothly into a bottle. Sample of approximately double the volume of bottle was overflowed. The bottle was plugged temporally with a ground glass stopper.

After sampling, 2 cm³ of seawater was removed from bottle to allow thermal expansion of sample. At all stations RF-4030, RF-4054 and RF-4059, at which more than 80 samples (corresponding to two stations) were waiting for analyses, 0.2 cm³ of saturated mercury (II) chloride solution was added to prevent change in pH_T caused by biological activity. At other stations, no mercury (II) chloride solution was added, and measurements of pH_T were started immediately and ended within 20 hours after samplings.

Bottle was sealed with greased (Apiezon-L) ground glass stopper. Sample bottles were stored at room temperature while awaiting analysis. Sample bottles were immersed in isothermal bath to keep in 25.0 °C for over 1 hour before analysis.

(5) pH_T measurement

(5.1) Calculation of pH_T from measured absorbance

pH_T was calculated from the measured absorbance based on the following equations (2)–(4).

$$\begin{aligned} \overline{\text{pH}_T} &= \overline{\text{p}K_2 + \log_{10}([\text{I}^{2-}]/[\text{HI}^-])} \\ &= \overline{\text{p}K_2 + \log_{10}\{(R - 0.0069_1)/(2.222_0 - 0.133_1 R)\}} \end{aligned} \quad (2)$$

$$R = (A_{578}^{\text{SD}} - A_{578}^{\text{S}} - A_{730}^{\text{SD}} + A_{730}^{\text{S}})/(A_{434}^{\text{SD}} - A_{434}^{\text{S}} - A_{730}^{\text{SD}} + A_{730}^{\text{S}}) \quad (3)$$

where $\text{p}K_2$ is the acid dissociation constant of *m*-cresol purple, $[\text{I}^{2-}] / [\text{HI}^-]$ is the ratio of *m*-cresol purple base form (I^{2-}) concentration over acid form (HI^-) concentration, which is estimated from absorbance ratio R and the ratios of extinction coefficients (*Clayton and Byrne, 1993*). $\overline{A_{\lambda}^{\text{S}}}$ and $\overline{A_{\lambda}^{\text{SD}}}$ in equation (3) are absorbances of seawater itself and dye plus seawater,

respectively, at wavelength λ (nm). The value of $\text{p}K_2$ ($= -\log_{10}(K_2/k^0)$, $k^0 = 1 \text{ mol kg}^{-1}$) had also been expressed as a function of temperature T (in Kelvin) and salinity S (in psu) by *Clayton and Byrne (1993)*, but the calculated value has been subsequently corrected by 0.0047 on the basis of a reported pH_T value accounting for “tris” buffer (*DelValls and Dickson, 1998*):

$$\begin{aligned} \overline{\text{p}K_2} &= \overline{\text{p}K_2(\text{Clayton \& Byrne, 1993}) + 0.0047} \\ &= \overline{1245.69/T + 3.8322 + 0.00211(35 - S)}. \end{aligned} \quad (4)$$

$$293 \text{ K} \leq T \leq 303 \text{ K}, 30 \leq S \leq 37$$

(5.2) pH_T Perturbation caused by addition of dye solution

The injection of *m*-cresol purple solution affects the pH_T of seawater sample because the acid base equilibrium of the seawater is disrupted by the addition of the dye acid-base pair (*Dickson et al., 2007*). We corrected the R in Equation (2) for the perturbation using empirical method (Equation (5)) in which a second aliquot of dye solution is added to the seawater sample (*Dickson et al., 2007; Clayton and Byrne, 1993*).

$$\begin{aligned} R &= R_1 - \Delta R, \\ \Delta R &= R_2 - R_1 = R_1 - R \text{ (Assumption)}, \end{aligned} \quad (5)$$

where, R_1 and R_2 are the absorbance ratio after the addition of first and second aliquot of dye solution, respectively. The value of ΔR depended on the pH_T of sample. We expressed ΔR as a quadratic function of R_1 based on experimental $R_2 - R_1$ data obtained at this cruise (Figure C.6.3). 6 samples at each station were analysed to obtain $R_2 - R_1$ data, ΔR was expressed as a

quadratic function of R_1 and the pH_T was evaluated from $R = R_1 - \Delta R$ using equation (2).

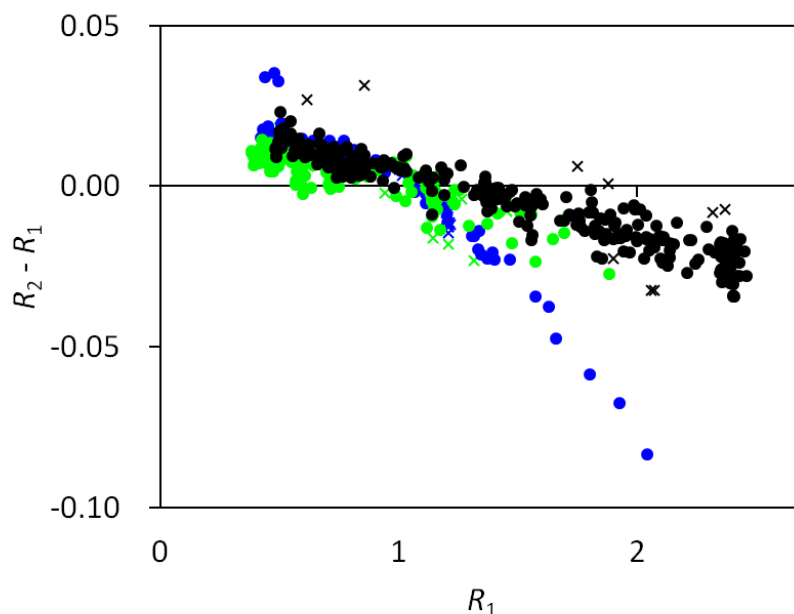


Figure C.6.3. pH_T perturbation caused by the addition of indicator dye solution. The perturbation was expressed as a difference in absorbance ratio between first and second aliquot, $\Delta R = R_2 - R_1$. The colour of plots denotes the cruise; blue: RF11-06, green: RF11-07, black: RF11-08. The result of quadratic regression was listed in Table C.6.1.

Table C.6.1. The coefficients of quadratic regression of the pH_T perturbation that was caused by the addition of *m*-cresol purple solution and was expressed as the difference in absorbance

ratio R . $\Delta R = C_2 \times R_1^2 + C_1 \times R_1 + C_0$

Cruise	C_2	C_1	C_0
RF11-06	-3.3202E-02	1.9195E-02	0.01651
RF11-07	-7.7805E-03	-3.6774E-03	0.01173
RF11-08	-1.1831E-03	-1.6008E-02	0.02138

(6) Quality assurance

(6.1) Results of pH_T measurements of CRM and working reference materials

To check the repeatability and/or reproducibility of measurements, we analysed two batches (103, 107) of certified reference materials (CRMs) that were prepared by Dr. A.G. Dickson at Scripps Institute of Oceanography. Two portions of sample were extracted and analysed from a bottle and the difference in two data were plotted (R-chart, Figure C.6.4a). The standard

deviation was estimated using equations described in SOP22 of *Dickson et al.* (2007). The standard deviation estimated from accepted data was 0.0020 ($n = 23$) in cruise RF11-07 (June, 2011) and 0.0013 ($n = 28$) in cruise RF11-08 (July and August, 2011), respectively.

Measured pH_T was compared with “reference value” that was calculated from certified values of DIC and TA using acid dissociation constants of carbonic acid and hydrogen carbonate ion described by *Lueker et al.* (2000). The concentrations of phosphate and silicate were also used for calculation, although the values are not certified. The difference in measured and reference values were plotted in Figure C.6.4 b). The offset of measured value was 0.0008 ± 0.0024 (mean \pm standard deviation, $n = 23$) in cruise RF11-07 and -0.0094 ± 0.0030 ($n = 28$) in cruise RF11-08, respectively.

In order to monitor the condition of apparatus, in-house standard seawaters (SSW) batch L, and M were analysed. The SSWs were made using the CRM’s manner. The mean and standard deviation was 7.7804 ± 0.0019 ($n = 19$) for batch L in cruise RF11-06, 7.7523 ± 0.0032 ($n = 51$) for batch M in cruise RF11-07 and 7.7479 ± 0.0023 ($n = 61$) for batch M in cruise RF11-08 (Figure C.6.5).

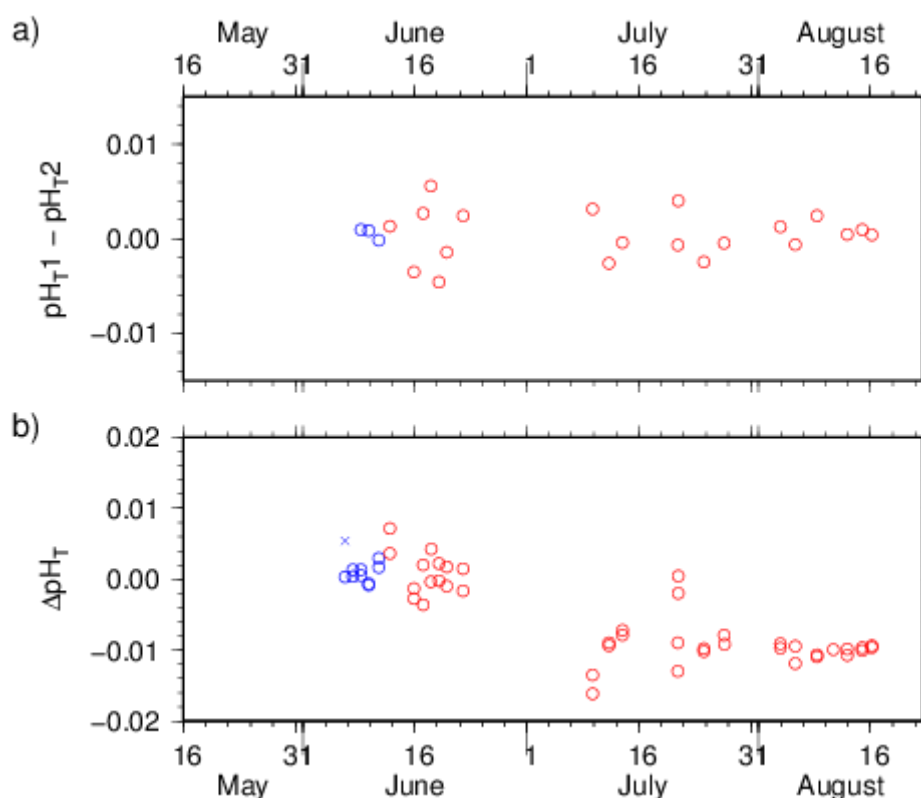


Figure C.6.4. a) Differences in replicate measurements of pH_T in CRM for each bottle (R-chart). b) Differences in pH_T of CRMs between measured and reference values that was calculated from certified values of DIC and TA using acid dissociation constants of carbonates described by *Lueker et al.* (2000). The colour of plots denotes the batch of CRM; blue: batch

103, red: batch 107. Cross plots denote the bad measurements.

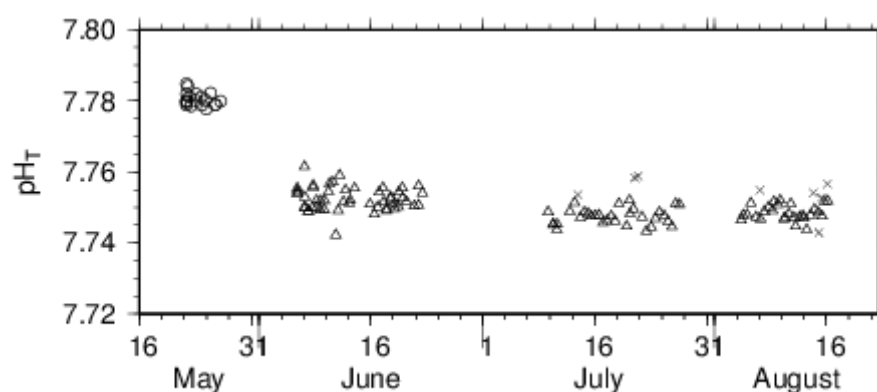


Figure C.6.5. Measured pH_T of working reference materials. The symbols denote the batch of working reference materials; circle: batch L, triangle: batch M and cross: bad measurements.

(6.2) Repeatability of water column samples measurements

To check the repeatability of water column samples measurements, we measured replicate and duplicate samples. At each hydrographic station where sea water samples were drawn, two or more Niskin bottles were closed at the same layer (“Duplicate” sampling) if Niskin bottles on carousel sampler are more than the layers to be sampled at the station. A couple of samples were drawn from each Niskin bottle of 3 layers to obtain 3 “Replicate” samples at each hydrographic station.

Total amounts of the duplicate and replicate sample pairs were 129 and 240, respectively. The control limits and standard deviations were calculated using the method described in SOP22 of *Dickson et al. (2007)*. The average differences and the standard deviations estimated from accepted data are listed in Table C.6.2.

Table C.6.2 Summary of replicate and duplicate samples measurements

	Duplicate		Replicate	
Number of measurement pairs (Accepted / Sampled)	RF11-06:	15 / 15	RF11-06:	18 / 18
	RF11-07:	30 / 31	RF11-07:	69 / 69
	RF11-08:	76 / 83	RF11-08:	150 / 153
	Total:	121 / 129	Total:	237 / 240
Average of absolute difference	RF11-06:	0.0024	RF11-06:	0.0043
	RF11-07:	0.0029	RF11-07:	0.0036
	RF11-08:	0.0022	RF11-08:	0.0025
	Total:	0.0024	Total:	0.0030
Standard deviation of measurements	RF11-06:	0.0026	RF11-06:	0.0042

RF11-07:	0.0026	RF11-07:	0.0035
RF11-08:	0.0026	RF11-08:	0.0023
Total:	0.0026	Total:	0.0028

(6.3) Quality flag assignment

Quality code was assigned for each of pH_T measurements based on the WHP quality code definitions for water sample measurements (Swift and Diggs, 2008, Swift, 2010). Summary of assigned quality control flags are listed in Table C.6.3. The replicate data were averaged and flagged 6 if both of the flag were 1. If either of the flag was 3 or 4, younger flag was selected.

Table C.6.3 Summary of assigned quality control flags.

Flag	Definition	Number of samples
1	Not finalized	2894
3	Questionable	111
4	Bad (Faulty)	20
5	Not reported	0
6	Replicate measurements	237
Total number of samples		3025

* Samples of flag 6 are counted as flag 1

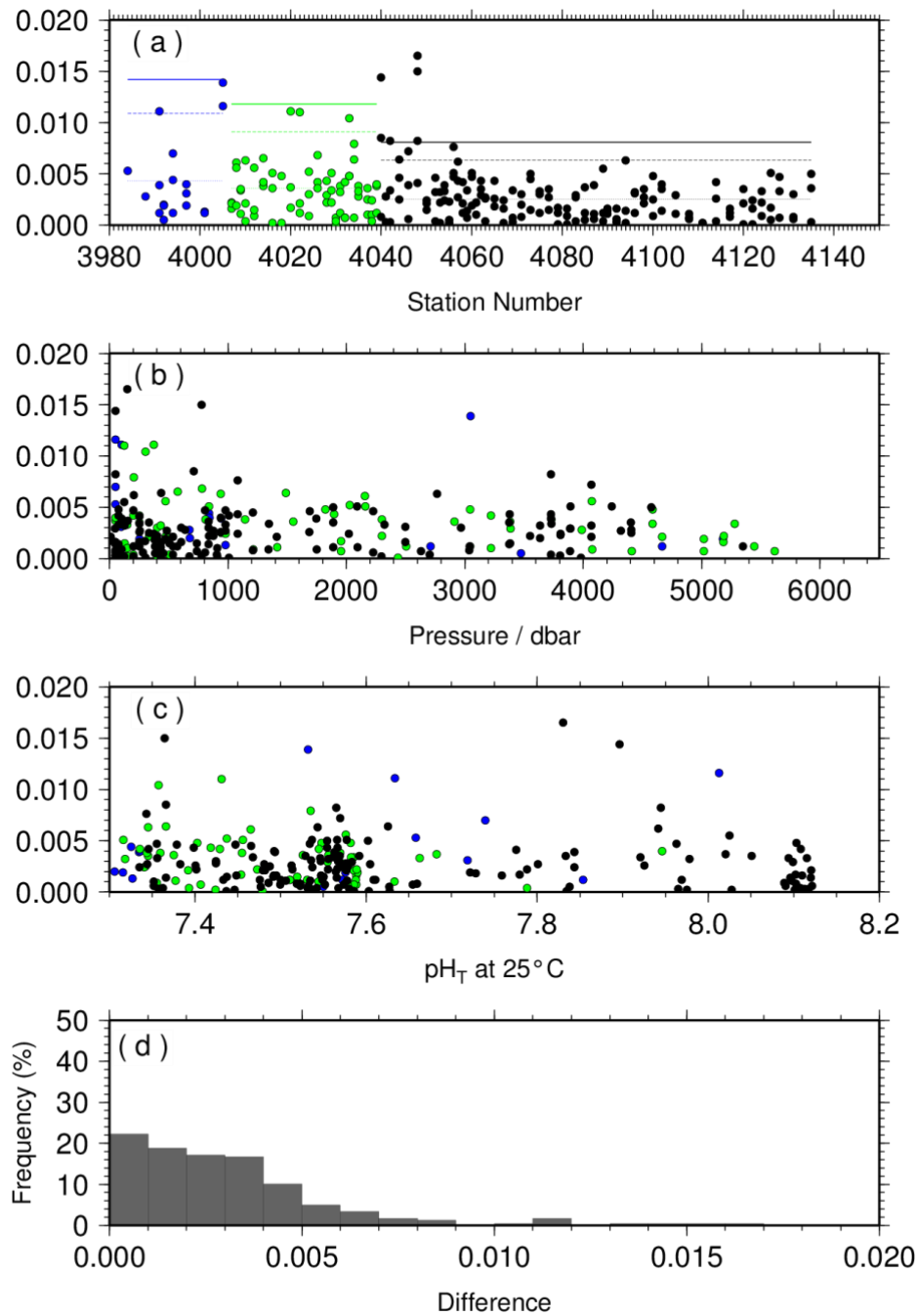


Figure C.6.7. Result of pH_T replicate samplings (n = 237) during the cruises RF11-06, RF11-07 and RF11-08 versus (a) Station number, (b) Sampling depth, (c) pH_T values and (d) Histogram of the result of replicate samplings. The lines in the panel (a) indicate upper control limit (thick), upper warning limit (dashed) and average of absolute difference (dotted), respectively. The colour of plots denotes the cruise (See Figure C.6.3).

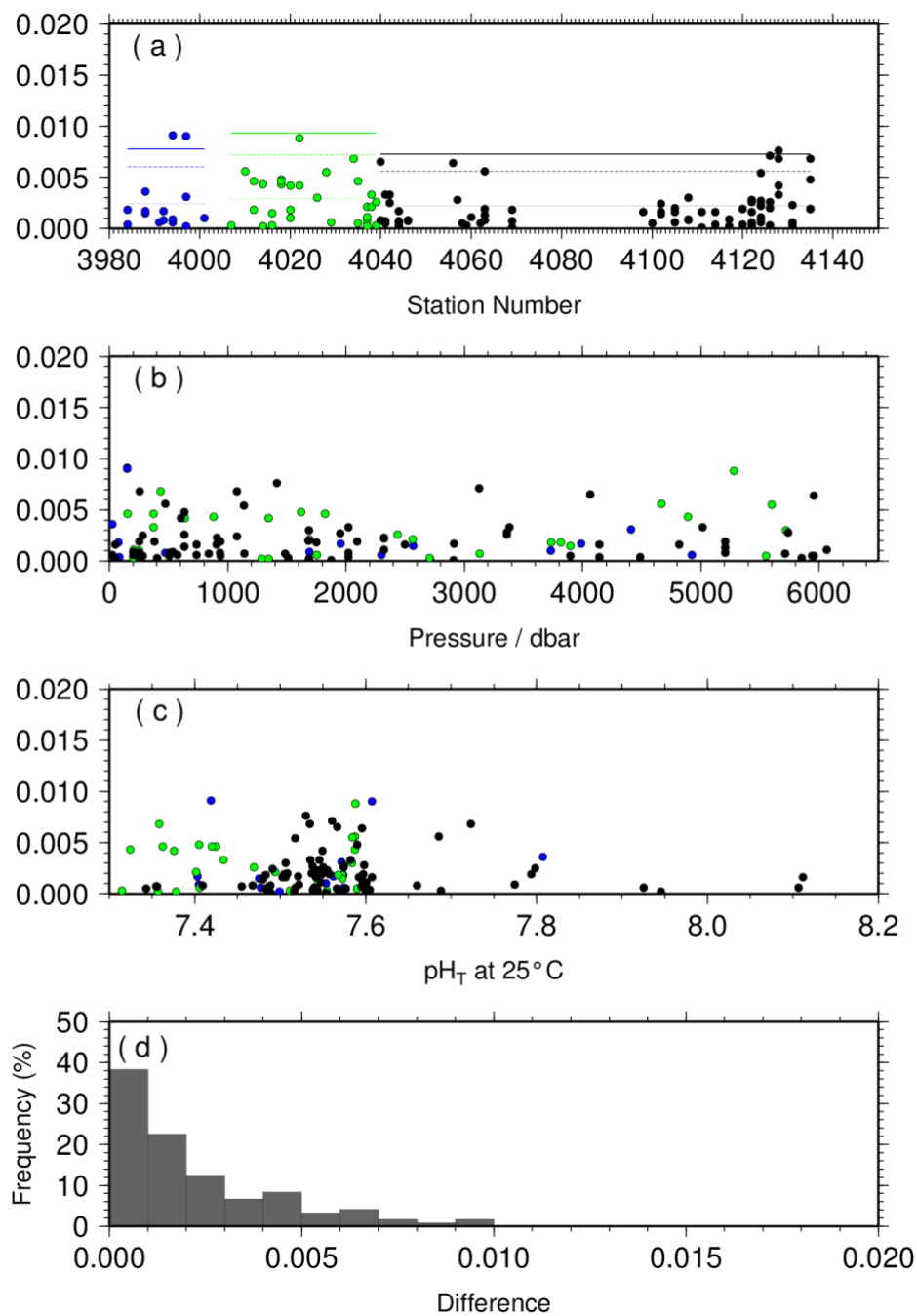


Figure C.6.8. Result of pH_T duplicate samplings (n = 121) during the cruises RF11-06, RF11-07 and RF11-08 versus (a) Station number, (b) Sampling depth, (c) pH_T values and (d) Histogram of the result of duplicate samplings.

(7) Problems

Although most data were on a smooth line of a vertical profile, pH_T values of samples obtained from deep layers at a cross over stations (see section (8)) were different between cruises. In addition, there were large offsets between pH_T values of CRMs or SSW analysed in different cruises. Therefore, we assigned all data as “not finalized” ($\text{QF} = 1$). It was found after the cruise that the linearity of CCD sensor of spectrophotometer to the light intensity was insufficient at the intensity range higher than 55000. The absorbance values will be corrected for the CCD sensor non-linearity.

pH_T data of 111 samples (Table C.6.3) were assigned as questionable data ($\text{QF} = 3$) because the data was sufficiently (approx. 2σ of measurements) apart from smooth line of vertical profile of a station. The pH_T data for these samples showed different characters from the data of DIC, TA, dissolved oxygen or nutrients. Possible reason for this problem was a lack of rinsing optical cell after a measurement, because of malfunction of circulation pump of pre-treatment unit. pH_T data of 20 samples (Table C.6.3) were assigned as bad (faulty) data ($\text{QF} = 4$). The absorbance at wavelength 730 nm of these data was anomalously high, which represented air bubbles remained in an optical cell. If all of five absorbance data per a sample measurement was faulty, the data was assigned as bad.

(8) Results

(8.1) Comparison at cross-stations during the cruise

There were two cross-stations during the cruise. The one was located at 40°N/165°E and another was located at 9°N/165°E. At stations of Stn.55 (RF4039) and Stn.56 (RF4040), hydrocast sampling for pH_T was conducted two times at interval of 18 days. At stations of Stn.105 (RF4089) and Stn.106 (RF4090), hydrocast sampling for pH_T was conducted two times. Interval between the first and the second was 14 days. These profiles are shown in Figure C.6.9.

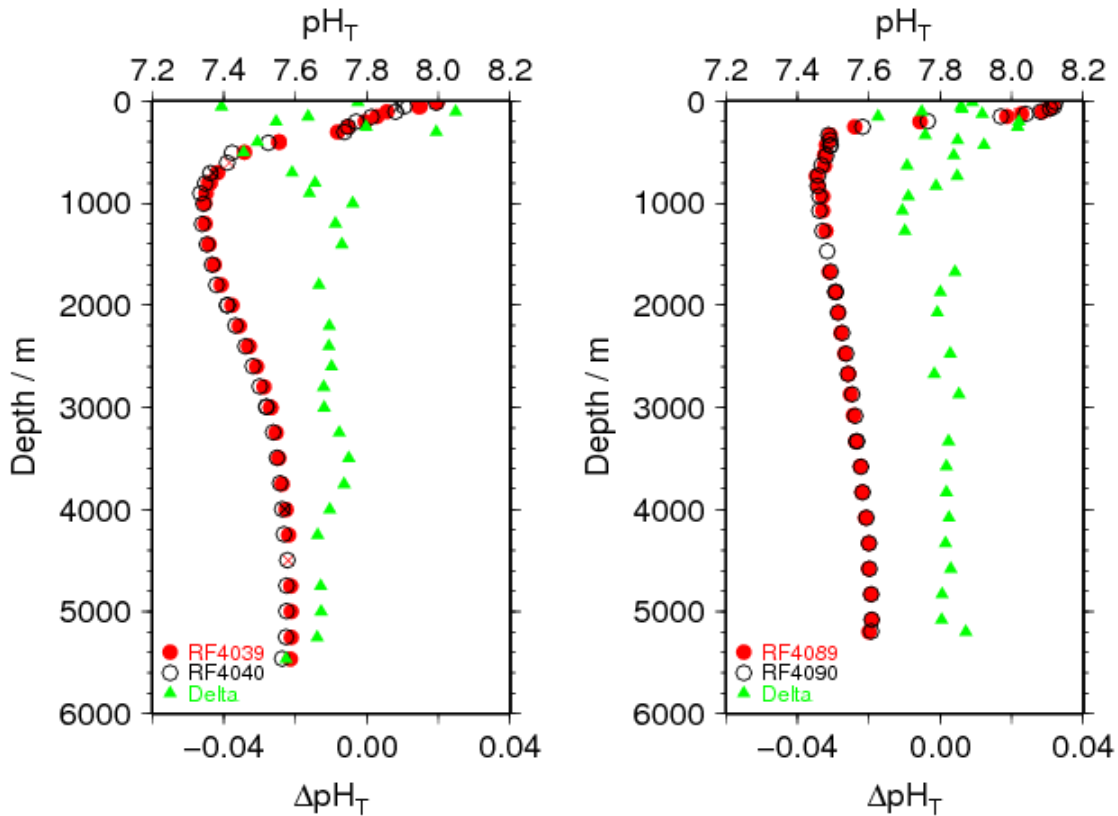


Figure C.6.9. Comparison of pH_T observed in this study at same location in different legs of this cruise. a) 40N, 165E in cruise RF11-07 (station RF4039) and in cruise RF11-08 (station RF4040); b) 9N, 165E in leg1 (station RF4089) and leg2 (station RF4090) of cruise RF11-08. The colour denotes the station shown in the legend. Triangle plot is the difference in pH_T analysed at same location in different legs.

(8.2) Comparison at cross-stations of WHP-P1 and P3 sections

We compared our pH_T data and WHP-P1 at a cross point (around $47^\circ\text{N}/165^\circ\text{E}$). WHP-P1 line was observed in 2007 by R/V Mirai that belongs to Japan Agency for Marine-Earth Science and Technology (JAMSTEC).

Summary of the comparison of these profiles is shown in Figure C.6.10.

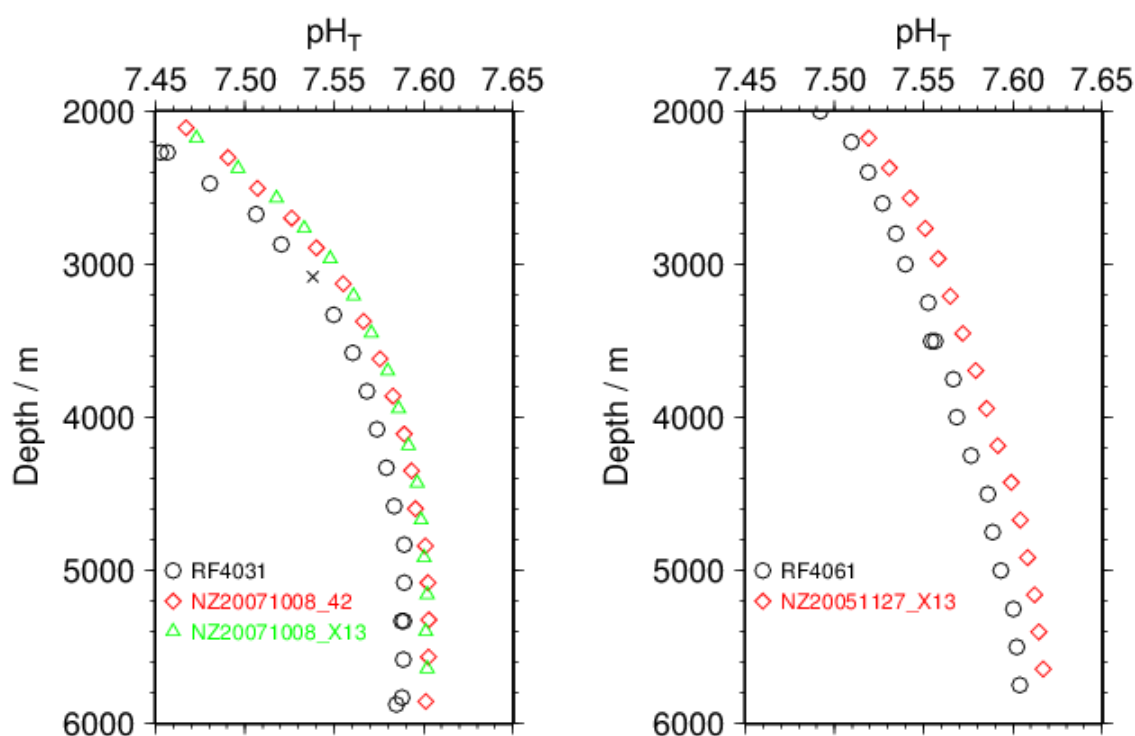


Figure C.6.10. Comparison of pH_T profiles at cross-stations of WHP-P1 (left panel), and WHP-P3 (right panel). Circle show this cruise.

References

- Clayton T.D. and R.H. Byrne 1993. Spectrophotometric seawater pH measurements: total hydrogen ion concentration scale calibration of m-cresol purple and at-sea results. *Deep-Sea Res. I*, **40**, 2115-2129.
- Dickson, A.G. 1990. Standard potential of the reaction: $\text{AgCl(s)} + 1/2 \text{H}_2(\text{g}) = \text{Ag(s)} + \text{HCl(aq)}$, and the standard acidity constant of the ion HSO_4^- in synthetic sea water from 273.15 to 318.15 K. *J. Chem. Thermodynamics*, **22**, 113-127.
- Dickson, A.G., Sabine, C.L. and Christian, J.R. (Eds.) 2007. Guide to best practices for ocean CO_2 measurements. *PICES Special Publication* 3, 191 pp.
- Lueker, T.J, A.G. Dickson and C.D. Keeling, 2000. Ocean pCO_2 calculated from dissolved

inorganic carbon, alkalinity, and equations for K_1 and K_2 : validation based on laboratory measurements of CO_2 in gas and seawater at equilibrium. *Marine Chem.*, **70**, 105-119.

Saito, S., M. Ishii, T. Midorikawa and H.Y. Inoue 2008. Precise Spectrophotometric Measurement of Seawater pH_T with an Automated Apparatus using a Flow Cell in a Closed Circuit. *Technical Reports of Meteorological Research Institute*, **57**, 1-28.

7. *Phytopigment (chlorophyll-a and phaeopigments)*

1 November 2019

(1) Personnel

Naoki NAGAI (GEMD/JMA)

Shinichiro UMEDA (GEMD/JMA)

(2) Station occupied

A total of 90 stations (RF11-06: 12, RF11-07: 27, RF11-08: 51) were occupied for phytopigment. Station location and sampling layers of phytopigment are shown in Figure C.7.1.

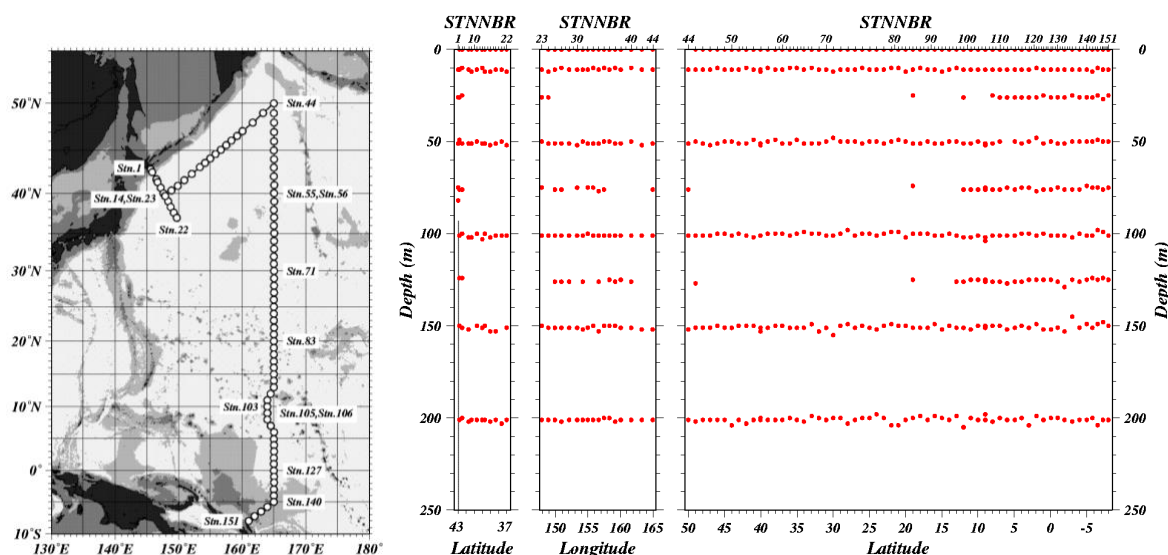


Figure C.7.1 Station location (left panel) and sampling layers of chlorophyll-a (right panels)

(3) Reagents

N,N-dimethylformamide (DMF)

0.5 N hydrochloric acid (0.5N HCl)

chlorophyll-a standard from *Anacystis nidulans* algae manufactured by Sigma Chemical Co.

Rhodamine WT manufactured by Turner Designs.

(4) Instruments

Fluorometer; 10-AU manufactured by Turner Designs

Spectrophotometer; UV-1800 manufactured by Shimadzu Co. Ltd.

Glass Fiber Filiter; Whatman GF/F filter (25 mm)

(5) Standardization

A chlorophyll-*a* standard calibration for fluorometric determination was performed by the method described by UNESCO (1994). Before standardization, fluorometer was calibrated by using 100 % DMF and a Rhodamine solution diluted to 1ppm with deionized water. Chlorophyll-*a* standard was dissolved in DMF. The concentration of chlorophyll-*a* solution was determined spectrophotometrically as follows;

$$\text{Chl } \alpha \text{ concentration } (\mu\text{g/ml}) = A_{\text{chl}} / \text{specific absorption coefficient}$$

where A_{chl} is the difference between absorbance at 663.8 nm and 750 nm. The specific absorption coefficient is 88.74 L/g·cm (Porra *et al.*, 1989). Using this precise chlorophyll-*a* concentration, the linear calibration factor (f_{ph}) and the acidification coefficient (R) were calculated. f_{ph} was calibrated for each cuvette as the slope of the unacidified fluorometric reading vs. chlorophyll-*a* concentration calculated spectrophotometrically. R was calculated by averaging the ratio of the unacidified and acidified readings of pure chlorophyll-*a*. Table C.7.1 shows f_{ph} and R in this cruise.

Table C.7.1 f_{ph} and R determined by the standardization

	RF11-06	RF11-07	RF11-08
Linear calibration factor (f_{ph})	1.755	1.741	1.775
Acidification coefficient (R)	7.084	7.571	7.202

(6) Seawater sampling and measurement

Water samples were collected from 10-liters Niskin bottle attached the CTD-system and a stainless steel bucket for the surface. A 200 ml seawater sample was immediately filtered through 25 mm GF/F filters by low vacuum pressure, the particulate matter collected on the filter. Chlorophyll-*a* was extracted in vial with 9 ml of DMF. Extracts were stored for 24 hours in the refrigerator at -30°C until analysis.

After the extracts were put on the room temperature for at least one hour in the dark, only the extracts except the filter were decanted from the vial to the cuvette. Fluorometer readings for each cuvettes were taken before and after acidification with 1-2 drops 0.5 N HCl. A chlorophyll-*a* and phaeopigments concentration in the sample are calculated using the following equations;

$$\text{Chl } (\mu\text{g/l}) = \frac{F_0 - F_a}{f_{\text{ph}} \cdot (R - 1)} \cdot \frac{v}{V}$$

$$\text{Phaeo } (\mu\text{g/l}) = \frac{R \cdot F_0 - F_a}{f_{\text{ph}} \cdot (R - 1)} \cdot \frac{v}{V}$$

F_0 = reading before acidification

F_a = reading after acidification

R = acidification coefficient (F_0/F_a) for pure chlorophyll-*a*

f_{ph} = linear calibration factor

v = extraction volume

V = sample volume

(7) Quality control flag assignment

Quality flag values were assigned to chlorophyll-*a* measurements using the code defined in IOCCP Report No.14 (Swift, 2010). Measurement flags of 2 (good), 3 (questionable), 4 (bad), and 5 (not repeated) have been assigned (Table C.7.2).

Table C.7.2 Summary of assigned quality control flags

Flag	Definition	Chl	Phaeo
2	Good	629	629
3	Questionable	0	0
4	Bad (Faulty)	3	3
5	Not reported	1	1
Total number		633	633

References

- Holm-Hansen, O., and B. Riemann (1978): chlorophyll *a* determination: improvements in methodology. *Oikos*, 30, 438-447.
- Holm-Hansen, O., C. J. Lorenzen, R. W. Holmes and J. D. H. Strickland (1965): Fluorometric determination of chlorophyll. *J. Cons. Perm. Int. Explor. Mer.*, 30, 3-15.
- Porra, R. J., W. A. Thompson and P. E. Kriedemann (1989): Determination of accurate coefficients and simultaneous equations for assaying chlorophylls *a* and *b* extracted with four different solvents: verification of the concentration of chlorophyll standards by atomic absorption spectroscopy. *Biochem. Biophys. Acta*, 975, 384-394
- Swift, J. H. (2010): Reference-quality water sample data: Notes on acquisition, record keeping, and evaluation. *IOCCP Report No.14, ICPO Pub. 134, 2010 ver.1*
- UNESCO (1994), Protocols for the joint global ocean flux study (JGOFS) core measurements: Measurement of chlorophyll *a* and phaeopigments by fluorometric analysis, *IOC manuals and guides 29, Chapter 14*.

8. $\delta^{13}\text{C}$ and $\Delta^{14}\text{C}$ of Dissolved Inorganic Carbon

1 November 2019

Yuichiro KUMAMOTO

Research Institute for Global Change,

Japan Agency for Marine-Earth Science and Technology

(1) Introduction

Stable and radioactive carbon isotopic ratios ($\delta^{13}\text{C}$ and $\Delta^{14}\text{C}$) of dissolved inorganic carbon (DIC) are good tracers for the anthropogenic carbon in the ocean. During RF11-07 and -08 cruises, named WHP-P13 revisit cruise along 165°E approximately in the North Pacific, seawater samples for $\delta^{13}\text{C}$ and $\Delta^{14}\text{C}$ analyses were collected at 12 stations. Here we report results of $\delta^{13}\text{C}$ and $\Delta^{14}\text{C}$ of DIC.

(2) Sample collection

The sampling stations are summarized in Figure C.8.1 and Table C.8.1. A total of 287 seawater samples, including four pairs of replicate samples, were collected between surface (about 10 m depth) and near bottom at 12 stations using 12-liter X-Niskin bottles. The seawater in the X-Niskin bottle was siphoned into a 250 cm³ glass bottle with enough seawater to fill the glass bottle two times. Immediately after sampling, 10 cm³ of seawater was removed from the bottle and the sample was poisoned by 200 μL of saturated HgCl_2 solution. Then the bottle was sealed by a glass stopper with Apiezon M grease and stored in a cool and dark space on board.

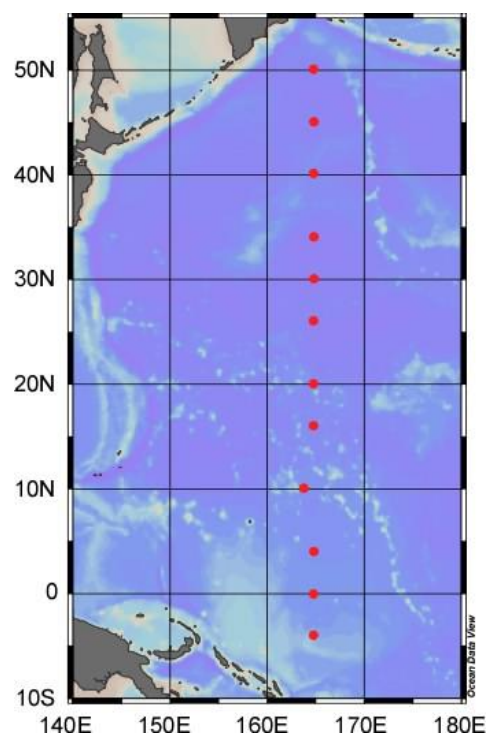


Figure C.8.1. Sampling stations for $\delta^{13}\text{C}$ and $\Delta^{14}\text{C}$ of DIC during RF11-07 and -08 cruises (June, 2011–September, 2011).

C.8.1. The sampling stations, number of samples, and maximum sampling depth for carbon isotopes in DIC during RF11-07 and -08 cruises.

Station		Number of samples	Max. sampling depth / m
P13-44	RF4028	24	5481
P13-49	RF4033	24	5914
P13-55	RF4039	24	5465
P13-66	RF4050	23	5997
P13-71	RF4055	24	5891
P13-75	RF4059	24	5737
P13-83	RF4067	24	5338
P13-91	RF4075	24	5378
P13-103	RF4087	24	4971
P13-116	RF4100	24	4478
P13-127	RF4111	24	4352
P13-138	RF4122	24	3317
	Total	287	

(3) Sample preparation

In our laboratory, DIC in the seawater samples were stripped cryogenically and split into three aliquots: Accelerator Mass Spectrometry (AMS) ^{14}C measurement (about 200 μmol), ^{13}C measurement (about 100 μmol), and archive (about 200 μmol). Efficiency of the CO_2 stripping from seawater sample was more than 95 % that was calculated from concentration of DIC in the seawater samples. The stripped CO_2 gas for ^{14}C was then converted to graphite catalytically on iron powder with pure hydrogen gas. Yield of graphite powder from CO_2 gas was estimated to be about 80 % in average by weighing of sample graphite powder. Details of these preparation procedures were described by Kumamoto et al. (2011).

(4) Sample measurements

$\delta^{13}\text{C}$ of the sample CO_2 gas was measured using Finnigan MAT252 mass spectrometer. The $\delta^{13}\text{C}$ value was calculated by a following equation:

$$\delta^{13}\text{C} (\text{‰}) = (R_{\text{sample}} / R_{\text{standard}} - 1) \times 1000. \quad (1)$$

where R_{sample} and R_{standard} denote $^{13}\text{C} / ^{12}\text{C}$ ratios of the sample CO_2 gas and the standard CO_2 gas, respectively. The working standard gas was purchased from Oztech Gas Co. $\delta^{13}\text{C}$ of the standard gas was assigned with VPDB (Vienna Pee Dee Belemnite) standards and calibrated relative to the appropriate internationally accepted IAEA primary standards. $\Delta\delta^{14}\text{C}$ in the graphite sample was measured in AMS facilities of Institute of Accelerator Analysis Ltd in Shirakawa, Japan (Pelletron 9SDH-2, National Electrostatic Corporation). The $\Delta^{14}\text{C}$ value was calculated by:

$$\delta^{14}\text{C} (\text{‰}) = (R_{\text{sample}} / R_{\text{standard}} - 1) \times 1000, \quad (2)$$

$$\Delta^{14}\text{C} (\text{‰}) = \delta^{14}\text{C} - 2 (\delta^{13}\text{C} + 25) (1 + \delta^{14}\text{C} / 1000), \quad (3)$$

where R_{sample} and R_{standard} denote, respectively, $^{14}\text{C} / ^{12}\text{C}$ ratios of the sample and the international standard, NIST Oxalic Acid SRM4990-C (HOxII). R_{standard} was corrected for decay since A.D. 1950 (Stuiver and Polach, 1977; Stuiver, 1983). Equation 3 is normalization for isotopic fractionation. When quality of $\delta^{13}\text{C}$ data was not "good", $\Delta^{14}\text{C}$ was calculated by interpolated $\delta^{13}\text{C}$ value derived from data at just above and below layers. Finally $\Delta^{14}\text{C}$ value was corrected for radiocarbon decay between the sampling and the measurement dates. Individual errors of $\delta^{13}\text{C}$ were given by standard deviation of repeat measurements. Errors of $\Delta^{14}\text{C}$ were derived from larger of the standard deviation of repeat measurements and the counting error. Means of the $\delta^{13}\text{C}$ and $\Delta^{14}\text{C}$ errors were calculated to be 0.004 ‰ and 2.6 ‰ ($n = 283$), respectively, corresponding to repeatabilities of our $\delta^{13}\text{C}$ and $\Delta^{14}\text{C}$ measurements.

(5) Replicate measurements

Replicate samples were taken at three stations. Results of 4 pairs of the replicate samples

are shown in C.8.2. The standard deviation of the $\delta^{13}\text{C}$ and $\Delta^{14}\text{C}$ replicate analyses was calculated to be 0.029 ‰ ($n = 4$) and 4.4 ‰ ($n = 4$), respectively. These were larger than the repeatability obtained from the individual measurements (0.004 ‰ for $\delta^{13}\text{C}$ and 2.6 ‰ for $\Delta^{14}\text{C}$) probably due to errors from sample preparation. We concluded that the uncertainty of our $\delta^{13}\text{C}$ and $\Delta^{14}\text{C}$ analyses including error due to the sample preparation were about 0.03 ‰ and 4 ‰, respectively.

C.8.2. Summary of replicate analyses.

Station	Btl	$\delta^{13}\text{C} / \text{‰}$				$\Delta^{14}\text{C} / \text{‰}$			
		$\delta^{13}\text{C}$	Error ^a	E.W.Mean ^b	Uncertainty ^c	$\Delta^{14}\text{C}$	Error ^d	E.W.Mean ^b	Uncertainty ^c
P13-116	29	0.011	0.003	0.014	0.004	-17.3	2.8	-19.7	3.3
		0.016	0.003			-21.9	2.8		
P13-127	28	0.713	0.004	0.696	0.024	47.1	3.0	46.9	2.1
		0.679	0.004			46.6	3.0		
P13-138	28	0.786	0.002	0.783	0.016	47.3	3.2	51.2	5.2
		0.763	0.005			54.7	3.0		
P13-138	1	0.093	0.005	01.62	0.051	-217.3	2.5	-212.9	6.3
		0.165	0.001			-208.4	2.5		

a. Standard deviation of repeat measurements.

b. Error weighted mean of the replicate pair.

c. Larger of the standard deviation and the error weighted standard deviation of the replicate pair.

d. Larger of the standard deviation of repeat measurements and the counting errors.

(6) Reference seawater measurements

During the sample measurements period in 2011 and 2012, we measured $\delta^{13}\text{C}$ and $\Delta^{14}\text{C}$ in reference seawaters together with those in the samples. The reference seawater was prepared from a large volume of surface seawater collected in an open ocean. The surface seawater was filtered, exposed to ultraviolet irradiation, poisoned by HgCl_2 , dispensed in 250 cm³ glass bottles, and then has been stored since March 2011. The $\delta^{13}\text{C}$ and $\Delta^{14}\text{C}$ of the reference seawater was measured at every station series. The results are shown in Table 3. The standard deviations of $\delta^{13}\text{C}$ ($n = 11$) and $\Delta^{14}\text{C}$ ($n = 12$) were 0.025 ‰ and 3.9 ‰, respectively. These are almost same as the uncertainty (0.029 ‰ for $\delta^{13}\text{C}$ and 4.4 ‰ for $\Delta^{14}\text{C}$) obtained from the replicate measurements.

Table 3 Summary of reference seawaters (RS) measurements.

No.	RS No.	$\delta^{13}\text{C} / \text{‰}$			$\Delta^{14}\text{C}^a / \text{‰}$		
		Measurement date	$\delta^{13}\text{C}$	Error ^b	Measurement date	$\Delta^{14}\text{C}$	Error ^c
1	RM1103-35	21-Sep-11	-0.302	0.005	28-Nov-11	32.1	2.9
2	RM1103-191	15-Sep-11	-0.357	0.005	28-Nov-11	40.4	2.7

3	RM1103-31	20-Sep-11	-0.319	0.001	28-Nov-11	44.0	2.7
4	RM1103-117	06-Dec-11	-0.350	0.003	17-Feb-12	38.0	3.0
5	RM1103-169	07-Dec-11	-0.344	0.003	17-Feb-12	38.6	2.9
6	RM1103-104	08-Dec-11	-0.343	0.002	17-Feb-12	30.6	2.8
7	RM1103-5	04-Jan-12	-0.354	0.003	12-Mar-12	39.0	2.8
8	RM1103-12	05-Jan-12	-0.344	0.004	12-Mar-12	32.3	2.8
9	RM1103-38	12-Jan-12	-0.353	0.007	12-Mar-12	34.6	2.9
10	RM1103-14	-	-	-	21-Mar-12	39.9	2.9
11	RM1103-96	31-Jan-12	-0.402	0.005	21-Mar-12	36.9	3.0
12	RM1103-16	01-Feb-12	-0.358	0.004	21-Mar-12	38.0	3.0

- Decay corrected for 28/Nov./2011.
- Standard deviation of repeat measurements.
- Larger of the standard deviation and the counting error.

(7) Quality control flag assignment

Quality flag values were assigned to all $\delta^{13}\text{C}$ and $\Delta^{14}\text{C}$ measurements using the code defined in Table 0.2 of WHP Office Report WHPO 91-1 Rev.2 section 4.5.2 (Joyce et al., 1994). Measurement flags of 2, 3, 4, 5, and 6 have been assigned (Table 4). For the choice between 2 (good), 3 (questionable) or 4 (bad), we basically followed a flagging procedure in Key et al. (1996) as listed below:

- On a station-by-station basis, a datum was plotted against pressure. Any points not lying on a generally smooth trend were noted.
- $\delta^{13}\text{C}$ ($\Delta^{14}\text{C}$) was then plotted against dissolved oxygen (silicate) concentration and deviant points noted. If a datum deviated from both the depth and oxygen (silicate) plots, it was flagged 3.
- Vertical sections against depth were prepared using the Ocean Data View (Schlitzer, 2012). If a datum was anomalous on the section plots, datum flag was degraded from 2 to 3, or from 3 to 4.

Table 4 Summary of assigned quality control flags.

Flag	Definition	Number	
		$\delta^{13}\text{C}$	$\Delta^{14}\text{C}$
2	Good	270	275
3	Questionable	6	4
4	Bad	3	0
5	Not report (missing)	0	0
6	Replicate	4	4
Total		283	283

(8) Data Summary

Figure C.8.2 shows vertical section of $\delta^{13}\text{C}$ against depth. Higher $\delta^{13}\text{C}$ values were observed in surface waters. The highest value (more than 1.3 ‰) was found in surface water of the equatorial region. Minimum layer of $\delta^{13}\text{C}$ was found in deep waters from 500 to 2,000 m depth approximately and the smallest value (-0.8 ‰ approx.) was around 300-m depth at the northernmost station 44. From the minimum in the deep waters to the bottom, $\delta^{13}\text{C}$ value increases gradually. The general distribution of $\delta^{13}\text{C}$ well agrees with that presented in a previous study (Kroopnick, 1985) and is mainly governed by biogeochemical process and ocean circulation.

Figure C.8.3 shows vertical section of $\Delta^{14}\text{C}$ against depth. Higher $\Delta^{14}\text{C}$ values were observed in the thermocline (< about 1,000 m depth), which is derived from the bomb-produced radiocarbon. Relative higher $\Delta^{14}\text{C}$ was measured below 4,000 m depth approximately where the high- $\delta^{13}\text{C}$ water was found. Minimum layer of $\Delta^{14}\text{C}$ was found in deep waters from 1,500 to 4,000 m depth approximately. The general distribution of $\Delta^{14}\text{C}$ in deep and bottom waters supports results in a previous study (Key et al., 2004) and indicates the global pattern of thermohaline circulation.

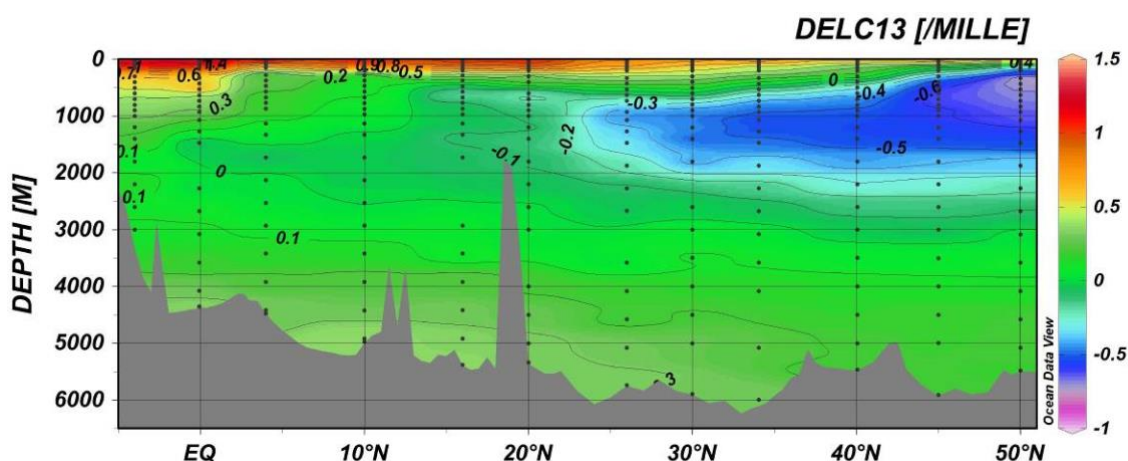


Figure C.8.2. Vertical sections of $\delta^{13}\text{C}$ (‰) against depth along the WHP-P13 line in 2011.

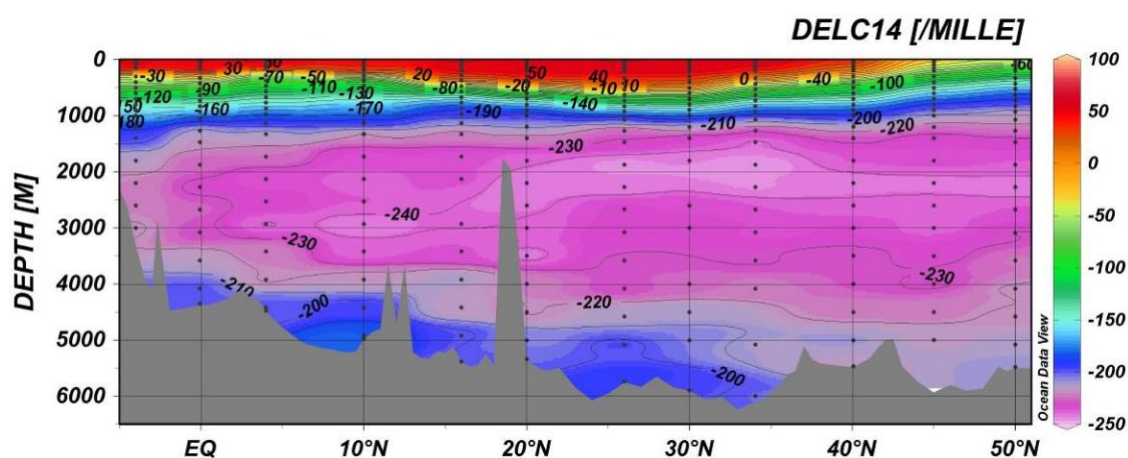


Figure C.8.3. Vertical sections of $\Delta^{14}\text{C}$ (‰) against depth along the WHP-P13 line in 2011.

References

- Joyce, T., and C. Corry, *eds.*, C. Corry, A. Dessier, A. Dickson, T. Joyce, M. Kenny, R. Key, D. Legler, R. Millard, R. Onken, P. Saunders, M. Stalcup, *contrib.*, 1994. Requirements for WOCE Hydrographic Programme Data Reporting, WHPD Pub. 90-1 Rev. 2, 145pp.
- Key, R.M., A. Kozyr, C.L. Sabine, K. Lee, R. Wanninkhof, J.L. Bullister, R.A. Feely, F.J. Millero, C. Mordy, T.H. Peng, 2004. A global ocean carbon climatology: Results from Global Data Analysis Project (GLODAP), *Global Biogeochemical Cycles*, 18, GB4031, doi:10.1029/2004GB002247.
- Key, R.M., P.D. Quay, G.A. Jones, A.P. McNichol, K.F. von Reden, R.J. Schneider, 1996. WOCE AMS radiocarbon I: Pacific Ocean results (P6, P16, P17), *Radiocarbon* 38, 425-518.
- Kroopnick, P.M., 1985. The distribution of ^{13}C of ΣCO_2 in the world oceans, *Deep-Sea Research*, 32, 57-84.
- Kumamoto Y, Murata A, Watanabe S, Fukasawa M., 2011. Temporal and spatial variations in bomb radiocarbon along BEAGLE2003 lines—Revisits of WHP P06, A10, and I03/I04 in the Southern Hemisphere Oceans, *Progress in Oceanography* 89, 49–60.
- Schlitzer, R., 2012. Ocean Data View, URL: <http://odv.awi.de/en/home/>
- Stuiver. M., 1983. International agreements and the use of the new oxalic acid standard, *Radiocarbon*, 25, 793-795.
- Stuiver, M. and H.A. Polach, 1977. Reporting of ^{14}C data. *Radiocarbon* 19, 355-363.